

The Poincaré Switch

Group 12 Authors:

Michelle Ngyuen	Austin “David” Rich	Joshua Hendry
<i>Electrical Engineering</i>	<i>Optical Engineering</i>	<i>Optical Engineering</i>

Review Committee:

Dr. Darren Hudson	CREOL	Associate Professor
Dr. Wayesh Qarony	ECE	Assistant Professor
Dr. Enxia Zhang	ECE	Assistant Professor
Gregory Jenkins	ASML Optical Engineer (Sponsor)	

Advisors:

Dr. Chung Yan Chan	ECE	Senior Lecturer
Dr. Aravinda Kar	CREOL	Professor

CHAPTER 1. SUMMARY	8
CHAPTER 2. BACKGROUND.....	8
2.1 BACKGROUND AND MOTIVATION	8
2.2 FEATURES AND FUNCTIONALITIES	9
2.3 PAST PROJECTS	10
2.3.1 <i>Basis Paper Summary</i>	10
2.3.2 <i>History of Birefringent Crystals as Optical Modulators</i>	12
2.3.3 <i>Use of Double – Pass set up to Characterize a PSA</i>	12
2.3.4 <i>Goals and Objectives</i>	12
2.4 SPECIFICATIONS	17
CHAPTER 3. RESEARCH	24
3.1 TECHNOLOGIES	24
3.1.1 <i>Light Sources</i>	24
3.1.2 <i>Birefringent Crystals</i>	29
3.1.3 <i>Motors</i>	34
3.1.4 <i>Motor Driver</i>	40
3.1.5 <i>High Level Motor Controller</i>	40
3.1.6 <i>Microcontrollers</i>	43
3.1.7 <i>Power Meter</i>	47
3.1.8 <i>Polarizers</i>	48
3.1.9 <i>Retroreflector</i>	50
3.1.10 <i>Lens</i>	51
3.1.11 <i>Beamsplitter</i>	52
3.1.12 <i>Mirror</i>	53
3.1.13 <i>LED Driver</i>	54
3.1.14 <i>Operational Amplifier</i>	55
3.1.15 <i>Digital-to-Analog Converter</i>	56
3.2 POWER MANAGEMENT	56
3.2.1 <i>Power Delivery</i>	56
3.2.2 <i>Power Adapter</i>	57
3.2.3 <i>Power Jack</i>	58
3.2.4 <i>Voltage Regulator</i>	59
3.3 COMMUNICATION PROTOCOL	61
3.3.1 <i>USB</i>	61
3.3.2 <i>UART</i>	61
3.3.3 <i>SPI</i>	61
3.4 SOFTWARE	62
3.4.1 <i>Programming Languages</i>	62
3.4.2 <i>Development Environment</i>	64
CHAPTER 4. STANDARDS AND DESIGN CONSTRAINTS	65
4.1 INDUSTRIAL STANDARDS	65

4.1.1 PCB Design Standards	65
4.1.2 Communication Protocol Standards	66
4.1.3 Lens Standards.....	67
4.1.4 Laser Safety Standards.....	67
4.2 DESIGN CONSTRAINTS	68
4.2.1 Power Constraints.....	68
4.2.2 Optical Constraints.....	68
4.2.3 Practical Constraints.....	69
4.2.4 Time Constraints.....	69
4.2.5 Economic	70
4.2.6 Scalability	71
4.3 OTHER CONSTRAINTS	72
4.3.1 Sustainability.....	72
4.3.2 Manufacturability.....	72
4.3.3 Political	72
4.3.4 Ethical.....	72
4.3.5 Health and Safety	73
4.3.6 Environmental	73
CHAPTER 5. APPLICATION OF LLMS.....	73
5.1 CHATGPT USE CASE 1	74
5.2 CHATGPT USE CASE 2.....	75
5.3 CHATGPT USE CASE 3.....	75
5.4 CHATGPT USE CASE 4.....	76
5.5 CHATGPT USE CASE 5.....	76
CHAPTER 6. HARDWARE DESIGN	77
6.1 SYSTEM HARDWARE DESIGN	77
6.1.1 Power Supply Delivery.....	77
6.1.2 TIA Circuit.....	79
6.1.3 Microcontroller Connection.....	82
6.1.4 Double-Pass Beam Calculations.....	85
6.1.5 Single-Pass Beam Calculations	86
6.1.6 Motor Mount Design.....	87
CHAPTER 7. SOFTWARE AND SIMULATION DESIGN.....	87
7.1 SIMULATION DESIGN.....	87
7.1.1 MATLAB.....	87
7.1.2 Mathematical Principles.....	88
7.1.3 Stokes' Theorem	89
7.1.4 Calculating Theoretical PER.....	89
7.1.5 Simulating the "Broadband" Response of the System.....	92
7.1.6 LTspice Simulation	93
7.2 SOFTWARE DESIGN	94
7.2.1 GUI	95
7.2.2 Motor Control	96

7.2.3 Data Collection.....	97
CHAPTER 8. SYSTEM FABRICATION AND PROTOTYPE CONSTRUCTION	100
8.1 PCB LAYOUT	100
8.1.1 Voltage Regulator.....	100
8.1.2 TIA Circuit Board.....	102
8.1.3 Main Board	103
8.2 PCB HOUSING	ERROR! BOOKMARK NOT DEFINED.
8.3 DC POWER SUPPLY HOUSING.....	ERROR! BOOKMARK NOT DEFINED.
8.4 OPTICS CAD DIAGRAM	106
CHAPTER 9. SYSTEM TESTING AND EVALUATION.....	107
9.1 OPTOELECTRONICS FEASIBILITY	107
9.2 HARDWARE TESTING	108
9.2.1 Switch Timing	108
9.2.2 Voltage Regulator.....	112
9.3 SOFTWARE TESTING.....	115
9.3.1 Motor Control System	115
9.3.2 Light Source Control System.....	115
9.4 PERFORMANCE EVALUATION	115
9.5 OVERALL INTEGRATION.....	116
9.6 PLAN FOR SENIOR DESIGN 2.....	ERROR! BOOKMARK NOT DEFINED.
CHAPTER 10. ADMINISTRATIVE CONTENT.....	117
10.1 BUDGET.....	117
10.1.1 Bill of Materials Double-Pass	117
10.1.2 Bill of Materials Single-Pass	118
10.2 MILESTONES	120
10.3 WORK DISTRIBUTIONS.....	121
CHAPTER 11. CONCLUSION.....	122
CHAPTER 12. APPENDIX A: REFERENCES	124
CHAPTER 13. APPENDIX B: DATA SHEETS AND REFERENCE FIGURES.....	131
CHAPTER 14. APPENDIX C: LLM PROMPTS AND RESPONSES.....	137
CHAPTER 15. APPENDIX D: SOFTWARE CODE.....	163

Table of Figures

Figure 2.3-1.....	16
Figure 2.4-1.....	20
Figure 2.4-2.....	21
Figure 2.4-3.....	22

Figure 2.4-4.....	23
Figure 3.1-1.....	30
Figure 3.1-2	30
Figure 3.1-3	31
Figure 3.1-4	31
Figure 3.1-5	32
Figure 3.1-6	32
Figure 4.3-1 Laser safety label for the laser we used in our setup identifying the hazards that come with this class of laser	73
Figure 6.1-1.....	78
Figure 6.1-2	79
Figure 6.1-3.....	79
Figure 6.1-4	80
Figure 6.1-5	81
Figure 6.1-6.....	81
Figure 6.1-7.....	82
Figure 6.1-8.....	83
Figure 6.1-9.....	83
Figure 6.1-10	84
Figure 6.1-11.....	84
Figure 6.1-12	85
Figure 6.1-13.....	87
Figure 7.1-1.....	89
Figure 7.1-2	89
Figure 7.1-3.....	90
Figure 7.1-4	91
Figure 7.1-5.....	92
Figure 7.1-6	92
Figure 7.1-7.....	93
Figure 7.1-8.....	94
Figure 7.2-1.....	95
Figure 7.2-2.....	96
Figure 7.2-3.....	96
Figure 7.2-4.....	97
Figure 7.2-5.....	98
Figure 7.2-6	98
Figure 7.2-7	99
Figure 7.2-8	100

Figure 8.1-1	101
Figure 8.1-2	101
Figure 8.1-3	102
Figure 8.1-4	102
Figure 8.1-5	103
Figure 8.1-6	104
Figure 8.2-1	105
Figure 8.2-2	105
Figure 8.2-3	106
Figure 8.3-1	106
Figure 8.3-2	107
Figure 9.1-1	108
Figure 9.2-1	109
Figure 9.2-2	109
Figure 9.2-3	113
Figure 9.2-4	114

Tables

Table 2.4-1 System Specifications	17
Table 2.4-2 Component Specifications	18
Table 3.1-1 Source Type Comparison	25
Table 3.1-2 LED Comparison	27
Table 3.1-3 Laser Comparison	28
Table 3.1-4 Motor Type Comparison	37
Table 3.1-5 Galvanometer Motor Comparison	39
Table 3.1-6 High Level Motor Controller Comparison	41
Table 3.1-7 DAQ Card Comparison	42
Table 3.1-8 Microcontroller Type Comparison	44
Table 3.1-9 ESP32 Comparison	46
Table 3.1-10 Power Meter Comparison	48
Table 3.1-11 Polarizer Comparison	49
Table 3.1-12 Retroreflector Comparison	51
Table 3.1-13 Lens Comparison	52
Table 3.1-14 Beam Splitter Comparison	53
Table 3.1-15 Mirror Comparison	54
Table 3.1-16 LED Driver	55

Table 3.1-17 Operation Amplifier	55
Table 3.1-18 Digital to Analog Converter	56
Table 3.2-1 Power Management.....	57
Table 3.2-2 Adapter Model Comparisons	58
Table 3.2-3 Jack Model Comparisons	58
Table 3.2-4 Voltage Regulator Type Comparison	60
Table 3.2-5 Switching Voltage Regulator Comparison	60
Table 3.4-1 Programming Language Comparison	63
Table 3.4-2.....	63
Table 3.4-3 Development Environment Comparison	64
Table 9.2-1	110
Table 9.2-2.....	111
Table 9.2-3.....	111
Table 9.2-4 Data Collected with LED Load	112
Table 9.2-5 Data Collected with Additional Load and LED Load	112
Table 9.2-6 Data Collected from the Voltage Regulator PCB	113
Table 9.2-7 Data Collected from the TIA Circuit PCB.....	114
Table 10.2-1 Senior Design 1 Milestones	120
Table 10.2-2 Senior design 2 Milestones	120

Chapter 1. Summary

The Poincare switch or Fast Polarization Switch is a device that is capable of rotating through all of the linear polarization states limited only by the smallest step size the motor can take. We were contracted by ASML to build this device for our senior design project while the switch itself needed to remain between Five thousand to Seven thousand dollars we were given some “padding” for testing and characterization equipment. Using The Poincaré Switch you are able to rotate between two small angles within 5 ms. The step response we tested corresponded to the angles of rotation that we calculated for the crystal to give us the desired output polarizations, we tested various crystals looked at different light sources and optical alignment elements, and compared between two different set ups, the single-pass and double-pass set up. Verifying the merits and costs of each. Through all of our research, combined with the expertise we have gained over the years here at the University of Central Florida, we were able to prove our basic objectives by the semester showing control of our Thorlabs Galvanometer rotating the necessary angle within the time frame given, we have Glan-Taylor polarizers that when combined gives us an extinction ration over 100:1 and we verified that over the visible spectrum. We deep dove into the math of the crystal showing how various wavelengths interact with it, simulating laser-like sources with a narrow line width and LED like sources with a FWHM around 28 nm. We utilized software like MATLAB, Labview, and ArduinoIDE to control our setup in a centralized way, on the user’s computer. We designed and built an optical system to test various light sources spanning across the visible spectrum without having to reach in and swap them out. While maintaining preferred spot size and power requirements for our client ASML. During this project we were in constant contact with ASML, The rest of our review committee and our faculty advisors. Once again thank you so much to ASML for sponsoring this project, the experience of working on this type of project for any of us would not have been made a reality without you. We were very lucky to play this small role in the project.

Chapter 2. Background

2.1 Background and Motivation

In the world of semiconductor technology, light and its manipulation are at its core. Being able to harness the power of light is crucial to staying on top of this innovative environment. For our senior design project, we task ourselves with mastering polarization control with the utmost precision. This mastery, while some see it as merely scientific fun, we understand is crucial to the furthering of metrology, sensing, and overall analysis of the smallest technological systems. We plan to create a fast polarization switch, that we call Fast Polarization Switch, that utilizes the fascinating features of birefringent crystals. Through careful selection of this crystal, we will be able to rotate it in such a way to rapidly alter the polarization of input light. This technology, while new and innovative, will considerably change the state of semiconductor manufacturing with its precision and stability. In a world where computers control our ecosystem, from the bottom of the sea to the heavens upon the stars, our project will be involved in the steppingstones that will change our future.

Inside of academia, the class senior design is modeled after the real-world hardships engineers are faced with on a daily basis. This course is designed to challenge up and coming engineers to take

what we have learned through our rigorous coursework and apply it to a product that will not only innovate but advance the technological world in a way that has never been done. As a team we must create a system that is reasonably accessible to our audience as well as fully capable of completing its intended goal. To do this our team must be highly skilled and coordinated, qualities that cannot be taught and must be achieved through dedication. This type of project is the best way to spring into the world of industry and prepare us for the upcoming problems we will face. This project, while useful, is a test of teamwork, knowledge, and commitment and will show those around us that we are prepared for what's to come.

The idea of Fast Polarization Switch came from ASML, a leader in the field of semiconductor technology. This collaboration not only challenges but also inspires us. We are challenged by the fact that we must live up to the high standards that come from working with a world leader in such innovative technology and inspired with the knowledge that the work we do here is being used to push the forefront of technology. With their insight into the newest technological advancements, they led us to the idea of using a rotating birefringent crystal as the cornerstone of a polarization switch. This idea will not only be technically challenging but also be immensely practically valuable in the world of metrology. With their guidance, Fast Polarization Switch will show the industry that we can provide a global impact in the same way ASML has for so long.

2.2 Features and Functionalities

The main functionality of our product is the ability to polarize light. This is done by using crystal and the properties of birefringence to change the refractive index of light as it passes through. This allows us to change the polarization of light by altering the angle at which the light is incident upon the crystal. This will allow us to quickly and accurately change the polarization by just rotating our crystal on a rotation mount connected to a motor.

This can also act as a power modulator. By passing the polarized light through a polarized beam splitter, we are able to output a fraction of the input light's power. By changing the polarization, the amount that gets reflected will also change. As the polarization output from the crystal changes the polarization of the beam splitter, we will increase power and as we get further away from the polarizers set polarization our power will decrease. Using this functionality, our polarizing crystal can also effectively act as a power regulator.

Our system will be able to work with the entire visible light spectrum. Birefringent crystals are transparent over a large range, from UV to IR. This allows us to function across a wide wavelength range so our product can be used across a variety of applications. Our product is also thermally and mechanically stable. This stability comes from the fact that we will be using a double pass system for our crystal, meaning that we will pass light through the crystal twice. This will eliminate the beam distortions that may be induced from other polarization modulators, like electro-optic modulators. Also, because we are only mechanically moving the crystal and not changing the refractive index by changing the electric field across the crystal, like electro-optic modulators, we will not be drastically heating our crystal. This means we do not have to worry about any thermal instability that may come from this heating.

We would also like to test a single pass system in our project. This single-pass setup will increase the angle difference between orthogonal polarization states. This means we will have to turn our motor more to achieve the same result. This would allow a user to use a less precise motor and could potentially save money. Also, it will limit the amount of power loss we will receive from our

system. This is because the double pass system has the light passing through a beam splitter twice that is not necessary for a single-pass setup.

Our design will avoid the need for high power input. Unlike other polarization modulators that use voltage to control polarization we will be using solely mechanical sources. This decreases power consumption as we will not need a constant source of power to alter our light. Also, more importantly, since our product will be used in high sensitivity metrology applications, we will need our product to be as accurate as possible. By not using high voltage to control polarization we will not be worried about problems like RF interference or electronic noise. This will help us drastically increase sensitivity.

2.3 Past Projects

2.3.1 Basis Paper Summary

Fast Polarization Switch is based on prior work completed at the University of Physics, KAIST, in Korea. The title of their work “Double-pass rotating z-cut quartz plate as a rapidly variable waveplate” (Lee, Kwon et al. 2025) was published online through Optica. This work establishes the feasibility of our goals. Elucidating paths of improvement and highlighting the math used to back up their results as well. Specifically, the Jones matrices provided are used to determine the output polarization depending on rotation angle of the crystal, and the difference in angle between the optical axis and the fast axis. The double-pass alignment they use can be a basis for the system to implement fiber and negates the need to adjust the alignment based on wavelength changes. Easing the process of measuring different depths using varied wavelength sources or a frequency sweeping light source. With the characterization of their system establishing our baseline. We have clear basic objectives to achieve. Namely the ability to change the polarization between orthogonal states within a millisecond. With an extinction rate of 99.9% reducing the output power of their system by 30dB. Comparing their chosen z – cut uniaxial quartz plate to the more widely used Pockels Cells, in terms of the electro-optical effect. The quartz offered more thermal stability and was capable of handling higher power without damaging functionality. It’s CTE or (Coefficient of Thermal Expansion) being smaller when compared to typical EOM crystals reduces thermal lensing and optical degradation. Fully rotating polarization of the light within $\sim 0.7^\circ$ of controlled angular change. Noting that typical zero-order waveplates require a 45° rotation. This was the key factor in bringing the switching time to below a millisecond they remarked. Finally, they provide a way to suppress the angular vibrations that come from such quick movements. These insights are the integral components, gleaned from this work, that we utilized to complete our objectives. Further details on how each of these are going to be achieved will be explained below.

The beam that was used in the past project was characterized by divergence angle and beam waist, which was determined to 2.2 mm with a divergence angle of 100 μ rads they chose the (Cening optics, AR coated at 1064 nm) their crystal had a thickness of 10 mm with refractive indices of $n_o = 1.534$ and $n_e = 1.543$ at 1064 nm. The rotation of their crystal between 10° to 20° is used to measure and map changes in polarization. This offset from normal reduces back reflections. Their experiment showed that even within this range they were able to have full control over polarization and power. It also shows that the double pass configuration reduces the period by a half cycle, further lowering transition time between orthogonal polarization states. To verify its use in a wide wavelength range they not only tested at 1064 nm but also 671 nm again measuring power in both single and double pass configurations the comparisons held true, phase delay was

slightly larger when comparing quartz angles to 1064 nm however the power showed similar variances with double – pass doubling the peaks and halving the period. The contrast for the 671 nm light increased with increased quartz angle, this was attributed to the AR coating being less effective and the back reflections playing a bigger role in the process.

One of the biggest hindrances to the use of quartz crystal as a variable wave plate has been the beam path shift. The comparison here between the two configurations showcase that the double-pass configuration due to the retro-reflection of the light shows no position shift in the reflected light. This can be proven using basic geometric optics. Where $D_o = \frac{d}{\cos \theta_o} \sin(\theta - \theta_o)$, $D_e = \frac{d}{\cos \theta_e} \sin(\theta - \theta_e)$ Here θ_o and θ_e can be found through Snell's law: $n_e \sin \theta_e = n \sin \theta = n_o \sin \theta_o$ to verify this in the double – pass set up they utilized a wave plate and a beam splitter, measuring the beam shift by looking at the position of the reflected beam from the beam splitter. Theorizing that due to negligible beam shifts, new opportunities for fiber coupling arise. They compared contrast in the single and double pass configuration between free space and the fiber coupled, comparisons were similar with contrast in the double pass being much higher. When comparing coupling efficiency, it was easy to see why. The efficiency was constant with varying quartz angle in the double pass. While the single pass suffered significantly increasing losses with higher quartz angle.

To experimentally prove the validity of rapid power conversion they use a pulse which rotates the crystal to an orthogonal state, in the double pass setup. With a rotation interval $\theta_f - \theta_i = 0.7^\circ$. Starting in the off position they find the pulse brings the output light to its full power within a millisecond. The pulse they used did cause some vibration in the crystal due to the stopping motion. They stated that this could be mitigated by shaping the pulse. Although their method increased the time to power conversion to 2.5ms. The rotator chosen could operate with an input sinewave signal with frequencies up to 300 Hz, this limit is due to its mechanical nature. Characterizing the power conversion in their experiment by measuring the power ratio between two polarizations in the double pass design. Calculating conversion ratio with $R_p = (P_{\max} - P_{\text{bg}})/(P_{\min} - P_{\text{bg}})$ where P_{\max} and P_{\min} are maximum and minimum power, P_{bg} is the background noise. They find the conversion ratio to be about 1000. They also determined the tolerance in offset of their retro-reflective mirror. Finding the ratio to stay above 900 when the degree change stayed between $\pm 0.015^\circ$ from the apex. They find a peak beam shift displacement of $9.1\mu\text{m}$, expecting a beam shift less than $9.3\mu\text{m}$, these are both unnoticeable when related to the beam diameter of 2.2 mm. Due to the rapid rotation and stopping there are vibrations in the angle of the quartz, causing erratic changes in power. They studied these power shifts by studying the shift in beam position at the stopping angle, in the single pass setup. This method led to more accurate extrapolation of these differences, and lead them to find that these power fluctuations due to stopping are less than 0.1%, furthermore finding that this holds true for various types of input signals they determine that the noise level introduced by their specific operating system is low enough that their system could be used in atomic quantum simulating platforms.

The team at the University of Physics, KAIST, in Korea, was able to demonstrate that implementing a rotating z-cut quartz plate in a double-pass configuration was not only possible but could push the boundaries on tolerances and what these types of EOM systems are capable of. Highlighting its application for systems that require larger beam sizes, unable to be addressed by acousto-optic modulators. The system they created is fast, precise, with a full range of control over

polarization, and intensity. With this paper as the backbone to our project we were able to not only meet those goals and objectives but push beyond.

2.3.2 History of Birefringent Crystals as Optical Modulators

The use of birefringent crystals as waveplates in optics has been documented for well over 50 years. Originally utilized as a retardation plate in 1964. Exact equations describing the phase difference and the electric field of the outgoing light were discovered using Maxwell's equations. Providing conventional solutions for calcite and quartz. Even going so far as to discuss Quartz as a quarter wave-plate and applying it to the investigation of elliptical polarization. Exploring it for the case of a monochromatic plane wave that is normally incident and briefly comparing some oblique incidences. (Holmes 1964) Later on in the "Handbook of optical constants of solids: Handbook of thermo-optic coefficients of optical materials with applications." Which came out in 1998 (Ghosh 1998) here Ghosh went into more detail on how to apply quarter – wave retardation plate as a polarizer, amongst others. Continuing in Volume 1 Section 12.7, the book references a few different ways of solving the polarization of outgoing light, using matrix mathematics and further describing the difference between positive and negative uniaxial crystals. A wonderful reference involving the finer details of Jones matrix calculations was included in this section as well.

In 2016 something akin to the single-pass setup was used to characterize the crystal using a polarizer and analyzer both orientated at a 45° angle to the crystal to maximize the power drop. Then rotating the crystal, they saw how the power fluctuated. Analyzing the data and using Jones matrices they were able to determine the angular orientation of the crystals Optical axis. (Paranin 2016) As well as Ghosh et al. in 1999 go over characterization of calcite and quartz crystals highlighting that the refractive indices. Quoting "The extraordinary and ordinary indices of refraction of the crystal are fundamental parameters to have when applying such a crystal to any optical device or system." (Ghosh 1999) These parameters were provided for both crystals as tables showing the respective indices across a variety of wavelengths. Further claiming that the progress made during that work would be foundational in discovering a standardized equation representing the birefringence of all other uniaxial crystals. (Tables to be Included in Appendix.)

2.3.3 Use of Double – Pass set up to Characterize a PSA

A paper written in 2012 uses the double pass technique to characterize a PSA (polarization state analyzer). Fascinatingly it only uses the PSA and no other polarizing element to do the characterization. Further demonstrating the possibility of this technique used do design broadband high-resolution spectropolarimetric systems. Claiming the system can be used to find the parameters of any chromatic retarder. (Zallat, Torzynski et al. 2012) This discovery in combination with the work done in the prior papers we looked into is what made us believe we can make a self-calibrating system that can work with any composition of birefringent crystal given the proper thickness. Being able to insert any crystal the right orientation and running a calibration protocol, it was possible to make our system find the minimum rotation needed to switch polarizations between orthogonal states. Allowing for more adaptability into various other applications.

2.3.4 Goals and Objectives

The idea of this project is to build a device that takes input light and produces light of a specific chosen polarization. Our goals and objectives are listed below.

Basic Goals

- Build a device to take in visible light and polarize it at the desired speed.

Achieving the desired speed of polarization is dependent solely on the motor speed. After inputting the desired polarization into the GUI, the system should know exactly how much the crystal needs to rotate to be able to output the desired polarization and then it needs to calculate how long it takes to activate the motor for the crystal to be in the location required. After this calculation the system will turn on the motor for the desired time and speed to rotate this crystal to the exact angle to achieve desired polarization. The wavelength range for our system needs to be between 500 and 800nm.

- Be able to produce any linear polarization desired

This goal relies solely on the crystal selected. We needed to pick a crystal such that we can achieve the angle of rotation for the desired polarization. This selection should be thought out carefully as choosing a crystal will decide how much is needed to rotate to achieve the full polarization spectrum and the larger this rotation angle is then the larger our device will need to be to be able to rotate. Also, if the angle needed to achieve the full spectrum is too small, we may not be able to rotate the crystal precisely enough to achieve this goal which would mean we would need a higher price for our motor.

Advanced Goals

- Polarize input light that has a bandwidth of 30nm.

For this goal we would like to be able to polarize light sources with a small bandwidth of at maximum 30nm. The system should be able to maintain a high extinction ratio and still do this in the allotted time of under 5 milliseconds.

- Maintain accuracy for long term use

For this goal, our system will have MTBF (Mean time between Failures) comparable to if not better than other polarization-based modulators.

Stretch Goals

- Operate with two different light source wavelengths at the same time

We would like to operate our system with two different light sources with different wavelengths at the same time while maintaining 80% of our extinction rate. These light sources would be at wavelengths separated by more than 100nm.

- Enable polarization modulation continuously

Allow the user to input a steady change between polarization states and the speed of change. This would allow the user to experience different polarizations without having to use several inputs into the system.

We can create specific objectives to be able to achieve these goals. These objectives are listed below.

Basic Objectives

- Switch between linear orthogonal polarizations in under 5ms

For this objective we will need a highly accurate motor and driver. This is because the computer will have to calculate the desired angle of incidence the crystal needs to achieve the chosen polarization.

- Have an extinction ratio of at least 100:1

This means that when we check our output power from our polarizing beam splitter, we should be able to have a maximum power that is 100 times higher than our minimum power. To do this, we need to have a highly accurate polarizing beam splitter. If the splitter has a low extinction rate, then we will not be able to accurately measure the crystals extinction rate as the PBS's extinction rate will be limiting the crystal.

- Works with a wavelength range of between 500-800nm

This device will be used with a range in the visible spectrum. This means we need to be able to accurately adjust the angle of incidence needed for a specific wavelength in this range.

- Build the switching mechanism for under \$7,000

This is the budget we were given by ASML. This budget includes everything that goes into making the polarizer, but not the sources or power meter. This means we will be able to use money from outside of this budget to buy light sources and testing equipment like a power meter.

Advanced Objectives

- Route light source output through fiber for extreme stability

For this objective we would like to send our light output into fiber and then into the power detector. This would allow us to show that our device is stable and allow for easy routing of output light for the actual product, since in the product the power detector would not be needed. The user would simply have the output light from a fiber.

- Create arbitrary polarization states

For this objective we would like to be able to create circular and elliptical polarization states. This would allow the user to have greater control over their polarizations and be able to hit every polarization state on the Poincaré sphere

- Create a GUI to control polarization state and which light source to use.

For this objective we create a user interface to easily control the polarization the user wants and which light they want to turn on. The user would input a polarization, and the system would take this input and be able to calculate the time and speed of rotation for our motor.

Stretch Objectives

- Achieve an extinction ratio of 1000:1

This is the overall goal set by ASML. This is a stretch goal as it correlates to a precision of 99.9% which is an extremely high goal to set.

- Achieve a Switch timing of under 1ms

This objective is also set by ASML. This is strictly determined by how fast our motor can rotate and since we are using a motor off the shelf not something we can change. This objective is achievable by choosing a faster motor.

- Able to handle powers of up to 20mW

Our system should be able to handle a light source of 20mW. It should keep its extinction ratio even at light sources of up to 20mW.

- Allow crystal swapping

For this objective, we would use a mount that would allow us to remove the crystal and swap it for another one. This means we could use crystals that are designed for wavelengths out of our range and allow us to change crystal thickness for desired effects. This drastically increases the versatility of our system.

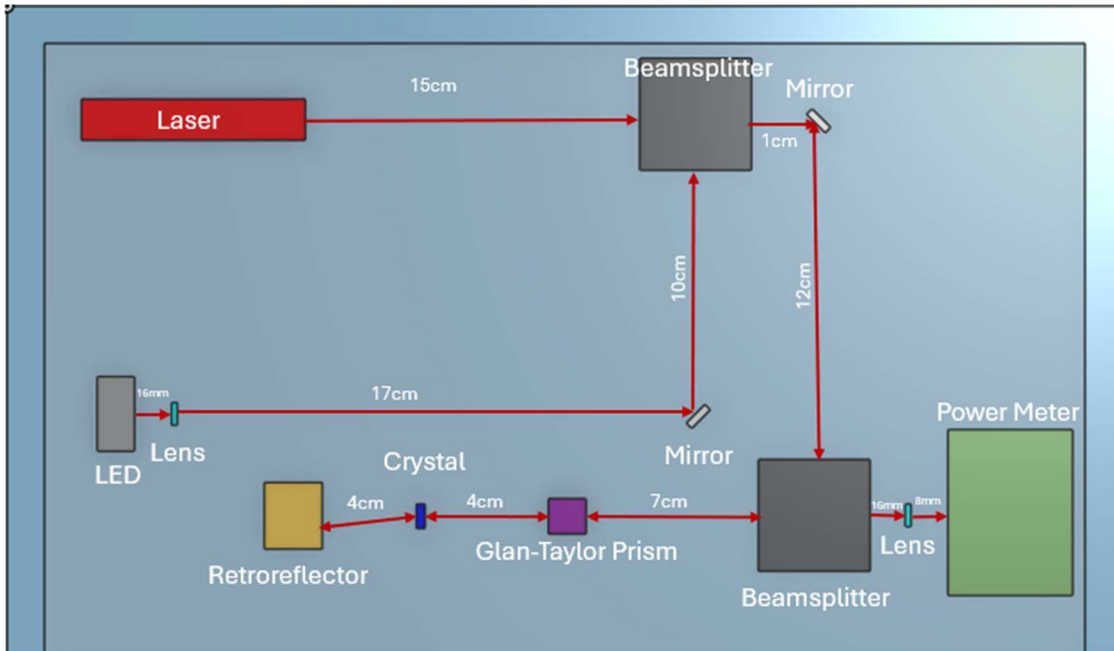


Figure 2.3.4-2

Optical design diagram is shown above. This demonstrates the double-pass optical setup that will be used to achieve our goals and objectives for this project. The red arrows indicate the laser direction of travel originating at the laser

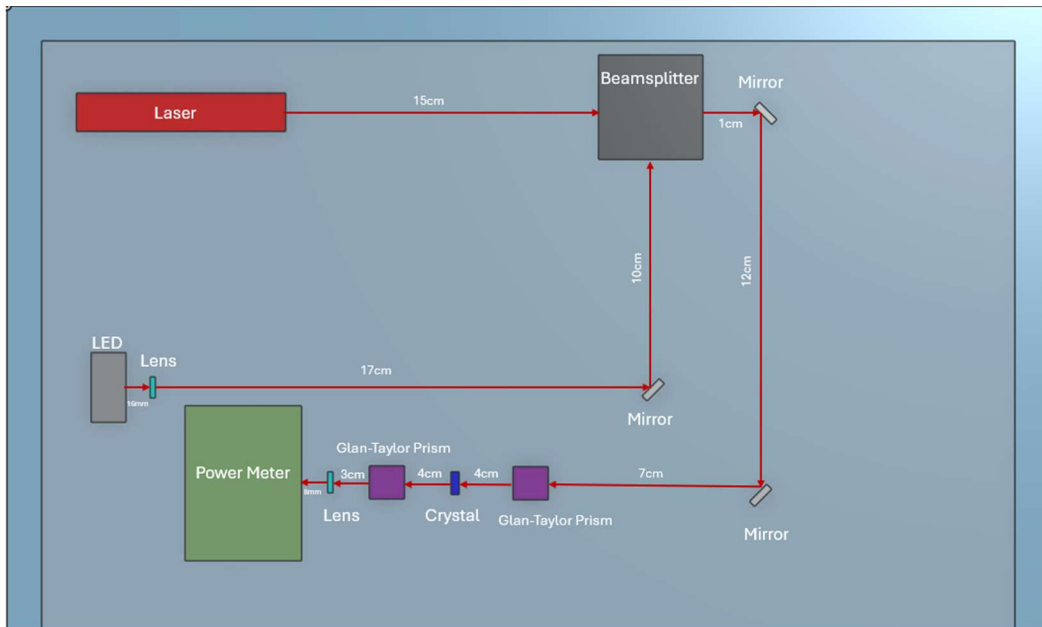


Figure 2.3-1

Optical design diagram is shown above. This demonstrates the single-pass optical setup that will be used to achieve our goals and objectives for this project. The red arrows indicate the laser direction of travel originating at the laser component.

2.4 Specifications

Table 2.4-1 System Specifications

Parameter	Description	Specification
Power Consumption	How much power our system will consume on average with normal use.	≤ 750 W
User Input to Output Measurement Time	The time it takes from the user to input a power reading from our system	≤ 3 seconds
Extinction Ratio Precision	This describes the precision of our polarization. This ratio describes the number of photons in the desired polarization to the photons with an orthogonal polarization	100:1
Motor Precision	This is the percent error we can expect when we use the motor.	$\pm 0.005^\circ$
Switching Time	This describes the time it takes for the motor to rotate the crystal to the position where the light is orthogonally polarized to the position we just left.	≤ 5 millisecond
Optical (Output) Power	This is the amount of power that will be detected by the photodetector after passing through the system.	Maximum 20 mW
Wavelength Range	This is the acceptable wavelengths for optimal use of our system	400 nm to 700 nm
Polarization Range	These are the polarization states that a user can input into the system and obtain an orthogonal output	0° to 180°
Step Response time	This is the amount of time for the motor to take one step towards the end distance it needs to travel	500 μ s
Total Cost of Polarization Switch	This is the cost of the polarization switch. This does not include light sources or power detector.	$< \$7,000$

Table 2.4-2 Component Specifications

Component(s)	Parameter	Specification
Electrical		
3.3 V Regulator	a) Max Output Current b) Max DC Input Voltage c) Min Output Voltage d) Max Output Voltage	a) 800 mA b) 15 V c) 3.267 V d) 3.333 V
5 V Regulator	a) Max Output Current b) Max DC Input Voltage c) Min Output Voltage d) Max Output Voltage	a) 1.5 A b) 35 V c) 4.8 V d) 5.2 V
Microcontroller (ESP32-S3 Series)	a) Max Output Current b) Average Output Current	a) 1500 mA b) 500 mA
Motor Driver (L298N Dual H-Bridge)	a) Input Voltage Range b) Output Voltage Range c) Peak Current d) Input Current Range e) Max Power Consumption	a) 3.2 V to 40 V b) 5 V to 35 V c) 2 A d) 0 to 36 mA e) 20 W
Motor (TBA)	a) Angle Range b) Step Size c) Speed d) Torque	a) 0° to 20° b) $\leq 0.1^\circ$ c) $\geq 1,000$ rpm d) TBD
Optics		
520 nm Compact Laser	a) Wavelength b) Output Power c) Size d) Beam Diameter e) Operating Voltage f) Operating Current g) Divergence	a) 520 nm b) 0.9 mW c) 11 mm x 60.2 mm d) 3 mm e) 4.9 V f) 80 mA g) -0.6 mrad
635 nm Compact Laser	a) Wavelength b) Output Power c) Size d) Beam Diameter e) Operating Voltage f) Operating Current g) Divergence	a) 635 nm b) 0.9 mW c) 11 mm x 60.2 mm d) 3 mm e) 4.9 V f) 70 mA g) -0.6 mrad
LED	a) Wavelength Peak b) Emitter Dimensions c) Dimensions d) Lifetime e) Output Power f) Forward Voltage g) Maximum Current	a) 470 nm b) 2 mm x 1 mm c) 30.5 mm Diameter d) >100,000 Hours e) 1161.7 mW f) 3.8 V g) 1000 mA

	h) Full Angle Divergence i) Bandwidth	h) 80 Degrees i) 28 nm
Plano-Convex Condenser Lens	a) Focal Length b) Wavelength Range c) Material d) Dimensions	a) 10 mm b) 350 nm x 700 nm c) N-BK7 d) 6 mm Diameter
Beam Splitter	a) Wavelength Range b) Size c) Split Ratio	a) 400 nm – 700 nm b) 30 mm x 16 mm c) 50:50
Retroreflector	a) Wavelength Range b) Diameter	a) 350 – 2000nm b) 10 mm
Photo Diode	a) Wavelength Range b) Aperture Size c) Dimensions d) Power Range	a) 400 – 1100 nm b) 9.5 mm Diameter c) 30.5 mm x 12.7 mm d) 50 nW – 50 mW
Power Meter Console	a) Dimensions b) Wavelength Range c) Power Range d) Repetition Rate e) Bandwidth	a) 180 mm x 38 mm b) 185 nm – 25 um c) 100 pW – 200 W d) 3 kHz e) DC – 100 kHz
Glan-Taylor Prism	a) Wavelength Range b) Aperture Size c) Extinction Ratio d) Dimensions	a) 350 nm – 700 nm b) 5 mm x 5 mm c) 100,000:1 d) 9.5 mm x 9.5 mm
Mirror	a) Diameter b) Reflectance c) Material d) Wavelength Range	a) 7 mm b) > 99% (400 – 750 nm) c) Fused Silica d) 400 nm – 750 nm
Crystal	a) Thickness b) Refractive Indices c) Absorption Spectra	TBD TBD TBD

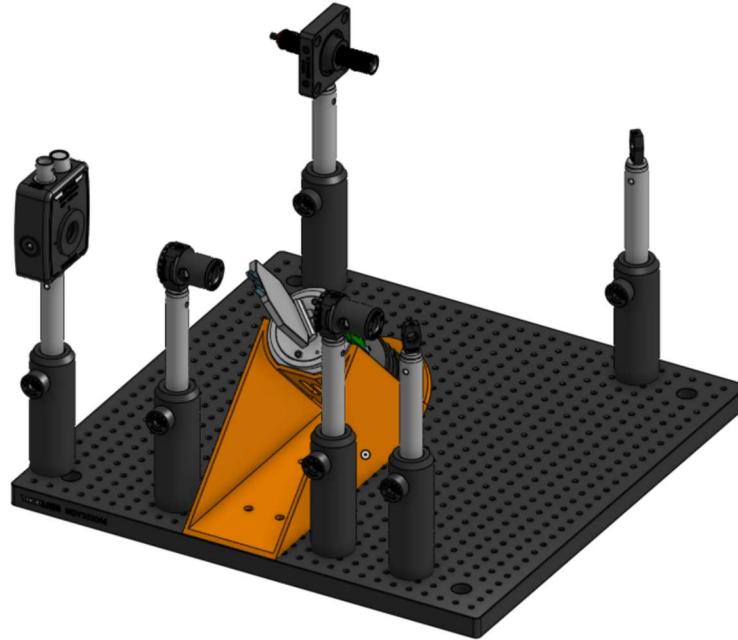


Figure 2.3.4-4

Prototype Illustration is shown above. This illustration is the general layout we will be using inside the housing of our system.

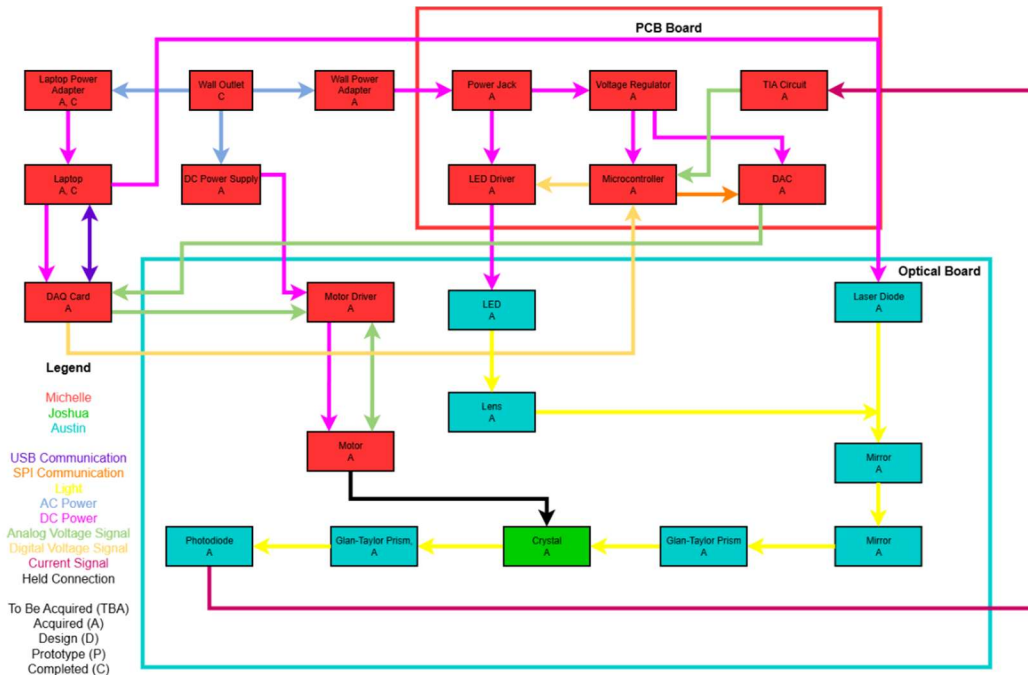


Figure 2.4-1

Hardware Diagram. This diagram shows how the components of our system will interact to ultimately produce our end goals. The colors of each block indicate the student tasked with researching and designing that component. The colors of each arrow indicate the connection between components.

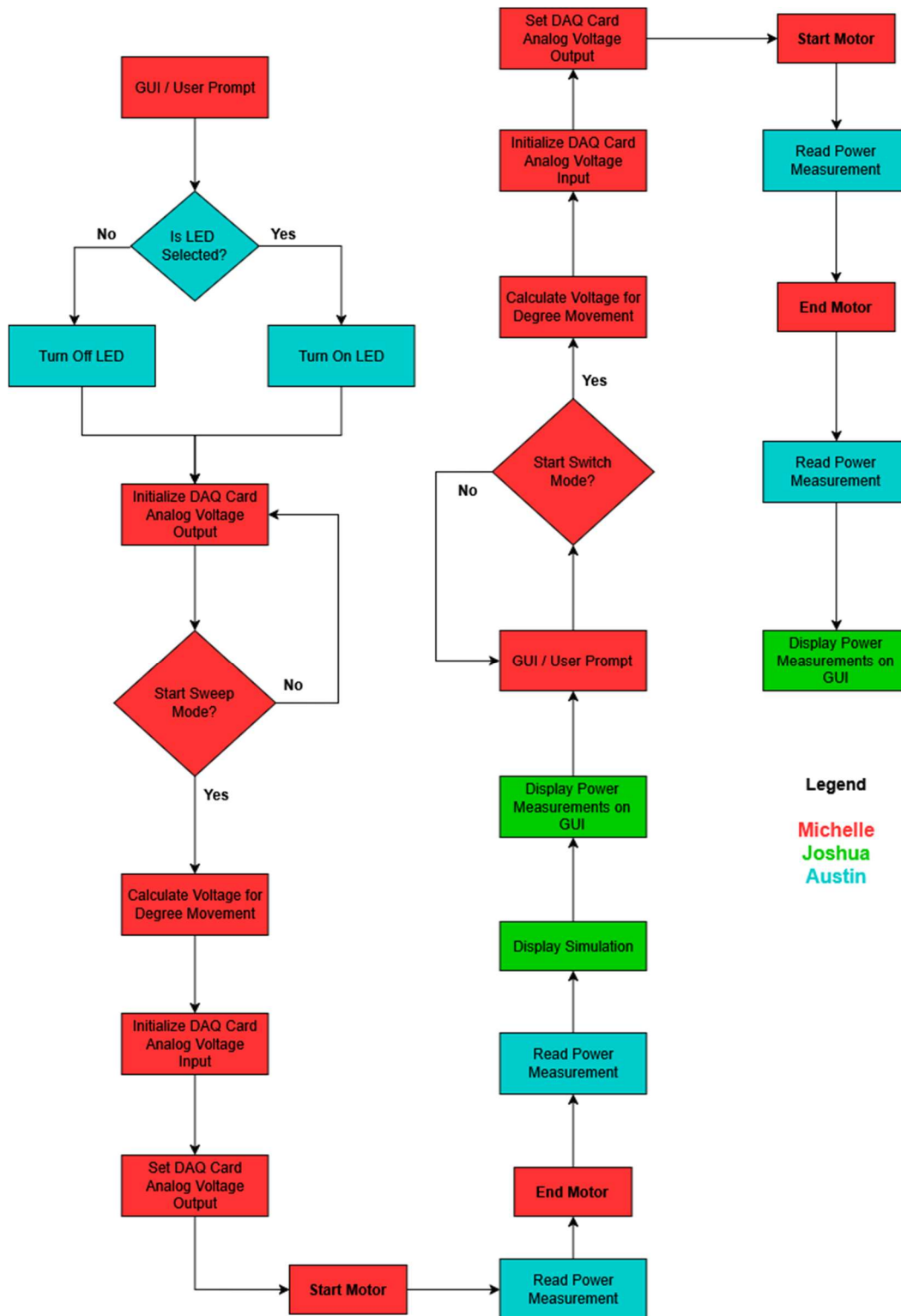


Figure 2.4-2

Software Diagram. This diagram shows how the software of our project interacted in the final product. The color of the boxes indicates who oversees which section of the software. The arrows indicate the timeline of events.

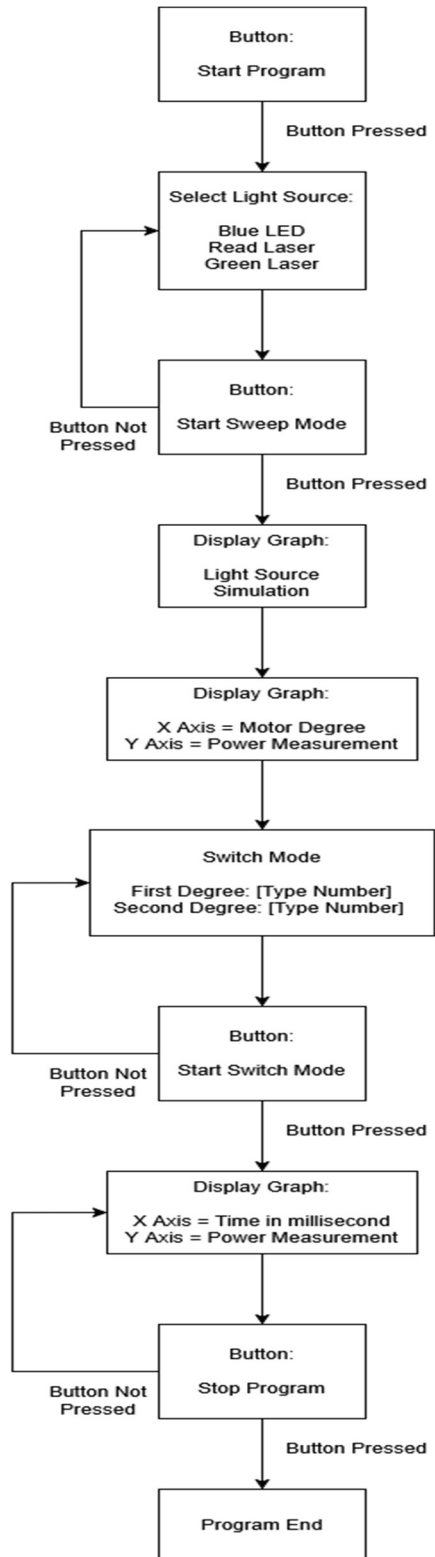


Figure 2.4-3

User Interface Diagram. This diagram shows how the GUI will function and the prompts it will give to the users.

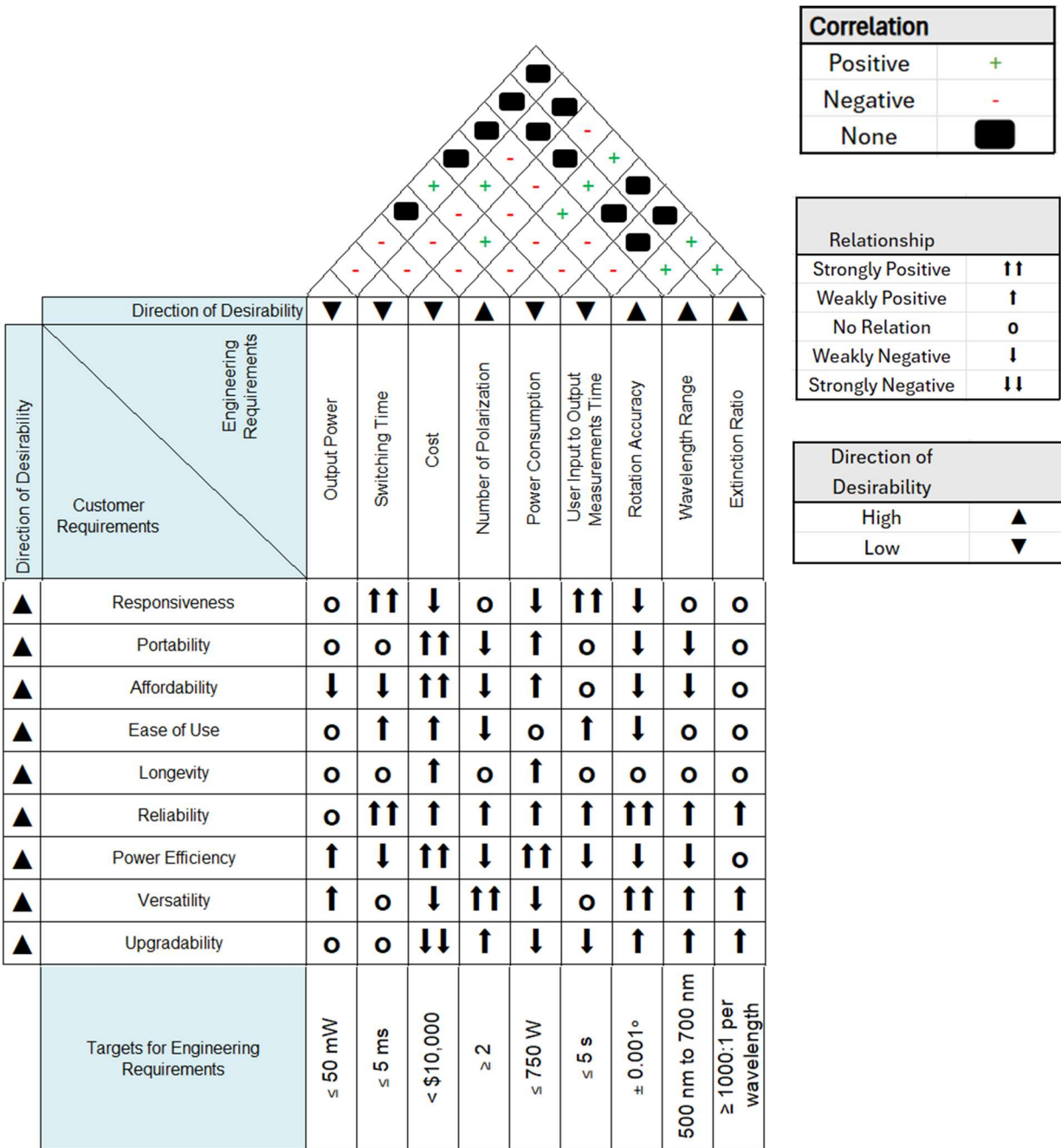


Figure 2.4-4

House of Quality. This figure provides a visual aid of engineering tradeoffs for the project. The left-handed column is the requirements important to the user. The top column indicates product requirements that we may need to make tradeoffs for.

Chapter 3. Research

3.1 Technologies

3.1.1 Light Sources

3.1.1.1 LED VS Laser

For our light source there is a choice between using light emitting diodes (LEDs) or using laser light. There are several advantages and disadvantages to either source. We also must consider the needs of our sponsor.

LEDs are a type of semiconductor technology. This device has two different regions known as the N-type and P-type. The N-type portion of this technology contains atoms that contain more valence electrons than the P-type which has more atoms that have less valence electrons. When these two parts combine the valence electrons of the N-type recombine with the holes of the P-type material. When these two combine the high energy electron gives off energy in the form of light. The energy and subsequent color of this light is based on the energy distance between the valence band and the band under it called the conduction band. This makes LEDs an efficient lighting technology because it can be turned on almost instantly unlike incandescent bulbs that need to heat up. Since these diodes only need to pump enough electrons into the N-type material to keep a steady flow of electrons in the valence band on the N-side, they are an energy efficient and fast device (Yam 2005). LEDs naturally have a broad linewidth because the semiconductor material has several thousand atoms that all have their valence bands at slightly different energy levels (Ojeda 1997). This means that as then electrons go from valence band to conduction band there is a bit different amount of energy that each electron must lose depending on the atom's valence band energy. When this effect is combined from several thousand atoms you get LEDs that have very large bandwidths.

Laser diodes work in a similar way to LEDs in the fact that they are also made of an N-type and P-type material. They are also similar in the fact that light gets created when the electrons and holes recombine in their respective material. The differences come from what happens when the light tries to escape the material. In a laser there are two mirrors set up on either side of the semiconductor creating a cavity. In this cavity one photon will get emitted like before, called spontaneous emission. As this photon is travelling through the cavity it will be passing through a gain material. This material amplifies photons as they pass through. To do this it is filled with excited electrons. As the light passes through this material the photons induce the excited electrons to begin to recombine with the holes in the gain material and then release light (Slusher 1999). These photons are an exact copy of the original passing photon in terms of wavelength, direction of propagation, and polarization. This process is called stimulated emission. These amplified photons will then reflect off one of the mirrors that create the cavity and make another trip through the gain material which amplifies them again. To release the light from the cavity one of the mirrors is not fully reflective. This means that some of the light escapes as it hits this mirror. Light moves so fast that it hits this slightly transparent mirror many times and effectively escapes after several trips, but because it has amplified so many times and there are so many photons being created there is a steady stream of light. To ensure this system works the user just needs to make sure that the gain material is constantly having a steady flow of electrons in its valence band. Since lasers use stimulated emission as their source of light the light that comes out of them have a very narrow linewidth in terms of wavelength. They also are a coherent source (Ojeda 1997).

Lasers come with several pros and cons. The pros of using a laser light source are that the light is mostly collimated. Laser lights being highly directional is mostly collimated and do not diverge much. This means we would not have to use lenses to collimate the light that comes out of the laser before it goes into our system. This would save us money. Also, we could use specialty lasers called fiber lasers that use doped fiber as a gain medium. This would mean our laser light is already coupled into fiber making the light much easier to work with. Laser light is also monochromatic, with a very small bandwidth (Ojeda 1997). This property of the light would make calculating the angle needed for our motor to turn much easier. Each wavelength of light will need a different incident angle to achieve the correct polarization. Using a light source that is monochromatic makes this calculation much easier as we will not have to calculate the angle for an entire range of wavelengths but only one. The cons of using laser light are also lengthy. Firstly, high quality lasers and drivers are extremely expensive. We are trying to make our system cheaper than others so including a light source that is expensive is a problem. Next, because most light is not monochromatic and collimated our system would not be as general if we use a laser light source. If our product goes into the market and has only been using monochromatic sources, it will not be adaptable for sources with a broad wavelength range. This would force the product to be used solely with lasers and could not be adapted to LEDs unless the software was changed. Lasers are also high-power consumers. This raises the cost of using the product as it costs more power than if we used the alternative light source.

LEDs solve many of the problems that are created by lasers. Firstly, LEDs are inexpensive. This drastically cuts down on the cost of our system by using LEDs instead of laser light sources. LEDs are often broadband sources. One of our goals is to use the product with a light source that has a bandwidth of 30nm. This is much easier to accomplish than laser light because LEDs have a naturally broader bandwidth than lasers. Instead of using multiple lasers to achieve this goal we could use one LED. To achieve a narrower bandwidth, we can use a bandpass filter. LEDs also use much less power than lasers, allowing us to cut cost of operation. One of the drawbacks of LEDs is that the light is not collimated. This ensures that we need to buy extra lenses to collimate the light. The cost of lenses does not outweigh the cost of lasers and their drivers. Also, using LEDs means we need to purchase a narrow bandpass filter if we want to test our device with singular wavelengths. This can significantly hurt our budget because extremely narrow bandpass filters come at a high price.

Table 3.1-1 Source Type Comparison

Criteria	Laser	LED
Low Power Consumption		X
Ease of Use	X	
Cost		X
30nm Bandwidth		X

3.1.1.2 Why LED and Laser

We have chosen to use both lasers and LEDs. If we use these technologies properly we can highlight the strengths of each and lessen their disadvantages. Cheaper laser diodes will allow for ease of use of the laser with a minimal cost. We will use these sources to test our visible spectrum range since this source has an extremely narrow bandwidth. We will then use a single higher power LED to test if our system works for a broadband source. When we are looking for specific LEDs we will be looking for:

- Low Cost
- High Power- at least 20mW
- Broad Bandwidth- at least 30nm, not more than 50nm

When we are looking for a laser, we are looking for:

- Low Cost
- Narrow Bandwidth – 10nm
- Wavelengths – Entire Visible Spectrum
- Ease of Use

3.1.1.3 599 SMD LED

These types of LEDs are small and packaged and come from Dialight. They are made of mostly indium gallium nitride. There are a couple of options with the 599 series that include single-color LEDs, bicolor microLEDs, and single pixel LEDs. These LEDs have a small full width half max (FWHM) wavelength, normally around 15nm. They come in several different colors in the visible spectrum from red to blue.

3.1.1.4 MWUVL1

This type of LED is from ThorLabs and emits white light. It is mounted on a heat sink to keep a constant temperature and ensure no optical losses. The emission spectrum peaks at 400nm but also has a large portion of the spectrum in the 600nm area. This would mean for this diode we would need a bandpass filter to narrow our spectrum to around 30nm bandwidth. It outputs 338mW of typical power so the losses from filtering will not affect our goal of a high-power system.

3.1.1.5 LED560L

This type of LED also comes from ThorLabs and is the simplest kind of LED. It is not mounted. It operates at a single wavelength with a bandwidth of 11nm. It has an optical power of 0.15mW. It has a current input max of 50mA and a large operating temperature of less than 80 degrees Celsius.

3.1.1.6 M470L5 ThorLabs

This is a blue LED similar to the MWUVL1 in the fact that it is sold with a cooling mount of the same size as the previous LED giving it a small volume. It has a central wavelength of 470nm and a bandwidth of 28nm. Since this bandwidth aligns with our 30nm bandwidth goal we would not need to use a chromatic filter to limit the LEDs bandwidth. There is an 80 degree full angle. It also has a 1161.7mW output power. It has a forward voltage of 3.8 V and an electrical power of 3820mW.

3.1.1.7 Why M470L5 ThorLabs

Table 3.1-2 LED Comparison

Features	599 SMD LED Dialight	MWUVL1 ThorLabs	LED560L ThorLabs	M470L5 ThorLabs
Peak Wavelength	587 nm	406 nm	562 nm	470 nm
Bandwidth	15 nm	300 nm	11 nm	28 nm
Output Power	3 mW	235 mW	0.15 mW	1161.7 mW
Electrical Power	42 mW	790 mW	46 mW	3820 mW
Forward Voltage	2.1 V	6.3 V	2.3 V	3.8 V
Cost	\$0.53	\$191.10	\$19.48	\$261.20

For our project we would like to use the LED for two reasons. First being we need to show that our system can handle a broadband source. This means for our first consideration we need a source that has a broad wavelength range. We would like to show that our system can handle a maximum of 30nm. The Dialight and 560L from Thorlabs come far under this requirement. This makes these two LEDs hard to use for this proof of concept. The MWUVL1 has a very large wavelength range, much larger than we are aiming for with our project. This means if we would like to use this diode we would need to place a bandpass filter in front of it. Since we are trying to minimize our costs to stay in budget, we would like to not add any other expenses like a chromatic bandpass filter. The 470L just under the 30nm bandwidth but effectively has the exact bandwidth we need without using any kind of filtering.

The next reason for using an LED is because we would like to test our system for higher power devices on the scale of 20mW. For our project we are going to be passing the beams of light through many different components each with their own absorption and reflection coefficients. This means we need a source of high enough power to be able to pass through all these systems and still have enough power to meet these requirements. The 560L and Dialight LEDs already have too little power to meet our requirements without passing through any optical devices. The MWUVL1 LED has enough power by itself, but after passing the light through a bandpass filter a large portion of the light would not pass through. The bandwidth of the LED is so large, and the power is distributed across the bandwidth. This means by cutting this bandwidth by 270 nm will drastically reduce this power. By using the M470L we can maximize the power going through our system because we do not need this bandpass filter and we can use the entire bandwidth of the LED.

While the M470L has the highest cost of all the LEDs it will save us money and achieve more of our goals. It will save us money because we will not have to buy a bandpass filter which can be expensive. Using this LED will also guarantee that we will have the power needed to achieve our goals.

3.1.1.8 TLB-6704 Tunable Diode Laser Newport

This impressive laser is tunable with respect to its wavelength. This specific type is tunable around the 650nm range but other products from Newport of the same line tune through different wavelengths. For example, another diode is tunable around the 790nm range. It offers an impressive switching speed of around 5-10ns. They offer output power ranging from 8mW for the product mentioned to 50mW of the TLB-6716. These lasers come with a driver that controls the

output wavelength and therefore may take up a lot of space within our system. This source however couples into a fiber which makes for very easy use.

3.1.1.9 ThorLabs PL20X

These compact lasers are extremely easy to use. They have a housing that is 11mm in diameter, making it easy to fit into our 30cm x 30cm optical breadboard. These lasers are connected through USB. They have an operating voltage of around 5V and an operating current of around 70mA. The beam diameter is 3mm. These sources are only single wavelength sources and are not tunable meaning we would need to buy more than one to demonstrate that we are able to use our system on the entire visible spectrum. These lasers are also inexpensive because they do not need to be run by a driver so no purchase of a laser driver would be needed.

3.1.1.10 0220-923-00 Coherent Visible Laser

These lasers from coherent are impressive because of their size and are sold by Edmund Optics. The largest of these lasers are 45.1mm in length and 14.8mm in diameter. This impressive size allows these lasers to be fit into any system and are easily small enough for our design. Unfortunately, they also need a power supply. These lasers are quite expensive for their size, being priced from \$200 to \$700 and the power supply being \$70.

3.1.1.11 Why Thorlabs PL20X

Table 3.1-3 Laser Comparison

Features	TLB-6704 Tunable Laser Newport	Thorlabs PL20X	0220-923-00 Edmund Optics
Wavelength	635 nm – 638 nm	635 nm, 520 nm, 405 nm	635 nm
Bandwidth	1 nm	1 nm	5 nm
Diameter	Fiber Diameter	11 mm	14.8 mm
Forward Voltage	100 V	5 V	5 V
Electrical Power	<170 W	0.35 W	0.4 W
Output Power	8 mW	0.9 mW	2 mW
Price	Quote (Related Products \$3,000)	\$146.40 - \$246.67	\$303.03

In our project we are using lasers to show that our system can work for the entire visible spectrum. This means unlike with the LED we do not require a high-power source. This allows us to buy a cheaper, lower power laser if we can test the entire visible spectrum. We chose to do this because high power lasers that can achieve wavelengths across the entire visible spectrum are extremely expensive and out of our budget.

The Newport laser does have a tunable wavelength which would allow us to show how the angle of crystal rotation changes as we change wavelengths. The problem with this laser is that it is extremely expensive. This is expensive because this type of laser is not only hard to build but needs a controller which can accurately change the wavelength of this laser. These controllers are normally large and would not fit inside of our optical breadboard. We would need to only pass the laser into our system using fiber and keep the other parts of the laser outside of the optical

breadboard. This makes this laser hard to transport and prone to accidents. We would like to keep our project as contained in the optical breadboard as possible to increase ease of use.

We chose the Thorlabs laser over the Edmund Optics laser because it is not only cheaper but more form fitting. The Thorlabs laser is not much smaller or cheaper than the Edmund laser but because we would like to increase the ease of use of our system we would like to minimize the size of the laser. Also, the Edmund laser needs a power supply attachment that is \$69 which further increases the price of the laser as opposed to the Thorlabs laser. The Thorlabs laser is easy to use because it is connected to a USB, and it is cheaper than its competitors.

3.1.2 Birefringent Crystals

3.1.2.1 Birefringent Crystals as Waveplates

Using Maxwell's equations with appropriate boundary conditions has enabled the discovery of exact solutions for the phase difference and amplitude shift of incident light. This phenomenon happens due to the nature of birefringence. Anisotropic also known as uniaxial or birefringent materials more aptly materials that have differing refractive indices due to the direction and polarization of the light. This difference in the indices often used as a measure of birefringence causes various polarizations of incoming light to experience myriad phase changes. These changes in phase can shape the polarization of the light. Waveplates come in 3 main types, a quarter-wave plate which shifts the phase by 90° , a 180° phase shift is achieved through implementation of a half – wave plate, and the full wave – plate subsequently is a 360° change. Phase Retardation is given by

$$\delta = \frac{2\pi \cdot \Delta n \cdot d}{\lambda}$$

where $\Delta n = \mathbf{Birefringence}$, $d = \mathbf{Thickness}$, and $\lambda = \mathbf{Wavelength\ of\ light}$

Birefringent crystals can be used in waveplates, electro-optical devices and as converters for high-order laser beams.(Paranin 2016) However they excel at polarization modulation, and polarization based methods are often used to characterize the thickness of the crystal. Generally, when linearly polarized light enters the crystal, it is divided by ordinary and extraordinary refractive indices. Each of the waves interacting with indices travels at its own speed. This difference in speeds creates a change in phase between the two light waves. As seen above the phase difference is not only determined by the Δn it is also influence by the wavelength of the light the thickness of the crystal as well as the angle of incidence. As the light recombines on leaving the crystal the waves undergo coherent interference with one another and reform as a new polarization state. Through this you can achieve elliptical and circular polarization states and of course dictating the angle of linearly polarized light. Furthermore, with the addition of a linear polarizer we will be able to control the output intensity as well. This interference is in the polarization space meaning their vectors create a new polarization state. You can visualize the polarization space through graphical models such as the Poincaré sphere, and Jones Vectors.

3.1.2.2 Quartz Crystal

Quartz Crystal (SiO_2) is a fundamental material that is widely used in electronics and optics. Implementation of Quartz crystal was explored using a MATLAB simulation. In the simulation we tested various thicknesses of the crystal. Keeping in mind the integration necessary onto a mechanical motor, and the timing goal of sub-millisecond switching time. The input light was set at 508 nm responding to a value near center of the visible spectrum and linearly polarized in the vertical direction, in reference to the optical axis. This corresponds to an ordinary refractive index of 1.54822 and an extraordinary index of 1.55746. Starting the simulation with a crystal thickness of 1 cm we get a plot of our output power. This gives us a minimum angle of 0.28° with a target of 0.1° rotation needed for the polarization this means Quartz would need to be a bit thicker to try and get the optimal timing of below 1 millisecond. Any increase in weight would mean greater torque and an increase in vibrations at the point where the motor stops. This implied Quartz may not be one of the better choices if we were looking to not only reduce the minimum angle but also the weight. Using the average density of SiO_2 a value of 2650 kg/m^3 we can calculate a mass of 2.65 grams for the cubic centimeter. If we were to achieve a target of 0.1° minimum rotation, the thickness of Quartz would need to be 2.65 cm. Leaving the other dimensions the same brings us to a mass of 7.0225 g. We also get a plot of our output power. Quartz is a foundational material in optics and to explore this crystal as one of the options to be used in this application was almost pre-determined. However, using our simulation created using Jones matrix calculus in MATLAB, we show which of the crystals will be the better fit.

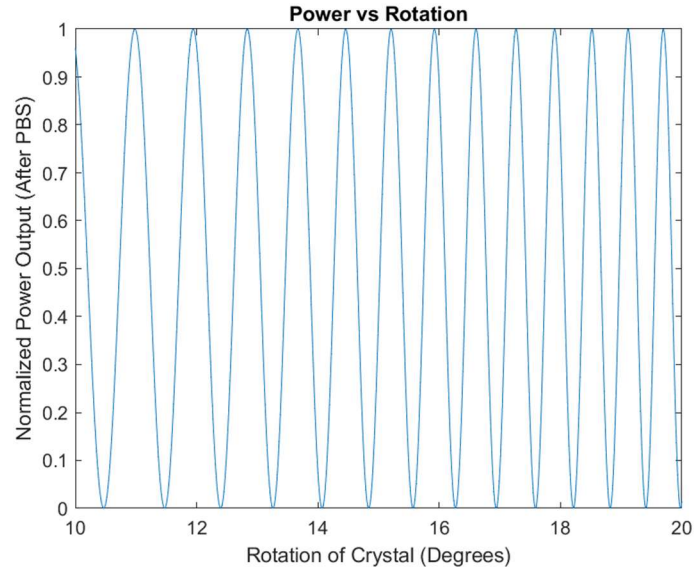


Figure 3.1-2

Plot of normalized power while rotating a quartz crystal with a 1 cm thickness, between 10° – 20° degrees with a step size of 0.01°

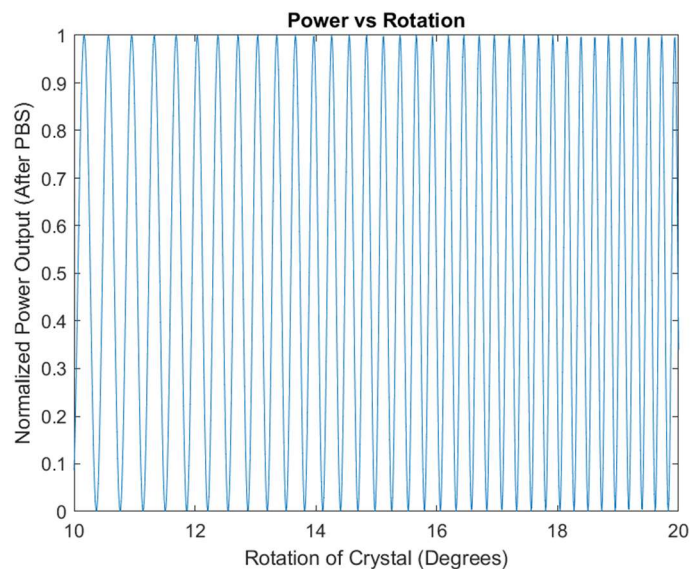


Figure 3.1-1

Plot of Normalized Power while rotating a quartz crystal with a 2.65 cm thickness using a 10° – 20° sweep, with a step size of 0.1°

3.1.2.3 Calcite Crystal

Calcite crystal CaCO_3 is a carbonate and is a particularly common material. Found in limestone its trigonal atomic structure make it uniaxial despite the many forms it can take. We can also see calcite formed with some opacity giving it a white color. We will be using the transparent calcite. This selection will decrease optical losses while passing through the calcite and will help maintain the contrast of intensity on the output. This variety is called “Iceland Spar.” Calcite crystal was first discovered to have birefringent properties by Danish scientist Rasmus Bartholin in 1669. The ordinary refractive index at a wavelength of 508 nm is 1.66527. Conversely the extraordinary refractive index is 1.48596. Using these values, we simulate the normalized output power of the crystal corresponding to a thickness

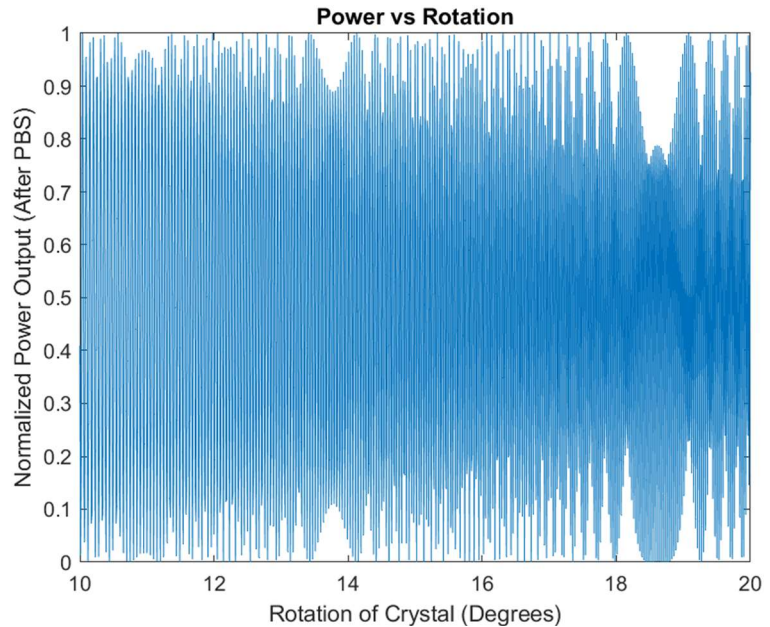


Figure 3.1-4

Plot of normalized power while rotating a calcite crystal with a 1 cm thickness, between 10 – 20 degrees with a step size of 0.01°

of 1 cm. The plot shows erratic and inconsistent power fluctuations with a minimum change required to switch between orthogonal polarizations states to be 0.01°. These values would need a mechanical motor that is outside of the budget range set by ASML. Deciding to go with a thinner crystal to both give us a little bit more room in rotation and to reduce the force put on the motor from stopping and accelerating, minimizing vibrations in the crystal due to those forces. To achieve a target of 0.1° minimum rotation angle, a thickness of 0.125 cm we get a plot of normalized power. Leaving the other dimensions the same, we see a reduction in overall mass too. Calcite has a density of 2710 kg/m³ this means the mass of our crystal would be 0.339 grams, a significant reduction therefore the forces exerted on our motor will be less compared to Quartz. Calcite crystal made a very promising option given more time and a larger

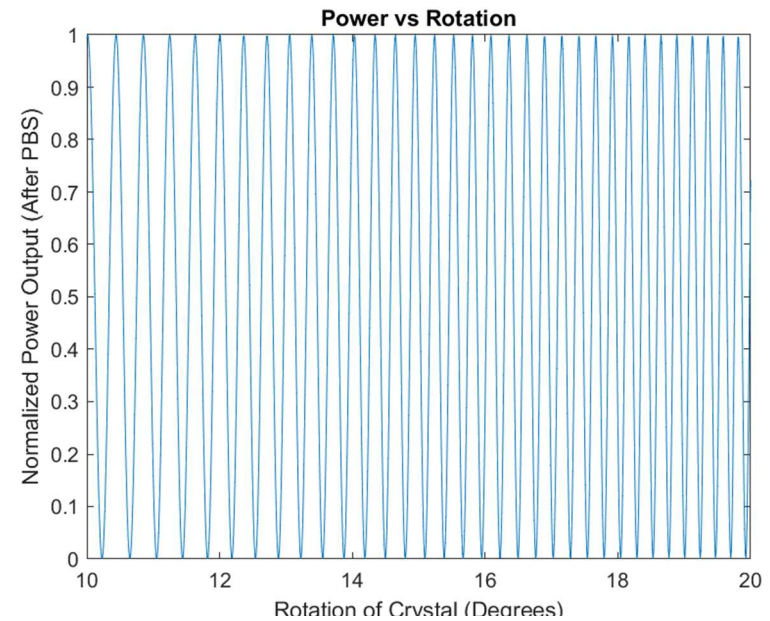


Figure 3.1-3

Plot of normalized power while rotating a quartz crystal with a 1.25 mm thickness, between 10 – 20 degrees with a step size of 0.01°

budget researching and purchasing the right rotation system or even getting one custom designed. It would open up the possibility for even faster devices. To a certain point the speed of the mechanics switching repeatedly may cause issues if it resonates with the device, this will cause the smallest vibrations to cascade into catastrophic failure.

3.1.2.4 α - BBO

Alpha Barium Borate or BaB_2O_4 is an inorganic compound that is a common optical material. It also has a Beta and Gamma structure, both of which have better use during nonlinear optics as they facilitate spontaneous parametric down conversion. α - BBO is used in many polarization-based devices such as Glan - Taylor prisms, beam splitters and has replaced other uniaxial crystals including lithium niobate, calcite and titanium dioxide. To check the crystal, we found known values of the ordinary and extraordinary refractive indices at a wavelength of 532 nm. With values of 1.6776 and 1.5534 respectively. Using these values in the MATLAB program we created. Starting out a thickness of 1 cm, we obtain a Power vs. Rotation plot. Showing consistent results supports the idea that with greater birefringence you have a greater change in polarization with rotation of the crystal. With a 1 cm thick crystal the minimum rotation needed to achieve orthogonal polarization states is 0.023° . This ends up being a little bigger than the minimum angle needed for calcite. This corresponds to a crystal that needs to be a little thicker to achieve our target of 0.1° for the minimum rotation needed. A thickness of 0.23 cm is what is required to hit the target minimum rotation. Once again assuming the other dimensions of the crystal stay the

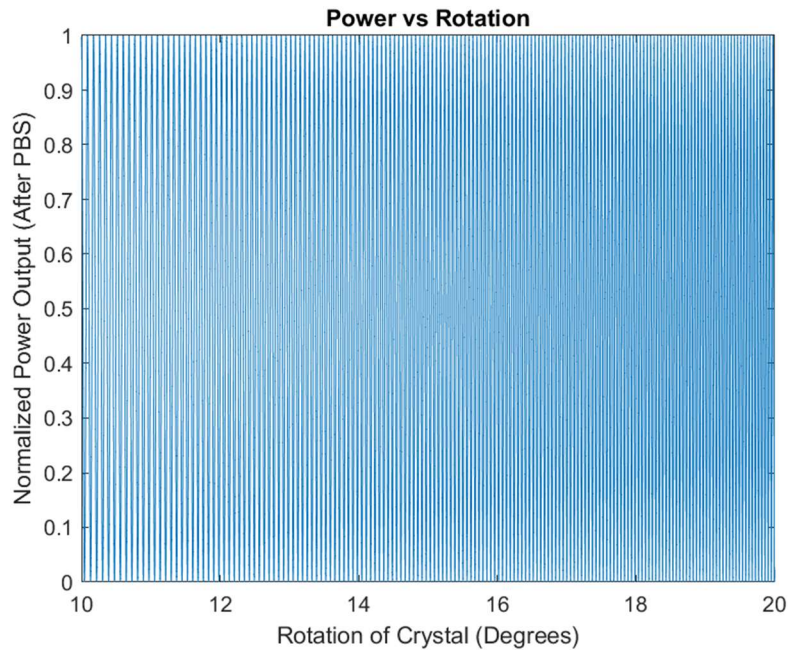


Figure 3.1-6

Plot of normalized power while rotating a α - BBO crystal with a 1 cm thickness, between 10 - 20 degrees with a step size of 0.01°

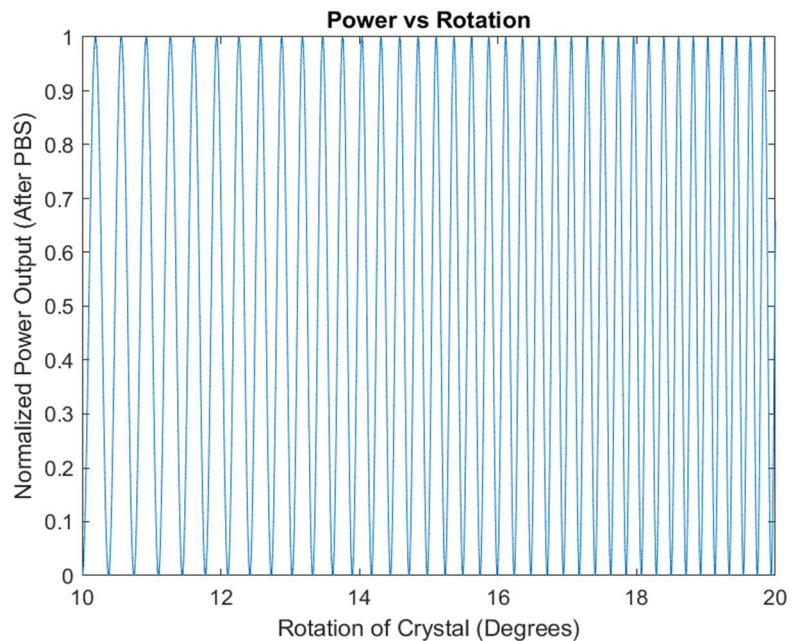


Figure 3.1-5

Plot of normalized power while rotating a α - BBO crystal with a 2.3 mm thickness, between 10 - 20 degrees with a step size of 0.01°

same and using the density of Alpha barium borate. 3.85 g/cm^3 this gives us an overall mass of crystal to be 0.8855 grams. Alpha Barium Borate is a fantastic crystal used in optical components and will be used as our second crystal that will be “unknown” to the system. However, for an optimal prototype design in this specific application case it falls short of calcite due to its slightly lower birefringence. The following Power vs Rotation plot corresponds to the thickness of 0.230 cm. These results match the previous targets in the other crystals within a margin error.

3.1.2.5 Non – Linear Crystals as Wave plates

Non – linear Crystals are optical elements that enable non – linear processes such as second – harmonic generation, sum/difference frequency generation and optical parametric oscillations. These effects change more than just the polarization of light. High birefringence is not a byproduct of engineering these crystals but a design target. Birefringence is essential to non-linear crystal as this property allows engineers to make use of a technique known as phase matching. Phase matching ensures that the light waves interact with each other, by maintaining a constant phase relationship energy transfer can be maximized.

Second harmonic generation (SHG) is a process where two photons of matching frequency are absorbed by a material, then subsequently a photon of twice the energy is emitted. A common example of this is the use of KTP to produce 532 nm light. This crystal takes in 1064 nm electro – magnetic radiation and through the absorption of two photons can emit radiation at half the wavelength of the incoming light. Note that this comes with a loss of power as some energy is still lost to phonons. Phonons are quanta of energy that are used to represent the vibrational energy absorption and distribution throughout a molecular structure. Second, harmonic generation will not be a helpful process in our application. Looking to finely control polarization states without any conversion of frequency in our light would be ideal. Trying to compensate for this process would require much higher power. In general, these crystals can be more expensive and have higher absorption coefficients as well. Absorption coefficients are determined based on the material you are looking at and can be used to determine the optical power losses with a given path length of the material.

Sum frequency generation while like SHG in that it takes in two photons and emits one. It interestingly does not require the photons to have the same frequency. These photons of varying frequency will join and produce a photon with a frequency corresponding to the sum of the input frequencies of the light. Difference frequency generation is the inverse process. Where the crystal takes in a singular photon and depending upon the properties, will emit two photons with reduced power and of different frequencies. Some of the applications of these processes include microscopy, spectroscopy, tunable light sources, and terahertz generation. These non – linear processes have many great uses and are a great example of the astounding things nature is capable of under the right circumstances.

3.1.2.6 Other Explored Crystals

A couple of the other crystal compounds that we investigated before settling upon calcite were TiO_2 as well as β – BBO Beta Barium Borate. Both of these exhibit some non-linear effects. TiO_2 is a compound that exhibits limited third – order effects such as self – phase modulation or the Kerr effect. In its bulk form TiO_2 exhibits minimal birefringence. However, a higher birefringence can be manufactured by engineering a grating or other microstructures using the material. Due to timeline and financial constraints, we opted for another route.

For the β – BBO we we’re already looking into α – BBO as a possible option, so to continue onto the other members of the family to see their strengths and weaknesses was only natural. β – BBO is a very commonly used non – liner crystal with a broad transparency range 200 nm – 3500 nm and an exceptional damage threshold which corresponds to 10 GW/cm². This crystal can be used in applications that require processes from SHG to even Fifth Harmonic Generation. This crystal is also utilized in optical parametric oscillators and electro-optical modulators. While although all of these applications are impressive. The high demand for this crystal and the limited power throughput, to reduce the nonlinear effects, proved this crystal to be an inconvenient solution to our problem.

3.1.2.7 Sellmeier Equations

Sellmeier equations are used to describe the wavelength dependent refractive indices of optical mediums. Each optical medium has it’s own formula that is dependent upon the material properties, many crystal production companies will include the refractive index at a few wavelengths as well as the Sellmeier formula for that material. During our research into finding calcite and α – BBO crystals to be used in our setup we documented the formulas for these materials to be implemented into our simulation, these formulas will allow us to see exactly how the refractive index of these materials will change over as broad of a wavelength range as we want. For both materials the Sellmeier equation we used, was provided by [Newlight Optical](#). Due to the birefringent nature of these materials, there is an equation for both the ordinary and extraordinary indices. **Calcite:** $n_o^2 = 2.69705 + \frac{0.0192064}{(\lambda^2 - 0.01820)} - 0.0151624\lambda^2$, and $n_e^2 = 2.18438 + \frac{0.0087309}{(\lambda^2 - 0.01018)} - 0.0024411\lambda^2$ for **α – BBO:** $n_o^2 = 2.67579 + \frac{0.02099}{(\lambda^2 - 0.0470)} - 0.00528\lambda^2$, and $n_e^2 = 2.31197 + \frac{0.01184}{(\lambda^2 - 0.01607)} - 0.00400\lambda^2$ and for **Quartz:** $n_o^2 = 2.3573 - 0.01170\lambda^2 + \frac{0.01054}{\lambda^2} + \frac{1.3414 \cdot 10^{-4}}{\lambda^4} - \frac{4.4537 \cdot 10^{-7}}{\lambda^6} + \frac{5.9236 \cdot 10^{-8}}{\lambda^8}$, and $n_e^2 = 2.3849 - 0.01259\lambda^2 + \frac{0.01079}{\lambda^2} + \frac{1.6518 \cdot 10^{-4}}{\lambda^4} - \frac{1.9474 \cdot 10^{-7}}{\lambda^6} + \frac{9.3648 \cdot 10^{-8}}{\lambda^8}$ These equations using our input wavelength range are used to create arrays for each of the indices, then using these refractive index arrays we solve for the output electric field in the same way you would for the individual wavelength. The outputs for a broadband source can be found in the following figures. Based on the equations and the limited range of wavelengths only as broad as 30 nm the refractive index change is negligible within the visible regime.

3.1.3 Motors

3.1.3.1 Stepper Motor

The benefits of a stepper motor are its precise positioning as stepper motors can move in exact steps based on the motor step angle ([HowEngineeringWorks.com](#)). Stepper motors can have a small step angle as small as 0.9 degrees and can go even smaller through the method of micro-stepping (dividing up the motor step angle to smaller angle increments). Another benefit of the stepper motor is its simple control due to being open-loop feedback. Steeper motor rotates based on the electric pulses sent by the motor driver with the number of pulses telling the stepper motor how many angle steps to take to reach the desired angle ([HowEngineeringWorks.com](#)). An additional advantage of the stepper motor is its holding torque. Stepper motors can remain in position without drifting as the mechanism of the stepper motor is able to produce holding torque to stop the motor in place ([HowEngineeringWorks.com](#)). Lastly, stepper motors are reliable and

durable due to the motors only having a few moving parts which leads to less maintenance, less wearing, and a long operational life (HowEngineeringWorks.com).

The disadvantages of a stepper motor are its limited speed. Stepper motors typically have a maximum speed of 3,000 rpm and when the motors start running at high speeds, the overall torque decreases which can lead to the stepper motors missing steps, decreasing the overall accuracy of the system (HowEngineeringWorks.com). Another disadvantage of the stepper motor is its power efficiency as stepper motor requires a full current draw for each step it takes which leads to higher energy consumption and heat generation (HowEngineeringWorks.com). This also leads to an overheating problem as long period of uses with the stepper motor can cause excess heat production which can damage the motor if there are not proper cooling procedures in place (HowEngineeringWorks.com). An additional disadvantage of the stepper motor is its vibration and noise as it rotates, which can impact the crystal as the vibration may resonate with the crystal, impacting our readings.

If a stepper motor is chosen to be used in our system, micro-stepping will need to be done to ensure the motor can have a maximum step angle of 0.1 degrees. Micro-stepping can also help with the vibration and noise issue to prevent the crystal from resonating and interfering with the data. Another benefit is the holding torque of the stepper motor which would help with stopping the motor and holding the crystal in place to be able to read the desired measurements we want from our system. However, a drawback of the stepper motor is its open-loop feedback system which would become a problem if the stepper motor skipped steps. This becomes an increasing issue as the stepper motor will need to go at high speed, and the accuracy of the system may not be met. Another problem is the overall torque of the system. As the stepper motor increase speed, the overall torque decreases which may become a problem as the stepper motor may not be able to produce the necessary torque needed to rotate with the crystal load within the necessary switching time.

3.1.3.2 Servo Motor

The benefits of a servo motor are its precision control due to having a closed-loop feedback system that allows precise control over the motor's position, speed, and torque (Retekdrones). This will permit accurate position with the motor rotation along with consistent speed and torque throughout the motor usage. Another benefit of the servo motor is its speed range as a servo motor can reach speeds upwards to 6,000 rpm. Not only can a servo motor reach such high speeds, the torque of the servo motor also remains consistent no matter what speed the servo motor goes. This permits more load flexibility with the overall motor system as the mass of the load can be changed and the servo motor would be able to handle this different load mass due to its consistent torque (Retekdrones). Servo motors are also energy efficient as they only consumed the needed power for the servo motor to rotate at its necessary speed for the desired rotational movement (Retekdrones).

The disadvantage of a servo motor is its complexity. Since a servo motor is a closed-loop feedback system, tuning is needed to ensure that the feedback system of the servo motor is working properly. This means that the person tuning the servo motor needs to have a deep understanding of control theory to tune the various parameters needed for the feedback device to work properly (Zhou). Another disadvantage of a servo motor is its cost. Due to being a closed-loop feedback system, the servo motor will have a higher complex control system that requires extra equipment such as an encoder and possibly a special controller for the system to work properly as intended (Retekdrones). Another drawback of the servo motor is the maintenance upkeep. The servo motor

has a lot more moving parts that needs to be inspected and maintained to ensure proper functionality of the servo motor (Retekdrones).

If a servo motor is chosen to be used in our system, the closed-loop feedback system will be beneficial to ensure that the servo motor is rotating 0.1 degrees as per the requirements. The load flexibility of the servo motor will also be helpful with being able to switch the crystals out as the change in the load would not significantly impact the performance of the servo motor. However, due to the complexity of the control system of the servo motor, it could possibly mean an increase in the workload for the team to configure the feedback system of the servo motor to ensure the 0.1 degrees movement in 1 millisecond switching time is met. Another concern with choosing to use a servo motor would be the cost of the servo motor due to needing an encoder, which could be a possible concern for the budget of the project.

3.1.3.3 Brushless DC Motor

The benefit of a brushless DC motor is its efficiency. Since the brushless DC motor does not have a brush in its motor, this decreases the overall friction in the system between the moving parts of a motor (Modar Motor). This overall decrease in friction leads to a more efficient motor system. Another benefit of the brushless DC motor is its low maintenance cost and the longevity of the system. The lack of a brush in the motor means less parts are rubbing against each other which leads to less wear in the motor system (Modar Motor). An advantage of the brushless DC motor is its speed control. A brushless DC motor has a speed control that can go up to 60,000 rpm without overheating which makes it effective in situations where precise accuracy is needed (Mechtex). Another advantage of the brushless DC motor is its low noise due to the lack of a brush in the motor, the motor rotates quietly with minimal vibrations (Modar Motor).

The disadvantage of a brushless DC motor is its cost. Due to the speed control of the motor, the motor requires hall sensors and encoders to assist with the speed control of the motor to ensure proper operation (Mechtex). Another disadvantage of the brushless DC motor is its complexity. Since the motor utilize a closed-loop feedback system, proper calibration needs to be conducted to ensure the motor system is working properly (Modar Motor). A drawback of using a brushless DC motor is its heat dissipation. The motor dissipation of heat increases as the speed of the motor increases which can lead to performance issues with the overall power efficiency of the motor system and potential damage to the components of the motor (Mechtex).

If a brushless DC motor is chosen to be used in our system, the low vibrations of the motor system would help ensure that the motor does not resonate with the crystal which can impact the output measurement of this system. The speed control of the brushless DC motor would also help with ensuring that the motor rotated 0.1 degrees with a switching time of 1 millisecond. However, the drawback to this is that the brushless DC motor does not have a position feedback system and thus, the accuracy of the position moved cannot be verified by the motor system. Another disadvantage with using a brushless DC motor is its complexity with having to configure the speed control of the motor which can lead to an increased workload for the team.

3.1.3.4 Galvanometer Motor

The benefits of a galvanometer motor are its precise position control. The galvanometer motor utilizes a closed-loop feedback system in which the sensors in the galvanometer motor sends the positioning information back to the controller for the controller to send information to correct the positioning errors to ensure accurate positioning of the motor (Artizono). Another benefit of the

galvanometer motor is its small step angle as the galvanometer motor can have a step angle as small as a single microradian (Sintec Optronics). Another advantage of the galvanometer motor is its step response time. The galvanometer motor has a small step response time in the sub-millisecond due to having a large bandwidth in its closed-loop feedback system that can be as high as several kilohertz, minimizing the settling time of the motor and ensuring proper time for the position control to function (Artizono , Sintec Optronics). An advantage of the galvanometer motor is its scanning field as the galvanometer motor has a scanning range up to 20 degrees (Artizono).

The disadvantage of a galvanometer motor is its complexity. Due to the galvanometer motor being a closed-loop feedback system, the galvanometer motor utilizes a Proportional-Integral-Derivative control system to minimize the positional error which means the person tuning the system needs to have a deep understanding of control theory (Sintec Optronics). Another drawback of the galvanometer motor is its cost. Since the galvanometer motor is a closed-loop feedback system, additional equipment needs to be brought, such as sensors or an integral position detector, for the controller to be able to receive information about the motor position to correct these positional errors (Sintec Optronics) A disadvantage of the galvanometer motor is its maintenance as the galvanometer motor may need periodic calibration to ensure the motor system is working properly as intended and parts may need to be replaced as constant use may lead to wear on the motor parts (Artizono).

If a galvanometer motor is chosen to be used in our system, the precise position control would be helpful to ensure that the motor is rotating 0.1 degrees with minimal positional error. The small resolution angle for the step size of the galvanometer motor would also be helpful with rotating the crystal in the small step angle to hit the desired polarization that the user may want. The large bandwidth of the closed-loop feedback system of the galvanometer motor would be helpful with ensuring that the 1 millisecond switching time is achieved for the motor system. However, an issue with using the galvanometer motor is its complexity as configuration of the closed-loop feedback system would be necessary to ensure the galvanometer motor is working properly as intended but this can lead to an increased workload for the team. Another issue would be the cost of the galvanometer motor due to the extra equipment the motor system would need to meet the requirements of the project which could lead to a strain in the budget of the project.

Table 3.1-4 Motor Type Comparison

Feature	Stepper Motor	Servo Motor	Brushless DC Motor	Galvanometer Motor
Step Angle (Degrees)	0.9 / 0.1125 (with micro stepping)	0.088 (with 12 bits encoder)	N/A	0.000057
Feedback System	Open-Loop	Closed-Loop	Closed-Loop	Closed-Loop
Control System	N/A	Position, Speed, Torque	Speed, Torque	Position
Energy Efficiency	High Power Consumption	Low Power Consumption	Medium Power Consumption	Low Power Consumption
Heat Generation	High	Low	High	Low
Cost	Small: \$5 - \$50	Small: \$5 - \$50	Small: \$15 - \$50	Small: \$50 - \$600

	Medium: \$20 - \$150 Large: \$50 - \$1,500+	Medium: \$100 - \$2,000 High Torque: \$1,000 - \$8,000	Mid-Range: \$150 - \$1,000 High Torque: \$1,000 - \$7,000	High Speed: \$300 - \$4,500 Industrial: \$3,500 - \$10,000+
Suitability for Motor System	Micro stepping needed for degree movement, Torque concerns with micro stepping	Position control for 0.1 degree movement, Speed control to reach 1 ms switching time, Torque control to rotate motor	Speed control to reach 1 ms switching time, Torque control to rotate motor, Additional sensor/encoder needed for position control	Position control for 0.1 degree movement

3.1.3.5 Why Galvanometer Motor?

The galvanometer motor was chosen as the motor for our motor system. The galvanometer motor was chosen for its small step angle which will be helpful in rotating the crystal to get the desired polarization for our system. The closed-loop feedback system of the galvanometer motor will ensure that the motor is rotating to the desired position. The galvanometer motor is also known for its fast-switching time which will ensure that the motor system can reach the required switching time of 1 millisecond.

3.1.3.6 SCANLAB's dynAXIS

The SCANLAB's dynAXIS series is a series of galvanometer motor that utilizes a precision ball bearing to reduce friction and heat to ensure the motor is backlash free. Typically, motor that utilizes a precision ball bearing in their system has the benefit of increasing motor lifespan, better load handling, and improved motor efficiency and reliability (Lumi Manufacturing Technology). These benefits in the precision ball bearing are reflected in the SCAANLAB's claims on their series of galvanometer motors to have high resolution, good repeatability, low drift, and fast acceleration with high accuracy. However, SCANLAB does not provide a datasheet for their product unless contacted through their website. Thus, the exact information behind these claims does not have quantitative data that can be utilized to be compared with other galvanometer motor brands.

3.1.3.7 Novanta 6210K

The Novanta 6210K is a single axis closed loop galvanometer motor scanner. There are two keys aspects of the Novanta 6210K that makes it stand out from its competitors, its combination of moving magnet actuator technology and its special position detector technology that the company claims are only available from them. The benefits of the moving magnet actuator technology are that it is durable due to having fewer moving parts, better thermal management system as water cooling can be utilized, and can bring down the overall cost since a position management system is not needed to control the current of the moving magnet actuator (Magnetic Innovations).

Novanta utilizes a PD (Proportional-Derivative) system with optical sensors and encoders to determine the positioning of the motor and to make any needed corrections which has the serve the company well as the motor can handle various load sizes as mirrors on the galvanometer motor can be as small as 3 mm to as large as 100 mm (Tedford, Berke et al.).

3.1.3.8 ThorLabs SS30Y-AG 1D Galvanometer

ThorLabs SS30Y-AG 1D Galvanometer motor is a moving magnet galvanometer motor that utilizes a cross-flexure pivot design. The cross-flexure pivot design is made up of three parts: the flexure, the core (or inner housing), and the mounting (or the outer housing) in which the flexure in an X shape is inside the inner housing and is meant to be flexible along one side to control the direction of the outer housing which would determine the motor angle (Seelig). The benefits of utilizing a cross-flexure pivot design is its precise motor movement with little to no friction wear on the motor system which would help with the longevity and the maintenance of the motor system (Peterson, Hardin et al.).

Table 3.1-5 Galvanometer Motor Comparison

Features	SCANLAB's dyn <i>AXIS</i>	Novanta 6210K Galvonometer	ThorLabs Cross-Flexure 1D Galvanometer
Cost	Quote	Quote	\$3,819.90
Lead Time	4 Months	6 Months	Available Now
Small Step Angle Response	Data Sheet Unavailable	100 μ s – 200 μ s	150 μ s
Repeatability	Data Sheet Unavailable	8 μ rad	< 10 μ rad

3.1.3.9 Why ThorLabs Cross-Flexure 1D Galvanometer?

The SS30Y-AG was one of two galvanometers that made the final cut, the other galvo being the the Noavanta 6210K, both have similar specifications with the key factor being repeatability. Repeatability of a galvanometer is the maximum deviation from the target position over repeated movements (IntelLiDrives Inc. Staff). Another key feature of this motor is the cross-flexure technology it employs, rather than other ball bearing galvos, which would improve the stability during scanning motion in small angle applications to achieve higher repeatability. With the ThorLabs motor achieving repeatability below 10 μ rads which keeps us below the margin of error needed for the chosen position, as well as claims of lifetimes in the billions of operating hours, under proper conditions and a small angle response time of about 1.2 ms for a 0.45° angle. Which gets us extremely close to our target, with a chosen target of around 0.1° we were likely to meet our timing goals. The Novanta motor actually had slightly improved specs. When it came to repeatability their motor boasted an even better repeatability of 8 μ rads, with a comparable lifetime and an easier out of the box assembly, as well as an operating software to easily program and control the motor. The 6210K from Noavanta was our first choice. However, after contacting them regarding our needs and how they could best be met. Noavanta gave us a 24-week lead time. This

conflicted with our timeline and was what ultimately led us to choose a more readily available solution of the ThorLabs SS30Y-AG 1D Galvanometer motor.

3.1.4 Motor Driver

Motor drivers are an important part of the motor system since the motor driver plays an essential role in taking the motor controller's low power command signals and converting them into high power voltage and current to be delivered to the motor for the motor to rotate to the desired position (McKay). The motor driver also plays a role in the control system of the closed-loop feedback system of the motor. The motor driver receives the encoder signal on the positioning error and either sends this signal back to its own control loop to correct the error or sends the signal to the motor controller for the controller to determine the best course of action to fix the error (McKay). It is essential to choose a motor driver that is compatible with the chosen galvanometer motor as choosing the wrong motor driver can impact the performance, efficiency, and reliability of the motor system which can prevent us from meeting the requirements of this project (FlexPCB).

The Class 1 Servo Amplifier for QS Series Galvo Scanners was chosen as the motor driver for our project since the chosen galvanometer motor for our project automatically comes with its own motor driver. The motor driver that comes with the chosen galvanometer motor is a Position, Integral, and Differential (PID) servo amplifier that has been factory tuned to be compatible with the chosen galvanometer motor. Utilizing the motor driver that comes with the chosen galvanometer motor instead of choosing our own motor driver to use will ensure that there is no compatibility issue between the motor and the motor driver along with decreasing the workload of the project as the PID settings of the motor driver has already been configured to work best with the galvanometer motor. Therefore, for the best performance of the motor, the motor driver that comes with the chosen galvanometer motor will be utilized in our project.

3.1.5 High Level Motor Controller

3.1.5.1 Computer

The computer can be used as the high level motor controller through hosting software that converts the user's command to digital marking data that holds the information needed for motor rotational movement (Google Gemini 2025). This digital marking data then gets sent to the interface card or galvo controller card to convert the digital position commands into analog voltage signals (Google Gemini 2025). The galvo controller card then sends this information to the motor driver of the system in which the driver amplifies the signals to drive the motor based on the received information (Artizono , Google Gemini 2025). The motor's sensors sense the position of the motor and sends this information back to the computer for the computer to decide on the best way to correct this error and sends this correction back to the interface card in which it goes through the whole process again (Artizono).

3.1.5.2 Microcontroller

The microcontroller can be used as the motor controller through generating the digital position commands for the motor rotational movement. These digital position commands are then sent to an external Digital to Analog Converter (DAC) for the digital position commands to be converted into analog signals (DeltaFlo , Google Gemini 2025). The motor driver expects a command input range from -5 Volts to +5 Volts but due to the microcontroller only being able to output a unipolar digital signal, the converted analog signals need to be sent through an inverting operational

amplifier (op-amp) to also get the negative range of the analog signals (DeltaFlo , Google Gemini 2025). Then both the positive and negative range of the analog signals gets sent to the motor driver in which the motor driver will then amplify the signals to drive the motor based on the received information (DeltaFlo , Google Gemini 2025). The motor’s sensors sense the position of the motor and sends this information back to the microcontroller in which the microcontroller decides on the best way to correct the positional errors and sends this correction to the DAC, starting the whole process again (Google Gemini 2025)

Table 3.1-6 High Level Motor Controller Comparison

Specification	Computer	Microcontroller
External Technology	Galvo Controller Card	Digital to Analog Converter
Software	Company Recommended Software	Arduino Libraries
Energy Efficiency	Low Power Consumption	Low Power Consumption
Cost	Computer: N/A (Personal Laptop) Galvo Controller Card: \$300 - \$750	Microcontroller: \$4 - \$35 DAC: \$5 - \$25

3.1.5.3 Why Computer?

Computer was chosen as the motor controller for our motor system due to its software capabilities. Utilizing the company recommended software from the galvo controller card chosen would help the workload of the team as the software would permit us to enter the position of the motor desired based on the user’s chosen polarization. On the other hand, a drawback of choosing the microcontroller would mean more DIY integration and coding which could lead to a greater workload for the team (Google Gemini 2025). A drawback to utilizing the computer as the motor controller is the overall cost to the budget. Using the microcontroller instead would help minimize the increase in cost and ensure we stay in budget. However, the workload benefits from choosing the computer were worth the cost that it would add to the budget in comparison to the low cost of the microcontroller but could potentially increase workload for the team.

3.1.5.4 Data Acquisition Card (DAQ)

The DAQ card was chosen as the interface card for the motor system. The reason the DAQ card was chosen was due to the chosen galvanometer motor’s company (Thorlabs) recommending the usage of the DAQ card with the galvanometer motor for more complex scanning patterns (Thorlabs). The purpose of a DAQ card is to receive analog signal from external equipment such as sensors for the computer to process and utilize the information (Masood). The DAQ card is also capable of outputting analog signals based on the data the computer wants to transfer to other external equipment (CDN Newswire and LabJack Corporation). The DAQ card can receive data from external equipment for the computer to analyze and utilize is due to the DAQ card having an Analog to Digital Converter (ADC) within its system (Masood). In turn, the DAQ card is able to transmit the data the computer wants to send to the other external equipment in the system is due to the DAQ card having a DAC within its own system (CDN Newswire and LabJack Corporation).

Table 3.1-7 DAQ Card Comparison

Features	USB-6002	PCIE-1812-B	MCC USB-160G
Analog Output Channel	2 Channels	2 Channels	2 Channels
Maximum Sample Rate	50,000 Samples per Second	250,000 Samples per Second	500,000 Samples per Second
Analog Input Resolution	16 bits	16 bits	16 bits
Maximum Update Rate	5,000 Samples per Second	3,000,000 Samples per Second	500,000 Samples per Second
Analog Output Voltage	±10 V	±10 V	±10 V
Cost	\$697	\$1,333	\$919

3.1.5.5 3.1.5.5 DAQ Card Chosen

The USB-6002 was chosen as the DAQ card for our project due to its price and sampling capabilities. The USB-6002 is the cheapest model out of the three models compared which will help with the budgeting of this project to make sure we stay under the given budget by our sponsor. The DAQ card also has a sample rate of 50,000 samples per second which translates to 50 samples per millisecond, which meets the requirements we want for this project. However, an issue with this DAQ card model is its update rate. This DAQ card model has an update rate of 5,000 samples per second which translates to 5 samples per millisecond to control the motor movement. This can lead to a tight control bandwidth to move the chosen galvanometer motor 0.1 degrees in 1 millisecond. However, due to the budget we have for the cost of the motor along with the optics devices, the USB-6002 model was chosen for our DAQ card to ensure that we stay within the given budget of the project.

3.1.5.6 DAQ Card Software

NI-DAQmx and LabVIEW are complementary tools developed by National Instruments that together enable powerful data acquisition and control systems. NI-DAQmx is a driver software that facilitates communication between your computer and National Instruments hardware, such as USB DAQ devices, PCI boards, or PXI modules. It provides a robust API for configuring and executing tasks like analog and digital input/output, counter operations, and timing synchronization. Users typically begin by using Measurement & Automation Explorer (MAX), a utility that comes with NI-DAQmx, to detect connected devices, configure channels, and test hardware functionality. Within LabVIEW, NI-DAQmx integrates seamlessly through the DAQ Assistant a program wizard that helps users set up acquisition tasks and automatically generates the corresponding LabVIEW code. For more advanced users, direct calls to NI-DAQmx VIs (Virtual Instruments) allow for fine-grained control and customization of data acquisition workflows.

LabVIEW itself is a graphical programming environment designed for engineers and scientists to build measurement, automation, and control systems. Instead of writing traditional code, users create programs by wiring together functional blocks in a flowchart-like interface. This visual

approach makes it easier to design complex systems, especially when dealing with real-time data acquisition, signal processing, and hardware control. LabVIEW supports modular design through subVIs, enabling reusable and scalable code structures. It also offers deployment options to real-time targets and FPGAs, making it suitable for high-speed and deterministic applications. When used with NI-DAQmx, LabVIEW becomes a complete solution for building interactive, responsive, and reliable experimental setups—from simple voltage measurements to sophisticated multi-channel control systems.

3.1.6 Microcontrollers

The purpose of microcontrollers in this project is to control the LED to turn on or off based on the user's input. If the user inputs to turn on the LED, the microcontroller will output a certain voltage value to turn on the LED driver. The LED driver will then turn on and then ensure the LED receives the proper current and voltage ratings. If the user inputs to turn off the LED, the microcontroller will not output any voltage which will turn off the LED driver. The user will input this information through a graphical user interface (GUI) that we will create and thus, the microcontroller will need to have Wi-Fi or Bluetooth capability to be able to receive information from this GUI.

3.1.6.1 ESP32

The ESP32 has many features that can be helpful and could be utilized for this project. The ESP32 has Wi-Fi capabilities (2.4 GHz Wi-Fi, 802.11 b/g/n) with being able to connect to a Wi-Fi network and is even capable with creating its own Wi-Fi wireless network for other devices to connect to the ESP32 (Random Nerd Tutorials , Starting Electronics). The ESP32 also has Bluetooth capabilities as it supports the Bluetooth Classic and Bluetooth Low Energy (BLE) functionality (Random Nerd Tutorials). The ESP32 also has the GPIO (general-purpose input/output) pins feature as the ESP32 can offer upwards to 32 GPIO pins (Starting Electronics). The ESP32 also supports a variety of development environments such as the Arduino IDE, MicroPython, ESP-IDF, and the PlatformIO (Starting Electronics). The ESP32 is also known for its low cost as the cheapest ESP32 cost as low as \$3 and the most expensive ESP32 only costs as high as \$14 (Zink). The ESP32 also has low power consumption capability as the ESP32 supports low-power mode states such as deep sleep (Random Nerd Tutorials).

3.1.6.2 MSP430

The MSP430 has many features that can be helpful for the project. The MSP430 is known for its ultra-low power consumption due to its lower sleep current functionality and efficient wake behavior which reduces the overall power consumption of the microcontroller (Unit Electronics). The MSP430 also supports its own developmental environment known as Code Composer Studio (IDE) that supports a variety of libraries and documentation to assist with the programming of the microcontroller (Allen). The MSP430 is also on the low side of microcontroller costs since the MSP430 can cost as low as \$2.07 and can be as expensive as \$21.93, which would help keep the cost of the project low (Allen). The MSP430 also offers the GPIO functionality with the microcontroller offering GPIO pins as low as 4 pins or as high as 90 pins depending on the model type (Ariat Technology). However, a drawback of utilizing the MSP430 in our project is its lack of built-in Wi-Fi or Bluetooth modules in its development boards. The MSP430 does not support Wi-Fi nor Bluetooth capabilities which means an external module must be brought to be used with the MSP430 if wireless communications want to be done for our project (Roberts , Sharma).

3.1.6.3 Arduino Uno

The Arduino Uno has many features that can be helpful for the project. The Arduino Uno has GPIO pins features with 14 digital pins that can act as inputs or outputs with the output pins being able to be set to output a voltage value of 5 Volts or 0 Volts (Linux Code , Mitchell). The Arduino Uno also supports its own developmental environment known as the Arduino IDE which supports a variety of libraries and provides a simple programming language as it utilizes a simplified version of the C/C++ programming language (Linux Code). The Arduino Uno is on the low side cost wise as the cheapest Arduino Uno cost \$20 while the most expensive Arduino Uno cost \$55.40, which means choosing the Arduino Uno would not lead to much strain on our budget. The Arduino uno also has low power consumption ability as the Arduino Uno supports a Low Power Library that can help with decreasing the overall power consumption of the microcontroller through a variety of methods such as sleep mode and stand-by mode (Chung and Bagur). However, an issue with utilizing the Arduino Uno for the project is its Wi-Fi and Bluetooth capabilities. The Arduino Uno has not have Wi-Fi and Bluetooth capabilities built into the board, but instead, external equipment must be added to the board for such features to be included in the Arduino Uno (Mitchell).

3.1.6.4 STM32

The STM32 has a variety of features that can be helpful for the project. The STM32 has GPIO pins feature as it hosts about 37 digital I/O pins on the board that can output a voltage of 3.3 Volts (Gariyal). The STM32 also supports a variety of development environments such as the Arm Keli MDK, PlatformIO IDE, and STM32CubeIDE that comes with various compliers and drivers to help the software development process (STM32-base). The STM32 also supports a variety of programming languages such as C, C++, BASIC, Python, and Ada which will offer more flexibility in the project with being able to choose the programming language we want when programming the microcontroller (Highleap Electronic). The STM32 also supports low power consumption through offering various low power modes such as a sleep mode and standby modes (Chatarjee). The STM32 also supports Bluetooth capabilities with its built-in Bluetooth Low Energy (BLE) module; however, the STM32 does not support Wi-Fi capabilities and an external module must be brought instead to be able to utilize wireless communications through the Wi-Fi method (Chatarjee). However, the STM32 in terms of cost is a bit more expensive in comparison to other microcontrollers due to its higher level of performance and functionality (Highleap Electronic). Another potential drawback of choosing the STM32 is its learning curve as the STM32 is known for offering more advanced features and capabilities which leads to more complex programming to utilize those features and capabilities (Highleap Electronic).

Table 3.1-8 Microcontroller Type Comparison

Features	ESP32	MSP 430	Arduino Uno	STM32
ADC Bit	12-bit	12- or 14- bit	10-bit	12-bit
GPIO Pins	34	4 to 90 (Depends on the Model)	14	37+ (Depends on the Model)
Energy Efficiency	Low Power Consumption	Low Power Consumption	Low Power Consumption	Low Power Consumption
Cost	\$3 - \$14	\$2 - \$25	\$20 - \$55.40	\$1 - \$25

Suitability for LED Control and ADC Reading	Supports Arduino IDE for simple C programming	Simple programming and more control over the bit values in the registers	Cost a bit more than the other microcontrollers	Too complex for the scale of programming in this project
---	---	--	---	--

3.1.6.5 Why ESP32?

The ESP32 was chosen as the microcontroller for our project. The reason being is that the ESP32 supports Wi-Fi and Bluetooth wireless connectivity unlike the MSP430 and the Arduino Uno which both require external equipment for Wi-Fi or Bluetooth capabilities which can increase the cost of the project. The STM32 supports Bluetooth capabilities and is similar in cost to an ESP32 but STM32 are often known for its advanced features and capabilities which leads to more complex programming. Since the microcontroller will only be used to turn on or off the LED based on controlling the voltage through the LED driver, only simple on/off I/O programming will occur and thus, the STM32 is too advanced for a microcontroller for this project. Thus, the ESP32 was chosen as the microcontroller for this project for its wireless connectivity, cost, and simple programming.

3.1.6.6 ESP32 Development Kit

For our prototype, a development kit will be utilized to test the code and to have USB communication protocol support. Having the USB protocol support would make it easy to compile the code onto the microcontroller to test the code and debug the code as needed.

3.1.6.7 ESP32-S3-DevKitC-1

This ESP32 model has a built in Wi-Fi and Bluetooth Low Energy MCU module that has Wi-Fi and Bluetooth Low Energy capabilities. This ESP32 model processing power consist of a dual core 32-bit LX7 CPU with a main frequency that goes up to 240 MHz which will ensure a fast processing time for simple and complex features that this development board offers (Electronikz). The ESP32-S3-DevKitC-1 comes in various variants with the N8R8 and 1U-N8R8 variants offering 8 MB for flashing while the N32R16V variant offers 32 MB for flashing. The ESP32 model also supports a USB port which will ensure an easy workflow of allowing an easy way to test the code of controlling the LED and laser diode. The ESP32 model also supports a 5 V to 3.3 V low dropout (LDO) regulator which allows the ESP32 to output a voltage of 3.3 V through its GPIO pins. This ESP32 holds a total of 42 pins with 34 of those pins being GPIO pins that can be used for our project. Most of the GPIO pins on this ESP32 model are broken out to pin headers which make it easy to prototype on the breadboard.

3.1.6.8 ESP32-C3-DevKitM-1

This ESP32 model is a compact size development board and is equipped with an ultra-low-power System on Chip (SOC) which allows this ESP32 model to be battery powered (Electronikz). The ESP32 model also offers additional power modes (such as active, modem-sleep, light-sleep, and deep sleep) to further lower the power consumption of the development board. This ESP32 model has a 32-bit RISC-V single core processor with a clock speed that goes upwards to 160 MHz. The ESP32 model also offers 4 MB for flashing within its chip package. The ESP32 model also has Wi-Fi and Bluetooth Low Energy capabilities along with having a total of 30 pins on the board, but only 15 of those pins can be used for I/O purposes. Most of these pins are also broken out to

pin holders which will be helpful when prototyping on the breadboard. This ESP32 model supports a micro-USB port along with a 5 V to 3.3 V LDO regulator.

3.1.6.9 ESP32-C5-DevKitC-1

This ESP32 model has Wi-Fi and Bluetooth Low Energy capabilities along with Zigbee and Thread functionality. A key component of this ESP32 model that separates it from other ESP32 models is its dual-band Wi-Fi support as it can support both 5 GHz and 2.4 GHz Wi-Fi (K). The ESP32 model is running on the high-performance RISC-V processor with a clock speed that goes up to 240 MHz which ensures fast response time for its more complex capabilities along with completing simple tasks even faster than usual in comparison to other ESP32 development boards. This ESP32 model supports a Type C USB port along with a 5 V to 3.3 V DC/DC voltage regulator and 8 MB for flashing the microcontroller. This ESP32 model has a total of 32 pins with 22 of those pins can be used for I/O purposes. Most of those pins are also broken out to pin holders which will be useful for prototyping on the breadboard.

Table 3.1-9 ESP32 Comparison

Features	S3-DevKitC-1	C3-DevKitM-1	C5-DevKitC-1
Processing Power	Dual-Core, 32-Bit LX7 CPU (240 MHz)	Single-Core, 32-bit RISC-V (160 MHz)	Single-Core, RISC-V (240 MHz)
I/O Pins	34	15	22
RAM	8 MB / 32 MB	4 MB	8 MB
Cost	\$15	\$9.80	\$13.90
Power Efficiency (in comparison)	Medium Power Consumption	Low Power Consumption	High Power Consumption
Suitability for LED Control and ADC Reading	Fast processing power, Dual core (permit parallel task execution), High amount of RAM for flashing, Decent power efficiency	Slower clock speed, Single-core, Low amount of RAM for flashing, Excellent power efficiency	Fast processing power but only single-core, Low power efficiency (in comparison to other models)

3.1.6.10 ESP32 Development Kit Chosen

The ESP32-S3-DevKitC-1 was chosen as the microcontroller for our project. The reason we choose this microcontroller over the other models is due to its power efficiency and simplicity. The ESP32-C3-DevKitM-1 was not chosen as the microcontroller for our project despite its low cost was due to its processing power as it was a bit slower in comparison to the other model options. The ESP32-C5-DevKitC-1 supported dual band Wi-Fi; however, there are limitations to the 5 GHz Wi-Fi. Limitations to the 5 GHz Wi-Fi is its compatibility with other devices as it is a relatively new Wi-Fi functionality and as such, older devices and routers may not be able to take advantage of the 5 GHz features (ESPBoards). Another limitation of the 5 GHz Wi-Fi is its range since the 5 GHz Wi-Fi offers faster data exchange speed and will experience less interference from external equipment, it comes at the cost of only being effective in short ranges and the Wi-Fi signals has a hard time of going through walls which can be an issue if the router is not in the same room as the

device connected to the Wi-Fi (ESPBoards). Thus, the advanced features of the ESP32-C5-DevKitC-1 were not needed in this project, and the extra power consumption was not worth it for the simple tasks of enabling a switch. Therefore, the ESP32-S3-DevKitC-1 was chosen for our project as it meets the wireless connectivity and processing power requirements needed for this project with a power efficiency that was agreeable for this section of the system.

3.1.7 Power Meter

Power meters are essential to almost every optical project. Mainly these devices work by using a photodiode which is a semiconductor device that works in reverse to an LED. By placing a P-side and N-side semiconductor together and applying a reverse voltage across them they no longer emit light like a semiconductor. Instead, when light comes in contact with the semiconductor it gets absorbed by the material which causes an electron to jump to the valence band of the material. Once this electron is in the valence band it is able to pass through the semiconductor (Murari 2009). We then read the amount of power being generated by the photodiode and can determine the amount of optical power incident on the power meter.

For our applications we need a power meter that is able to measure quick changes in power. We would like to achieve sub-millisecond switching and therefore need a power meter to be able to take readings much faster than 1ms, so we are able to monitor the power modulation. We also need to be able to read small powers. Our goal is up to 20mW so we need to read a large range around 20mW.

3.1.7.1 ThorLabs S120C and PM100D

The photodiode has a wavelength range of 400nm – 1100nm. It measures power from 50nW to 50mW. It has a response time of less than a microsecond and a resolution of 1nW. This is a silicon detector. It has a diameter of 30.5mm and a thickness of 12.7mm. The aperture size is 9.5mm in diameter. This diode is used for measuring low power lasers which is perfect for our application. We can also use the power meter that is compatible with the diode and is the PM100D. It has a power range from 100pW to 200W. The responsivity is 1pA/W which means that the diode is the limiting factor for response time.

3.1.7.2 Thorlabs S120C and PM103

This power meter setup uses the same photodiode as the previous setup but a new meter. This meter has a sampling speed of 100,000 samples per second. The minimum and maximum power readings depend on the photodiode. This meter connects to a computer using Mini USB.

3.1.7.3 Newport 918D-SL-OD2R and 844-PE-USB

This power meter combination from Newport offers a much wider range of power detection with a range of 2W to 20pW for the diode and the meter. The diode has a rise time of less than 2 microseconds but the meter itself has a sampling rate of 15Hz so we are limited by the meter. The aperture size is 11.3mm in diameter and the power meter connects through USB. The detector semiconductor is made of silicon.

3.1.7.4 DET100A2

This photodiode is unique because it can be connected directly to an oscilloscope for its power reading. This means we can borrow an oscilloscope from our labs to directly connect to this diode. It is rated for a wavelength range between 320nm – 1100nm. It has a very fast response time of

35ns. The detector has a diameter of 9.8mm. The diode connects to any power meter or oscilloscope using a BNC cable

3.1.7.5 Why DET100A2 Thorlabs

Table 3.1-10 Power Meter Comparison

	ThorLabs S120C and PM100D (Obsolete)	Thorlabs S120C and PM103	Newport 918D-SL-OD2R and 844-PE-USB	DET100A2 Thorlabs
Wavelength Range	400 nm – 1100 nm	400 nm – 1100 nm	400 nm – 1100nm	320 nm – 1100 nm
Power Range	50 nW – 50 mW	50 nW – 50 mW	20 pW – 2 W	Unknown
Diode Diameter	9.5 mm	9.5 mm	11.3 mm	9.8 mm
Minimum Sampling Rate	<1us	<1 us	0.066 ms	Meter Dependent
Diode Material	Silicon	Silicon	Silicon	Silicon
Price	\$1740.66	\$1109.61	\$1762	\$204.65

For our project the most important part of the power meter is how fast it can detect power changes. Since we need to switch the polarization states quickly, we need to be able to see the power reading changes throughout the process. This means we need many samples in under a millisecond. This makes the Newport meter setup unusable for our purposes. The PM100D went obsolete but it is a fantastic choice. We decided to use the DET100A2 because it can read powers very quickly with its 35ns rise time. We also chose this detector because with its ability to connect to a borrowed oscilloscope that makes this meter setup easy to use and versatile. It also saves us money from having to buy another power meter.

3.1.8 Polarizers

A polarizer is a very similar product to the one we will be making. A polarizer transmits one polarization while blocking or absorbing orthogonal polarization. There are several different kinds of polarizers like wire grid polarizers. These devices use metal wires aligned vertically. When vertical electric field from a photon encounters the wire grid it induces a current in the wires. This current oscillates back and forth across the wire which then creates another electric field which opposes the incident field. This causes the electric field that is parallel to the wire grid to be reflected or absorbed and the electric field that is perpendicular passes through. By turning the direction of these wires, we can control which polarizations get absorbed and which pass through (Young 1965). Another group of polarizers use birefringent crystals to change the speed of the extraordinary and ordinary polarizations. Then in polarizers like a Glan-Taylor prism you create an airgap in the crystal. This gap has a very specific angle so that one ray gets reflected and one transmits. This allows only one polarization to pass through (Protopopov 2014).

We need a polarizer because as light passes through our system it will be either polarized into a random linear angle or randomly polarized depending on whether we use a laser or LED. Using a polarizer before the light passes through our system ensures that the light is initially polarized in a specific known direction. Rotating the birefringent crystal is going to shift the polarization around the Poincare Sphere but we need to have a known starting point so that we know how much to turn

the crystal to achieve a specific desired polarization. The beam also needs to pass through a polarizer after going through the crystal. The reason for this is that by passing through a second polarizer we turn a change in polarization into a change in power. When the light is aligned with this secondary polarizer we will achieve a max power reading on our power meter. Then as we rotate the polarization on the Poincare Sphere the power will fluctuate until we reach the orthogonal polarization which will then allow us to achieve a minimum power reading. This is how we will determine that we can achieve orthogonal polarization states.

The most important factor for a polarizer in our application is that it achieves a high extinction ratio. This ratio describes how much light passes through of a desired polarization vs how much light is of orthogonal polarization. We would like to achieve >100:1 extinction ratio so our polarizer needs to have an extinction ratio higher than this so that we are not limited to this products extinction ratio.

3.1.8.1 CCM5-PBS201/M Thorlabs

One option is to replace the beam splitter that the light will pass through twice with a polarizing beam splitter. This will allow the light to be linearly polarized in a known direction as we enter our crystal subsystem. Then the light will retroreflect back into the polarizing beam splitter and again turn change in polarization into a change in power as described before. These polarizers work specifically by reflecting one polarization and transmitting another like the Glan-Taylor prism. This beam splitter is a 30mm cube that has a wavelength range from 420nm – 680nm. This beamsplitter is also relatively inexpensive with a price of \$331.76. This beam splitter has an extinction ratio of 1000:1 when transmitting and 100:1 when reflecting.

3.1.8.2 Newport 46-575

With this type of polarizer, the light with a polarization that aligns with the polarizer’s transmission axis will pass through and the light that does not, will either get reflected or absorbed. This polarizer is easy to work with because it is in the shape of a glass lens and is mounted. It has a diameter of 22.5mm. It is uncoated so there will be unwanted reflections, and the product will work with a wavelength from 400 nm – 700 nm. The highest extinction ratio this polarizer achieves is 2,700:1. This ratio is above our limit allowing it to work in our system; however, this ratio is only achieved with a wavelength range of 550 nm – 650 nm. When in the 400 nm range the extinction ratio is 19:1.

3.1.8.3 Thorlabs GT5

This is a Glan-Taylor polarizer as described before. These polarizers are useful because their specific design allows for extremely high extinction ratios. Specifically for this device the ratio is 100,000:1. This polarizer is uncoated and works with a wavelength range from 350 nm – 2.3 um.

Table 3.1-11 Polarizer Comparison

	Thorlabs GT5	Newport 46-575	CCM5-PBS201/M Thorlabs
Wavelength Range	350 nm – 2.3 um	400 nm – 700 nm	420 nm – 680 nm
Extinction Ratio	100,000:1	19:1 at 400nm 200:1 at 500nm >2700:1 at 550nm-650nm	1000:1 transmission 100:1 reflection

		600:1 at 700nm	
Aperture Size	6.5 mm x 6.5 mm	22.5mm	16mm
Price	\$626.65	\$49.29	\$331.76

3.1.8.4 Why Thorlabs GT5

The most important feature of a polarizer for our needs is its extinction ratio. For this reason, the GT5 polarizer is the best option. If the polarizer does not have a high extinction ratio, then our overall extinction ratio will be limited by the polarizer. We would like to show that our polarizer can achieve at least a 100:1 extinction ratio across the entire wavelength range. This means that the Newport polarizer would not work as well for us even though its price is extremely attractive. The Newport polarizer can only achieve higher than 1000:1 at a specific wavelength range in the visible spectrum, so we would be limited unless we only use a light source in this range. The CCM5 has a high enough extinction ratio as we are transmitting through the system, but it is only the minimum that we would like to achieve. We would like to show that our system can achieve higher than 100:1 extinction ratio so we need a polarizer that far exceeds this ratio and the GT5 offers this. Unfortunately, it achieves our goal at a high price range.

3.1.9 Retroreflector

A Retroreflector and a mirror are very similar devices in the fact that they reflect light. These two devices do these things in different ways, however. A mirror reflects light at an angle that is the same as its incident angle. This follows from the law of reflection that states $\theta_i = \theta_r$. A retroreflector reflects light back to its source no matter the incident angle. To do this we use vector math. If we write our incoming light as three motion vectors depending on how the light is coming at our reflector. These mirrors are aligned so that the reflected light has a direction vector that is exactly opposite of the incoming ray (Egidi 2018).

3.1.9.1 Thorlabs PS974M-A

These retroreflectors from Thorlabs are compact at a 10mm diameter which means they can fit easily into our setup. The design of these reflectors is a prism shape from the three mirrors to be able to reflect the light back at exactly the opposite direction it came in at. This device works from a wavelength range from 350 nm – 700 nm.

3.1.9.2 Newport 50441-0505AL

This reflector has a diameter of 12.7mm which also allows it to fit into our system with ease. This product is made of aluminum and has a reflective coating on the inside to reflect the light with high efficiency. This mirror is also not wavelength dependent on allowing any beam to enter and work the same.

3.1.9.3 Edmund Optics 49-079

This reflector has a diameter of 25.4mm. This reflector is made of silver and has a protective overcoat which makes this product inexpensive. This device has a wavelength range from 400 nm – 2500 nm.

Table 3.1-12 Retroreflector Comparison

	Thorlabs PS974M-A	Newport 50441-0505AL	Edmund Optics 49-079
Diameter	10mm	12.7mm	7.16mm
Material	N-BK7	Al	Silver
Beam Deviation	<3 arcsec	5 arcsec	5 arcsec
Price	\$205.91	\$390	\$286.20

3.1.9.4 Why Thorlabs PS974M-A

For our project one feature that stands out is the beam displacement in our output is very small since we are retroreflecting the light and doing a double pass setup. This setup allows us to achieve very small beam deviations from refraction through the crystal known as beam walk-off. This feature depends solely on how well the retroreflector can keep the light on its initial path which means that the beam deviation is the most important factor for this reflector. This led us to choose the Thorlabs reflector because it has the smallest beam deviation. This reflector also has the smallest price which matches our goal of the cheapest system.

3.1.10 Lens

In this project, a lens will be an important technology when combined with the LED. LEDs, while having a larger bandwidth than lasers, also have a larger divergence angle than lasers. We need our light to follow a singular path over a relatively large distance. That means to accomplish this with an LED we need to have it collimated. To collimate a light source, we just need a lens. If we place the LED at the focal point of a lens, we will output a collimated beam (Qiao 2022). Some important qualities of the lens affect how much optical power leaves the lens as a collimated beam. The amount of light that gets collimated is called numerical aperture (NA). The higher NA value is the higher the power of the collimated beam will be. NA is determined by the diameter of the lens as well as the focal length of the lens (Piston 1998). To achieve the highest NA and power of the beam, we need a large diameter lens with a small focal length.

3.1.10.1 ACL25416U Thorlabs

Thorlabs has a large selection of aspheric lenses. This type of lens means that the curvature of the lens is not constant. This leads to having sharper focusing and larger NAs. This lens has a staggering NA of 0.79. This means it will be able to collect a large portion of the light from our LED. This lens also has a diameter of 25.4mm and a focal length of 16mm. These qualities allow us to use this lens in a very confined space and be able to gather a large portion of our light that escapes the LED.

3.1.10.2 KPA19AR.14 Newport

This is another aspheric lens. Unlike the ThorLabs lens this lens is coated with an antireflective coating which is designed for 430 nm – 700 nm, so more light from our design will pass through with this coating. This Newport lens is also specifically designed for the purpose of light collection and has a diameter of 25mm. It also has a focal length of 18.8mm. This gives this lens an NA of 0.66.

3.1.10.3 23-813 Edmund Optics

This condenser lens is used for light collimation like the other two lenses. It is also an aspheric lens. This lens offers an extremely high NA compared to most other lenses. It has a diameter of 16mm and a focal length of 8.3mm. The combination of this small focal length and large diameter means that this lens has a NA of 0.96

3.1.10.4 Why ACL25416U Thorlabs?

Table 3.1-13 Lens Comparison

	ACL25416U Thorlabs	KPA19AR.14 Newport	23-813 Edmund Optics
Diameter	25.4 mm	25 mm	16 mm
Focal Length	16 mm	18.75 mm	8.3 mm
Material	B270	L-BAL 35	H-K9L
Numerical Aperture	0.79	0.66	0.96
Price	\$22.00	\$459	\$62.54

We are using lenses in the system to collect light from our LED. The amount of light collected by a lens is measured by its NA. While the Edmund Optics lens has the highest NA we decided to use the Thorlabs lens for a couple of reasons. We used the LED's viewing angle which is 80 degrees to make this choice. By using this value and the diameter and focal length of the lens we can determine how much light gets collected by the lens. We use the formula $r_{\text{beam}} = f_{\text{lens}} \times \tan(\theta)$ to calculate the radius of the beam when it hits the lens. For the Thorlabs lens this value is 13mm which leads to a 26mm diameter. For the Newport lens this radius is 15.7mm which leads to a 31.4mm diameter. Finally, for the Edmund Optics lens the radius of the beam is 6.96mm and the diameter is 13.93mm. By these calculations the Thorlabs lens and the Edmund Optics lens both have diameters of lens that would encompass the entire LED diameter. This means that both lenses would effectively collimate the light for our purposes. We chose to use the Thorlabs lens because it is 3 times cheaper than the Edmund optics lens. Since we need two of these lenses, one for collimation and one for focusing on the power meter, we chose the Thorlabs lens to save \$80.

3.1.11 Beamsplitter

For our project, we are using beamsplitters to combine light sources for the light collection subsystem. Beamsplitters do this by acting as a semitransparent mirror angled at 45 degrees to incoming light. To create this semitransparent mirror these technologies are two pieces of glass that when put together form a cube. These two pieces of glass are each right triangle and when put together another material is added between them. This change in materials is how the splitters get their semitransparent mirror. When the light hits the mirror, some of it will pass through and some of it will get reflected (Gilo 1992). For our case the beamsplitter is allowing us to take two beams and combine them into one beam. This will allow us to have as many light sources as we want, and they all, after going through the beamsplitters, overlap as they continue through the system. We will only be using one light source at a time, so doing this will let us align all our light sources and just turn them on and off as we need them. To achieve this goal from our beamsplitters we need beamsplitters with a 50:50 transmission to reflection ratio. We are going to need one beam splitter to take the light pass through our crystal and one beam splitter for every light source after

the first one. The amount of beamsplitters we need is substantial, so we need our beamsplitters to be inexpensive so we can stay under budget.

3.1.11.1 47-122 Edmund Optics

This beamsplitter from Edmund Optics has an antireflective coating rated for the wavelength range of 430 nm – 670 nm. It has a beam splitting ratio of 50% transmission and 50% reflection. This splitter is made from BK7 glass. This cube also has a size of 20mm.

3.1.11.2 10BC17MB.1 Newport

This splitter from Newport is designed to work well for combining different lasers. The splitter has a higher absorption rate than normal but also has minimal polarization sensitivity. This is important for us because we do not want the beamsplitter to interfere with our extinction ratio. If we have a beamsplitter that has different reflection coefficients for different polarizations, then we will have a lower extinction ratio. This cube has a size of 25.4 mm and has an antireflection coating that is rated for 400 nm – 700 nm.

3.1.11.3 CCM5-BS016/M Thorlabs

This beamsplitter from Thorlabs comes in a 16mm cage system. There is a coating applied between the two pieces of glass to ensure the correct amount of light is transmitted and reflected. All the faces of this cube have an antireflective coating rated for 400 nm – 700 nm. The cage system for this beam splitter allows for easy mounting and maneuvering.

Table 3.1-14 Beam Splitter Comparison

	47-122 Edmund Optics	10BC17MB.1 Newport	CCM5-BS016/M Thorlabs
Wavelength Range	430 nm – 670 nm	400 nm – 700 nm	400 nm – 700 nm
Size	20 mm x 20 mm	25.4 mm x 25.4 mm	16 mm x 16 mm
Transmission to Reflection Ratio	50:50	45:45	50:50
Price	\$306.34	\$282	\$224.99

3.1.11.4 Why CCM5-BS016/M Thorlabs

Since we are using multiple beam splitters, we need these to be cheap. We will be using three light sources which means we will need 3 light sources. This leads us to choose the Thorlabs beamsplitter. This splitter has low loss from absorption unlike the Newport beamsplitter and is the cheapest of the three options. This splitter also comes in a cube that is easy to mount unlike the other beamsplitters which we would need to mount separately. Using this beamsplitter will save us the most money.

3.1.12 Mirror

Mirrors play a crucial role in optical projects. Mirrors are used to guide light along a select path. Mirrors have a property called reflectivity that allows them to bounce light off of themselves. In our project we use these mirrors to guide the light from the sources to beamsplitters and then into the crystal. We need high reflectivity mirrors for our wavelength which means we need dielectric mirrors. Dielectric mirrors use layers of transparent material with different refractive indexes to

reflect light. These layers are spaced specifically for certain wavelengths of light which make them not applicable for every wavelength. This is different from metallic mirrors because metallic mirrors have a much higher absorption and generally lower reflectivity's than dielectric mirrors (Perry 1965).

3.1.12.1 70-667 Edmund Optics

This is a dielectric mirror that reflects a broad range of wavelengths. This mirror is rated for 400nm – 750nm. The spacing between the material layers in the mirror is 1/4th of the wavelength. This mirror has a reflectivity of greater than 98%.

3.1.12.2 BB03-E02 Thorlabs

This is a smaller diameter lens with only 7mm in diameter. It also has a wavelength range of 400nm – 750nm. This mirror has an average reflection of over 99%. This mirror also has a spacing of 1/4th of the wavelength between each layer.

3.1.12.3 05Q20BB.HR2 Newport

This mirror has an average reflectance of 98%. It has a diameter of 12.7 mm. This mirror has a larger bandwidth than others being from 350nm – 1100nm. This mirror is made from silica substrates and has metallic dielectric coatings.

Table 3.1-15 Mirror Comparison

	BB03-E02 Thorlabs	05Q20BB.HR2 Newport	70-667 Edmund Optics
Diameter	7 mm	12.7 mm	12.5 mm
Wavelength Range	400 nm – 750 nm	350 nm – 1100 nm	400 nm – 750 nm
Reflectivity	99%	98%	>98%
Price	\$49.85	\$161	\$66.25

3.1.12.4 Why BB03-E02 Thorlabs

The most important factor for our application is that we have inexpensive mirrors. This is because we are using several of them so the more expensive they are, the more they impact our budget. We also want mirrors that have high reflectivity so that we lose as little power as possible. This will maximize the optical power we can receive on our power meter. This led us to choose the mirrors from Thorlabs. Since most of our optics come from Thorlabs we save money on delivery fees by ordering these mirrors from them as well. These are also the cheapest mirrors that have the highest reflectivity.

3.1.13 LED Driver

For the LED chosen, an LED driver will be utilized to ensure the proper current and voltage is powering the LED. There are two different types of LED drivers, constant current LED drivers and constant voltage LED drivers. A constant current LED driver ensures a steady flow of current goes into the LED by changing the voltage that the LED receives, usually around the forward voltage rating value of the LED (Unitop , Wan). A constant voltage LED driver maintains a steady voltage value but has the drawback of not limiting the current flow to the LED (Unitop , Wan). For our LED, the datasheet recommends selecting an LED driver that does not go over the maximum

current (which in our case is 1 A) and sufficient forward voltage is supplied (which in our case is 3.8 V). Thus, based on the recommendations of the LED’s datasheet, a constant current LED driver will be utilized in our system to power the LED.

Table 3.1-16 LED Driver

Features	TLM4036DC-1000	LDDS-1000HW	RCD-24-1.00/W
Max Current	1 A	1 A	1 A
Input Voltage	10 V – 30 V	12 V – 56 V	6 V – 36 V
Output Voltage	2 – 26 V	2 – 45 V	3 V – 31 V
Power	26 W	45 W	33 W
Cost	\$22.98	\$8.87	\$24.44

The LDDS-1000HW model was chosen as the LED driver for our system. The reason the LDDS-1000HW model was chosen was due to its on/off switch and the cost. The TLM4036DC-1000 model did not offer on/off switch capability while the LDDS-1000HW and RCD-24-1.00/W models did which will be utilized in our system with the ESP32 microcontroller to turn on or off the LED based on the user’s input. The LDDS-1000HW model turns on when voltage is applied to the switch pin while the RCD-24-1.00/W model turns on when no voltage is applied to the switch pin. Thus, the LDDS-1000HW model would be more power effective for our system since the LED only turns on when the user wants the LED to be turned on. The LDDS-1000HW model is also the cheapest model amongst the three models compared. Therefore, the LDDS-1000HW model was chosen for its on/off switching mode and its cost in comparison to the other LED driver models.

3.1.14 Operational Amplifier

For the operational amplifier (op-amp), it will be utilized to build the transimpedance amplifier (TIA) circuit of our system to verify the switching time of the motor. When deciding on the op-amp of the circuit, the gain bandwidth of the op-amp must be high enough to handle the speed of converting the current into voltage in less than 5 ms. The op-amp must also have a low offset voltage to ensure the accuracy of the output voltage of the op-amp (Toshiba). The op-amp chosen would ideally have no input bias current to ensure the accuracy of the output of the TIA circuit but due to the non-ideal condition of the real world, the chosen op-amp would need to have a low input bias current to help with the performance of the TIA circuit (everything PE).

Table 3.1-17 Operation Amplifier

Features	OPA357	OPA354	OPA863A	OPA2863A
Gain Bandwidth	100 MHz	100 MHz	50 MHz	50 MHz
Offset Voltage	8 mV	8 mV	0.095 mV	0.095 mV
Input Bias Current	50 pA	50 pA	730,000 pA	730,000 pA
Supply Voltage Range	2.5 V – 5.5 V	2.5 – 5.5 V	2.7 V – 12.6 V	2.7 V – 12.6 V
Cost	\$2.38	\$2.39	\$2.39	\$3.77

The OPA354 was chosen as the op-amp for the TIA circuit due to its gain bandwidth, low input bias current, and its PCB design layout. The OPA357 and OPA354 has a better gain bandwidth and lower input bias current in comparison to the other two op-amps that were compared. The OPA354 was chosen over the OPA357 due to its simpler PCB design layout. In the datasheet of the OPA357, there were more requirements in what to considering in laying out the op-amp in the PCB in comparison to the OPA354. Thus, to help with the time constraint of this project, the OPA354 was chosen as the op-amp utilized in the TIA circuit.

3.1.15 Digital-to-Analog Converter

An external digital-to-analog converter (DAC) must be chosen for our project as the ESP32-S3 chosen does not include an internal DAC functionality. When choosing a DAC chip for our system, it is important to consider the digital input interface of the DAC chip to ensure that the ESP32-S3 is able to communicate with the DAC chip (Menges). Another consideration when choosing a DAC chip is the sampling rate in which we need to choose a DAC chip that can output a voltage value fast enough for the sampling rate of the analog input reading of the DAQ card.

Table 3.1-18 Digital to Analog Converter

Features	DAC6571	DAC6311	DAC53202	DAC53001
Update Rate	125,000 samples per second	83,000 samples per second	25,000 samples per second	25,000 samples per second
Output Voltage	0 V to 5.5 V	0 V to 5.5 V	0 V to 5.5 V	0 V to 5.5 V
Interface Type	I2C	SPI	I2C, SPI	I2C, SPI
Package Type	SOT-23 (DBV)	SOT-SC70 (DCK)	WQFN (RTE)	WQFN (RTE)
Cost	\$2.05	\$2.01	\$3.15	\$3.33

The DAC6311 was chosen as the DAC chip for our system. The reason being is that the DAQ card has a sampling rate of upwards to 50,000 samples per second for its analog input reading. Thus, the DAC6571 and DAC6311 are the only DAC chips available in our selection that can keep up. When comparing the DAC6571 and the DAC6311, the interface type was the last factor in considering which one to choose. The DAC6311 was chosen for its SPI interface type since the output frequency of the voltage value can be adjusted unlike the I2C interface type which only has a couple of frequency rates to choose from (eVision Instruments).

3.2 Power Management

3.2.1 Power Delivery

For our system, the main power source will be from the wall outlet. The reason for this is the wall outlet supplies a constant power source without worry of losing charge unlike the battery. Another reason is that various components for our system already use the wall outlet as their power source such as the laptop and the motor with its DC power supply. Thus, to make the power delivery system simple, the power source will focus on the wall outlet as supplying the power to the whole system. The next challenge comes from figuring out how to utilize the wall outlet power to power the various components in the system.

For the laptop, a simple laptop charger will be used to power the laptop and ensure it does not lose charge while it is running the system. The motor system gains its power from the DC power supply with the DC power supply being powered by the wall outlet. The DAQ card for the motor utilizes a USB device to power its system and to transfer data between the laptop and the motor; thus, the DAQ card will be connected to the laptop to get its required voltage and current it needs to be powered and for it to transfer data between the DAQ card and the laptop. This leaves the microcontroller, LED, and the laser diode to be powered by the system. The microcontroller, LED, and laser diode cannot connect directly to the wall outlet and there is a limited amount of USB ports that the laptop can handle. Thus, a power adapter along with a power jack will be utilized to be able to deliver power to these devices. Voltage regulators will be used to ensure that the proper voltage is being delivered to the microcontroller and laser diode while an LED driver will be utilized to ensure the proper current and voltage is being delivered to the LED.

Table 3.2-1 Power Management

Component	Power Consumption	Operating Voltage	Operating Current
ESP32	Typical: 1,500 mW Max: 2,160 mW	Min: 3 V Max: 3.6 V	Typical: 500 mA Max: 1000 mA
LED	Typical: 3,800 mW Max: 3,820 mW	Typical: 3.8 V Max: 3.82 V	Max: 1000 mA
Laser Diode (520 nm)	Min: 392 mW Max: 520 mW	Min: 4.9 V Max: 5.2 V	Typical: 80 mA Max: 100 mA
Laser Diode (635 nm)	Min: 343 mW Max: 468 mW	Min: 4.9 V Max: 5.2 V	Typical: 70 mA Max: 90 mA
Motor Driver	Typical: 60 W Max: 240 W	± 15 V to ± 24 V	Typical: 4 A Max: 10 A
Motor	Typical: 60 W Max: 240 W	± 15 V to ± 24 V	Typical: 4 A Max: 10 A
Laptop	45 W	19.5 V	2.31 A
DAQ Card	727.5 mW to 772.5 mW	4.85 V to 5.15 V	Max: 150 mA
Total System	Typical: 171.76 W Max: 532.74 W	Min: ± 24 V	Typical: 12.11 A Max: 24.65 A

3.2.2 Power Adapter

The purpose of the power adapter in our system is to convert the AC power of the wall outlet to DC power since our devices use DC voltage and current to power on. It is essential to choose a power adapter that can meet the power, voltage, and current ratings of the overall system. If the voltage rating of the power adapter is too low, the device may not be able to turn on or will not work properly as intended; however, on the other hand, if the voltage rating is too high, the device can be damaged or lower the life span of the device (Busch). If the power rating of the power adapter is too low, the power adapter could be damaged from the devices in the system trying to draw more current than the power adapter can handle (Busch). On the other hand, if the power rating of the power adapter is too high, the devices in the system can still work properly as intended since the devices will only draw the current needed for them to function (Busch). This, however,

does not apply to the LED device since it is a current control device in which we need to create a constant current driver that will ensure that only the needed amount of current the LED needs to function is flowing into the device. Therefore, it is essential when we choose the power adapter for our system that it can meet the overall power, voltage, and current ratings of the whole system.

Table 3.2-2 Adapter Model Comparisons

Features	MDS-030AAC07 AB	B00ZWU5L0C	16-00216
Output Voltage	7 V	3 V - 12 V	12 V
Output Current	3 A	2 A	3 A
Power Rating	21 W	24 W	36 W
Plug Size	5.5 mm x 2.1 mm	5.5 mm x 2.1 mm	5.5 mm x 2.1 mm
Cost	\$27.64	\$13.90	\$11.81

3.2.2.1 Why 16-00216?

The 16-00216 model was chosen as the power adapter due to its output voltage and output current ratings. The 16-00216 model outputs a voltage value of 12 V which meets the requirements of this system to power the microcontroller and LED. The 16-00216 model also outputs a current rating of 3 A which ensures a stable current supply for the system. The system requires a current rating of at least 1.8 A but to ensure that there is enough current in the system to power the devices, the 16-00216 model was chosen for its 3 A current rating. The 16-00216 model is also the cheapest model in comparison to the MDS-030AAC07 AB model and the B00ZWU5L0C model. Thus, the 16-00216 model was chosen to meet the output voltage and current ratings needed for our system as well as being the cheapest model choice out of the three models compared.

3.2.3 Power Jack

For our system, the power adapter needs to be able to deliver the power from the wall outlet to the PCB board for the microcontroller, LED, and laser diodes to be powered on. This will be done through having the power adapter connect to a power jack that will deliver the needed voltage and current to the devices through the soldering of the exposed wires of the power jack to the PCB board. The power jack needs to meet the voltage and current ratings of the power adapter to ensure reliability in delivering the power to our system (Smoot). Another aspect that needs to be considered is the gender of the power adapter (Smoot). The chosen power adapter had a male connector and thus, the power jack needs to be a female connector. Another consideration is the plug size of the power adapter in which the barrel size of the power jack needs to be the same size as the plug size of the power adapter to ensure that the power adapter can be plugged into the power jack (Smoot). Lastly, the polarity of the power adapter needs to be considered as well (Smoot). The chosen power adapter had a polarity in which the center pin was connected to the positive polarity while the outer sleeve was connected to the negative polarity. Thus, when considering the power jack, the power jack also needs to be connected to the positive polarity in the center pin and the outer sleeve needs to be connected to the negative polarity.

Table 3.2-3 Jack Model Comparisons

Features	B07CTMY9KG	B072BXB2Y8	B08PYT6HZ2
Voltage Rating	12 V	12 V	12 V
Current Rating	3 A	5 A	15 A
Barrel Size	5.5 mm x 2.1 mm	5.5 mm x 2.1 mm	5.5 mm x 2.1 mm

Gender	Female	Female	Female
Polarity	Center Positive	Center Positive	Center Positive
Cost	\$5.99	\$9.49	\$9.99

The B072BXB2Y8 was chosen for meeting the voltage and current ratings required to handle the chosen power adapter along with having a barrel size that would ensure proper connection. The B072BXB2Y8 was also chosen for its female gender and having a positive polarity at its center. The B072BXB2Y8 was chosen over the other wires due to being an 18 AWG wire. The 18 AWG wire is often used to power low voltage devices along with being cost friendly while still having great performance and durability (Origin Data Global Limited). The B07CTMY9KG model is also an 18 AWG wire type; however, the B072BXB2Y8 model was chosen instead as the power jack due to its increased current capability which ensures proper current control between the power adapter and our system.

3.2.4 Voltage Regulator

Voltage regulators will be used in our system to regulate the voltage going into the microcontroller which operates at 3.3 V. Thus, when deciding on a voltage regulator, the voltage regulator needs to be able to output a 3.3 V value and can take an input voltage of 12 V.

3.2.4.1 Linear Voltage Regulator

A linear voltage regulator works by having a resistive method (usually a BJT or MOSFET) to regulate the output voltage by varying the current that goes through the resistive method (IC Components Limited, Teja). However, a drawback with this voltage regulation method is the heat dissipation that comes with regulating the voltage through the transistor which would lead to the need to have a heat sink method to ensure that the voltage regulator would not cause damage to the PCB board (Teja). Another drawback of the linear voltage regulator is its efficiency due to the heat dissipation, which causes the linear voltage regulator to have an efficiency of between 20% and 60% (Teja). Linear voltage regulator also has the limitation of only being able to decrease the input voltage to the desired output voltage (Teja). However, for our system, we want to decrease the input voltage to the desired output voltage and thus, this limitation of the linear voltage regulator would not be an issue for our system. An advantage of utilizing the linear voltage regulator is its simplicity since they are easy to use and implement into a circuit system due to only needing a few extra components to ensure it is working properly as intended (Teja). Another advantage of the linear voltage regulator is its noise free output voltage which makes the linear voltage regulator helpful for audio systems and analog circuits where it is favorable for noise to be minimized for performance (IC Components Limited).

3.2.4.2 Switching Voltage Regulator

A switching voltage regulator works by utilizing the transistor as a high-speed switch in which the transistor is turned on or off to keep the output voltage consistently at the desired value (IC Components Limited, Teja). This leads to the advantages that the switching voltage regulator presents. Due to the on or off state of the transistor within the switching voltage regulator, the heat dissipation of the voltage regulator is a lot smaller in comparison to the heat dissipation of the linear voltage regulator (Teja). This efficiency in heat dissipation leads to the switching voltage regulator having better efficiency as it can be as efficient up to 95% (Teja). Another benefit of the switching voltage regulator is that the output voltage can be lower or higher than the input voltage,

but for our system, only having the output voltage being lower than the input voltage will be our focus (Teja). However, a drawback of the switching voltage regulator is its complexity as the switching voltage regulator requires additional components such as inductors and capacitors to ensure it works properly as intended (IC Components Limited , Teja). Another drawback of the switching voltage regulator is that the output voltage could have a lot of interference and noise which leads to the switching voltage regulator being often used in circuit systems that need a lot of current or needs to save power (IC Components Limited , Teja).

Table 3.2-4 Voltage Regulator Type Comparison

Features	Linear	Switching
Output Voltage	Fixed or Adjustable	Fixed or Adjustable
Heat Generation	High	Low
Efficiency	Low (30% to 60%)	High (70% to 95%)
Complexity	Simple	High
Step Movement	Step-Down	Step-Down, Step-Up

3.2.4.3 Voltage Regulator Type Chosen

The switching voltage regulator will be chosen as the voltage regulator in our system. The reason being is that the heat dissipation and the efficiency of the switching voltage regulator would be helpful in the creation of PCB boards as heat dissipation of components is often a consideration that must be considered when creating the design of a PCB board. However, a drawback of the switching voltage regulator is its complexity due to the use of inductors and capacitors to ensure the switching voltage regulator is working as intended. This drawback may lead to additional workload for the team but utilizing circuit simulations such as Webench by Texas Instruments can help with this additional workload and would ensure the circuit design will meet the requirements needed to power the devices in our system.

3.2.4.4 Buck Regulators

Buck regulators are a type of switching voltage regulator in which the output voltage is smaller than the input voltage (Teja). Buck regulators work by switching on and off the transistor in which the energy from the input voltage is stored in magnetic fields to keep the output voltage constant at a certain value (IC Components Limited).

Table 3.2-5 Switching Voltage Regulator Comparison

Features	BD9781HFP-TR	LM2575	LM27402
Max Output Current	4 A	1 A	30 A
Efficiency	75% – 80%	75% – 88%	90% – 97%
Input Voltage	7 V – 35 V	4.75 V – 40 V	3 V – 20 V
Output Voltage	1 V – 35 V	1.23 V – 37 V	0.6 V – 18.6 V
Cost	\$5.69	\$3.63	\$3.12

3.2.4.5 Why LM2575?

The LM2575 model was chosen as the switching voltage regulator for our system. The reason the LM2575 model was chosen was due to its cost while still meeting the requirements needed for the circuit since the LM2575 model was the second cheapest model amongst the three options. The switching voltage regulator has an output current of 1 A which meets the current requirements to power the devices along with the current flow from the chosen power adapter. The voltage output has enough range to power the microcontroller. The input voltage range also offers a wide range which allows a more variety of options when choosing a power adapter that can power our system.

3.3 Communication Protocol

3.3.1 USB

The USB (Universal Serial Bus) protocol will be the communication protocol that will be utilized in our system. The USB protocol will be utilized to transfer data between the laptop and the DAQ card along with flashing the ESP32 microcontroller with our code. The USB protocol works by have a series of hubs that connect the external devices to the main host hub (which in our case will be the laptop) to determine the timing of how the data is transmitted from the main host hub to the external devices or vice versa (ElProCus). When a new device is connected to the USB port, the main host hub will read the data on that particular device USB hub to determine how to communicate with the new device and assigned the device with its own unique address (ElProCus). The USB protocol has four lines that it utilizes, a power bus (VBus), data transfer lines (D- and D+), and a ground pin (GND) with the data transfer lines indicating the flow of the data transfer (ElProCus). Thus, when utilizing the USB protocol in our system, the USB protocol will be used to communicate between the laptop and DAQ card along with flashing the ESP32 microcontroller and to provide power to the laser diode.

3.3.2 UART

The UART (Universal Asynchronous Receiver-Transmitter) was utilized to flash code onto the ESP32-S3 that is on the main PCB. The UART is a physical IC chip on the microcontroller in which its main purpose is to transmit and receive serial data from the USB (Campbell). The UART communication protocol works by utilizing two data lines (receiver and transmitter) to transfer data to another device bit by bit as when the UART chip receives the data, the data is converted into parallel to be transmitted to the receiving device (Pena and Legaspi). The UART communication protocol was utilized in our project to flash code onto the ESP32-S3. On the main PCB with the ESP32-S3 module, a UART chip will be included on the board. The UART chip will be the middleman between the USB and the ESP32-S3 in which the UART will take the data from the USB and convert it into usable UART data to be transmitted to the ESP32-S3.

3.3.3 SPI

The SPI (Serial Peripheral Interface) was utilized for the ESP32-S3 to communicate with the DAC chip. The SPI communication protocol works by utilizing 4 lines between the Master and Slave device: MOSI (Master Out, Slave In), MISO (Master In, Slave Out), SCLK (Signal Clock), and SS (Slave Signal) with the SCLK determining the timing of the data transfer between the devices to keep them in sync (yida). The benefit of utilizing SPI is that it can send and receive data simultaneously and this type of communication protocol is faster in its data transfer in comparison to other communication protocols like the I2C and UART (yida). The SPI communication was

utilized between the ESP32-S3 and DAC chip in which the MOSI, SCLK, and SS lines were utilized. The DAC chip is not sending data back to the ESP32-S3 and thus, the MISO line was not utilized. The ESP32-S3 sends a digital voltage signal to the SS line to let the DAC chip to begin outputting the voltage value to the DAQ card while the MOSI line is used to transmit the data and the SCLK line is used to keep the ESP32-S3 and DAC chip in sync with the timing of the data transfer.

3.4 Software

3.4.1 Programming Languages

3.4.1.1 C

The C programming language offers a variety of benefits. The C programming language is a general-purpose, middle-level programming language that offers usage in low-level programming and supports the function of high-level programming (Greeks for Greeks). C is also a popular choice for embedded system programming due to its direct access to machine level hardware and its dynamic memory allocation (Greeks for Greeks). C is also a heavily supported programming language that offers a variety of library to utilize for various programming projects (Greeks for Greeks). If the C programming language is chosen to program the ESP32 for our project, multiple development environments (such as Arduino IDE and Espressif IDE) support the C programming language for the ESP32 which will be useful in choosing a development environment for this project.

3.4.1.2 Python

The Python programming language offers a variety of benefits. One of the benefits of Python is the fact that it is a general-purpose programming language that supports object-oriented programming and functional programming (Atwell). Another benefit of Python is its simple syntax programming due to utilizing English keywords instead of punctuation like the C programming language and Python is a forgiving language as well due to simple syntax issues will still be accepted by Python as an acceptable expression (Atwell). Python also supports a variety of libraries to help with programming projects to add a feature or functionality to the program without having to write additional code (Mikke). If the Python programming language is chosen to program the ESP32, a limited amount of development environments support Python specifically as the programming language for the ESP32. Typically, if a person wants to program in Python to code the ESP32, MicroPython or CircuitPython programming languages would be utilized instead.

3.4.1.3 MicroPython

The MicroPython programming language utilizes the Python 3 programming language to code microcontrollers and embedded systems (Atwell). The benefit of using MicroPython is its simple syntax programming like Python but has the drawback of being unable to utilize the same amount of libraries as Python can and is not a forgiving language like Python (Atwell). Another benefit of the MicroPython is its small memory usage as the MicroPython can work on devices that has a small storage as little as 256 KB of storage and 16 KB of RAM (Rakshit). If the MicroPython programming language is chosen to program the ESP32, multiple development environments (such as Thonny) support the MicroPython programming language for the ESP32 which offers a variety of choices to choose from for our project.

3.4.1.4 CircuitPython

The CircuitPython builds off the MicroPython programming language but made it more beginner friendly to be more approachable for the wider public (Jacob). CircuitPython offers the benefit of interpreting the code directly which allows the user to see the effects of their code immediately without the need to compile the code (Jacob). CircuitPython also offers the benefit of turning the microcontroller into a plug-and-play device which avoids the hassle of configuring the microcontroller to work with the development environment and the programming language (Jacob). CircuitPython also offers the benefit of supporting a wide variety of libraries but does not offer the full range of libraries support on Python due to CircuitPython being unable to access low-level hardware on the microcontroller (Jacob).

Table 3.4-1 Programming Language Comparison

Features	C	Python	MicroPython	CircuitPython
Description	Low-level programming and supports high level programming	Object-oriented programming	Python 3 programming for embedded and MCU	Simplified version of MicroPython
Embedded Programming	Direct access to machine level hardware, Dynamic memory allocation	Not supported, Have to use MircoPython or CircuitPython	Can be used to code MUC that has small storage and RAM	No need to compile code, Turns the MCU into a plug and play device, Lacks access to low level hardware on MCU
Syntax	Complex	Simple	Simple	Simple
Library Support	Lots of libraries available	Lots of libraries available	Less libraries available for usage	Less libraries available for usage
Development Environments	Arduino IDE, Espressif IDE	N/A	PyCharm Professional, Visual Studio Code	Visual Studio Code

Table 3.4-2

3.4.1.5 Why C?

The reason the C programming language was chosen was for its development environment support. The Python programming language has a limited amount of development environment support and while the MicroPython and CircuitPython have more development environment support, their limited library support may not support the scope of this project. Thus, the C programming language was chosen as the programming language that will be utilized in our project to program the ESP32.

3.4.2 Development Environment

3.4.2.1 Arduino IDE

The Arduino IDE offers the benefits of being easy to use due to an easy user interface and little configuration needs to be done to start coding which makes the Arduino IDE a beginner friendly development environment to use (Voss). Another benefit of the Arduino IDE is its extensive library support with many of them can be utilized with the ESP32 microcontroller along with the large community support that offers a variety of help and tutorials to get started with utilizing the Arduino IDE to program an ESP32 (Voss). Another benefit of the Arduino IDE is its fast compiling time as even complex Wi-Fi or Bluetooth programs can be compiled within minutes which would be helpful with developing and prototyping the code (Voss). If the Arduino IDE is chosen as the development environment to program the ESP32, its fast-compiling time and beginner friendly setup would be helpful with prototyping and developing the code for the ESP32.

3.4.2.2 Espressif IDE (ESP-IDF)

The ESP-IDF is the official ESP32 development environment supported by the ESP32's company (Espressif) and is typically utilized through the Espressif IDE or an extension in Visual Studio Code (Voss). The benefit of utilizing the ESP-IDF is its full hardware control since the ESP-IDF has access to the ESP32's subsystems which permits further hardware performance customization (Voss). Another benefit of the ESP-IDF is its scalability as the ESP-IDF can scale from prototypes to commercial production with minimal rework of the code along with continuously support to update the program to ensure compatibility with new versions of the ESP microcontrollers (Voss). The ESP-IDF also has extensive documentation support that explains the subsystems, configuration file, and API when utilizing this development environment. If the ESP-IDF is chosen as the development environment to program the ESP32, its extensive documentation would be helpful with starting out but runs at the risk of having a steep learning curve.

Table 3.4-3 Development Environment Comparison

Arduino IDE	Espressif IDE (ESP-IDF)
Extensive Library and Community Support	Extensive Documentation on its subsystems, configuration file, and API
Beginner Friendly – easy user interface and little configuration required	Steep learning Curve – more complex to use
Fast compiling time – helpful for developing and prototyping the code	Easy Scalability and continuously software updates, ensures compatibility with future ESP32 MCU

3.4.2.3 Why Arduino IDE?

The reason the Arduino IDE was chosen as the development environment for our project was due to its beginner friendly nature and its fast prototyping. The ESP-IDF has more hardware control over the ESP32, but this complexity is not needed for our project since the ESP32 will be enabling the switches on the load switch and the LED driver. The most complex part of the ESP32 is the Bluetooth capability but the Arduino IDE has multiple libraries that support Bluetooth capability for the ESP32. Thus, the Arduino IDE will be the development environment for our project to code the ESP32 for its beginner friendly nature, fast prototyping, and libraries that support the scope of what we want the ESP32 to do.

Chapter 4. Standards and Design Constraints

4.1 Industrial Standards

4.1.1 PCB Design Standards

4.1.1.1 IPC-2221

PCB design standards are developed by the Association Connecting Electronics Industries (formerly known as Institute for Printed Circuits – IPC) to establish a standard of practices in regards to PCB design, fabrication, and assembly (Ayodele). The IPC-2221 standard focuses on the practice for PCB design to ensure the creation of the design will lead to the manufactured of a PCB that is high-quality, manufacturable, and reliable (Ayodele). The standard goes over the material selection, board size and shape, component placement, trace and space, trace thickness, and thermal management.

4.1.1.2 Material Selection

The IPC-2221 goes over the guidelines on selecting the material the PCB should be made of based on the electrical and mechanical performance the designer is trying to create for the PCB. The IPC-2221 goes over common PCB material and explains which material should be selected based on the requirements of the PCB such as signal integrity, thermal management of the board, and the durability of the board (Smith). Choosing the proper material for the PCB ensures the reliability of the PCB to meet the required electrical performance, the board is thermal stable, and can safely operate within the desired environment (Wu).

4.1.1.3 Board Size and Shape

The IPC-2221 goes over the guidelines on the board size and shape to ensure the best compatibility and functionality of the board along with ensuring a smooth manufacturing and assembling process of the PCB (Smith). The guidelines goes over the aspect ratio of the board, the size limitations of the board, the placement of mounting holes, and the thickness of the board based on the intended use of the board and the environment it will function in (Wu). Following these guidelines will assist with the safety of manufacturing and assembling these boards and ensure the reliability of the PCB to fulfill its intended purpose and keeps the PCB to be secure when being mounted and structurally sound (Wu).

4.1.1.4 Component Placement

The IPC-2221 goes over the guidelines on the component placement to ensure the functionality of the PCB and the avoidant of thermal hotspots and interface between the components (Smith). The guidelines go over where the components should be placed on the board in relations to the other components and the trace routing between the components (Wu). Following these guidelines ensure the components function as intended without interference, prevent electrical shorts, considers the thermal management of the board, and allow easy accessibility to the components and traces for easy troubleshooting and adjustment (Wu).

4.1.1.5 Trace and Space

The trace and space guidelines in the IPC-2221 goes over the trace width and the trace spacing between traces to ensure the PCB are safe and efficient (Smith). Numerous IPC trace width calculators can be utilized to determine what is the best trace width for the PCB based on the current, temperature rise limit, and the board material (Smith). It is important to utilize the proper

trace width to ensure the required amount of current can travel through the traces without overheating the board and possibly melting the traces (Smith). Ensuring the proper trace width and trace spacing is important for the manufacturing process and the prevention of electrical shorts and tracing interferences amongst the traces (Wu).

4.1.1.6 Thermal Management

The thermal management in the IPC-2221 goes over different methods that can be utilized to dissipate heat from the PCB to ensure the reliability and increase the lifespan of the components on the board (Smith). The IPC-2221 offers the methods of considering the thermal conductivity of the material the PCB is made of, selecting the right amount of copper to utilize for the thermal dissipation, utilize thermal vias for components that dissipate a lot of heat, and the usage of heat sinks and fans to minimize thermal damage (Wu). It is important to manage the heat generation of the PCB to ensure an easier assembly process along with the proper current rating is being delivered to the necessary components to ensure the dependability on the performance of the PCB (Wu)

4.1.2 Communication Protocol Standards

4.1.2.1 USB-IF

The USB standard was developed by USB Implementers Forum (USB-IF), a non-profit corporation made up of various companies with the goal of developing a standard for USB (Poole). Establishing a standard for USB is important as it informs the customers that the USB cable is safe and reliable to use, the USB cable is compatibility with a variety of devices, and the USB cable has the ideal performance for data transfer and power delivery (Cablink). There are two different types of guidelines the USB-IF creates for the USB, cable type and USB versions.

4.1.2.2 Cable Type

Ensuring the proper USB cable type is utilized for the system is important as it ensures compatibility between the USB port and the USB plug. The two different types of USB cables utilized in our project are the USB Type-A cable and the Micro-USB.

The USB Type-A cable is utilized by the laser diode module to power the device. The USB Type-A cable is the most common USB cable type with its rectangular shape and used in a variety of devices such as computers, chargers, and wall adapters (Cablink). The USB Type-A cable supports a variety of USB versions (USB 1.0 to USB 3.2) but has the drawback of not being reversible in which the user is required to align the USB plug correctly when inserting into the USB port (Cablink).

The Micro-USB cable is utilized by the ESP32 to flash the code onto the microcontroller and to provide a connection between the laptop and the ESP32 when developing the code for our system. The Micro-USB cable is often utilized for data transfer and charging small, portable devices such as smartphones and tablets (Anker). There are two different types of the Micro-USB, Micro-A and Micro-B. Micro-A has a rectangular shape that is smaller than the USB Type-A version while the Micro-B has a rectangular shape that has tapered ends (Anker). The Micro-USB often support a variety of USB versions with the most common one being the USB 2.0 version (Anker).

4.1.2.3 USB Version

The USB-IF developed different USB versions with its own performance on data transfer and power delivery. The USB version that our project utilizes is the USB 1.1 to flash the ESP32 with our code and to prototype our code on the ESP32. The USB 1.1 was developed to improve upon various issues with the USB 1.0 version (Poole). The USB 1.1 offer Master/Slave interface with the main device being the Master while the other devices connected to the main device through the USB were the Slave (Poole). The USB 1.1 had a data transfer rate of 1.5 Mbps on the low speed side while at full speed, the data transfer rate was 12 Mbps (Poole). The USB 1.1 does not include the feature of having extension cables due to timing and power limitations (Poole). When a device connects to the main device through the USB 1.1, the device is limited to 100 mA on start-up and on steady use, the device is limited to 500 mA (Poole).

4.1.3 Lens Standards

ISO 10110 is an optical standard for the testing and classifying lenses. This is highly important when working with our collimating lens. ISO 10110 is used in optical applications involving lenses and optical surfaces. The standard first discusses material imperfections including bubbles and stress birefringence. This standard allows engineers to talk about certain optical parameters like focal length and curvature of lenses. We are using lenses in our project to collect light from an LED and then later focus the light onto a power meter. The key parameters we are using for our lens are focal length, diameter of the lens, and numerical aperture. These parameters are key in light collection. Since we are looking to maximize light collection we need a large diameter lens with a small focal length.

The focal length of the lens will also be crucial in focusing the beam onto our power meter. ISO 10110 defines clearly how to define focal length. This allows for easy determination of lens parameters for manufacturers and buyers of optical lenses. The coating of a lens is also defined by this standard. This ensures that the lens will perform to the desired specifications for a user. For example, in our project we have antireflective coatings for the visible range of wavelengths. These specifications are critical when designing optical systems that include lenses or mirrors. We used these standards to choose a lens that has a small focal length and large diameter to collect as much light as possible.

4.1.4 Laser Safety Standards

Laser safety is extremely important when operating any kind of laser. IEC 60825-1 defines how a laser is classified in terms of safety. The key parameters for a laser in terms of safety are wavelength and power of the beam. This standard classifies a laser with numbers from class 1 to class 4 with 1 being the least dangerous to 4 being the most. These parameters are key when working with lasers and tell a user how much safety is needed for normal use. This standard also defines a permissible exposure time called MPE. This exposure time is the maximum amount of time a person can be exposed to each class of laser. This MPE is determined by laser class. Also determined by laser class is the warning labels required to be placed onto different classes of lasers.

This standard is important in our project as we use lasers. Our lasers are class 2 lasers which is defined as visible lasers under 1 mw of power. The safety required for these lasers is minimal but careful protection is required. According to the standard the natural reflex to blink will protect the eye fast enough for these types of lasers. No filter glasses are required when working with these types of lasers. Safety is always key when working with optics and this standard helps anyone be safe with any laser devices in any project. If any high-power lasers are used this Standard would

tell the user how to properly use this laser with the safety required. This may include just wearing safety glasses or may include not being in the same room with the active laser. Each laser is different and therefore there needs to be a standard that tells the user how to be careful not matter which laser they are using.

4.2 Design Constraints

4.2.1 Power Constraints

A power constraint for our system is the AC to DC power conversion and ensuring the proper voltage rating is going into the components of our system. The AC to DC power conversion is an important consideration for our system since we are utilizing the power outlet to supply the power to our system. Thus, various adapters must be utilized to ensure the AC power from the outlet can be converted into DC power, the type of power that all our components in the system utilize. Three adapters are utilized in our system, the laptop adapter to power the laptop, the power adapter for the PCB, and the transformer in the DC power supply that converts the AC power to usable DC power for the motor.

When setting up the transformer of the DC power supply to convert the AC power to DC power, proper wiring and grounding must be done to ensure the DC power supply is working properly. Failure to ensure the proper wiring is being done can lead to the possibility of a fire starting or damage to the DC power supply itself. Thus, when setting up the DC power supply, extensive research was done to ensure the proper terminals were being connected, the proper AWG wire rating was being utilized to connect the terminals, and the proper grounding was being conducted.

Another consideration is stepping down the voltage rating of the DC power to the proper voltage rating that the component in the system utilizes. This will be done through the switching voltage regulator that will drop the 12 V DC power to 3.3 V for powering the ESP32. The LED driver chosen can utilize a 12 V input and thus, no voltage regulator would be needed for the LED driver. The USB-6002 is powered by the USB port connection to the laptop and the laser diode is powered by its own USB driver. When utilizing the DC power supply for the motor, we must ensure that the DC power supply is set to output a voltage of 15 V. Failure to do so can result in damage to the motor due to having too much voltage or can lead to the motor not working properly as it should be due to the faulty power line. Thus, a digital multimeter must be utilized to measure the output voltage of the DC power supply and a screwdriver will be used to adjust the potentiometer of the DC power supply.

Another power consideration is the effectiveness of the power management of the system. The ESP32 is constantly being run to blink a LED diode to showcase that the ESP32 was flash properly but it does lead to the ESP32 being on constantly. Another power management consideration is the movement of the motor in which even holding the motor at a certain angle led to the motor constantly consuming power to hold that position. This can lead to a large power consumption from our system and the possibly heating up of the servo amplifier.

4.2.2 Optical Constraints

When designing an optical system for our polarization switch we are limited by several optical constraints. Firstly, we must consider that to change polarization using a birefringent crystal the

light entering the crystal must already be polarized. This is not the case with LEDs but lasers do have polarized beams. This means we need to polarize the light as it enters our system.

Also, our extinction ratio is critically important to us. Extinction ratio is the amount of desired polarization divided by the amount of undesired polarization. This needs to be above 100:1 for our project. This is going to be limited by whichever optical component has the lowest extinction ratio. This means we need to choose polarizers with a high extinction ratio so that we can have the best chance at achieving a ratio above 100:1 from our crystal. However, the more precise our polarizers are the higher the cost.

Another constraint is the angle at which we need to turn our birefringent crystal. The retardation is solely dependent on incident angle into the crystal. This is because this angle changes the optical path length the light experiences as it passes through the system. If our incident angle is too large the path length increases to a point where our motors precision is not enough to achieve the desired polarization. This means we need to choose a range of angles to rotate our crystal that maximizes speed but also is not too large so that we cannot achieve enough precision for our system.

Our project sponsors are going to be using this system with visible light, so we need to make sure our coatings are for the visible range. This is a constraint for our components like lenses and power meter. These components need to have coatings that are antireflective for the visible range.

4.2.3 Practical Constraints

The fast polarization switch we are building uses many sensitive components that need to be maintained and kept in an environment where they remain secure from extreme temperature fluctuations, vibrations, and electric shock discharge. This prevents our system from operating outdoors or to be used in a mobile environment. Our MCU power supplies and DAQ all operate with a sub millisecond and microvolt level of precision to achieve such fine motor control these along with our servo amplifier are integral components and our system can not function without them. The servo amplifier, when in constant use generates heat that must be dissipated as the operating temperature must be kept below 130°F this ensures smooth and accurate control of our motor which is required to achieve the necessary precision in movement of our crystal. We are able to relieve some of the impacts by reducing the travel time, applying an offset in the optical design to reduce strain on the motor, reduce the load on the motor by selecting smaller and thinner crystals and to return to the zero position and the end of every operation cycle. These procedures along with mounting the servo amplifier onto a large thermally conductive surface while operating in temperature-controlled environment is key. The motors stopping precision and holding precision are just as integral to the operation and making sure the system meets the desired operating standards can be ensured by keeping the optical setup in a stable environment away from vibrations, preferably on a table that mitigates such influence, as any additional forces upon the crystal and motor during the operation of our device would increase the time it takes for the feedback on the servo to correct and for the crystal to stop rotating within the required time.

4.2.4 Time Constraints

Requirements of the project. The second and third months were spent researching parts and further narrowing down the overall system to fulfill the requirements. The final month was spent building the prototype to test and troubleshoot to present the prototype to showcase the validity of our final product. Another constraint is the delivery time. When researching parts, we had to consider the

possible lead time, availability of the product, and the delivery time of those parts. To migrate this issue, we made sure to choose parts that were available immediately (no lead time) unless the parts were highly specialized such as the crystal. Another consideration we had to consider was the sponsor's process in ordering these parts. Due to October being the start of a company's fiscal year, our sponsor gave us the deadline of the end of October to send a Bill of Material (BOM) list to them for the cost of the project to be added to next fiscal year budget consideration. Thus, when researching parts, we had to make sure to compile the BOM by the end of October and to make sure the parts were available to be delivered to us in November for us to assemble our prototype.

Additionally, another constraint is testing and troubleshooting. When we receive the parts, we need to make sure we have enough time to assemble these parts and test them to ensure they meet the requirements of the project. However, there may be issues and we would need to make sure we have enough time to troubleshoot those issues while still meeting the deadline to present our prototype. To migrate this issue, we made sure to immediately start working on building the prototype once the parts were delivered to us.

To migrate all these time constraints on our project, communications was a key part of ensuring we kept up with the deadlines of our project. As a group, we made sure to meet up at least once a week to discuss our task for the week. We would also have another meeting in the week to discuss the status of our tasks and to ask each other questions about the information we needed to complete the task. We would also have bi-weekly meetings with our sponsor to give updates on the project and ask questions to clarify the requirements of the project and what the sponsor was looking for from our product.

4.2.5 Economic

The other constraint in our project was the economic constraint. Our project has the benefit of having a sponsor that will pay for our parts with a budget limit of upwards to \$7,500. However, further discussion with our sponsor about the project budget reveals the budget was allocated to the cost of the motor and additional budget can be given to the project if goes beyond the \$7,500 cost due to the optics parts. Thus, when researching parts for our project, we had more flexibility in deciding parts that were higher in quality even with the higher cost.

However, there are some constraints that we need to keep in mind while researching parts. For our project, we wanted to keep the overall cost around \$10,000 to migrate the potential denying of parts from the financial department of the company. However, this constraint became an issue as we began to research parts for the motor system and the optics system. The optics system became increasingly expensive due to the number of parts we needed and the quality of those parts to ensure we meet the requirements the sponsor deemed necessary for this project. The motor system was also expensive due to its usage of the DAQ card and the galvanometer motor. The galvanometer motor also requires an additional DC power supply that led to a strain on the budget. Thus, a decision had to be made to decide which system would receive a greater portion of the budget to have higher quality parts. When discussing the requirements of the project with our sponsor, the sponsor emphasized the importance of the optics system and thus, it was decided that the optics system would receive a greater portion of the budget to meet the wants of our sponsor.

Therefore, due to a greater portion of the budget going into the optics system, some compromises had to be made with the motor system. When deciding on the DAQ card, we had to keep the budget in mind and thus, a cheaper DAQ card was chosen which led to the DAQ card having a smaller

update rate of 5,000 samples per second instead of choosing a more expensive DAQ card that has a higher update rate. Another compromise made was the choice of the motor in our system. Due to our group choosing a galvanometer motor for our motor system, we had to make sure that we chose a galvanometer motor that displayed its price. This is important to consider the strain the motor would have on our budget along with ensuring we would be able to receive the motor in time to build our prototype for the overall system; however, this did limit our galvanometer motor choice which led to us choosing a galvanometer motor from ThorLabs.

Another constraint with the economic side of the project is the potential unexpected troubleshooting. When submitting BOM to our sponsor, backup parts were not considered into the material list and thus, if any parts need to be replaced, they will most likely have to come out of our pockets. However, as mentioned earlier, some of the parts utilized in our project are expensive and thus, extra precautions will have to be taken to ensure these parts do not break while we are building our prototype such as following the recommended safety procedures as noted in the datasheet.

4.2.6 Scalability

Another constraint is the scalability constraint. Since this project is sponsored, when creating the overall system, we must keep in mind the potential uses our sponsor has for this project and the possibility of our sponsor expanding upon this project or potentially upgrading this project through changing certain parts for their use. When designing and creating our system, a couple of aspects of the project had to be kept in mind.

When choosing the software for our system, we had to consider the possibility of our sponsor wanting to edit the code for their use. This has become important as our system utilizes two software environments, Arduino IDE for the ESP32 and LabView for the motor control. When creating the system, it becomes important for us to have a detailed code commenting to ensure the sponsor understands what the code does so they can have an easier time adjusting the code for their usage.

Another consideration of the scalability constraint is the utilization of the crystal in the system. In the future, the sponsor may want to utilize a different type of crystal with the system and thus, having an easy way for the user to change out the crystal based on their needs would be beneficial to this task. Thus, when designing the motor system, it was kept in mind that the load might change especially since throughout the planning stage of the project, a defined crystal was not chosen yet and thus, the motor system needs to be flexible enough to handle a wide range of load while still meeting the requirements of this project.

Furthermore, our sponsor may want to change the motor for better performance. Thus, when setting up the motor system and the optics system, there needs to be a consideration of being able to easily change out the motor if our sponsor chooses to. This constraint can be migrated by designing a system in which the height of the optics system can be easily adjustable which would help free up our sponsor being restricted to choose a new motor with a similar height of our current motor.

4.3 Other Constraints

4.3.1 Sustainability

Sustainability is another constraint in our project. When designing the overall system, the lifespan of the system must be kept in mind as the sponsor will want a system that lasts a long time if they decide to use our system in the long term. This means that when we were choosing the parts for our system, we had to make sure the parts can be relatively easy to maintain and have a long-life span use.

A challenge to this sustainability is galvanometer motor usage. Motors generally have a lot of moving parts and need to be maintained to ensure the motor is performing at its best. This leads to a bit of a labor commitment to the maintenance of the galvanometer motor along with the potential understanding that the galvanometer motor may need to be replaced in the future if it no longer works.

4.3.2 Manufacturability

A constraint in our project is manufacturability since due to being college students, we are limited to utilizing the materials we have in the University labs to build our prototype and final product. This limits the complexity of our project as we must ensure that we can utilize the lab equipment to build the overall system and since the lab is a shared space, we also must consider how busy the lab is and how much of the equipment is available for use.

Another constraint of manufacturability is the replication of the project. If our sponsor decides to build another system like ours, the sponsor must also be able to reorder the same material as before. However, a challenge with this is the fact that our system utilizes a custom PCB board which means the sponsor would need to have a copy of the PCB board layout or create their own custom PCB board that would work with the system.

4.3.3 Political

ASML, the sponsor of our project, is a semiconductor company that has a large incentive to continue to improve their semiconductor products, especially with the rising demand for semiconductors throughout the world. Thus, when designing and building our system, a heavy emphasis from our sponsor was placed on ensuring the optics system meets the requirements of the project along with potentially meeting the stretch goals of our optics system.

Another political constraint of our project is the delivery of items. If parts in our system have to be delivered from a warehouse or from a company that produces the product outside of the country, the part may experience supply chain and trade regulation issues as the rules regarding tariffs are constantly changing, which may lead to delays in shipping. Thus, when researching parts, it was best for us to choose parts from companies that produce those items or the items are being held in a warehouse currently within the country.

4.3.4 Ethical

Ethical constraints in our project mean honesty in research and science, awareness for safety and societal impact. Following guidelines and Non – disclosure agreements given to us by our client ASML. Responsibly using our time and finances to be good stewards of the resources given to us by our client to achieve the goals they have asked of us. It means communicating with them on

what we could do and what we needed to do it. It also means being responsible for using AI in an appropriate way and properly referencing the sources we used to support our design and justify the component selection as well as the theoretical capabilities of our system. Another ethical constraint we should be aware of is the societal impact. Although ASML plans on using this product as a peripheral, this system has broader applications in many polarizations sensitive applications from biomedicine to communication security. Another constraint we kept in mind was repeatability we wanted to design a system based on existing technologies and experiments while expanding scope, pushing the capabilities of the system and achieving client goals. While documenting our process and choosing components that are readily available or where comparable technologies can also be applicable.

4.3.5 Health and Safety

A health and safety constraint of our project is the handling of the power supply in our system. For our system, we had to directly connect an AC power cord to the DC power supply. This handling of an AC power line in our project led to us being careful while utilizing the DC power supply in which we had to ensure the AC power line had proper grounding and the capacitors were discharged before turning on the DC power supply. Furthermore, the datasheet of the motor recommends connecting all the wires between the motor and the motor driver before turning on the power supply which led to us double checking the wiring to ensure everything is connected before turning on the power supply. During our experiment and characterization of our system we

will be utilizing class 2 Laser products these devices will have reflections that will be high power especially in our off state we need to be



Figure 4.3-1 Laser safety label for the laser we used in our setup identifying the hazards that come with this class of laser

aware of the direction of these beam dumps. As well as ensuring that they are blocked sufficiently to safely operate our devices. There are a variety of ways to do this our solution involved modifying the mounts of our Glan-Taylor prisms and surrounding our optical setup with beam blocks on the breadboard with cutouts for the wires.

4.3.6 Environmental

Another constraint of our project is the environmental constraint. The sponsor of the project did not note special conditions the system will be working under and thus, it can be assumed that the system will be working in an average office room at room temperature. Thus, when creating the PCB of our system, the PCB needs to be created with these average room conditions in mind. The system should be operated in a controlled indoor environment to ensure consistent operation and longer device lifetimes.

Chapter 5. Application of LLMs

Large language models (LLMs) have evolved immensely with the most popular of these platforms being ChatGPT. This model is developed by Open Ai and was released in 2022. These types of

platforms generate text based on a given input from a user. These models are given large amounts of text, hence the ‘large’ in LLM, to study and are designed to respond to users using the information they are given. Essentially the model “learns” from the internet and can quickly search for users’ questions and go through several sources to find correct answers. I have had this tool for several pieces of the project to quickly search for the answers to my questions. This model can effectively be used for research, but careful consideration is needed. Since LLMs searches the internet for answers it may come across misinformation and present it to the user as fact. This means while using software like this; one needs to carefully check the answers that come from it and cross-check it with your own knowledge and knowledge that you have researched. The best feature I have found using LLMs is finding specific technologies that can be used in the project like lenses. By telling ChatGPT I was able to input information like our LEDs full viewing angle and power to find a lens that would collect most of the light emitted from the LED. In this chapter we plan to show how LLMs have aided or hurt our progression in this project.

Each member of the team used these applications differently and of varied frequencies, but each of us tried to explore how LLMs could affect our research and the project as a whole. Our team decided to see how ChatGPT could help us with our project instead of other LLMs because of its popularity among laymen. We used this model for things like part acquisition even to general understanding of our project. Below we are going to explain how ChatGPT was able to respond to our questions and how we used this information.

5.1 ChatGPT Use Case 1

For the prompt given and the response from ChatGPT please refer to Appendix C [10a] and [10b].

ChatGPT was able to do a fantastic job explaining the main physics of our project. I appreciate how the model started with a basic understanding of polarization being defined on a fast and slow axis. The model seems to understand that since I am asking this question, I have a basic understanding of what polarization is and gives me an important clarification to my understanding. The model also starts with a brief answer to the question and then dives further into each component. This allows users to see the information they are looking for if they understand the topic and allows users who don’t understand to read further to gain further insight. The model does not give any mathematical equations for changing polarization which makes it difficult for the laymen to do a project like this because they will not be able to calculate the necessary factors to determine what kind of polarization one would get using a variable waveplate. The model should go over Stokes parameters and an overview of the Jones matrices for a simple setup of this type of experiment. The model gives a general overview of how to perform an experiment like the one used in this project and what is physically happening to the light as it goes through the waveplate. The model gives a general overview of the resulting polarization if the variable waveplate is tuned to different retardances and mentions the Poincare Sphere. These two points were never proven so it is important to fact check the model to make sure that the information output is accurate. In this case the model is correct about the outcomes of specific retardances and how this relates to the Poincare Sphere.

Asking more questions specifically aimed at these points would prompt ChatGPT to dive deeper into these points that it previously had lacked information on. I believe that ChatGPT was able to provide useful information and knowledge on how a system like the one we are designing in this project works. It does not dive into the math of the topic or the specific physics heavy information

probably because it is designed for laymen who would have a hard time understanding these topics. ChatGPT was able to give me enough information to understand the basic principles of variable retardance and its effect on polarization.

5.2 ChatGPT Use Case 2

For the prompt given and the response from ChatGPT please refer to Appendix C [11a] and [11b].

ChatGPT did a great job at deciding what kind of lens I may need to collimate my LED. It started by going into the math behind collimating an LED. It begins by showing how a user would find a lens with the correct diameter to create a beam of a specific size. The model does not know if I have any size constraints where certain focal lengths would not be suitable and so gives multiple examples of focal lengths and what kind of diameter lens one would need for these focal lengths. Importantly the model gives the equation showing how big a beam would be at a specific distance and tells the user that to collimate the beam the distance between the LED and the lens needs to be the focal length. This is important because it tells us exactly how to set up this system even though I did not ask for this specific information. This is useful in case a user thought that just placing the lens in front of the LED at any distance would collimate the beam. The equation that ChatGPT uses is also correct and it is also correct about the information on how to use the lens. Next ChatGPT gave only limited results for lenses. By just using this model it would be challenging to know all the options for lenses but the lenses they do give are viable options to use in this project. It is also good that ChatGPT gives links to these products so users know where they can purchase them. By using the method ChatGPT used to find these lenses the user would ensure that they capture all the light emitted in an 80-degree cone.

The model also gives the user insight into the potential mistakes that a user may face when buying a lens. This allows the user to understand how to use their desired lens. ChatGPT does not give the user any information on the different types of lenses and their uses, which would be helpful in finding other similar products. The model also does not give sources on how it finds the equation used to find the lens. The model also correctly gives further insight into other considerations for finding a lens like if we were looking to make a flat top beam and antireflective coatings.

I think ChatGPT successfully solved the problem of finding lenses for this case. It could have been more helpful if the model gave specific equations for finding how much power goes into the lens in case this is an important consideration for the audience. The model could have also given sources so we could find further information on how to compare lenses and how they differ from one another.

5.3 ChatGPT Use Case 3

For the prompt given and the response from ChatGPT please refer to Appendix C [9a] and [9b].

ChatGPT gave a short and concise response to this prompt. It first explains to the user that the price of these products depends greatly on what you need them for and how accurate they need to be. The LLM then gives a very long list of commercially sold items. It orders these items so that a user can easily see what the cheapest option is and what is the most expensive option. ChatGPT should have given a brief description of each item it gives the user and a comparison between items. It makes little sense to tell a user that the difference in prices depends on how well you need the system to run and then not tell how each system is run at a price range. It does give a concrete

option of 1 product from each of the low middle and high-cost groups of the product. It is very good that ChatGPT gave us a wide variety of price ranges and told us when we should use each price range.

We also noticed that ChatGPT has “remembered” other prompts that we have given it. At the end of the message, it gives us a tailored message to our needs asking if we need any DACs for engineering uses. This is a nice feature because it allows us not to have to describe to ChatGPT the entire project to get a specific answer to a question. To perform this feature ChatGPT reads through every previous conversation a user has had with it and then responds to the current prompt. The downside of this is that it uses quite as much processing power each time a user wants an answer to one question.

5.4 ChatGPT Use Case 4

For the prompt given and the response from ChatGPT please refer to Appendix C [13a] and [13b].

Unlike the normal routine of ChatGPT giving short concise responses in this case we have received a long response from this prompt. This makes sense because for all other prompts the questions were specific and showed an understanding of the topic from the user. This means ChatGPT already knew that the user had some background knowledge and therefore did not need to go as in depth as before. In this case with such a broad prompt ChatGPT seems to try to give as much information as possible for the user to be able to understand how a galvanometer works. The LLM gives few equations that show why a galvanometer performs the way it does in terms of speed and precision. Unfortunately, ChatGPT seems to also run into the same problem it has previously and gives no sources for the information it gives. Fortunately, on the other hand the information it gives is correct. Also, we wanted to test how the LLM responds to a multiple part question. ChatGPT does this effortlessly as it tailored its response to include speed throughout the entire explanation. Each time the software added a new point to its answer it tied this point back into how the speed of a galvanometer is affected.

The software also gave the user an idea of the smaller aspects of the motor and how to care for it. For example, the LLM mentions that because the motor is moving so quickly we are going to need to keep the motor cool for optimal function. At the end of the response ChatGPT gives an overall summary of everything it talked about. This summary is not as in depth as it should have been and anyone with a knowledge of galvanometers would have been able to give a more in-depth summary that someone would be able to understand. This summary should have included more details like how to use high bandwidth servo electronics or what the high-resolution sensors would do in the system.

5.5 ChatGPT Use Case 5

For the prompt given and the response from ChatGPT please refer to Appendix C [14a] and [14b].

We next wanted to see how ChatGPT handles visualization and specifically asked how to visualize a complicated topic. With all the questions that have been asked to ChatGPT it has understood that we have some optical background and made that assumption throughout the response it gave. We think this is a useful approach as mentioned before. It is useful for a software like this to gain an understanding of the user’s knowledge level. It does this by re-reading all the previous prompts it

has been given. This type of knowledge about a user is essential to answer questions to the best of the LLMs abilities.

The LLM begins by talking about Stokes Parameters. This is crucial to understanding the Poincare sphere. This would also be hard for a layman to understand. The LLM does not go into much detail into these parameters because it understands that the user has some optical background and assumes we already understand these parameters. It then nicely describes what the Poincare Sphere is using the Stokes Parameters. This shows strong continuity. The LLM understands the order in which to teach the user a topic. This is important because it allows the user to start from a point of understanding. This is exactly how we teach students in academia. We first start from a place of understanding and then move on to what we can learn from this understanding. This is a very smarty and thoughtful way to teach the user, and it is a very smart way for ChatGPT to teach a user.

The LLM describes where the different polarization states lie on the sphere. The LLM does not describe what polarization is, but we assume this is because it assumes we already know. Also, the LLM gives sufficient knowledge on how to achieve these different polarization states with waveplates. ChatGPT does not however give a picture of the sphere anywhere in the response. It supplements this picture for a MATLAB code that when run shows the entire sphere and gives an example of how to plot a polarization on this sphere. This is a very good way to allow an engineer to visualize the data, but it is not a good idea to tell a layman this information. This is also another case of the LLM understanding the users background knowledge. The best part of the response is something we have not seen yet in a prompt like this and that is recommended videos of the topic. This is extremely important for visual learners. This is the first time we have seen the LLM consider different learning styles when writing out a response and is a very thoughtful way of teaching a topic.

Overall, ChatGPT gave a great response to the topic and dove into many aspects of the sphere and what different points represent. The model should have provided a picture of the sphere instead of just giving the code to visualize the sphere, however the information the LLM gave was accurate and insightful. This prompt, like the previous also gives no source for any information given so it is highly important to check any and all information coming out of a system like this.

Chapter 6. Hardware Design

6.1 System Hardware Design

6.1.1 Power Supply Delivery

For our system, a single power input will be utilized to power our system. The single power input will be from the power adapter that will be plugged into the power jack. The power jack will then supply the overall voltage and current to our system which will be done through the voltage regulator and the LED driver. The system will have a 3.3 V regulator. The 3.3 V regulator will be utilized to power the ESP32-S3 microcontroller, the op-amps in the TIA circuit, and the DAC chip. The 3.3 V regulator will be on a separate board from the main PCB board for easy testing and troubleshooting of the voltage regulator to ensure it works properly before being added to the main PCB board. The TIA circuit will also be on a separate board from the main PCB board for easy

testing and troubleshooting to ensure the proper current to voltage conversion is being done before being added to the main PCB board. The LED driver will be utilized to power the LED and will be on the main PCB board. The DAC chip will also be on the main PCB board.

6.1.1.1 Voltage Regulator for Microcontroller

The 3.3 V regulator schematic was built based on the recommendations of the WEBENCH Power Designer given the requirements of a voltage input of 12 V, output voltage of 3.3 V, output current of 1 A, and utilizes the LM2575 component. However, a few adjustments were made to the recommended circuit to better match the needs of our system. An adjustment made to the circuit was the addition of the Blue LED to give an indication that the voltage regulator is working. The R1 resistor was added in series to the Blue LED to minimize the voltage and current going through the LED to ensure that the LED works as intended.

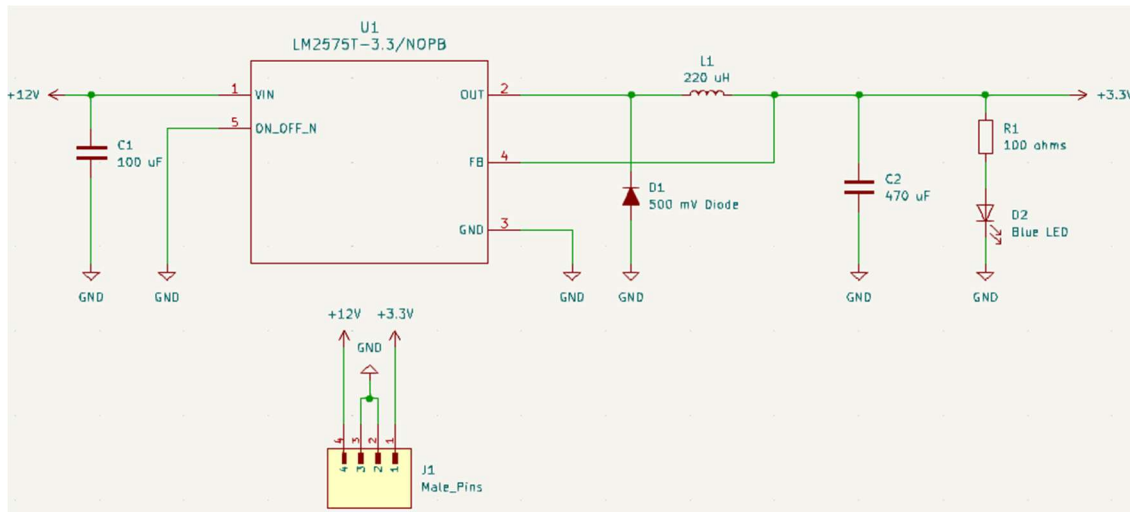


Figure 6.1-1

3.3 V Regulator Schematic with Male Pins for connection to main PCB board.

6.1.1.2 LED Driver

The LED driver will be utilized on the main PCB board. The J5 is utilized in the schematic to note where in the PCB board the screw terminal connectors are in which the wires of the LED driver will be inserted into for it to be connected to the PCB. The J6 notes the screw terminal connector in which the wires of the LED will be inserted into for it to be connected to the PCB for the LED to be powered by the LED driver. The blue LED was added as an LED indicator to assist with troubleshooting and to test the digital output of that ESP32-S3 pin.

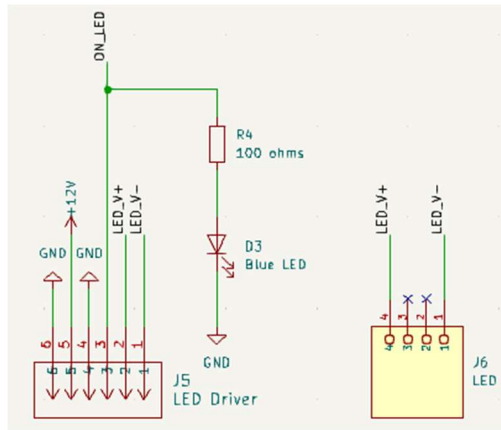


Figure 6.1-2

Screw terminal connectors for the LED driver and LED connection to the main PCB.

6.1.1.3 Voltage Regulator, TIA Circuit, and Power Adapter

The J2, J7, and J3 are utilized in the schematic to note where on the main PCB board the 3.3 V regulator, the TIA circuit, and the power adapter will be held. The 3.3 V regulator and the TIA circuit will be on a separate board and thus, the size and positioning of the 3.3 V regulator and the TIA circuit will need to be considered when designing the PCB board. The power adapter wires will be inserted into the screw terminal connectors and thus, the J8 will act as the connector indicators.

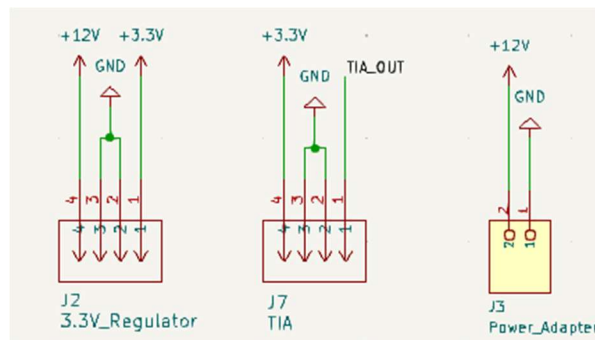


Figure 6.1-3

Female Headers for 3.3 V Regulator and TIA circuit to connect to the main PCB board and screw terminal connectors for the Power Adapter connection to the main PCB to power the system.

6.1.2 TIA Circuit

6.1.2.1 TIA Op-Amp

The R2 is the feedback resistor of the TIA circuit. It was calculated with the formula:

$$\frac{V_{max} - V_{min}}{I_{max} - I_{min}}$$

The max output voltage from the TIA circuit is set as 3 V to ensure that we do not saturate the op-amp. The max input current going into the TIA circuit is set as 9 mA. Inserting these numbers into the formula, we get R2 to be a resistor value of 332 Ω .

To help with the noise issue, C2 was added to the TIA circuit as a feedback capacitor. It was calculated with the formula:

$$\frac{1}{(2\pi)(R_f)(BW)}$$

The bandwidth is set as 10 MHz as this is the bandwidth of the chosen photodiode in our system. Inserting these numbers into the formula, we get C2 to be about 43 pF.

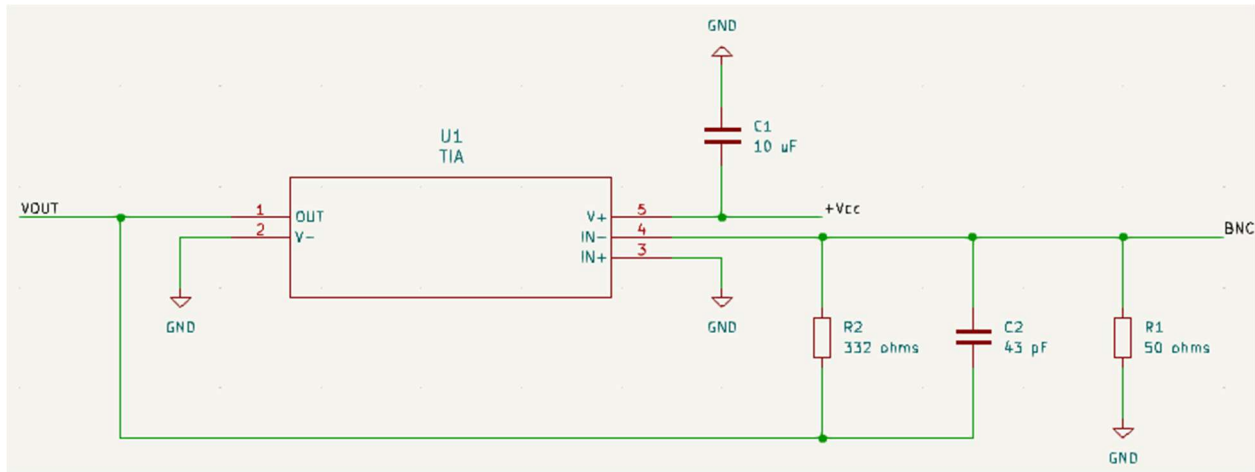


Figure 6.1-4

TIA Circuit that converts the input current from the photodiode into a voltage value.

During Senior Design 2, there were issues with soldering the TIA circuit onto the PCB. The R1 component was left off the board to help with troubleshooting the issue.

6.1.2.2 Gain Op-Amp

The TIA circuit was originally designed to be utilized with both the LED and the lasers. However, it was decided to only use the TIA circuit with the LED to verify the switching time of the motor. Thus, the gain op-amp became a unity gain op-amp.

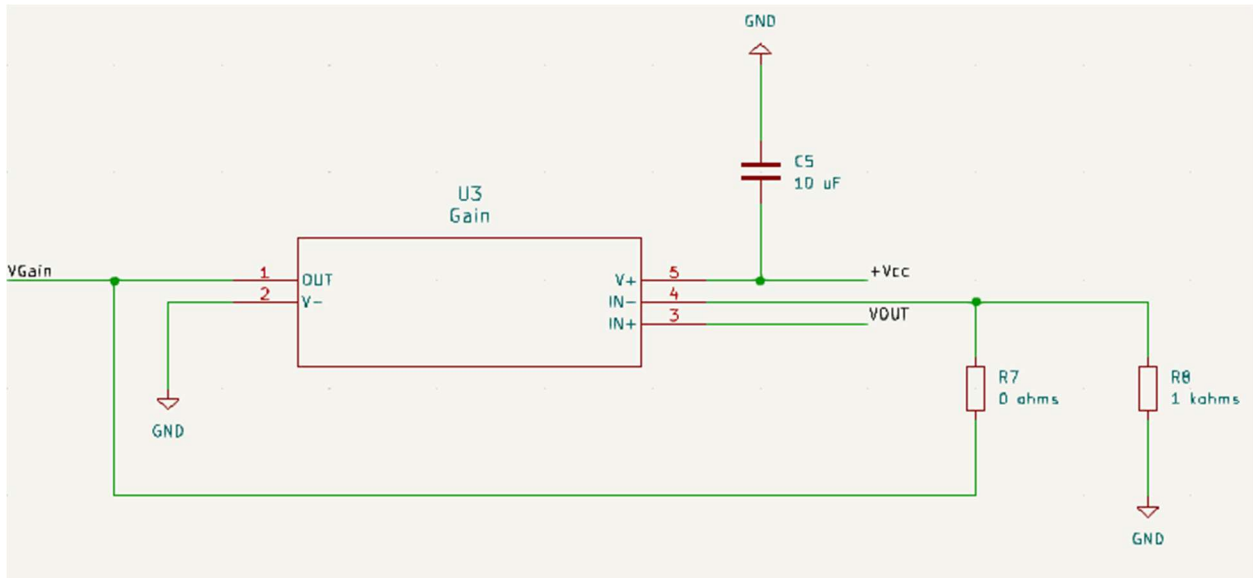


Figure 6.1-5

Unity op-amp that can be changed into a gain op-amp if needed.

During Senior Design 2, when testing our optical setup, it was realized that the LED was outputting a much lower power than expected. Thus, it was decided that the laser would be utilized instead to verify the switching time of the motor. R7 was changed to be 51 k Ω and R8 remained the same at 1 k Ω for a gain of about 52.

6.1.2.3 Low Pass Filter Op-Amp

The low pass filter was designed to have a cutoff frequency of 25 kHz since the ESP32-S3 analog-to-digital converter (ADC) was set to have a frequency reading of 50 kHz. The R3 and R4 was utilized to have a resistor value of 800 Ω to achieve the 25 kHz cutoff frequency.

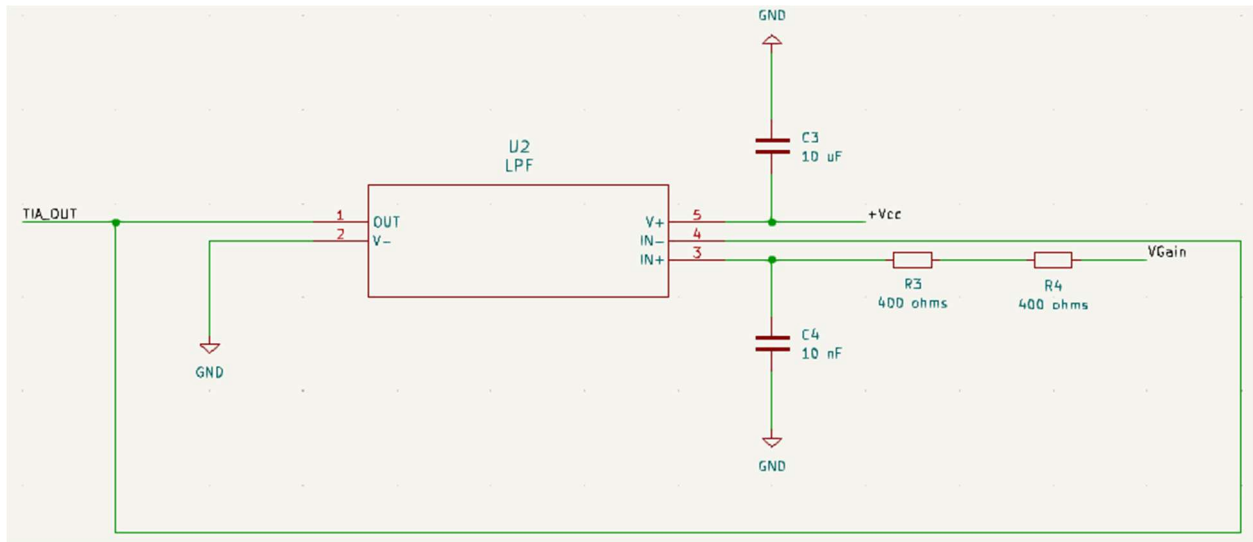


Figure 6.1-6

Low Pass Filter Op-Amp with a cutoff frequency of 25 kHz.

6.1.2.4 TIA Circuit Headers Connection

The TIA Circuit PCB utilized male pins (J1) to connect to the main PCB board. A voltage divider was utilized to bring the 3.3 V from the voltage regulator down to 3 V to ensure we do not accidentally fry the ESP32-S3 by sending too much voltage to the module. The BNC connector (J2) was utilized to connect the TIA circuit PCB to the photodiode since the chosen photodiode utilizes a BNC connector to transfer the output current to the oscilloscope.

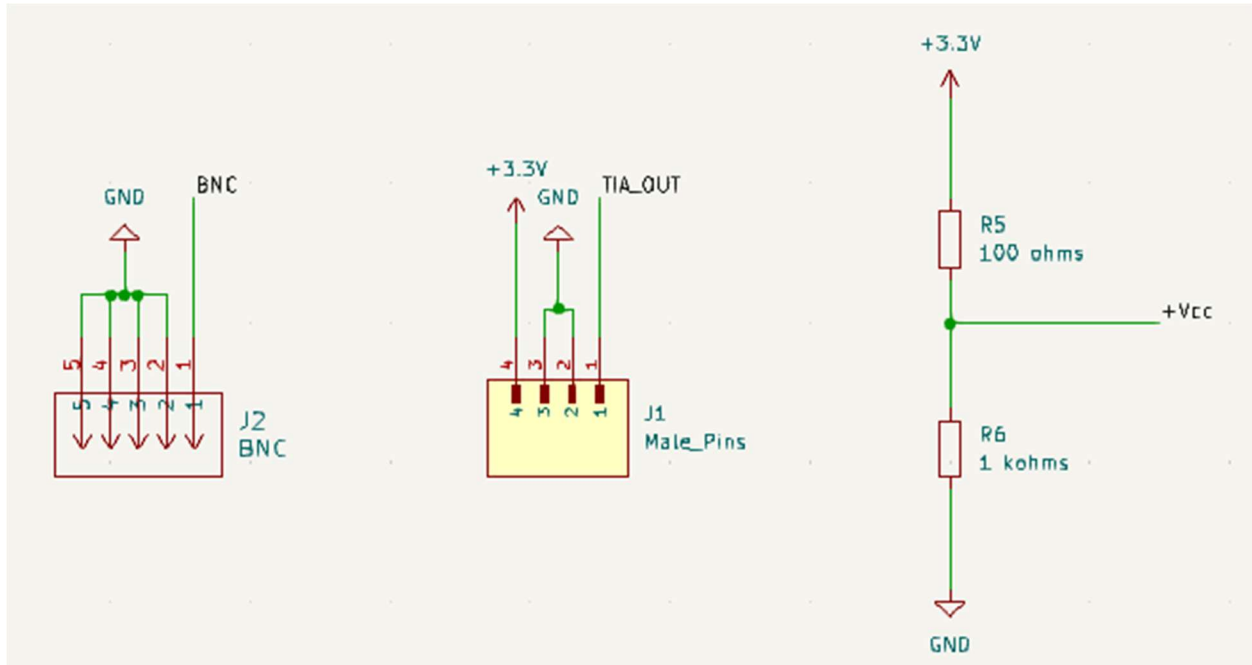


Figure 6.1-7

BNC Connector for the TIA circuit to connect to the chosen Photodiode, Male Pins for the TIA circuit to connect to the main PCB board, and Voltage Divider for 3 V.

During Senior Design 2, the voltage divider did not properly bring the voltage down to 3 V and was instead bringing the voltage value down to 1.5 V. It was decided to get rid of R6 and the R5 was replaced with a 0 Ω resistor.

6.1.3 Microcontroller Connection

6.1.3.1 Microcontroller Pins Configuration

For our prototype, an ESP32 development board will be utilized but for the PCB board, a ESP32-S3-WROOM-1U-N8 module will be implemented instead. The schematic was created based on the ESP32-S3 development board schematic datasheet. The ESP32-S3 development board can take 5 V due to having an internal voltage regulator that takes the 5 V to 3.3 V. Thus, for our PCB board, the ESP32 will be powered directly by the 3.3 V regulator through the 3.3 V pin on the ESP32.

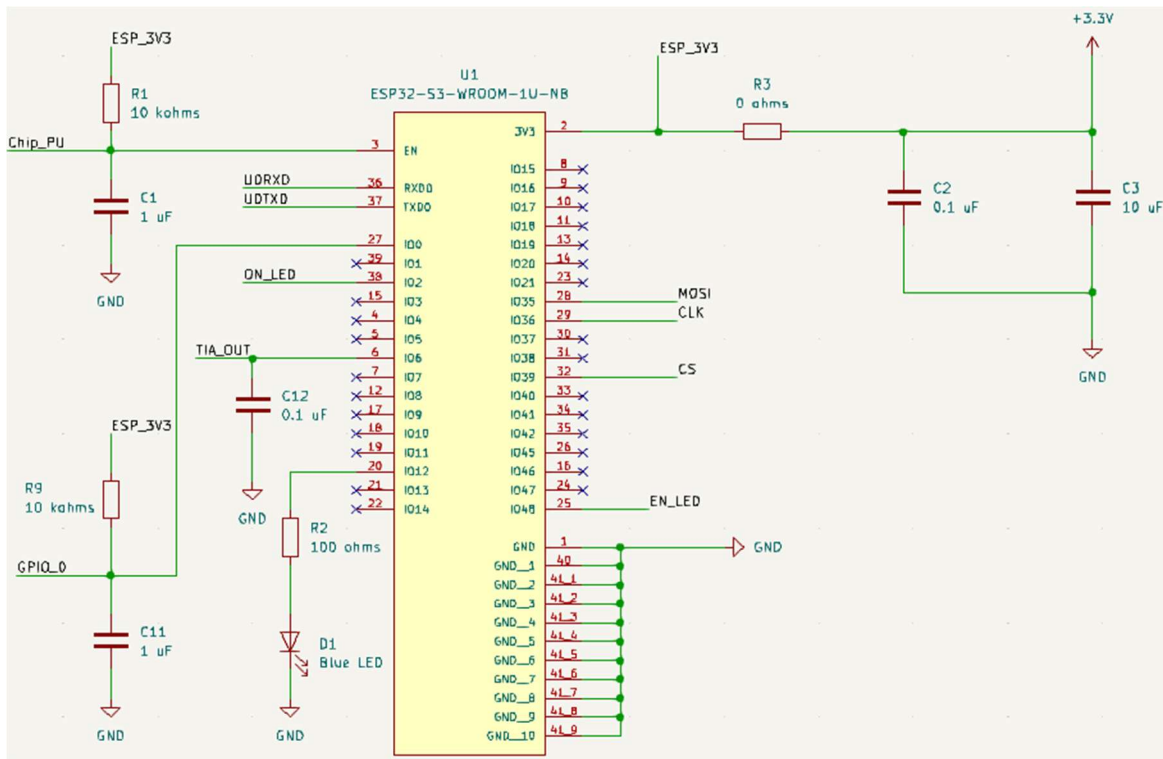


Figure 6.1-8

ESP32-S3 Pin Configuration Schematic on the main PCB.

6.1.3.2 Boot and Reset Buttons

The schematic for the buttons was created based on the ESP32-S3 development board schematic datasheet. The buttons the ESP32-S3 utilizes were not available and thus, an alternative button had to be used instead. The buttons will connect to the Boot and Reset pins of the ESP32 and will function in assisting the process in flashing the code to the ESP32-S3 as the ESP32-S3 needs to be in download mode to receive new code. The Reset button was utilized to reboot the ESP32-S3 to begin executing the latest flash code on the module.

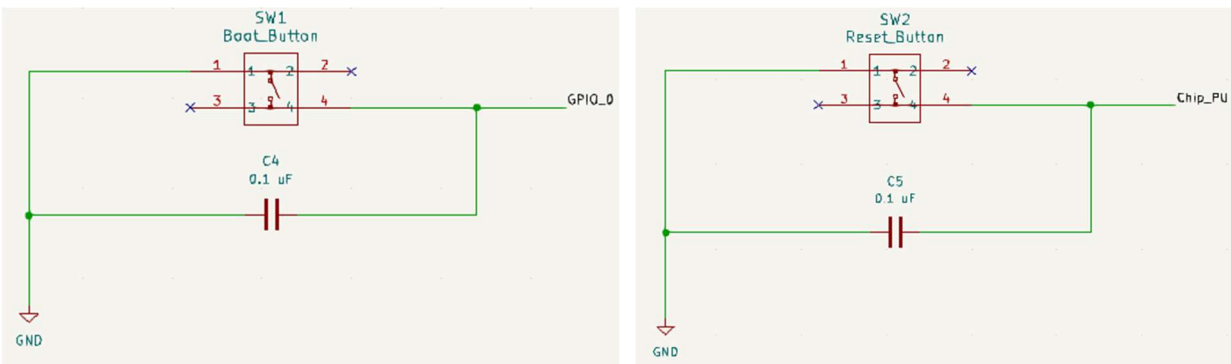


Figure 6.1-9

Boot and Reset Buttons connection to the ESP32-S3 pins.

6.1.3.3 USB and UART Connection

The ESP32-S3 development board supports USB connection and UART connection to flash code onto the ESP32-S3 but for our PCB, we need to build the connection itself. It was decided to utilize the UART flash method as it is more reliable than the USB in flashing the code. Thus, the USB connector in its data and power buses is connected to the chosen USB to UART chip in order to flash the code onto the ESP32-S3 on the main PCB.

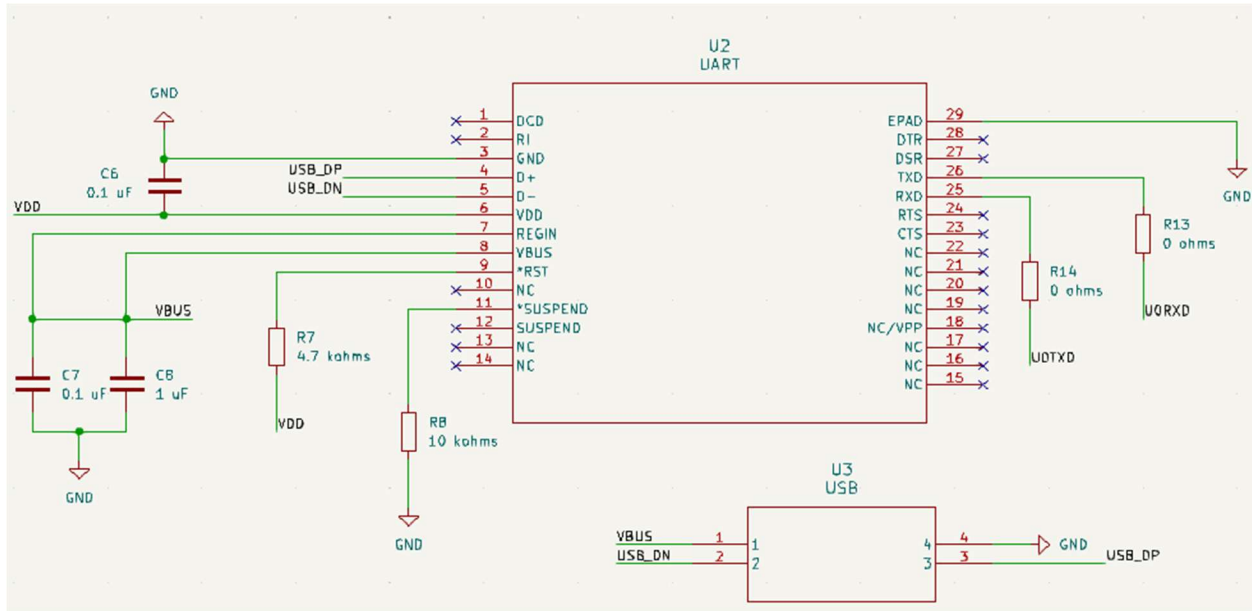


Figure 6.1-10

USB Connector connection to the USB to UART chip to flash code onto the ESP32-S3 on the main PCB.

6.1.3.4 DAC Chip Connection

The R11, R12, and R10 are series resistors for the SPI communication protocol of the DAC chip to assist with the noise issue and the performance of the data transfer (Cadence System Analysis). The C9 and C10 are added based on the PCB layout recommendation from the DAC chip datasheet to assist with minimizing the power supply noise to ensure a clean output voltage value.



Figure 6.1-11

SPI Communication connection between the DAC Chip and the ESP32-S3.

6.1.3.5 DAQ Card Connection

J4 is a screw terminal that was utilized to connect the output digital pin of the DAQ card to the PCB board to be transmitted to a pin on the ESP32 for the ESP32 to read to know when the user wants to turn on the LED. This was done instead of utilizing the Bluetooth/Wi-Fi capability of the ESP32-S3 since it was simpler solution. A Green LED was added as an indicator to showcase that the DAQ card is outputting a digital voltage with R1 being added in series to the Green LED to ensure the proper voltage and current ratings are going to the Green LED. The R6 and R15 were added as a voltage divider to bring the 5 V from the DAQ card down to 3.3 V for the ESP32-S3. Pins on the ESP32-S3 are only able to receive a maximum voltage rating of 3.3 V. Thus, the voltage divider was added to ensure the proper voltage is going into the ESP32-S3. J1 is a screw terminal that was utilized to connect the output voltage from the DAC chip to be read by the analog input reading of the DAQ card as this information will be displayed to the user.

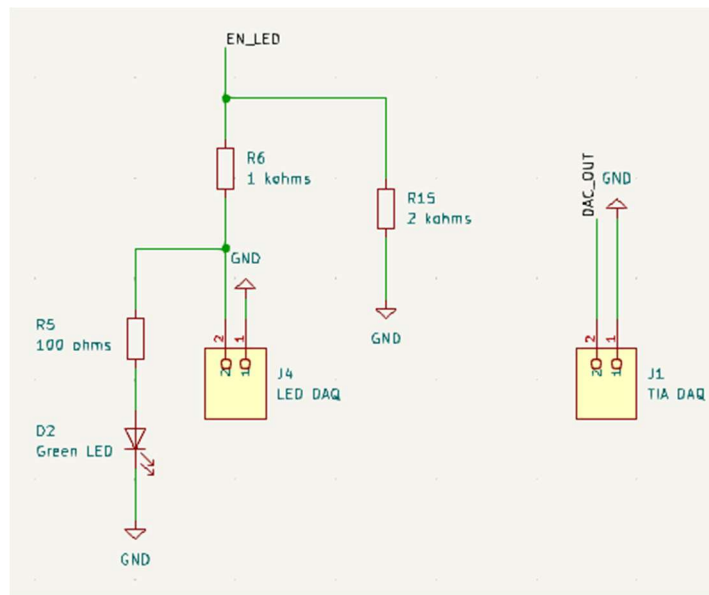


Figure 6.1-12

Screw Terminal Connections between the PCB and DAQ Card.

6.1.4 Double-Pass Beam Calculations

It is important to know the beam diameter and power of the beam as we get to the power detector. This will tell us how much power difference we can expect when switching polarization states. We need to achieve 20mW of optical power so that we can achieve our goal.

6.1.4.1 Beam Diameter

First we need to make sure all of our LED light is being collected by our lens. To do this we use the divergence of the LED which is 80 degrees full angle. At the focal length of the lens the LED beam will be 0.013m which leads to a beam diameter of about an inch. This means that all our beam will go into the lens and be collimated. To find the beam diameter we find the diameter of our collimating lens for our LED. This is a 1-inch diameter lens which means our beam is going to be 1 inch. From the lens our beam is going to approach our mirror. This mirror has a diameter of 7mm which means our beam is now going to be 7mm.

This will be focused by our focusing lens. The diameter of the beam will then be determined by the distance from our meter to the lens. This distance will be 8mm. To find the diameter of the beam on the power meter we use the formula:

$$w(z) = w_0 \sqrt{1 + \left(\frac{\Delta z}{z_R}\right)^2}$$

Which leads to a beam diameter of 3.5mm at the diode.

To find the diameter of the laser we use its divergence which is 0.6mrad. We use geometry and laser information to find the beam diameter and when it's greater than our mirror diameter since this is the smallest diameter optics we have. We know that the beam diameter is 3mm at 50mm distance. Using the formula

$$\tan(\theta) = \text{radius}/\text{length}$$

we can find our beam diameter at any length from the laser diode. We first need to get our original beam diameter at the face of the laser. To find this we use $\tan(0.6 \text{ mrad}) = D/50 \text{ mm}$. This means our original beam divergence at 50mm is 0.00003 m. If we subtract this from the diameter measured at this distance, we get our original distance $D_0 = 2.97 \text{ mm}$. Using this we can determine that to get to a diameter of 7 mm the laser would have to travel 6.72 m using the same method we used to find the diameter at 50 mm. Since our beam will not travel anywhere near this distance, we will collect all this light into our detector. We find the diameter of the beam to be 3.27 mm at the lens.

6.1.4.2 Power and Irradiance Considerations

If our LED is collimated at 1 inch diameter from the lens and only 7mm gets reflected from the mirror we are losing 72.44 % of power. This leads to our beam having a power of 320 mW after the first mirror. The limiting factor for using the LED is divergence after the lens. Using the divergence formula of

$$\theta = d/f$$

and inputting our lens and LED information we get a divergence angle of 3.6°. This divergence is going to constantly bleed optical power from the LED depending on how large the optical path length is. We expect that we will experience a much lower power due to the

For each laser there will be no power loss because there is no divergence. This leads to a power of 0.9mW for the laser power measured by the detector. Since the power meter has a noise equivalent power down to the 10^{-14} W we will easily be able to see this power.

6.1.5 Single-Pass Beam Calculations

6.1.5.1 Power calculations

The diameter of both beams will be approximately the same in each case. This is because the optical path length is changing by a negligible amount between setups. The power will drastically change. This is because we are using less beam splitters. Using the same calculations as before we see that we will have a power still dependent on the distance traveled by the LED beam because of the divergence. Since the beam diameter stays the same between systems this gives us an irradiance of 3.33 W/cm^2 . The laser will have a power of 0.9 mW.

6.1.6 Motor Mount Design

The angle of the motor needs to be very precise. The crystal needs to sit at a 45 degree angle from the optical axis and rotate on the 45 degree axis. This means we need to design our motor mount to hold the motor at a 45 degree angle as well as allow it to rotate at this angle. To achieve this we used Onshape to model a mount that the motor can screw into that will hold it at this angle. The mount will be able to screw into the optical breadboard for stability. Below a model of the mount can be seen with the motor attached.

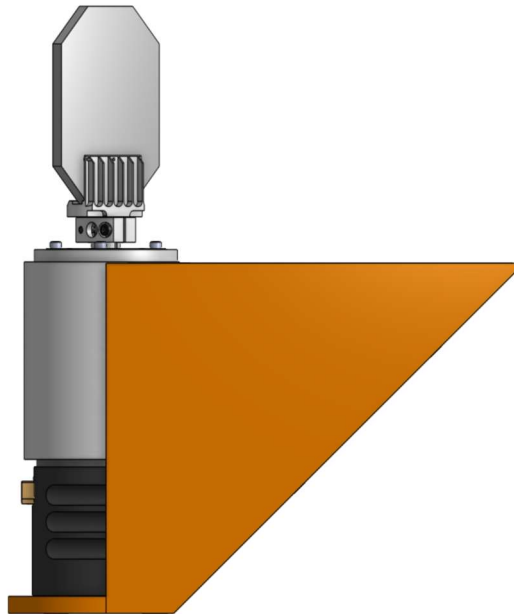


Figure 6.1-13

This figure shows the motor sitting on the designed mount. The mount will then be screwed into the optical breadboard with the angled piece being the part of the mount that creates the angle of the motor that the crystal will have.

Chapter 7. Software and Simulation Design

7.1 Simulation Design

7.1.1 MATLAB

MATLAB is an environment that is well suited to the task of simulating polarization experiments allowing us to work with stokes parameters easily by employing toolkits. MATLAB's matrix-oriented architecture and visualization tools allow for easily implementing Jones's calculus. The native syntax makes it easy to perform the calculations intuitively by representing light using Jones vectors and modeling optical components like polarizers and wave plates using matrices. Then simulate the effects of these components through matrix multiplication. Visualizing the results with built in tools to plot polarization as well as changes in power by function of changing the rotation of the crystal.

The addition of toolboxes and community contributed libraries that provide functions for computing the polarization parameters such as degree of polarization and the components for the Poincare sphere. These resources streamline the simulation process and ensure consistency with established models. MATLAB's integration with experimental hardware via serial communication and data acquisition toolboxes allows you to compare simulated results directly with live measurements, making it a platform for modeling and validation. With clear reusable code that allows for adapting our experimental setups for adjustments to different types of crystal or various powers and frequencies of light.

7.1.2 Mathematical Principles

The mathematical principals behind the polarization control using the z – cut quartz can be determined when assuming a monochromatic and collimated beam. The change in phase delay $\Delta\phi(\theta)$ as a function of rotation angle is written as

$$\Delta\phi(\theta) = 2\pi \frac{\Gamma(\theta)}{\lambda} = \frac{2\pi}{\lambda} n_o d \left(\sqrt{1 - \frac{\sin^2 \theta}{n_e^2}} - \sqrt{1 - \frac{\sin^2 \theta}{n_o^2}} \right) \quad (1)$$

Here λ is the wavelength d is the thickness of the quartz plate and n_o , n_e are the refractive indices for the ordinary and extraordinary components. Where the Jones Matrix of the Rotating z – cut quartz is shown to be

$$\mathbf{Q}(\beta, \theta) = \begin{pmatrix} Q_{xx} & Q_{xy} \\ Q_{yx} & Q_{yy} \end{pmatrix} = \begin{pmatrix} \cos^2 \beta + e^{i\Delta\phi} \sin^2 \beta & (1 - e^{i\Delta\phi}) \sin\beta \cos\beta \\ (1 - e^{i\Delta\phi}) \sin\beta \cos\beta & \sin^2 \beta + e^{i\Delta\phi} \cos^2 \beta \end{pmatrix} \quad (2)$$

Here β is the angle of pitch applied to the crystal by how the rotator is mounted, if $\beta = 0, \pi/2$, Parallel or orthogonal to the x - axis, the \mathbf{P} and \mathbf{S} polarizations will not experience rotation due to \mathbf{Q} becoming a diagonal matrix. These positions of the mounted crystal will not function as a waveplate, ensuring those off diagonal components having a value for β of $\pi/4$ can be achieved by applying a 45° pitch to the rotator mount.

Using the Jones matrix, we can solve the electric field of the output beam for single and double pass configurations. Those expressions are

$$\mathbf{E}^{(S)} = \begin{pmatrix} E_x^{(S)} \\ E_y^{(S)} \end{pmatrix} = \mathbf{Q} \left(\frac{\pi}{4}, \theta \right) \cdot \mathbf{E}_i = \frac{1}{2} \begin{pmatrix} 1 - e^{i\Delta\phi} \\ 1 + e^{i\Delta\phi} \end{pmatrix} \quad (3)$$

$$\mathbf{E}^{(D)} = \begin{pmatrix} E_x^{(D)} \\ E_y^{(D)} \end{pmatrix} = \mathbf{Q} \left(-\frac{\pi}{4}, \theta \right) \cdot \mathbf{M} \cdot \mathbf{E}^{(S)} = \frac{1}{2} \begin{pmatrix} 1 - e^{i2\Delta\phi} \\ -(1 + e^{i2\Delta\phi}) \end{pmatrix} \quad (4)$$

Here \mathbf{M} is the Jones matrix for a mirror under normal incident light and $\mathbf{Q} \left(-\frac{\pi}{4}, \theta \right)$ is the matrix representing the retro – reflected light. Implementation of a polarizing beam splitter (PBS) allowed them to vary the transmitted power this variance is given by $P_x^{(S)}, P_y^{(D)}$ for the single and double pass configurations respectively. These are

$$P_x^{(S)} = \left| E_x^{(S)} \right|^2 = \sin^2 (\Delta\phi/2) \quad (5),$$

$$P_x^{(D)} = |E_x^{(D)}|^2 = \sin^2(\Delta\phi) \quad (6)$$

7.1.3 Stokes' Theorem

The mathematical theorem we employed to determine the output polarization state of our light was based on the Stokes' parameters. This method involves converting the E_x and E_y fields into parameters that allow us to map this field into a 3-Dimensional sphere, this sphere is called the Poincaré sphere. This sphere contains every possible polarization state where the parameters are defined by the electric fields and then converted to x, y, and z values. With an electric field defined as $E = \begin{pmatrix} E_x \\ E_y \end{pmatrix}$, a Jones vector is converted to Stokes' parameters using the following formulas. $S_0 = |E_x|^2 + |E_y|^2$, $S_1 = |E_x|^2 - |E_y|^2$, $S_2 = 2 \cdot \text{Re}(E_x E_y^*)$, $S_3 = 2 \cdot \text{Im}(E_x E_y^*)$

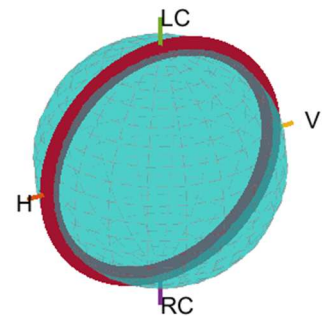
- pAfter evaluating the Stokes' parameters namely S_0 , which defines the magnitude of intensity. S_1 , being the portion of the magnitude that is in the horizontal or vertical polarization direction, or x direction in the Poincaré space. S_2 corresponds to the portion of magnitude in the $\pm 45^\circ$ polarization or the y direction. Lastly the S_3 parameter represents the portion of the magnitude in the Left/Right-handed circular polarization or the z direction. The formulas used to convert the parameters to the x, y and z values are $x = \frac{S_1}{S_0}$, $y = \frac{S_2}{S_0}$, $z = \frac{S_3}{S_0}$. The Poincaré sphere that is created by these equations verifies the findings in our background paper. Showing an axis of transition that goes from our input state moving through circular polarizations eventually reaching the orthogonal target state. The plot that corresponds to the conditions that match the paper is represented in this figure. This figure corresponds to a total crystal rotation angle, of 10° , namely from $10^\circ - 20^\circ$. This rotation angle shows multiple rotations through the Poincaré space. This finding went against our initial interpretation of the paper. With our original assumption being that the transitional states would correspond to an axis that traveled through the $\pm 45^\circ$ axis of rotation to further verify the accuracy of our results by introducing a quarter-wave plate to the system, which should convert circular polarization states into 45° ones and vice versa. The results of that implementation are as follows. This result further verifies the accuracy of our simulation being supported by the current understanding of polarization modulation and allows us to move forward with confidence into the next part of the simulation, a broadband source, as well as accounting for optical losses due to the components within the system.

7.1.4 Calculating Theoretical PER

To estimate the PER (Polarization Extinction Ratio) we calculated the power contained in each of the electric field components of the Jones vector and converting to dB we are able to estimate the PER through our chosen Calcite crystal, we are able to do this across various wavelength ranges using the aforementioned Sellmeier equations the formula used to compare the electric field

Poincare Sphere

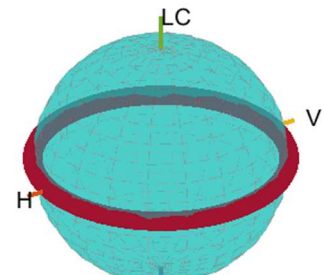
Figure 7.1-2



The corresponding polarization response of our system when going through multiple cycles.

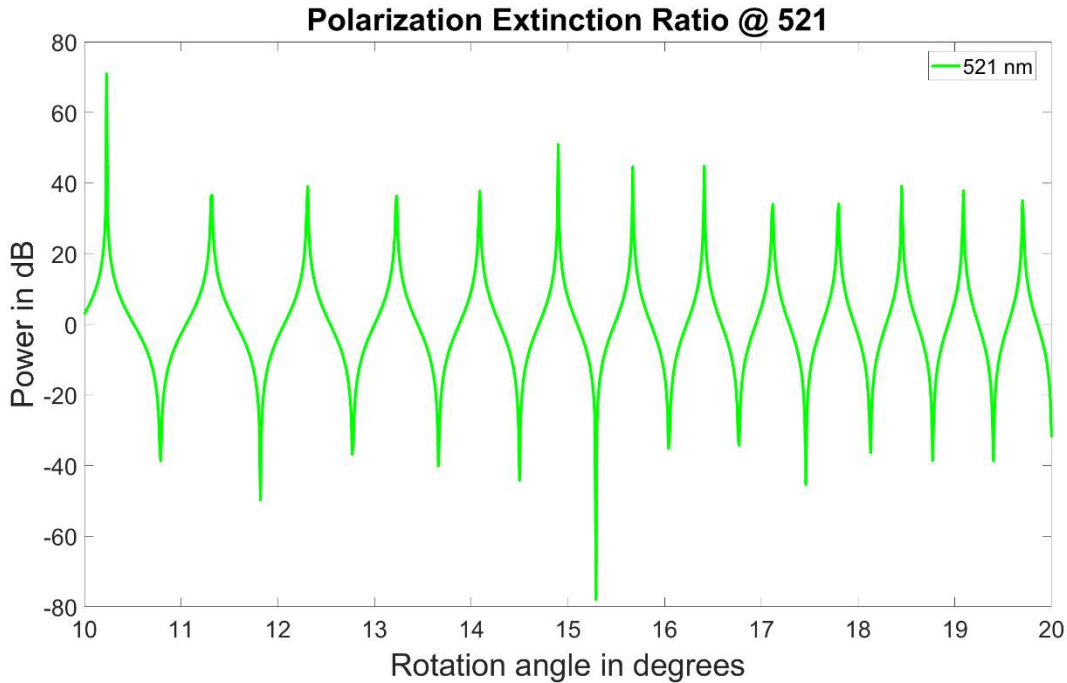
Poincare Sphere

Figure 7.1-1



Polarization response of our system when passing through multiple cycles with a static QWP

components and calculate the PER using this formula $PER = 10 \log_{10} \frac{|E_x|^2}{|E_y|^2}$ to look at the PER from the perspective of the horizontal polarization this corresponds to our cross polarizers having the horizontal orientation on our output polarizer.



This plot shows PER using our designed calcite crystal a sweep of 10°-20° showing the relative dB where any location on the plot that corresponds to 30 dB and the closest deep negative dB corresponds to the Ideal point for this single Wavelength.

Figure 7.1-3

This plot elucidates the response for a single wavelength which can be sufficient to estimate a narrowband emission on your light source or a single nanometer linewidth laser. To simulate the PER response of our broadband source and identify locations that will work over a range of about 30 nm more work is required, starting with gathering information on the light source. Namely finding the normalized/relative intensities or each wavelength of the emission spectrum, accurately weighting the intensity of each wavelength, then by utilizing the Sellmeier equations we can now see how the refractive index and intensity is dependent on wavelength this allows us to select a position that will maximize the number of wavelengths that achieve a 30 dB change between on and off states. The corresponding plot follows on the next page

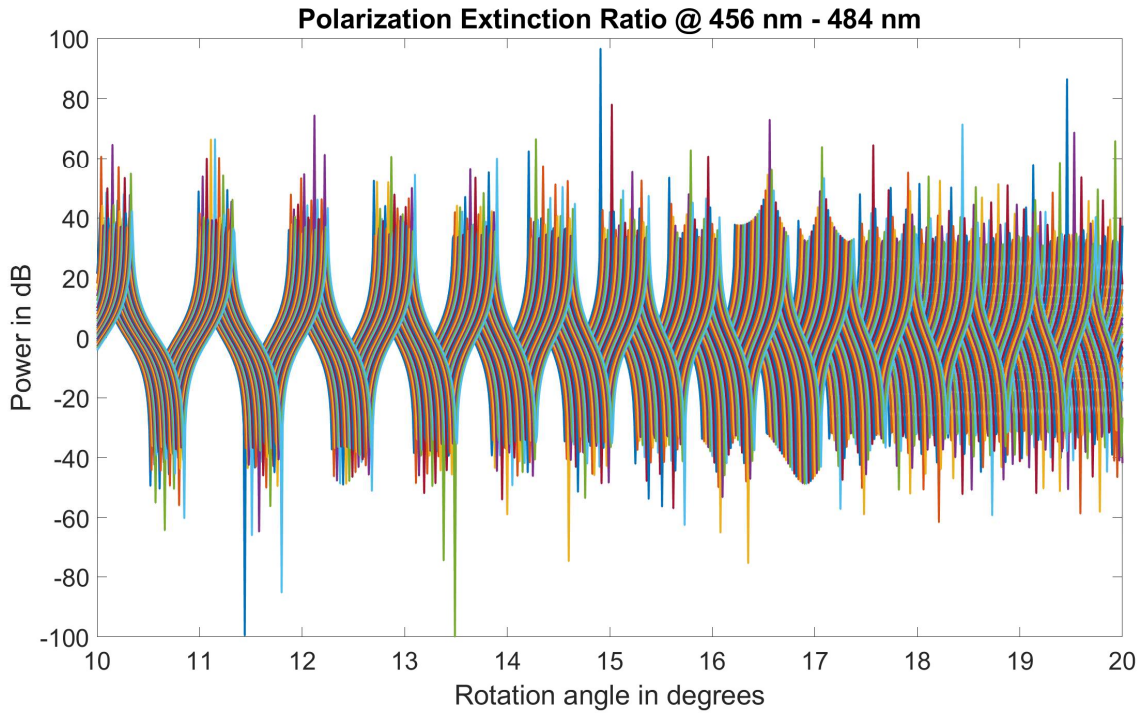


Figure 7.1-4

This plot shows PER depending on rotation of our crystal and wavelength it shows the response of 1 mm thick calcite being rotated between 10° - 20° The wavelength range plotted corresponds to 456 nm-484 nm which is the same range as the full width half max of the LED we chose, with a center wavelength estimated around 470 nm.

It's important to note that early on namely in the 10° - 13° range, we see narrower peaks in the pattern this means that staying in the regime that is closest to normal will give us more overlap between wavelengths. However, there is a tradeoff between getting closer to normal and the distance our motor must travel being extended as well as more power lost to back reflections. We believed it was best to stay between 10°-12° due to this factor.

7.1.5 Simulating the “Broadband” Response of the System

7.1.5.1 Simulating Power Response

From the PER we can estimate the best rotation angles to choose and zoom in further to get a closer look at the exact response of our operation protocol.

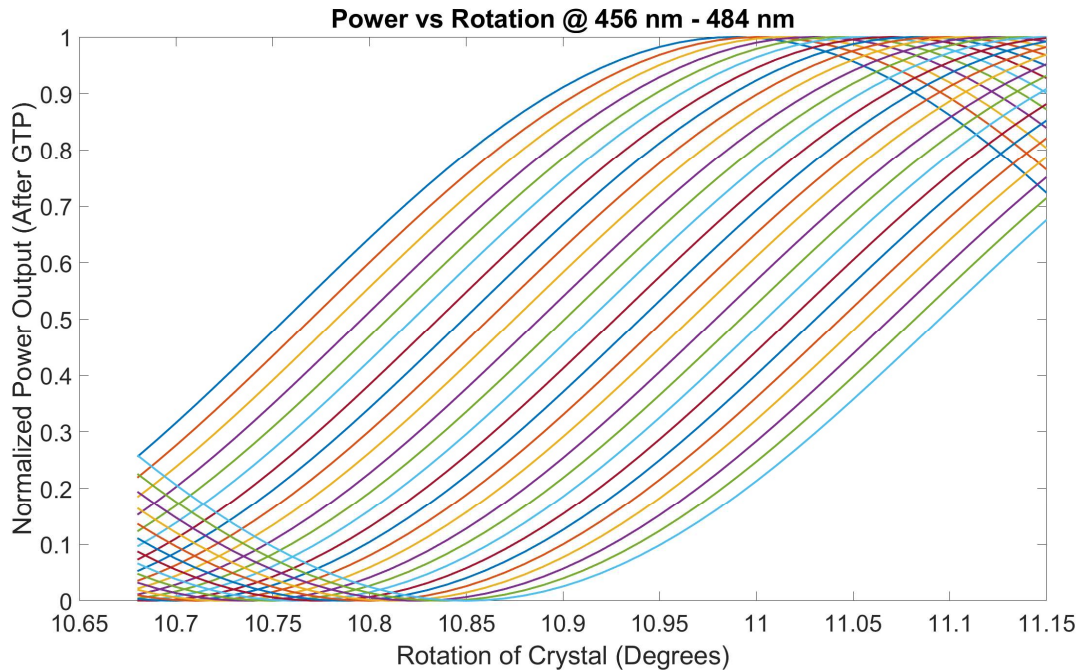


Figure 7.1-5

Power plotted dependent upon rotation of the crystal and the wavelength emitted from the LED with a rotation range of 10.8°-11.3° and a wavelength range of 456 nm-484 nm the response is weighted with the normalized emission intensity corresponding to the full width half max of the LED we used and the step size of our motor.

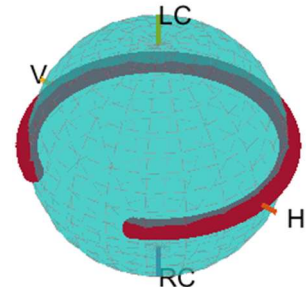
This plot shows a smooth response however it does highlight that the peaks of each of the wavelengths are asynchronous with what would seem to be a 0.05° step per nm change in the area of rotation. This does show that one of the wavelengths we are using is at 0.132 and a few more wavelengths at lower ranges. This does show that some power will be coming through and not perfectly polarized at our start and stop locations.

7.1.5.2 Simulating Broadband Polarization States

We can show this by using the Poincare spheres created previously plotting each wavelength as we rotate through this range. This plot highlights the fact that when we stop at this location and even in our starting locations there are some wavelengths that go to linear polarization states that are well off the center. Meaning some of these wavelengths will be filtered on our output polarizer when we are in

Poincare Sphere

Figure 7.1-6



*Poincare sphere showing the broadband polarization states achieved in our setup.
Poincare sphere showing the broadband polarization states achieved in our setup*

our on state and then in our off state we will have a bit of bleed through.

The total bleeding through is hard to visualize without a closer look at our PER. Which we will look at in the following plot

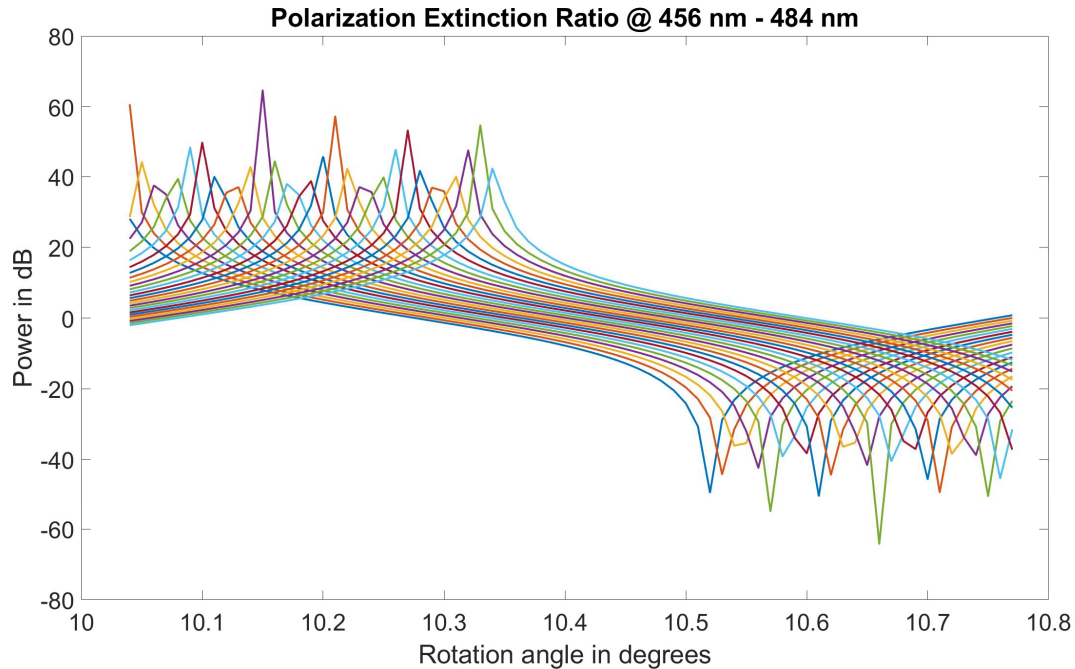


Figure 7.1-7

This shows PER dependent on rotation of a 1 mm Calcite Crystal and a source with a FWHM between 456 nm-484 nm we rotate between two target locations 10.82°-11.28° this is a target movement of 0.5° having verified this movement with an oscilloscope as taken place within 4.5 ms within our target time of 5 ms.

This plot shows that our selected targets to rotate the crystal between bring differences in extinction ratio at our stopping locations however, the max and min at each location are positive and negative dB showing at least that this location is close.

7.1.6 LTspice Simulation

An LTspice simulation was created to simulate the behavior of the TIA circuit to ensure the proper current to voltage conversion was occurring and the proper cutoff frequency was realized from the low pass filter. The LTspice simulation was used to help verify the TIA circuit PCB was working properly as expected.

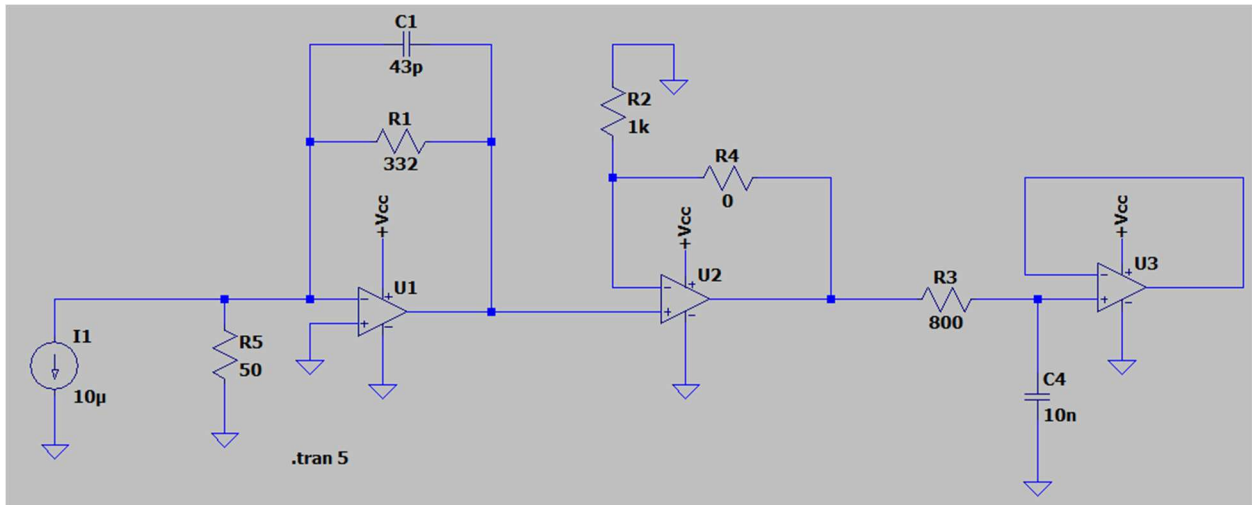


Figure 7.1.6

LTspice schematic of the TIA circuit, Unity op-amp circuit, and the Low Pass Filter.

During Senior Design 2, it was realized that when utilizing the LED in the optical setup, the power was a lot lower than expected. Thus, the lasers were utilized instead to determine the switching time of the motor which led to adjustments to the TIA circuit design.

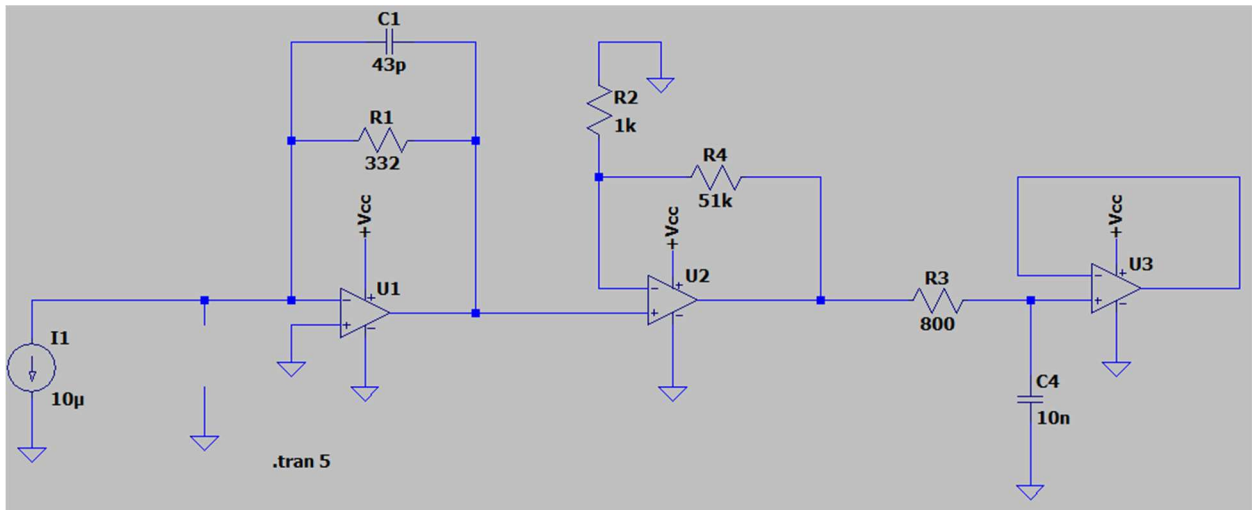


Figure 7.1-8

Updated version of the LTspice schematic of the TIA circuit, Gain op-amp circuit and the Low Pass Filter.

7.2 Software Design

Our project integrates multiple technologies into a unified graphical user interface (GUI) to enable robust data acquisition, control, and visualization. At the core, we use NI-DAQmx, a driver and API suite from National Instruments to interface with data acquisition hardware. This allows precise control over analog and digital I/O, timing, and triggering. We embed LabVIEW, a graphical programming environment, to handle real-time data visualization and user interaction.

LabVIEW’s modular design and seamless integration with NI-DAQmx make it ideal for building responsive measurement systems.

For low-level hardware control and custom logic, we use C programming, particularly for performance-critical routines and direct communication with embedded systems. Additionally, we incorporate ESP32 microcontroller programmed in the Arduino IDE (based on C/C++) to manage the light sources in our system. The ESP32 microcontroller communicates with the GUI via digital signals, allowing simple communication between the GUI and the ESP32 microcontroller.

All components LabVIEW, NI-DAQmx, and Arduino IDE will all receive an input from a single GUI framework. This unified interface streamlines user interaction, consolidates data streams, and provides centralized control over the entire system. The result is a cohesive, multi-platform solution that bridges high-level visualization with low-level hardware control.

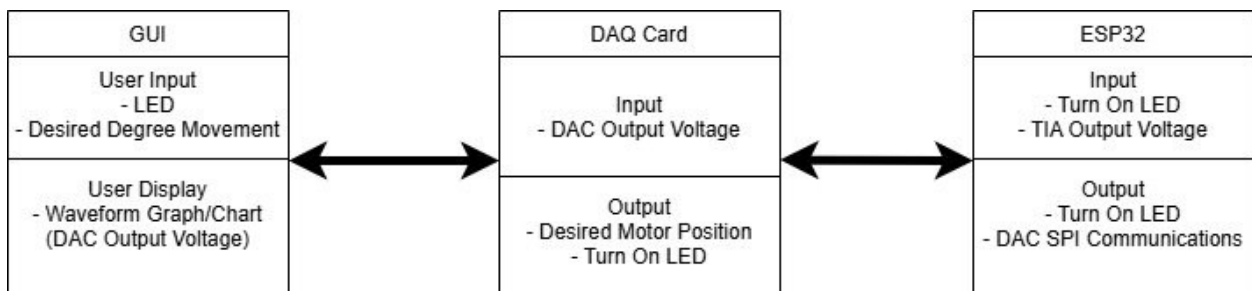


Figure 7.2-1

Overall Software System. Figure showcases what each part of the software subsystem does and what information its needs from the other software subsystems to complete their task.

7.2.1 GUI

7.2.1.1 LabView Front Panel Design

LabView has two components to its program, a front end and a back end. The front end is known as the Front Panel due to having various panels that the user can interact with to get a certain outcome. The back end or Back Panel is the coding part of the program in which the programmer can use various blocks to code their program to complete a certain task based on the user’s input on the Front Panel. For our program, the Front Panel will serve two purposes, one to control the on and off switch for the LED and the other is to control the motor movement based on the user’s desired motor angle movement.

The program works by having a drop down block in which the user selects what light source they are using. The user will then have a Start block in which the user presses when they want to start the sweep protocol. Afterwards, the MATLAB block will display the graph of the light source simulation and the graph of the collected measurements of the degree of the motor vs the power of the light source. The user will then insert the first degree movement into the Insert block and then insert the second degree movement into the other Insert block. The user will then press the Start block for the Switching mode. Once again, the MATLAB block will display the graph of the collected data of the time in milliseconds vs the power of the light source.

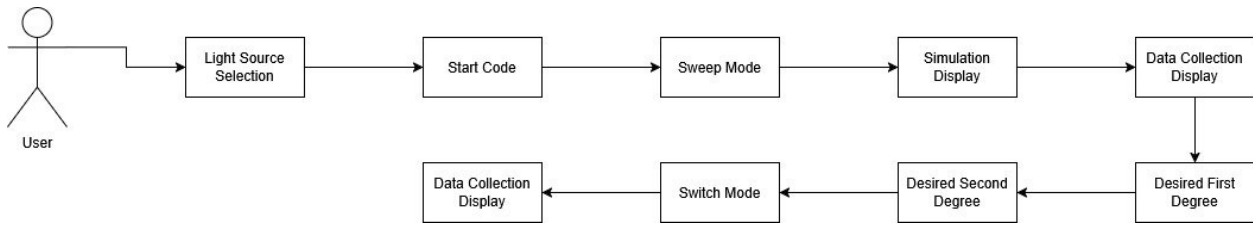


Figure 7.2-2

LabView Front Panel User Interface. Figure showcases the interaction between the user and the LabView Front Panel User Interface.

7.2.2 Motor Control

7.2.2.1 LabView Design

LabView is a program that utilizes various blocks to program instead of the traditional coding with words, but the basic coding concepts still carry over into LabView such as while and for loops. One such feature is LabView utilization of what is known as case structure which serves as the program's if else statement and shift registers which serve as a way for the program to pass one value of an iteration within a while or for loop into the next iteration. Utilizing both these methods, we can develop a system that will receive the user's input to move the motor between two desired angles.

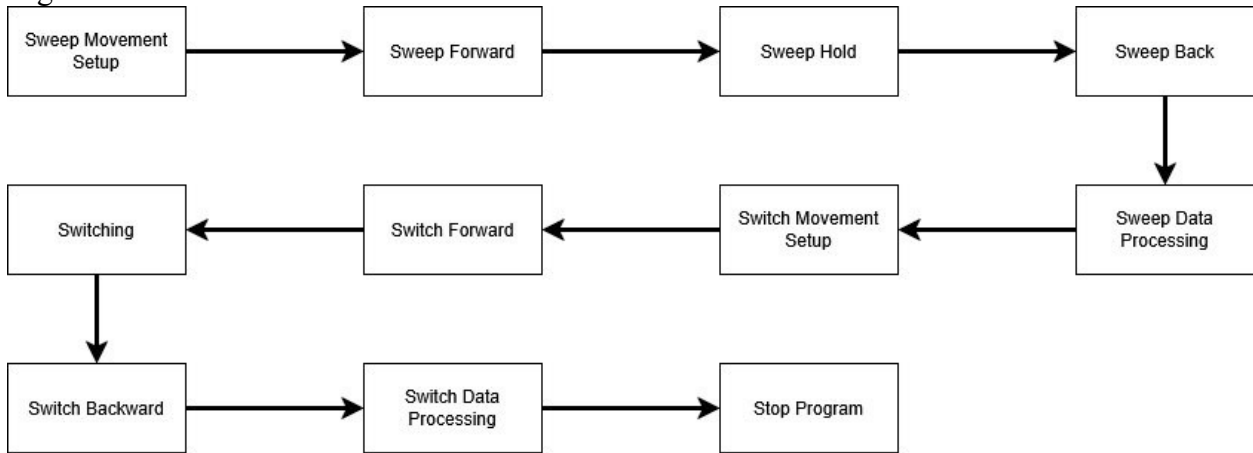


Figure 7.2-3

Case Structure Flow Chart. The figure showcases the interaction between the different case structures from the sweep mode to data collection display to switching mode.

7.2.2.2 Motor Movement

The motor movement utilizes set point generator to determine what voltage value the DAQ card should output to the motor driver to achieve the desired timing of the motor system. LabVIEW takes the desired degree movement and converts it to the voltage value that would achieve this degree movement. Then, the voltage value gets inserted into the set point generator with the desired timing that it should achieve that degree movement. For Sweep Mode, the motor moves to 5 degrees in 20 seconds, holds at 5 degrees for 2 seconds, and then returns to 0 degree in 6 seconds.

For Switching Mode, the motor moves to the first desired degree movement in 3 seconds, holds at first degree for 50 ms, switches to the second desired degree movement in 2.5 ms, holds at the second degree for 50 ms, and switches back to the first degree in 2.5 ms. This movement gets repeated multiple times for 1 second.

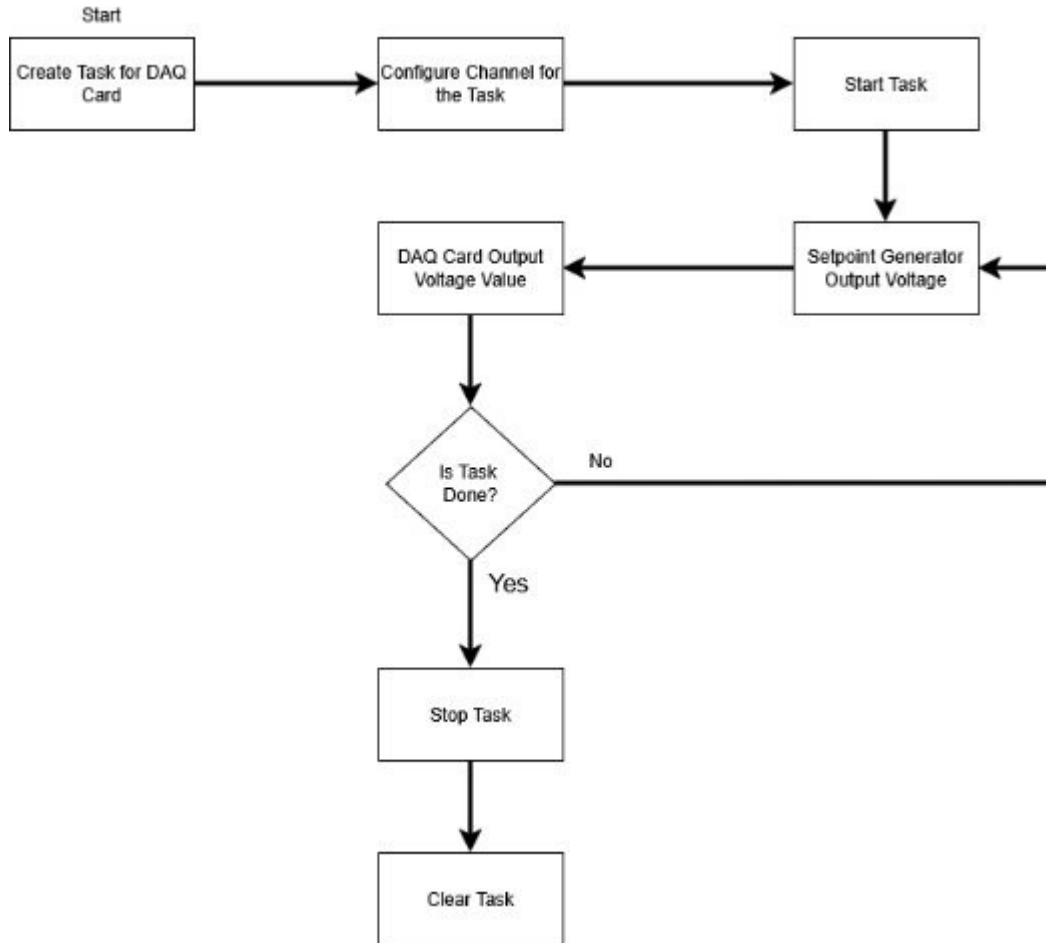


Figure 7.2-4

Motor Movement. The figure shows how the motor movement is configured in the Back End of LabVIEW.

7.2.3 Data Collection

7.2.3.1 Overall ESP32 Design

The ESP32 has three functions: control the Blue LED, read the voltage output from the TIA circuit, and utilize SPI communication with the DAC chip to output the voltage value to the DAQ card. This will be done through parallel execution of the code in which controlling the Blue LED and reading the voltage output from the TIA circuit was done on Core 1 of the ESP32 and the SPI communication with the DAC chip was done on Core 0. FreeRTOS was utilized in the ESP32 code to safely exchange data between the two cores.

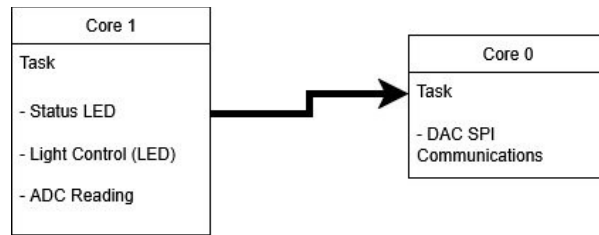


Figure 7.2-5

ESP32 Software Overview. The figure showcases the interaction between Core 1 and Core 0 along with what tasks are done in the respective cores.

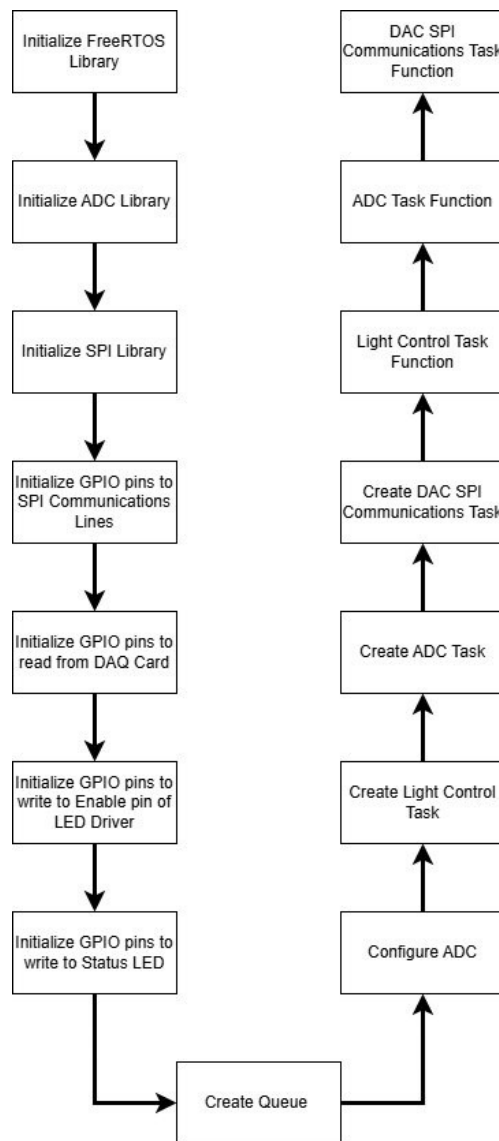


Figure 7.2-6

ESP32 Library. The figure shows what libraries were utilized in the ESP32 code and in what order the pins, libraries, and tasks are configured.

7.2.3.2 ESP32 Core 1

If the ESP32 reads a digital input from the DAQ card, the ESP32 outputs a digital voltage to the enable pin of the LED driver for the LED to turn on and the status LED turns on. The ESP32 then starts the continuous ADC reading functionality to read the output voltage from the TIA circuit. Then, queues were utilized to send the voltage value to Core 0. The ESP32 checks again if it reads a digital voltage signal from the DAQ card. If there is still a digital voltage signal, it continues to read the voltage value from the TIA circuit and sends the data to Core 0. If no digital voltage signal was read, it stops the continuous ADC reading and turns off the Blue LED.

If the ESP32 does not read a digital input from the DAQ card, the ESP32 does not output a digital voltage to the enable pin of the LED driver which leads to the LED to be off. It then checks the last time the status LED was blinked. If it has been more than a second, the status LED is toggled once more.

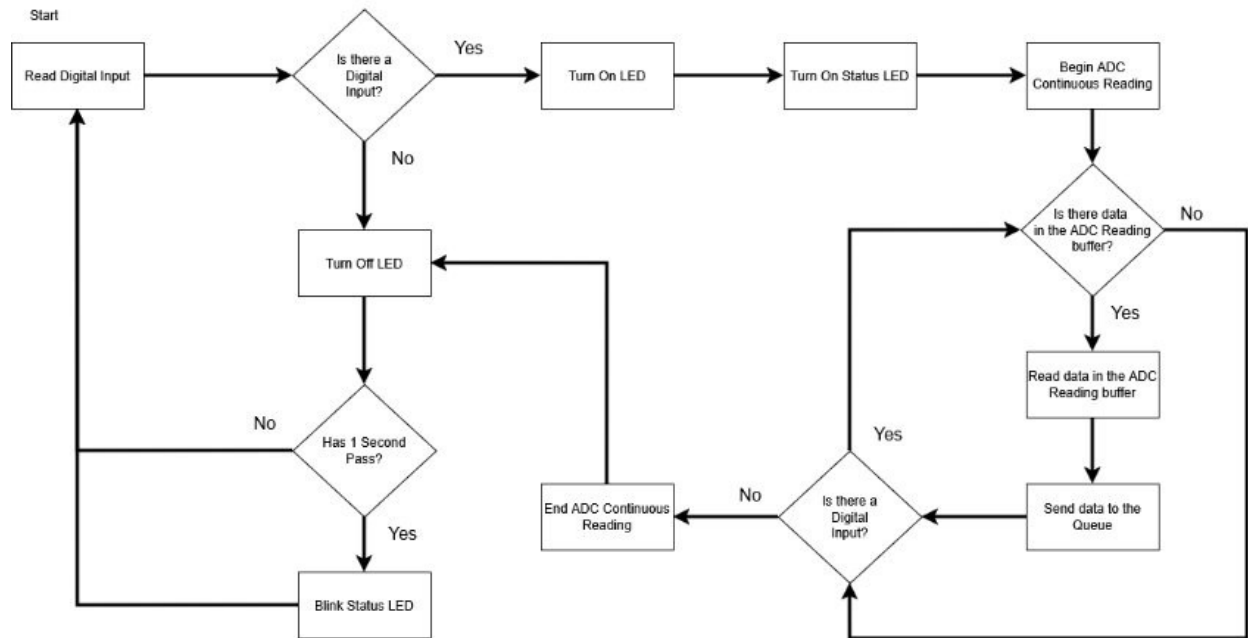


Figure 7.2-7

ESP32 Core 1. The figure shows the code logic in Core 1 of the ESP32 in controlling the Blue LED and collecting the data from the TIA circuit.

7.2.3.3 ESP32 Core 0

In Core 0 of the ESP32, the core waits until there is data in the queue. Once there is data in the queue, the data gets taken out of the queue and is added to the total sum. Once 16 data have been taken out of the queue, the total sum is averaged out. The ESP32 ADC reading by default is set to 12 bits but the DAC chip has a 10 bit resolution. The averaged voltage value is bit shifted from 12 bits to 10 bits. The data gets bit shifted once again to match the register values that the DAC chip is expecting. Then, the SPI communication starts, data is transferred to the DAC chip, and the SPI communication is stopped. The ESP32 once more checks if there is any data in the queue.

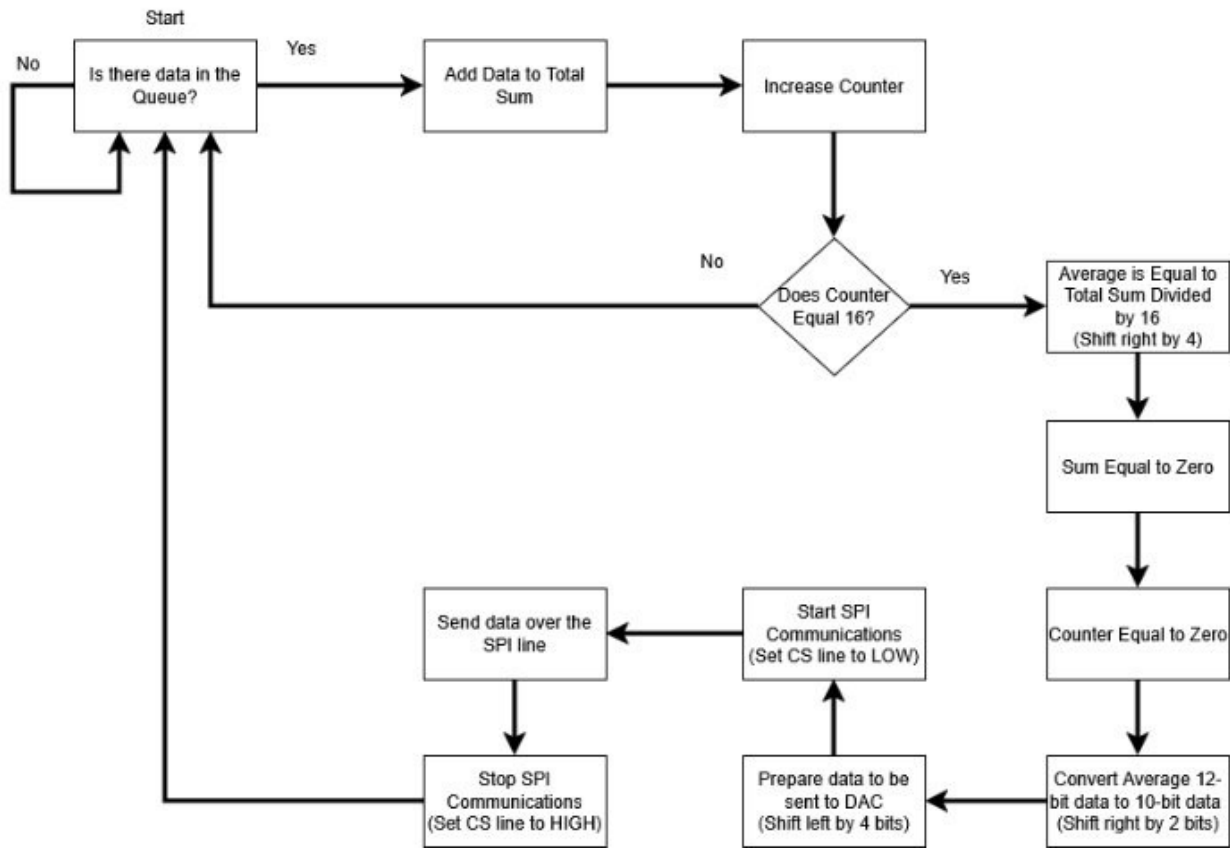


Figure 7.2-8

ESP32 Core 0. The figure shows the code logic in Core 0 in processing the voltage value sent from Core 1 and the SPI communication protocol with the DAC chip.

Chapter 8. System Fabrication and Prototype Construction

8.1 PCB Layout

8.1.1 Voltage Regulator

8.1.1.1 Voltage Regulator for ESP32

PCB design was done in KiCad due to its simple PCB design process and its Design Rules Checker functionality ensures that the PCB meets the constraints of the design and the manufacturer which helped streamline the work progress. When creating the PCB design, placement of the components was greatly considered in which bypass capacitors were placed close to the power line to ensure noise was minimized. Another consideration was labeling the components to help with the soldering process to ensure the proper components went into the right place. Trace width was also established to be a constant 40 mill throughout and the manufacturer's constraints were considered as well. All PCB includes a ground plane to help with the grounding of the components. The

voltage regulator was created to be separate from the main board to allow proper testing of the voltage regulator and easy troubleshooting of issues.

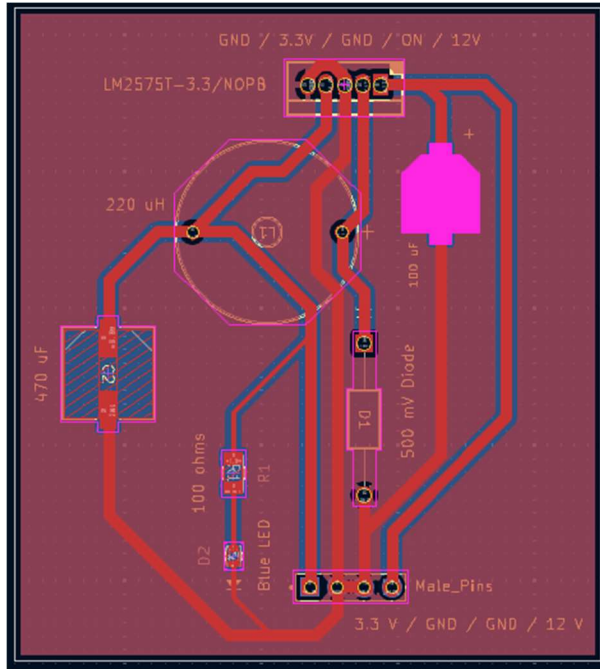


Figure 8.1-1

LM2575 (3.3 V) Voltage Regulator PCB Board.

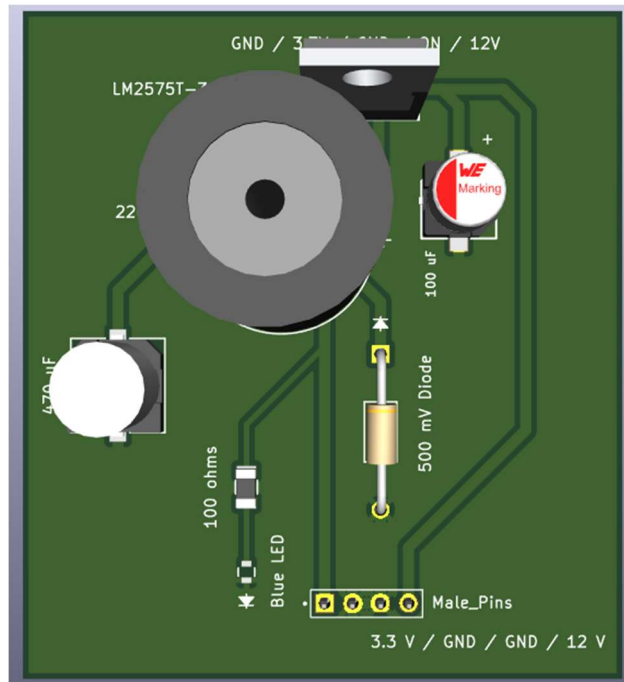


Figure 8.1-2

3D Model of the LM2575 (3.3 V) Voltage Regulator PCB Board.

8.1.2 TIA Circuit Board

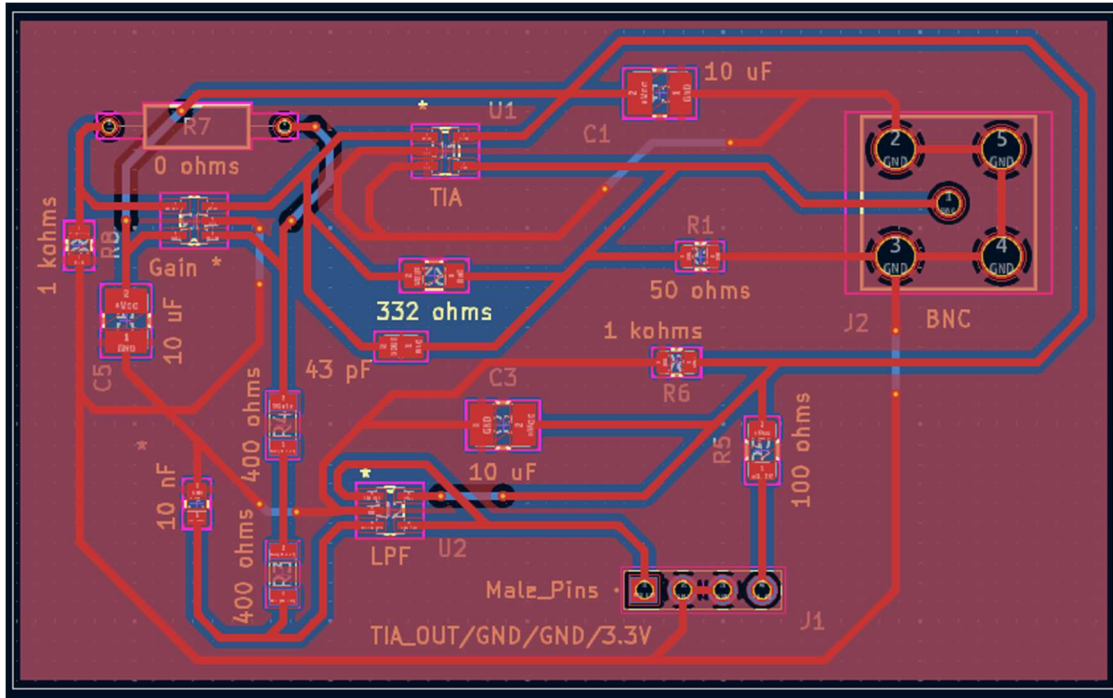


Figure 8.1-3

TIA Circuit PCB Layout with the TIA Circuit, Unity Op-Amp, and Low Pass Filter.

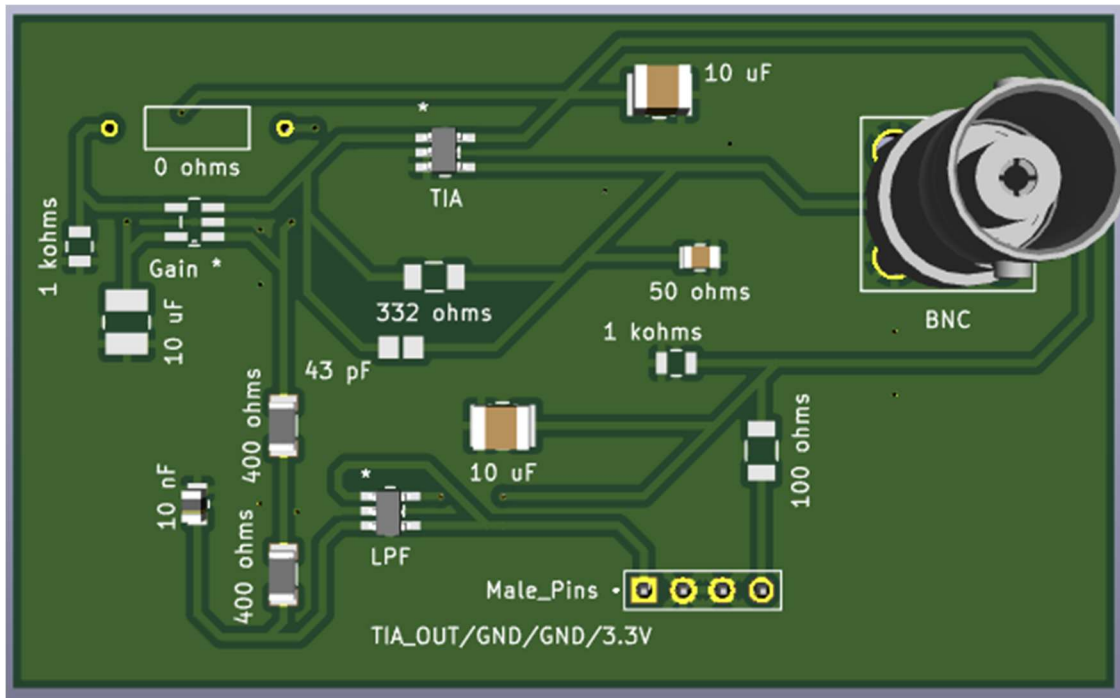


Figure 8.1-4

3D Model of the TIA Circuit PCB with the TIA Circuit, Unity Op-Amp, and Low Pass Filter.

8.1.3 Main Board

8.1.3.1 Main Board Considerations

Trace width was a constant 20 mil throughout the board; however, there were some sections that had to utilize a larger trace width due to transferring a higher current value. From the power supply, a trace width of 40 mil was utilized from the power supply to the input of the voltage regulator board and LED driver. 40 mil was also used from the LED driver to the LED.

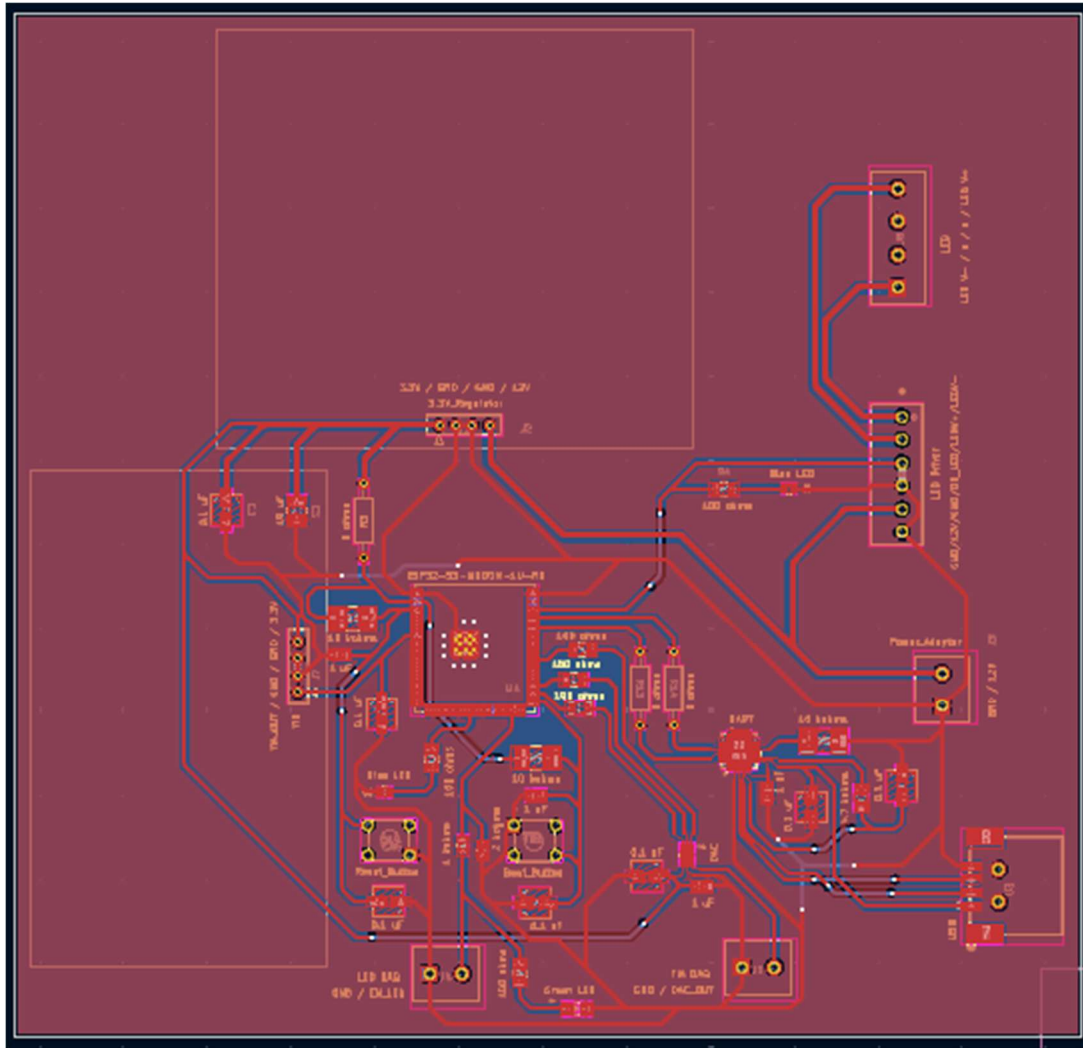


Figure 8.1-5

Main PCB Board with the ESP32, USB Connector, 3.3 Voltage Regulator, TIA Circuit, Power Adapter, LED Driver, LED, and DAQ Card.

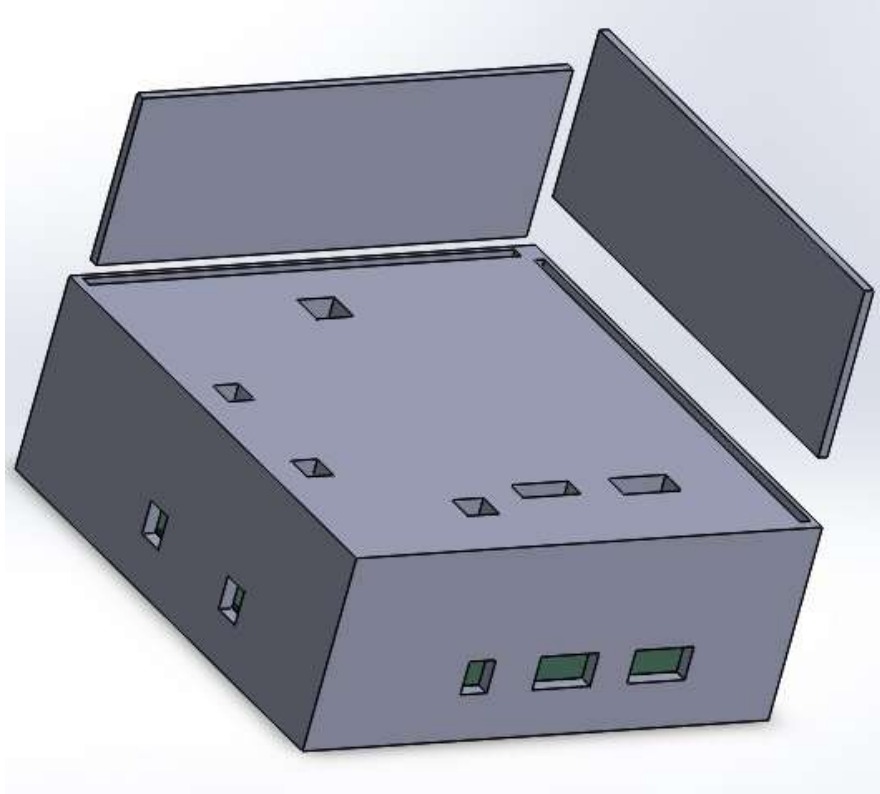


Figure 8.2-1

An angle aerial view of the PCB Housing CAD Design.

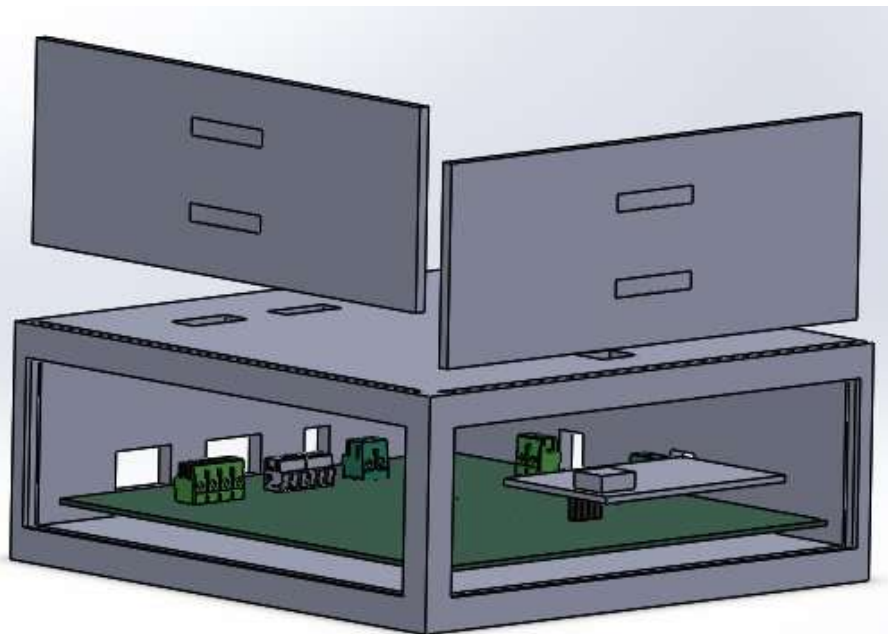


Figure 8.2-2

An angled view of the PCB Housing with the PCB inserted into the housing.

8.2.2 DC Power Supply Housing

8.2.2.1 DC Power Supply Housing CAD Design

Holes were left on the top above the AC to DC transformer and the DC to DC PCB to allow proper heat dissipation of the power supply. The hole in front was left to allow access to the output of the DC to DC PCB to easily power the motor.

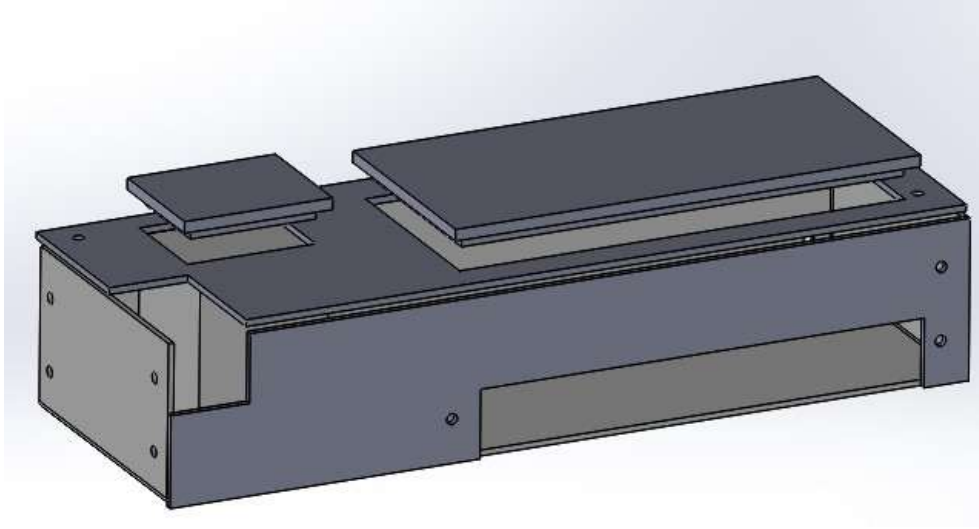


Figure 8.2-3

Front angled view of the DC Power Supply Housing CAD Design.

8.3 Optics CAD Diagram

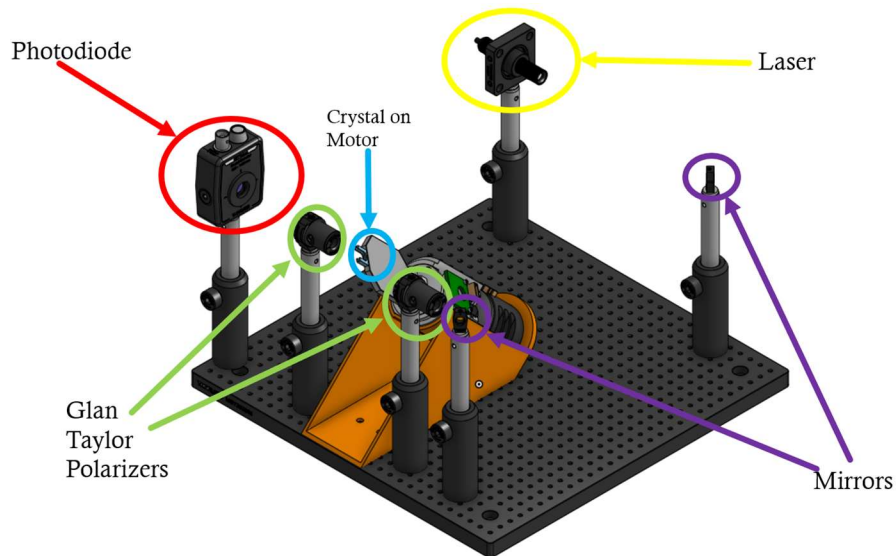


Figure 8.3-1

3D model of optical setup. Made by authors

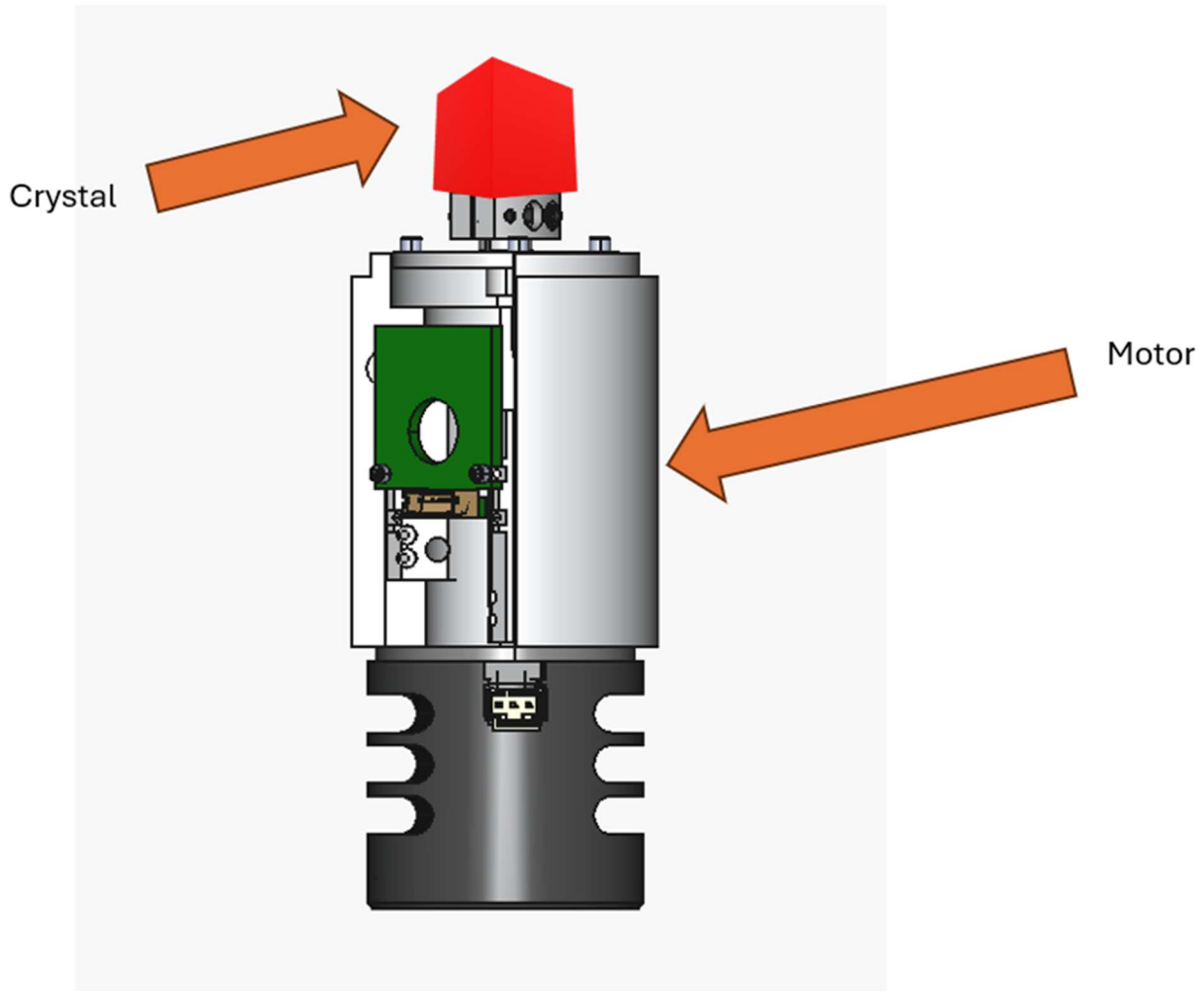


Figure 8.3-2

Motor and crystal created by authors

Chapter 9. System testing and Evaluation

9.1 Optoelectronics Feasibility

The Fast polarization switch project utilizes a photodiode as a way to measure the efficacy of our system. With a target 30 dB difference between the off and on states of our output power. The photodiode will be combined with an oscilloscope to offer an analog measurement of the output providing high enough fidelity of measurements to clearly see any vibrational effects and accurately compare the experimental results to the simulated results, the photo diode we are using is a biased Si detector from Thorlabs the DET100A2 with a detector size of 75.4 mm^2 , 35 ns Bandwidth of 10Mhz. Taking the output of our sources both the beam size and the overall optical losses due to the absorption and scattering cause by the optical components we can simulate the intensity incident on the detector. The Responsivity graphs of the other comparable photo detectors from Thorlabs are shown here as well.

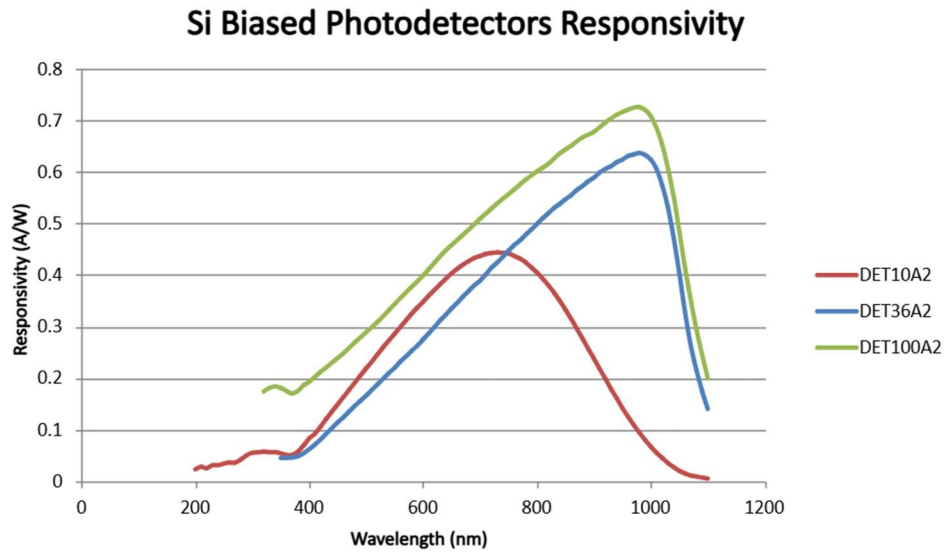


Figure 9.1-1

9.2 Hardware Testing

The results of our system and subsystem testing were tabulated and analyzed to show the demonstrable system specifications. That the Fast Polarization Switch is not only capable of meeting the proof-of-concept basic objectives but meets them consistently as well. Providing a good foundation for future development of similar systems as well as exploring other possible applications for this type of system.

9.2.1 Switch Timing

9.2.1.1 Experimental Setup and analysis

To test our switching time, we put our photodiode on the output of our system, The Fast Polarization switch. Then looked at the resulting waveform that was read through our TIA circuit and ESP32. We ran multiple tests averaging out the timing over the course of 10 switches during one run – cycle. Then looked at the deviation in those averages to determine the overall consistency in the timing. This proves our system was able to reach below the proof-of-concept 5 ms timing. Down to an average just above 2.5 ms.

9.2.1.2 Example of Waveform Results for Sweep

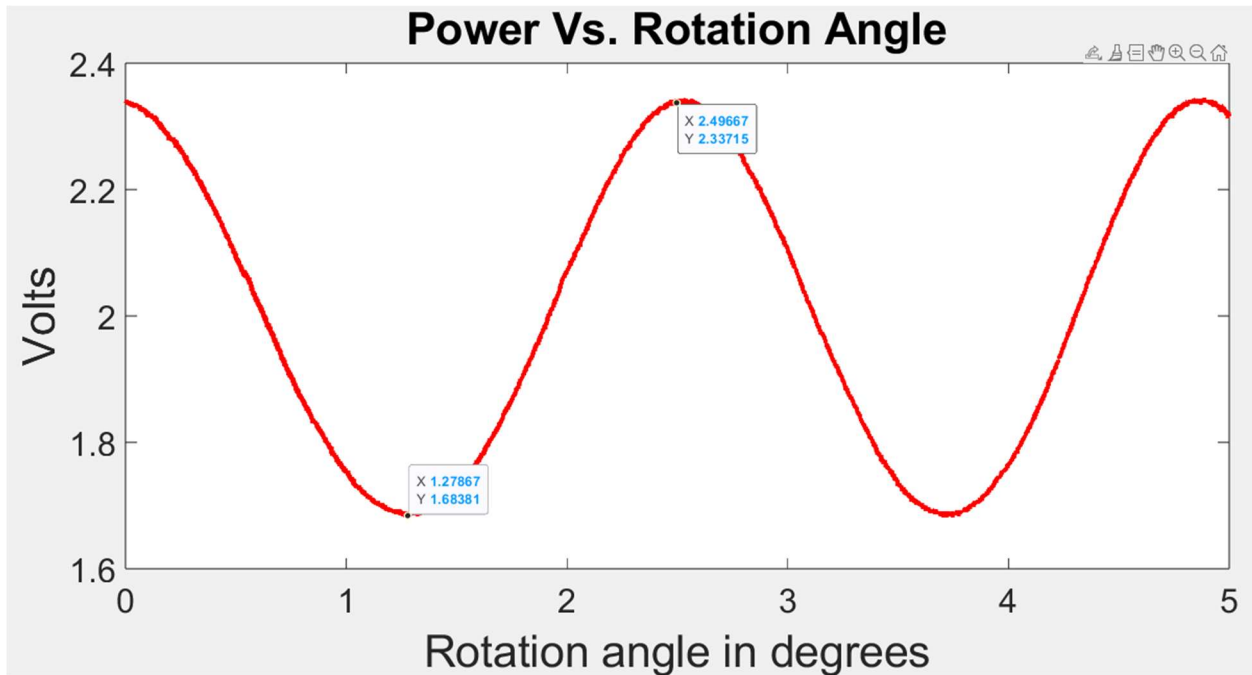


Figure 9.2-1

9.2.1.3 Example Waveform Results Switch

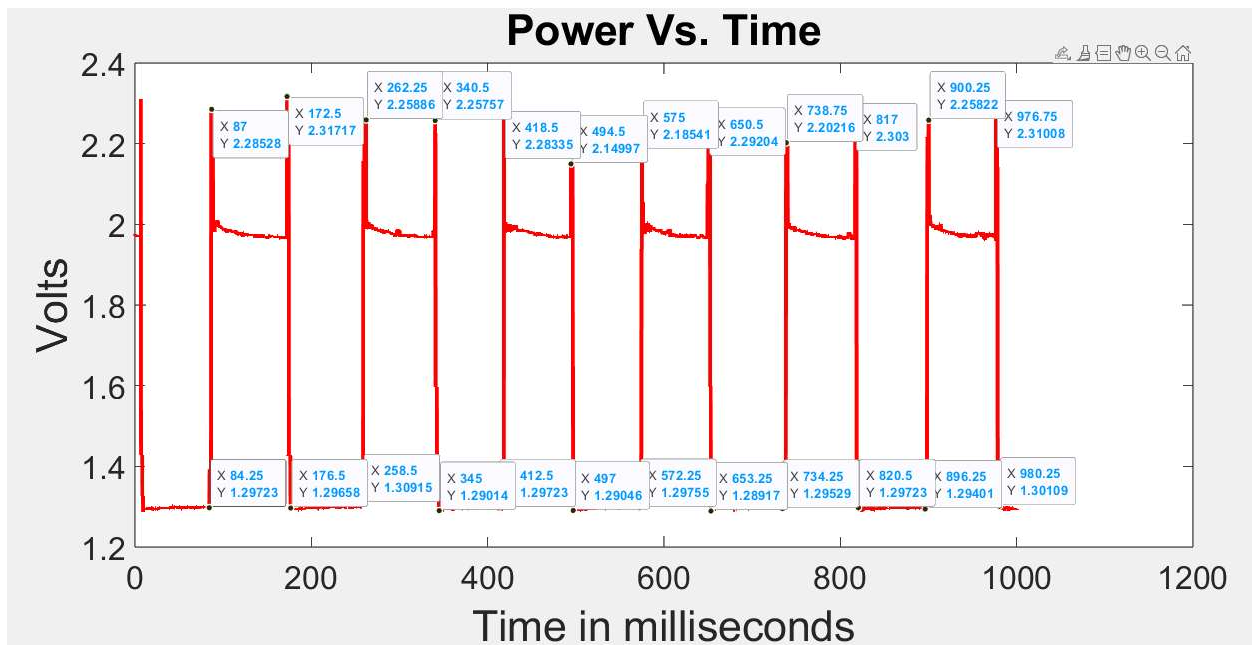


Figure 9.2-2

9.2.1.4 Example Tables of Testing Data Speed

Table 9.2-1

Test #	Min Power Time ms	Max Power Time ms	Total Time ms
1	334.1	332.5	1.6
2	90.25	93	2.75
3	175.75	171.5	4.25
4	257.25	261.5	4.25
5	341.75	343.75	2
6	423.5	424.25	0.75
7	505.75	508.5	2.75
8	585.5	590	4.5
9	671.75	671.5	0.25
10	748	750.5	2.5
			Avg = 2.56

Test #	Min Power Time ms	Max Power Time ms	Total Time ms
1	92.5	95.75	3.25
2	177.5	175.25	2.25
3	259.75	263.5	3.75
4	347	343.75	3.25
5	429.25	431.25	2
6	511.5	508.75	2.75
7	596.25	599.25	3
8	687.25	681.5	5.75
9	767.5	769.25	1.75
10	860	859.25	0.75
			Avg = 2.85

Test #	Min Power Time ms	Max Power Time ms	Total Time ms
1	86.75	89.25	2.5
2	174.75	170.5	4.25
3	253	259	6
4	344.25	340.5	3.75
5	429.75	433.5	3.75
6	515	512.5	2.5
7	603.5	605.75	2.25
8	690.75	688	2.75
9	772.75	775	2.25
10	854.75	852.75	2
			Avg = 3.2

9.2.1.5 Polarization Extinction Ratio Testing

To test the polarization extinction ratio, we used a couple of different methods. Towards the beginning of the development of the system, we tested PER by using the simulation to assist us in approximating where the low would be and then using an iterative move here and hold protocol, we painstakingly found the maxima and minima. This was an arduous process and increased the overall calibration time of the system, which is why we came up with the sweep protocol you saw above. As after running that protocol, we can quickly identify where the degrees of the maxima and minima are located. This drastically reduced this testing time.

9.2.1.6 Polarization Extinction Ratio Tables

639 nm Wavelength

Table 9.2-2

Test #	Max Power uW	Min Power uW	PER	Deviation
1	481	2.47	194.7368421	-16.61686969
2	485	2.24	216.5178571	31.46038588
3	484	2.29	211.3537118	0.340495931
4	483	2.61	185.0574713	-26.34603751
5	479	2.27	211.0132159	-3.209006363
6	482	2.28	211.4035088	25.24966262
7	482	2.25	214.2222222	-3.877325289
8	484	2.6	186.1538462	-30.4380821
9	482	2.21	218.0995475	11.5845324
10	483	2.23	216.5919283	10.44760683
			206.5150151	0.098650295

521 nm Wavelength

Table 9.2-3

Test #	Max Power uW	Min Power uW	PER	Deviation
1	481	2.47	194.7368421	-16.61686969
2	485	2.24	216.5178571	31.46038588
3	484	2.29	211.3537118	0.340495931
4	483	2.61	185.0574713	-26.34603751
5	479	2.27	211.0132159	-3.209006363
6	482	2.28	211.4035088	25.24966262
7	482	2.25	214.2222222	-3.877325289
8	484	2.6	186.1538462	-30.4380821
9	482	2.21	218.0995475	11.5845324
10	483	2.23	216.5919283	10.44760683
			206.5150151	0.098650295

9.2.1.7 Wavelength

To show the proof-of-concept wavelength specification we tested our system using a variety of light sources across the visible spectrum from 639 nm – 471 nm we have shown that the system can polarize light across the visible spectrum.

9.2.2 Voltage Regulator

9.2.2.1 Voltage Regulator for ESP32

To test the 3.3 V regulator for the ESP32, the output voltage and output current will be measured with a simple LED load and an additional load on top. This will allow us to see if the voltage regulator is working properly in which a constant voltage is occurring no matter the load. In addition, we will also be calculating the efficiency of the voltage regulator to see the power loss of the voltage regulator is significant enough to warrant the need of a heat sink when implementing the voltage regulator onto the PCB board.

Table 9.2-4 Data Collected with LED Load

Data Type Collected	Data Result
Input Voltage	12 V
Input Current	13 mA
Output Voltage	3.3114 V
Output Current	17.215 mA

Table 9.2-5 Data Collected with Additional Load and LED Load

Data Type Collected	Data Result
Input Voltage	12 V
Input Current	23 mA
Output Voltage	3.3012 V
Current through LED	17.133 mA
Current through Load	31 mA
Output Current	48.133 mA

Thus, with the data collected, it was found that the voltage regulator with just the LED load had an efficiency of 36.40% with a power loss of about 0.09899 W. With the additional load to the LED load, the voltage regulator was found to have an efficiency of 57.57% with a power loss of about 0.1171 W. Thus, with the efficiency being around the 40% to 60% range with a power loss of less than 1 W, the voltage regulator is efficient enough to be used as a constant voltage source to power the ESP32 and a heat sink is not required for the voltage regulator on the PCB board.

9.2.2.2 Voltage Regulator PCB Testing

To test the power efficiency of the PCB of the voltage regulator, the input of the voltage regulator PCB is connected to the DC Power Supply. The DC Power Supply is set to output a voltage value of 12 V, and the current is set to a limit of 1 A. At the output of the voltage regulator PCB, the

electronic load is connected. The electronic load is set to constant current mode and will draw current from 100 mA to 900 mA.

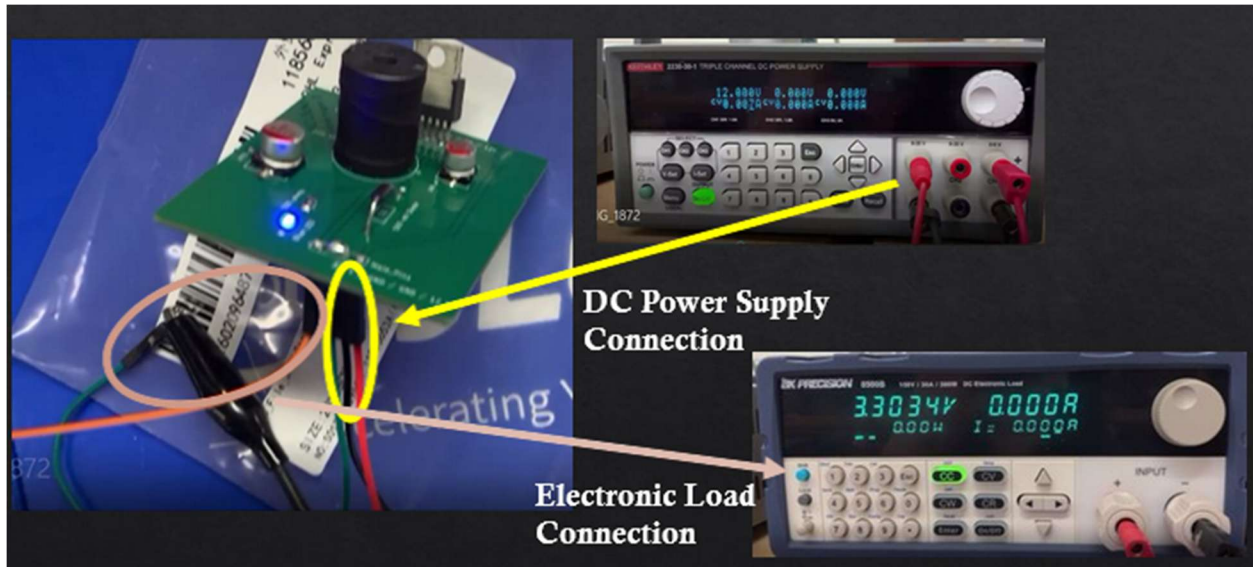


Figure 9.2-3

Voltage Regulator PCB Testing setup to the DC Power Supply and the Electronic Load.

Table 9.2-6 Data Collected from the Voltage Regulator PCB

Current Load Draw	Input Power	Output Power	Power Efficiency
100 mA	0.53 W	0.33 W	62.26415%
200 mA	0.92 W	0.64 W	69.56522%
300 mA	1.32 W	0.96 W	72.72727%
400 mA	1.73 W	1.26 W	72.83237%
500 mA	2.14 W	1.56 W	72.8972%
600 mA	2.56 W	1.85 W	72.26563%
700 mA	2.98 W	2.14 W	71.81208%
800 mA	3.41 W	2.42 W	70.96774%
900 mA	3.84 W	2.69 W	70.05208%

Thus, with the data collected, it was found that the voltage regulator PCB has an average power efficiency of about 70.60% which is expected from a LM voltage regulator. This supports the data collected from Senior Design 1 of the voltage regulator prototype and emphasizes that the voltage regulator PCB does not need a heat sink.

9.2.3 TIA Circuit

9.2.3.1 TIA Circuit PCB Testing

To test the accuracy of the TIA circuit, the output of the TIA circuit PCB will be compared with the voltage output from the LTspice simulation. The TIA circuit PCB is connected to the DC Power Supply to power the op-amp on the board. A separate breadboard is utilized to mimic the output

current of the photodiode going into the TIA circuit. The output voltage of the TIA circuit PCB is being read by the digital multimeter.

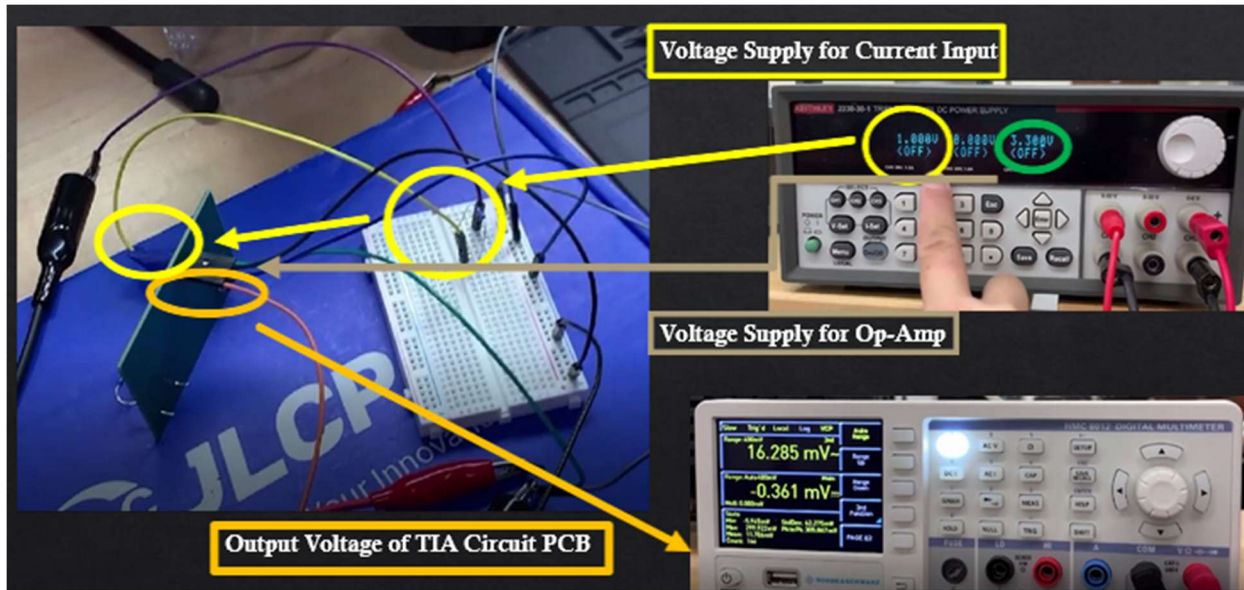


Figure 9.2-4

TIA Circuit PCB setup to the DC Power Supply, separate breadboard, and the digital multimeter.

Table 9.2-7 Data Collected from the TIA Circuit PCB

Input Current	Simulation	Experiment	Error Percentage
10 μ A	172.58 mV	2.67581 V	1450.475%
20 μ A	345.21 mV	2.72787 V	690.206%
30 μ A	517.84 mV	2.78422 V	437.6603%
40 μ A	690.47 mV	2.84454 V	311.9716%
50 μ A	863.10 mV	2.89913 V	235.8973%
60 μ A	1.0357 V	2.95894 V	185.6947%
70 μ A	1.2083 V	3.01498 V	149.5225%
80 μ A	1.3809 V	3.06964 V	122.2927%
90 μ A	1.5536 V	3.13900 V	102.0469%
100 μ A	1.7262 V	3.18472 V	84.49311%

Thus, with the data collected, it can be seen that the TIA circuit PCB has an average error percentage of 377.026%. This high average error percentage can be explained by the adjustments made to the circuit. The TIA circuit was originally designed to receive an input current of upwards to 9 mA, but with lower than expected optical power, the TIA circuit only receive upwards to 100 μ A in current. Thus, the LTspice simulation is not an accurate way to determine what is happening in the real world with the TIA circuit PCB.

9.3 Software Testing

9.3.1 Motor Control System

When programming the motor control system in LabView, there are various steps that can be taken to test the code while ensuring that we do not damage the motor while doing so. One such precaution is within the LabView program in which the programmer can press the light blue button to slow down the code to see it go one step at a time. Thus, when testing the code, we run it through this functionality first to see if there are issues with the code before testing it on the motor itself.

Once the code has been developed, it was time to test the code on the motor. The purpose of the testing is to see if the code can move the motor and to see if the motor did go to the desired angle, large angle movements were chosen to be able to see the movement of the motor with our bare eyes. Thus, for testing purposes, the first-degree movement was chosen to be 10 degrees, and the second-degree movement was chosen to be 20 degrees.

Following these procedures, we were able to develop a code that works with the motor that would move the motor to the desired degree based on the user's input. Once that was completed, timing was the next issue in which a laser system was set up to test the timing of the motor to ensure the motor achieves the desired switching time.

9.3.2 Light Source Control System

The light source control system was tested by connecting a simple LED diode to the output of the DAQ card and the ESP32. The LED diode being connected to the output of the DAQ card showcases whether the DAQ card is outputting a digital voltage when it is supposed to. Connecting an LED diode to the output of the ESP32 shows that the ESP32 is outputting a digital voltage when it is supposed to which acts as the ESP32 sending a digital voltage to the enable pin of the LED driver. Another LED diode was connected to the ESP32 in which the ESP32 would blink this LED diode every 1 second to test whether the code was properly flash to the ESP32.

Following these procedures, we test the light source control system by first having the user not want the LED to be on. This means the only LED diode that should be on is the LED diode that is constantly being blinked by the ESP32. Next is to have the user input that they want the LED to be turned. This would lead to all the LED diodes to be on. Following these procedures, we were able to verify that the DAQ card can properly communicate with the ESP32 to turn on or off the LED diode which will eventually become the LED.

9.4 Performance Evaluation

For the performance of our entire system, we evaluate our testing results. We were able to achieve an average PER of 206:1 with our red laser and 163:1 with the green. These results were enough to achieve our basic objective of 100:1 but not the stretch objective of 1000:1 that ASML wanted. We were also able to achieve an average switch time around 2.5ms which achieves our basic goal of under 5ms but not under 1ms for the stretch objective. From these two results we show that our system achieves all basic goals and objectives but struggles to reach the stretch objectives set. We believe we could not hit these goals because we lacked the fine tune adjustments to get perfect alignment. We also believe that there may have been some more success if we tried using other crystals and experimented with their results. We could not see these results with our LED, however.

We believe that since the LED is a diverging source there was some physics that we did not have time to study that was preventing us from achieving good results with this light source. We were able to achieve any desired polarization on the Poincare sphere by rotating the polarizer and crystal to achieve the polarization desired, including elliptical and circular polarizations. We also showed that our system can work across a range of wavelengths in the visible spectrum if they were narrowband sources that were mostly collimated. Our simulations showed that a user would be able to use this system to polarize a source with a larger bandwidth, but they would have worse PER. Unfortunately, due to budget constraints we could not test this since the only broadband source we had was too divergent to rule out if the broadband or diverging source was the root cause of the PER. We were also able to build an efficient GUI to control the motor and overall control our system. Overall, we were successful in meeting our basic goals and objectives as well as some of the advanced goals and objectives we set.

9.5 Overall Integration

The software we are utilizing namely, MATLAB, ArduinoIDE, and LABVIEW, the latter being the environment we are integrating our software into. MATLAB will be utilized to calculate and generate target angles to select, and predict the power over time response of our system. While LabView will take those target signals and utilizing the DAQmx “VI” kit send signals through our 6001USB NI DAQ card that will move the motor to the desired positions rotating the crystal the correct amount within the required time. The ArduinoIDE control is integrated into LabView transferring the control of the Led to our LabView GUI. Our LabView GUI will therefore be the central user interface and how one can best troubleshoot the software.

9.6 Future Improvements

This project shows lots of promise. The more we worked on it as a group the more we wish we had more time to optimize the system. Narrowing down the limiting factors for a variety of system parameters. Starting from an optics perspective, some of the properties of our crystal may have been affecting our PER. The Polarization Extinction Ratio (PER) could have been limited due to the reflection from our crystal utilizing an anti-reflective coating may have helped push our PER even further. Furthermore, the crystals fast axis needs to be aligned with the rotation axis and the rotation axis needs to be 45° exactly to achieve maximum PER. Adding a tilt stage, getting a motor designed to mount our crystal in, exploring both of these options would mitigate this issue we were running into. Impurities in the crystal, our math and PER estimates assume a pure calcite crystal. If there is other material in the crystal this may be influencing our results. Using spectroscopy to measure the absorption spectrum of the crystal could be used to determine the purity of the calcite. The internal structure of the calcite may have stresses introduced to it during the manufacturing and polishing process. Finally, the thickness of the crystal may not be uniform. We did not investigate the thickness tolerances of the crystal and the scratch dig being rated for 80/60 if there is a dig on the crystal in the right spot this could be throwing off our PER.

The other thing that could be improved upon is the timing of the motor, reducing the time it takes to switch by using a motor tuned to the weight and moment of inertia to the crystal will push this even further. When controlling the motor we saw some inconsistencies when pushing the motor to go faster than 5 ms, namely when it tried to stop and hold at the high or low it would sometimes incur kickback, lowering max power of the signal. This could be improved by adding additional movement positions in between the two. Or having the motor move a little bit past the position

then back toward it. Another improvement to the motor control is to monitor the positioning of the motor. This can be done by connecting wires from the motor driver that deal with the motor positioning monitoring and comparing it to the voltage that is being output from the DAQ card to the motor driver. In LabVIEW, there is a set point generator graph that compares the ideal voltage values to the actual voltage values which can be utilized to determine the ideal motor control movement vs what is happening in the real world. Determining the motor movement will allow us to determine what is causing the spikes in the switching time graph.

We believe that improving these aspects of our system, the PER and the motor movement during our switch, would be great next steps to getting The Fast Polarization switch application ready. We look forward to seeing what future engineers will be able to accomplish using this solid foundation.

Chapter 10. Administrative Content

10.1 Budget

Our project was sponsored by ASML, and they therefore set limits on the design. One of these limits is our budget which they selected to be under \$7,500 and preferably below \$5,000. This budget encompasses every component that we may need including a light source and polarized beam splitter which are expensive items. This budget also encompasses any replacements we may need, including the PCB and other electronic parts that may be changed in the production of our project. A breakdown of expected costs and budget distribution is provided in the Bill of Materials section.

10.1.1 Bill of Materials Double-Pass

10.1.1.1 Thorlabs

Part Name	Part Number	Quantity	Unit Price	Total Price
BNC Cable	2249-C-36	1	\$ 21.23	\$ 21.23
Glan-Taylor	GT5	1	\$ 626.65	\$ 626.65
Optical Post	MS1R/M	7	\$ 7.96	\$ 55.72
M3 Screw Kit	HW-KIT5/M	1	\$ 123.30	\$ 123.30
Post Holder	MSH075	7	\$ 39.10	\$ 273.70
LED Connector	CON8ML-4	1	\$ 39.10	\$ 39.10
Retroreflector	PS974M-A	1	\$ 205.91	\$ 205.91
Lens	ACL25416U	2	\$ 22.00	\$ 44.00
1/2 Wave Plate	LCC1111U-A	1	\$ 388.95	\$ 388.95
Beamsplitter	CCM5-BS016/M	3	\$ 224.99	\$ 674.97
Post Clamp	PCM/M	1	\$ 48.63	\$ 48.63
Photo Detector	DET100A2	1	\$ 204.65	\$ 204.65
Mirror	BB03-E02	4	\$ 49.85	\$ 199.40
Mirror mount	MFM7/M	4	\$ 31.15	\$ 124.60

520 nm Laser	PL201	1	\$ 199.63	\$ 199.63
635 nm Laser	PL202	1	\$ 146.40	\$ 146.40
Galvo Cables	CBLS3F	1	\$ 105.72	\$ 105.72
Power Supply	GPWR15	1	\$ 600.27	\$ 600.27
Galvanometer	SS30Y-AG	1	\$ 3819.90	\$ 3819.90
LED	M470L5	1	\$ 261.20	\$ 261.20
Breadboard	MBY3030/M	1	\$ 369.15	\$ 369.15

10.1.1.2 Amazon

Part name	Part number	Quantity	Unit price	Total price
USB 2.0 Socket	B09WQHXPXH6	1	\$ 5.89	\$ 5.89
ESP32-S3	B0BX2MSCRT	1	\$ 15.00	\$ 15.00
M8 Plug IP67	B0DGXB6PPQ	1	\$ 9.98	\$ 9.98

10.1.1.3 DigiKey

Part name	Part number	Quantity	Unit price	Total price
Breadboard	1738-1326-ND	1	\$ 2.90	\$ 2.90
3.3 V REG	LM2575T-3.3/NOPB	1	\$ 3.63	\$ 3.63
LED Driver	LDDS-1000HW	1	\$ 8.87	\$ 8.87
IC PWR Switch	296-34970-1-ND	1	\$ 0.77	\$ 0.77
AC/DC Adapter	16-00216	1	\$ 11.81	\$ 11.81
DC Power Jack	2057-ADC-002-1-ND	1	\$ 0.33	\$ 0.33
22AWG Jumper Kit	BKWK-3-ND	1	\$ 5.60	\$ 5.60
DAQ DEVICE	2270-782606-01-ND	1	\$ 784.12	\$ 784.12

10.1.2 Bill of Materials Single-Pass

10.1.2.1 Thorlabs

Part Name	Part Number	Quantity	Unit Price	Total Price
BNC Cable	2249-C-36	1	\$ 21.23	\$ 21.23
Glan-Taylor	GT5	2	\$ 626.65	\$ 1253.30
Optical Post	MS1R/M	7	\$ 7.96	\$ 55.72
M3 Screw Kit	HW-KIT5/M	1	\$ 123.30	\$ 123.30
Post Holder	MSH075	7	\$ 39.10	\$ 273.70

LED Connector	CON8ML-4	1	\$ 39.10	\$ 39.10
Retroreflector	PS974M-A	1	\$ 205.91	\$ 205.91
Lens	ACL25416U	2	\$ 22.00	\$ 44.00
1/2 Wave Plate	LCC1111U-A	1	\$ 388.95	\$ 388.95
Beamsplitter	CCM5-BS016/M	1	\$ 224.99	\$ 224.99
Post Clamp	PCM/M	1	\$ 48.63	\$ 48.63
Photo Detector	DET100A2	1	\$ 204.65	\$ 204.65
Mirror	BB03-E02	3	\$ 49.85	\$ 149.55
Mirror mount	MFM7/M	3	\$ 31.15	\$ 93.45
520 nm Laser	PL201	1	\$ 199.63	\$ 199.63
635 nm Laser	PL202	1	\$ 146.40	\$ 146.40
Galvo Cables	CBLS3F	1	\$ 105.72	\$ 105.72
Power Supply	GPWR15	1	\$ 600.27	\$ 600.27
Galvanometer	SS30Y-AG	1	\$ 3819.90	\$ 3819.90
LED	M470L5	1	\$ 261.20	\$ 261.20
Breadboard	MBY3030/M	1	\$ 369.15	\$ 369.15

10.1.2.2 Amazon

Part name	Part number	Quantity	Unit price	Total price
USB 2.0 Socket	B09WQHXPXH6	1	\$ 5.89	\$ 5.89
ESP32-S3	B0BX2MSCRT	1	\$ 15.00	\$ 15.00
M8 Plug IP67	B0DGYB6PPQ	1	\$ 9.98	\$ 9.98

10.1.2.3 DigiKey

Part name	Part number	Quantity	Unit price	Total price
Breadboard	1738-1326-ND	1	\$ 2.90	\$ 2.90
3.3 V REG	LM2575T-3.3/NOPB	1	\$ 3.63	\$ 3.63
LED Driver	LDDS-1000HW	1	\$ 8.87	\$ 8.87
IC PWR Switch	296-34970-1-ND	1	\$ 0.77	\$ 0.77
AC/DC Adapter	16-00216	1	\$ 11.81	\$ 11.81
DC Power Jack	2057-ADC-002-1-ND	1	\$ 0.33	\$ 0.33
22AWG Jumper Kit	BKWK-3-ND	1	\$ 5.60	\$ 5.60
DAQ DEVICE	2270-782606-01-ND	1	\$ 784.12	\$ 784.12

10.2 Milestones

Table 10.2-1 Senior Design 1 Milestones

Milestone	Start Date	End Date
D&C Report Submission	08/26/2025	09/05/2025
Committee Formation	09/02/2025	09/05/2025
D&C Meeting	09/08/2025	09/08/2025
Rough Draft Midterm	09/08/2025	10/03/2025
Midterm Report	09/08/2025	10/24/2025
Beginning Simulation Results	09/15/2025	10/24/2025
Compile and Submit	10/25/2025	10/30/2025
Mid Project Demo component acquisition	10/30/2025	11/18/2025
Final Report Draft	10/31/2025	11/18/2025
Sim Results	10/25/2025	11/18/2025
Compile and submit final	11/18/2025	11/25/2025
Mid Project Demo assembly	11/18/2025	11/24/2025

Table 10.2-2 Senior design 2 Milestones

Milestone	Start Date	End Date
Acquisition of Final Components	11/23/2025	01/31/2026
Program Software Control	11/23/2025	02/13/2026
Build GUI to Control System	11/23/2025	02/13/2026
Sim results for timing of System	12/12/2025	02/13/2026
Characterization of polarization switch	02/13/2026	02/28/2026

Final adjustments to meet expectations for basic and advanced	02/13/2026	02/28/2026
Review and adjust report or sim	02/13/2026	02/28/2026
Accomplish Stretch Goals	02/28/2026	EOS (End of Semester)

10.3 Work Distributions

Electrical Engineering	Responsibilities: Software	Hardware
Michelle Nguyen	<ul style="list-style-type: none"> • Initialize Motor Library • Initialize MCU pins to motor • Set motor speed • Function: Calculate time for motor to spin to reach calculated degree • Set motor spin time • Break out of Switch Statement • Start motor • Stop motor 	<ul style="list-style-type: none"> • Power Supply • Microcontroller • Motor Driver • Motor
Optical Engineering		
David “Austin” Rich	<ul style="list-style-type: none"> • Initialize MCU pins for laser diodes • If / Else Statement: Turn on/off laser diodes based on User Prompt • Read Power Measurement 	<ul style="list-style-type: none"> • Laser Driver • Laser Diode • Power Detector

Joshua Hendry	<ul style="list-style-type: none"> • GUI / User Prompt • Function: Calculate needed degree for selected polarization • Switch Statement: Case selection based on User Prompt (polarization selected) • Set motor angle • Display Power Measurement on GUI 	<ul style="list-style-type: none"> • Laptop • Mirror • Retro-Mirror • Crystal
---------------	--	---

Chapter 11. Conclusion

The Fast Polarization switch was a fantastic project that pushed the boundaries of our skills and expertise as well as challenging our teamwork and time management skills throughout this year. We were able to accomplish our goals in the best way we could, given constraints. that took place throughout the year, namely the delay in the Crystal being sent to us by Crylink there has been myriad issues communicating with them however they had the shortest lead time responded to us readily however it did not arrive in time for our final demo. Designing peripheral experiments to verify that the components of our project have come in, we were able to prove the highlighted objectives showing that the current components will not be the limiting factor of our system. Our motor was able to achieve a rotation of 1.4° within 5 ms with a measured consistent timing of 2.56 ms,. Our polarizers achieving their advertised polarization extinction ratio of 100,000:1, and our diode being able to respond to sub millisecond response time as well.

The main optical design of the fast polarization switch works by rotating a birefringent crystal on a motor. The birefringent crystal, having two different refractive indices based on the polarization of light, works as a retarder for both polarizations. The retardation introduced leads to a phase difference between polarizations. When the light escapes the crystal this phase difference leads to a change in polarization. This rotating crystal is essentially acting as a variable waveplate for us to change polarization. To test if this is working, we use crossed polarizers. Since the crystal is changing polarization. This leads to a sinusoidal change in power with the maximum power and minimum power being orthogonal linear polarizations. With the combination of another variable waveplate this will allow a user to achieve any polarization desired from our system.

The design of our switch allows for a wide range of flexibility. This system works for the entire visible spectrum and allows for a large range of power. This means the system can be used as a fast power modulator. As a polarization switch the device would not include a power meter or cross polarizers, making this system easy to use and low maintenance.

Calcite was chosen as the crystal for our project, early on due to the desire to have a custom designed crystal and for the lead times of such a product, we settled on this early, using mathematical simulations to compare between three chosen crystals calcite with its high birefringence was chosen as we could achieve a target distance of rotation to be 0.1° in the double pass set up. Reducing the load on the motor drastically. Conserving power over the planned extended uses as well as enabling faster times, ensuring that fast switch time with sufficient PER is achieved.

Chapter 12. Appendix A: References

Allen (August 28, 2023). "A Comprehensive Guide about MSP430." Retrieved October 27, 2025, from <https://www.estartrade-ic.com/a-comprehensive-guide-about-msp430/>.

Anker (February 28, 2025). "What is a Micro USB Cable? A Complete Guide." Retrieved November 12, 2025, from <https://www.anker.com/blogs/cables/what-is-a-micro-usb-cable>.

Ariat Technology (October 1, 2024). "Understanding MSP430 Datasheet: All You Need to Know." Retrieved October 27, 2025, from <https://www.ariat-tech.com/blog/understanding-msp430-datasheet-all-you-need-to-know.html>.

Artizono (May 29, 2025). "Understanding Laser Galvanometers: Technical Deep Dive." Retrieved October 18, 2025, from <https://artizono.com/understanding-laser-galvanometers-technical-deep-dive/>.

Atwell, C. (April 17, 2023). "What's the Difference Between Python and MicroPython?". Retrieved November 6, 2025, from <https://www.electronicdesign.com/technologies/embedded/article/21264036/electronic-design-whats-the-difference-between-python-and-micropython>.

Ayodele, A. (March 31, 2025). "IPC Standards: The Definitive Guide for Electronics Engineers and PCB Designers." Retrieved November 11, 2025, from <https://www.wevolver.com/article/mastering-ipc-standards-the-definitive-guide-for-electronics-engineers-and-pcb-designers>.

Busch, J. (December 20, 2023). "Complete Guide to Using the Correct Charger or Power Adapter (and What Happens If You Don't)." Retrieved October 25, 2025, from <https://www.groovypost.com/howto/choose-right-power-adapter-charger-phone-laptop/>.

Cablink (May 3, 2025). "USB IF Certified 101: A Guide for USB Cables." Retrieved November 12, 2025, from <https://www.hdmiusb-cable.com/usb-if-certified-101-a-guide-for-usb-cables/>.

Cadence System Analysis. "Series Resistor and RC Termination for Digital Signals ". from <https://resources.pcb.cadence.com/blog/series-resistor-and-rc-termination-for-digital-signals>.

Campbell, S. "Basics of UART Communication." from <https://www.circuitbasics.com/basics-uart-communication/>.

CDN Newswire and LabJack Corporation (May 19, 2023). "An Introduction to DAQ Boards: Understanding the Basics." Retrieved October 19, 2025, from <https://www.digitaljournal.com/pr/news/cdn-newswire/an-introduction-to-daq-boards-understanding-the-basics>.

Chatarjee, S. (October 15, 2024). "STM32 Programming: A Comprehensive Beginner's Guide." Retrieved October 20, 2025, from <https://evelta.com/blog/stm32-programming-a-comprehensive-beginners-guide/>.

Chung, T. and J. Bagur (February 28, 2025). "The Arduino Guide to Low Power Design." Retrieved October 19, 2025, from <https://docs.arduino.cc/learn/electronics/low-power/>.

DeltaFlo. "Arduino Laser Show with Real Galvos." Retrieved October 18, 2025, from <https://www.instructables.com/Arduino-Laser-Show-With-Real-Galvos/>.

Elektronikz (May 12, 2025). "Comprehensive Review of the ESP32-S3-DevKitC-1 Development Board." Retrieved October 21, 2025, from <https://elektronikz.com/products/esp32-s3-devkitc-1-development-board>.

Elektronikz (June 9, 2024). "Review of ESP32-C3-DevKitM-1: Perfect for Wireless Projects." Retrieved October 21, 2025, from <https://elektronikz.com/products/esp32-c3-devkitm-development-board>.

ElProCus. "USB Protocol : Architecture, Working, Synchronisation, DataFormat & Its Applications." Retrieved November 6, 2025, from <https://www.elprocus.com/usb-protocol/>.

ESPBoards (November 25, 2024). "Can ESP32 Connect to 5 GHz Wi-Fi? Exploring Wi-Fi Connectivity Options with ESP32." Retrieved October 22, 2025, from <https://www.espboards.dev/blog/connect-esp32-to-5ghz-wifi/>.

everything PE (November 29, 2023). "What do you mean by Input Bias Current of an op-amp?". from <https://www.everythingpe.com/community/what-do-you-mean-by-input-bias-current-of-an-op-amp>.

eVision Instruments. "I2C vs SPI Protocol: Differences and Similarities." from <https://evision-webshop.eu/blog/i2c-vs-spi-protocol-differences-and-similarities>.

FlexPCB (August 16, 2024). "How to Choose a Motor Drive and Motor Controller." Retrieved October 19, 2025, from <https://flexpcb.org/how-to-choose-a-motor-drive-and-motor-controller/>.

Gariyal, V. (March 16, 2024). "STM32 Bluepill Pinout, Board Layout & Specifications." Retrieved October 20, 2025, from <https://www.etechnophiles.com/stm32-bluepill-pinout/>.

Ghosh, G. (1998). Handbook of optical constants of solids: Handbook of thermo-optic coefficients of optical materials with applications, Academic Press.

Ghosh, G. (1999). "Dispersion-equation coefficients for the refractive index and birefringence of calcite and quartz crystals." Optics Communications **163**(1): 95-102.

Google Gemini (2025). Flash 2.5. from <https://gemini.google.com/app>.

Greeks for Greeks (August 4, 2022). "Benefits of C Language over Other Programming Languages." Retrieved November 6, 2025, from <https://www.geeksforgeeks.org/c/benefits-c-language-programming-languages/>.

Highleap Electronic. "Beginner's Guide to STM32 Microcontroller." Retrieved October 20, 2025, from <https://hilelectronic.com/beginners-guide-to-stm32-microcontroller/>.

Holmes, D. A. (1964). "Exact Theory of Retardation Plates*." Journal of the Optical Society of America **54**(9): 1115-1120.

HowEngineeringWorks.com. "What are the advantages and disadvantages of stepper motors?". from <https://www.howengineeringworks.com/questions/what-are-the-advantages-and-disadvantages-of-stepper-motors/>.

IntelLiDrives Inc. Staff (July 16, 2018). "Repeatability in Motion Control." from <https://www.machinedesign.com/mechanical-motion-systems/article/21836934/repeatability-in-motion-control>.

Jacob (September 7, 2024). "Why Use CircuitPython? 10 Compelling Reasons You Can't Ignore [2024]." Retrieved November 6, 2025, from <https://roboticcoding.com/why-use-circuitpython/>.

K, V. (February 8, 2025). "ESP32-C5 DevKitC-1 Elevate Your IoT Projects with Next-Gen Wireless Capabilities." Retrieved October 21, 2025, from <https://embeddedhardwaredesign.com/esp32-c5-devkitc-1-elevate-your-iot-projects-with-next-gen-wireless-capabilities/>.

Lee, B., et al. (2025). "Double-pass rotating z-cut quartz plate as a rapidly variable waveplate." *Optics Express* **33**(13): 28739-28751.

Linux Code (December 30, 2024). "Introduction to Arduino Microcontrollers." Retrieved October 19, 2025, from <https://thelinuxcode.com/introduction-to-arduino-microcontrollers/>.

Lumi Manufacturing Technology (August 15, 2025). "How to Choose Suitable Precision Ball Bearings for Your Motor." from <https://lumimt.com/blogs/news/how-to-choose-suitable-precision-ball-bearings-for-your-motor>.

Magnetic Innovations. "What is a Moving Magnet Voice Coil Actuator?". from <https://www.magneticinnovations.com/faq/what-is-a-moving-magnet-voice-coil-actuator/>.

Masood, S. (November 24, 2024). "The Ultimate Guide to DAQ Systems: Everything You Need to Know." Retrieved October 19, 2025, from <https://2amagazine.com/the-ultimate-guide-to-daq-systems-everything-you-need-to-know/>.

McKay, J. (May 30, 2025). "Servo Drive Applications: Top Benefits for Motion Control Applications." Retrieved October 19, 2025, from <https://www.a-m-c.com/servo-drive-top-benefits-motion-control-applications/>.

Mechtex. "Advantages and Disadvantages of Brushless DC Motor (BLDC Motor)." Retrieved October 18, 2025, from <https://mechtex.com/blog/advantages-and-disadvantages-of-blcdc-motors>.

Menges, C. (October 10, 2025). "Exploring DAC Types: A Comprehensive Guide to DAC Architecture." from <https://www.moon-audio.com/blogs/expert-advice/dac-types-deciphered>.

Mikke (January 14, 2025). "12 Essential Advantages of Python (Why Learn Python in 2025)." Retrieved November 6, 2025, from <https://mikkegoes.com/advantages-of-python/>.

Mitchell, A. (September 6, 2024). "The Definitive Guide to Arduino Microcontrollers." Retrieved October 19, 2025, from <https://expertbeacon.com/the-definitive-guide-to-arduino-microcontrollers/>.

Modar Motor. "What are the pros and cons of brushless motors?". Retrieved October 18, 2025, from <https://www.modarmotor.com/what-are-the-pros-and-cons-of-brushless-motors/>.

Origin Data Global Limited (February 19, 2025). "18 AWG Wire: Specifications, Applications & Best Practices." Retrieved October 25, 2025, from <https://www.origin-ic.com/blog/18-AWG-Wire-Specifications-Applications-Best-Practices/47511>.

Paranin, V. D. (2016). "Determination of the optical axis in Z-cut uniaxial crystals by a polarization-based method." *Technical Physics Letters* **42**(6): 559-562.

Pena, E. and M. G. Legaspi (December 2020). "UART: A Hardware Communication Protocol Understanding Universal Asynchronous Receiver/Transmitter." from <https://www.analog.com/en/resources/analog-dialogue/articles/uart-a-hardware-communication-protocol.html>.

Peterson, B. T., et al. (April 2024). "Cross-Axis Flexural Pivots in Mechatronic Applications: Stress-Based Design for Combined Tension and Bending." from <https://ieeexplore.ieee.org/document/10342672/citations#citations>.

Poole, I. "USB Standards: USB 1, USB 2, USB 3, USB 4 - Capabilities & Comparisons." Retrieved November 12, 2025, from <https://www.electronics-notes.com/articles/connectivity/usb-universal-serial-bus/standards.php>.

Rakshit, S. (September 28, 2024). "What is MicroPython? Everything You Need to Know." Retrieved November 6, 2025, from <https://pyseek.com/2024/09/what-is-micropython/>.

Random Nerd Tutorials (August 5, 2024). "Getting Started with the ESP32 Development Board." Retrieved October 19, 2025, from <https://randomnerdtutorials.com/getting-started-with-esp32/>.

Retekdrones (July 25, 2025). "What are the Pros and Cons of Servo Motors?". Retrieved October 16, 2025, from <https://retekdrones.com/blog/what-are-the-pros-and-cons-of-servo-motors/>.

Roberts, C. (November 11, 2015). "\$20 WiFi Connected Hardware Solution with ESP8266." Retrieved October 27, 2025, from <https://www.hackster.io/ctroberts/20-wifi-connected-hardware-solution-with-esp8266-fb5995>.

Seelig, F. A. "Flexural Pivots for Space Applications." from <https://ntrs.nasa.gov/api/citations/19690002472/downloads/19690002472.pdf>.

Sharma, A. (July 17, 2019). "Interfacing HC-05 Bluetooth Module with MSP430 Launchpad to control an LED." Retrieved October 27, 2025, from <https://circuitdigest.com/microcontroller-projects/interfacing-hc-05-bluetooth-module-with-msp430-launchpad-to-control-an-led>.

Sintec Optronics (September 3, 2020). "Choosing the Right Galvanometer and Servo for the Job." Retrieved October 18, 2025, from <https://www.sintec.sg/ApplicationNotes/335.html>.

Smith, H. (November 12, 2024). "IPC-2221 | PCB Design." Retrieved November 11, 2025, from <https://www.pcbasic.com/blog/ipc-2221.html>.

Smoot, R. (June 23, 2020). "How to Select DC Power Connectors: The Basics." Retrieved October 25, 2025, from <https://www.allaboutcircuits.com/industry-articles/how-to-select-dc-power-connectors-the-basics/>.

Starting Electronics (February 20, 2025). "Introduction to the ESP32: A Comprehensive Guide for Beginners." Retrieved October 19, 2025, from <https://startingelectronics.org/articles/ESP32/esp32-introduction/>.

STM32-base. "Getting started with STM32." Retrieved October 20, 2025, from <https://stm32-base.org/guides/getting-started.html>.

Tedford, M., et al. "Analog vs. Digital Galvanometer Technology – An Introduction." from <https://novantaphotonics.com/analog-vs-digital-galvanometer-technology-an-introduction/>.

Thorlabs. "Cross-Flexure Single-Axis VantagePro Galvo Systems." Retrieved October 18, 2025, from https://www.thorlabs.com/newgrouppage9.cfm?objectgroup_id=14123&pn=SS30Y-AG.

Toshiba. "What is the input offset voltage of an op-amp?". from https://toshiba.semicon-storage.com/us/semiconductor/knowledge/faq/linear_opamp/what-is-the-input-offset-voltage-of-an-op-amp.html.

Unit Electronics (August 8, 2025). "2025 MCU Selection Guide: Unitsemi MSP430 Series Advantages." Retrieved October 27, 2025, from <https://www.unitsemi.com/mcu-selection-guide-unitsemi-msp/#:~:text=This%20guide%20is%20for%20engineers%2C%20buyers%2C%20and%20product,%E2%80%94%20from%20ultra-low-BOM%20parts%20to%20FRAM-based%2C%20touch-capable%20models>.

Voss, W. (November 3, 2025). "Programming the ESP32: Choosing the Right IDE for Your Workflow." Retrieved November 6, 2025, from <https://copperhilltech.com/blog/programming-the-esp32-choosing-the-right-ide-for-your-workflow/>.

Wu, J. "IPC-2221: The Standard for Printed Circuit Board Design." Retrieved November 11, 2025, from <https://www.nextpcb.com/blog/ipc-2221>.

yida (September 13, 2022). "SPI – Introduction to Serial Peripheral Interface." from <https://www.seeedstudio.com/blog/2019/11/22/spi-introduction-to-serial-peripheral-interface/>.

Zallat, J., et al. (2012). "Double-pass self-spectral-calibration of a polarization state analyzer." *Optics Letters* **37**(3): 401-403.

Zhou, B. (July 7, 2025). ""What Are The Disadvantages of Servo Motors?"" Retrieved October 17, 2025, from <https://www.hlt-cnc.com/blog/what-are-the-disadvantages-of-servo-motors-428283.html>.

Zink, O. (February 21, 2025). "ESP32 Buying Guide: Find the Best ESP32 Board for Your Projects." Retrieved October 20, 2025, from <https://coolplaydev.com/best-esp32-buying-guide>.

Chapter 13. Appendix B: Data Sheets and Reference Figures

Table 2. Comparison of the experimental and computed values of refractive index for the ordinary rays of calcite crystal

Wavelength (μm)	Refractive index		Difference	R.I. (calculated) [2]	Difference
	Experimental [1]	This work			
0.2040	1.88224	1.882184	0.000056	1.884897	-0.002657
0.2080	1.86733	1.866589	0.000741	1.868397	-0.001067
0.2110	1.85692	1.855997	0.000923	1.857550	-0.000630
0.2140	1.84558	1.846232	-0.000652	1.847669	-0.002089
0.2190	1.83075	1.831551	-0.000801	1.832931	-0.002181
0.2260	1.81309	1.813794	-0.000704	1.815199	-0.002109
0.2310	1.80233	1.802752	-0.000422	1.804197	-0.001867
0.2420	1.78211	1.782239	-0.000129	1.783761	-0.001651
0.2570	1.76038	1.760496	-0.000116	1.762065	-0.001685
0.2630	1.75343	1.753303	0.000127	1.754873	-0.001443
0.2670	1.74864	1.748894	-0.000254	1.750460	-0.001820
0.2740	1.74139	1.741830	-0.000440	1.743380	-0.001990
0.2910	1.72774	1.727493	0.000247	1.728974	-0.001234
0.3030	1.71959	1.719253	0.000337	1.720668	-0.001078
0.3120	1.71425	1.713869	0.000381	1.715229	-0.000979
0.3300	1.70515	1.704727	0.000423	1.705972	-0.000822
0.3400	1.70078	1.700410	0.000370	1.701590	-0.000810
0.3460	1.69833	1.698037	0.000293	1.699179	-0.000849
0.3610	1.69316	1.692717	0.000443	1.693764	-0.000604
0.3940	1.68374	1.683418	0.000322	1.684272	-0.000532
0.4100	1.68014	1.679808	0.000332	1.680578	-0.000438
0.4340	1.67552	1.675209	0.000311	1.675864	-0.000344
0.4410	1.67423	1.674022	0.000208	1.674645	-0.000415
0.5080	1.66527	1.665186	0.000084	1.665564	-0.000294

Wavelength (μm)	Refractive index		Difference	R.I. (calculated) [2]	Difference
	Experimental [1]	This work			
0.5330	1.66277	1.662745	0.000025	1.663052	-0.000282
0.5600	1.66046	1.660471	-0.000011	1.660711	-0.000251
0.5890	1.65835	1.658364	-0.000014	1.658543	-0.000193
0.6430	1.65504	1.655139	-0.000099	1.655229	-0.000189
0.6560	1.65437	1.654470	-0.000100	1.654542	-0.000172
0.6700	1.65367	1.653788	-0.000118	1.653842	-0.000172
0.7000	1.65207	1.652444	-0.000374	1.652465	-0.000395
0.7680	1.64974	1.649868	-0.000128	1.649834	-0.000094
0.7950	1.64886	1.648985	-0.000125	1.648935	-0.000075
0.8010	1.64869	1.648797	-0.000107	1.648745	-0.000055
0.8330	1.64772	1.647844	-0.000124	1.647778	-0.000058
0.8670	1.64676	1.646908	-0.000148	1.646831	-0.000071
0.9050	1.64578	1.645937	-0.000157	1.645852	-0.000072
0.9460	1.64480	1.644964	-0.000164	1.644874	-0.000074
0.9910	1.64380	1.643964	-0.000164	1.643873	-0.000073
1.0420	1.64276	1.642899	-0.000139	1.642812	-0.000052
1.0970	1.64167	1.641811	-0.000141	1.641732	-0.000062
1.1590	1.64051	1.640638	-0.000128	1.640572	-0.000062
1.2290	1.63926	1.639359	-0.000099	1.639311	-0.000051
1.2730	1.63849	1.638570	-0.000080	1.638535	-0.000045
1.3070	1.63789	1.637965	-0.000075	1.637940	-0.000050
1.3200	1.63767	1.637734	-0.000064	1.637714	-0.000044
1.3690	1.63681	1.636866	-0.000056	1.636862	-0.000052
1.3960	1.63637	1.636388	-0.000018	1.636392	-0.000022
1.4220	1.63590	1.635926	-0.000026	1.635939	-0.000039
1.4790	1.63490	1.634910	-0.000010	1.634940	-0.000040
1.4970	1.63457	1.634587	-0.000017	1.634623	-0.000053
1.5410	1.63381	1.633793	0.000017	1.633841	-0.000031
1.6090	1.63261	1.632548	0.000062	1.632614	-0.000004
1.6820	1.63127	1.631183	0.000087	1.631263	0.000007
1.7610	1.62974	1.629666	0.000074	1.629756	-0.000016

Wavelength (μm)	Refractive index		Difference	R.I. (calculated) [2]	Difference
	Experimental [1]	This work			
1.8490	1.62800	1.627922	0.000078	1.628012	-0.000012
1.9460	1.62602	1.625924	0.000096	1.626000	0.000020
2.0530	1.62372	1.623621	0.000099	1.623659	0.000061
2.1720	1.62099	1.620926	0.000064	1.620888	0.000102
			RMSD=0.0003		RMSD=0.0009

Table 3. Comparison of the experimental and computed values of refractive index for the extraordinary rays of calcite crystal

Wavelength (μm)	Refractive index		Difference	R.I. (calculated) [2]	Difference
	Experimental [1]	This work			
0.2040	1.57081	1.570667	0.000143	1.571153	-0.000343
0.2080	1.56640	1.566086	0.000314	1.566326	0.000074
0.2110	1.56327	1.562883	0.000387	1.562984	0.000286
0.2140	1.55976	1.559863	-0.000103	1.559855	-0.000095
0.2190	1.55496	1.555197	-0.000237	1.555060	-0.000100
0.2260	1.54921	1.549340	-0.000130	1.549099	0.000111
0.2310	1.54541	1.545575	-0.000165	1.545298	0.000112
0.2420	1.53782	1.538317	-0.000497	1.538024	-0.000204
0.2570	1.53005	1.530226	-0.000176	1.529982	0.000068
0.2630	1.52736	1.527455	-0.000095	1.527240	0.000120
0.2670	1.52547	1.525733	-0.000263	1.525538	-0.000068
0.2740	1.52261	1.522933	-0.000323	1.522775	-0.000165
0.2910	1.51705	1.517101	-0.000051	1.517029	0.000021
0.3030	1.51365	1.513654	-0.000004	1.513638	0.000012
0.3120	1.51140	1.511364	0.000036	1.511386	0.000014
0.3300	1.50746	1.507405	0.000055	1.507492	-0.000032
0.3400	1.50562	1.505505	0.000115	1.505623	-0.000003
0.3460	1.50450	1.504452	0.000048	1.504587	-0.000087
0.3610	1.50224	1.502071	0.000169	1.502242	-0.000002
0.3940	1.49810	1.497838	0.000262	1.498069	0.000031
0.4100	1.49640	1.496173	0.000227	1.496425	-0.000025
0.4340	1.49430	1.494035	0.000265	1.494310	-0.000010

Wavelength (μm)	Refractive index		Difference	R.I. (calculated) [2]	Difference
	Experimental [1]	This work			
0.4410	1.49373	1.493481	0.000249	1.493762	-0.000032
0.5080	1.48956	1.489333	0.000227	1.489643	-0.000083
0.5330	1.48841	1.488186	0.000224	1.488499	-0.000089
0.5600	1.48736	1.487121	0.000239	1.487433	-0.000073
0.5890	1.48640	1.486139	0.000261	1.486449	-0.000049
0.6430	1.48490	1.484658	0.000242	1.484955	-0.000055
0.6560	1.48459	1.484355	0.000235	1.484648	-0.000058
0.6700	1.48426	1.484049	0.000211	1.484336	-0.000076
0.7000	1.48353	1.483452	0.000078	1.483728	-0.000198
0.7680	1.48259	1.482345	0.000245	1.482589	0.000001
0.7950	1.48216	1.481980	0.000180	1.482209	-0.000049
0.8010	1.48216	1.481904	0.000256	1.482129	0.000031
0.8330	1.48176	1.481522	0.000238	1.481729	0.000031
0.8670	1.48137	1.481159	0.000211	1.481345	0.000025
0.9050	1.48098	1.480798	0.000182	1.480958	0.000022
0.9460	1.48060	1.480451	0.000149	1.480582	0.000018
0.9910	1.48022	1.480114	0.000106	1.480211	0.000009
1.0420	1.47985	1.479776	0.000074	1.479832	0.000018
1.0970	1.47948	1.479455	0.000025	1.479463	0.000017
1.1590	1.47910	1.479135	-0.000035	1.479087	0.000013
1.2290	1.47870	1.478817	-0.000117	1.478700	0.000000
1.3070	1.47831	1.478503	-0.000193	1.478305	0.000005
1.3960	1.47789	1.478185	-0.000295	1.477887	0.000003
1.4970	1.47744	1.477861	-0.000421	1.477441	-0.000001
1.6150	1.47695	1.477516	-0.000566	1.476942	0.000008
1.7490	1.47638	1.477155	-0.000775	1.476389	-0.000009
1.9090	1.47573	1.476745	-0.001015	1.475729	0.000001
2.1000	1.47492	1.476269	-0.001349	1.474921	-0.000001
3.3240	1.47392	1.472766	0.001154	1.468373	0.005547
			RMSD=0.0004		RMSD=0.0008

Table 4. Comparison of the experimental and computed values of refractive index for the ordinary rays of quartz crystal

Wavelength (μm)	Refractive index		Difference	R.I. (calculated) [2]	Difference
	Experimental [1]	This work			
0.1980	1.65087	1.650902	-0.000032	1.652553	-0.001683
0.2310	1.61395	1.613860	0.000090	1.614267	-0.000317
0.3400	1.56747	1.567554	-0.000084	1.567528	-0.000058
0.3940	1.55846	1.558504	-0.000044	1.558488	-0.000028
0.4340	1.55396	1.553960	0.000000	1.553956	0.000004
0.5080	1.54822	1.548240	-0.000020	1.548257	-0.000037
0.5893	1.54424	1.544206	0.000034	1.544238	0.000002
0.7680	1.53903	1.538998	0.000032	1.539048	-0.000018
0.8325	1.53773	1.537711	0.000019	1.537763	-0.000033
0.9914	1.53514	1.535126	0.000014	1.535179	-0.000039
1.1592	1.53283	1.532823	0.000007	1.532872	-0.000042
1.3070	1.53090	1.530905	-0.000005	1.530949	-0.000049
1.3958	1.52977	1.529752	0.000018	1.529792	-0.000022
1.4792	1.52865	1.528651	-0.000001	1.528687	-0.000037
1.5414	1.52781	1.527813	-0.000003	1.527846	-0.000036
1.6815	1.52583	1.525857	-0.000027	1.525883	-0.000053
1.7614	1.52468	1.524690	-0.000010	1.524712	-0.000032
1.9457	1.52184	1.521832	0.000008	1.521845	-0.000005
2.0531	1.52005	1.520048	0.000002	1.520056	-0.000006
			RMSD=0.0003		RMSD=0.0004

Table 5. Comparison of the experimental and computed values of refractive index for the extraordinary rays of quartz crystal

Wavelength (μm)	Refractive index		Difference	R.I. (calculated) [2]	Difference
	Experimental [1]	This work			
Empty Cell			Empty Cell	Empty Cell	Empty Cell
0.1980	1.66394	1.663972	-0.000032	1.665774	-0.001834
0.2310	1.62555	1.625459	0.000091	1.625948	-0.000398
0.3400	1.57737	1.577457	-0.000087	1.577594	-0.000224
0.3940	1.56805	1.568093	-0.000043	1.568306	-0.000256
0.4340	1.56339	1.563393	-0.000003	1.563673	-0.000283

Wavelength (μm)	Refractive index		Difference	R.I. (calculated) [2]	Difference
	Experimental [1]	This work	Empty Cell	Empty Cell	Empty Cell
0.5080	1.55746	1.557478	-0.000018	1.557888	-0.000428
0.5893	1.55335	1.553306	0.000044	1.553871	-0.000521
0.7680	1.54794	1.547917	0.000023	1.548871	-0.000931
0.8325	1.54661	1.546583	0.000027	1.547698	-0.001088
0.9914	1.54392	1.543901	0.000019	1.545459	-0.001539
1.1592	1.54152	1.541508	0.000012	1.543614	-0.002094
1.3070	1.53951	1.539513	-0.000003	1.542172	-0.002662
1.3958	1.53832	1.538312	0.000008	1.541337	-0.003017
1.4792	1.53716	1.537166	-0.000006	1.540556	-0.003396
1.5414	1.53630	1.536292	0.000008	1.539970	-0.003670
1.6815	1.53422	1.534253	-0.000033	1.538623	-0.004403
1.7614	1.53301	1.533036	-0.000026	1.537831	-0.004821
1.9457	1.53004	1.530055	-0.000015	1.535911	-0.005871
2.0531	1.52823	1.528194	0.000036	1.534722	-0.006492
			RMSD=0.00004		RMSD=0.003

(Ghosh 1999)

Appendix C: LLM Prompts and Responses

[1a] Case Study 1 Prompt: “average stepper motor cost”

[1b] Case Study 1 Google Gemini Outcome: “The cost of a stepper motor can range significantly, typically from **\$5 to over \$1,500** per unit, but most common motors for hobbyists and light industrial use fall between **\$10 and \$200**.”

The wide price range is due to several key factors, primarily **size (NEMA standard), torque, speed, and additional features** like integrated drivers or encoders.

Typical Price Ranges by NEMA Size and Application

Stepper motors are often categorized by their **NEMA frame size**, which indicates the mounting face dimensions in inches (e.g., NEMA 17 has a 1.7" x 1.7" face). Generally, a larger NEMA size corresponds to higher torque and a higher price.

NEMA Frame Size	Typical Price Range (USD)	Common Applications
NEMA 8 to NEMA 14	\$5 - \$40	Small devices, precise optics, light-duty linear actuators, small 3D printers.
NEMA 17	\$10 - \$50	The most common size for 3D printers, CNC routers (desktop/small), and general hobby robotics.
NEMA 23	\$20 - \$150	Medium-duty CNC machines, larger 3D printers, industrial automation equipment requiring more power.
NEMA 34 and larger	\$50 - \$1,500+	Heavy-duty industrial CNC machinery, high-power robotic systems, and demanding motion control applications.

Factors Influencing Stepper Motor Cost

- **Holding Torque:** This is the most significant factor. Motors with **higher holding torque** (more powerful) require larger magnets and more robust construction, leading to a higher cost.

- **Integrated Electronics:** Motors with a built-in **driver** or **closed-loop encoder** system (sometimes called *servo-stepper* or *easy-servo*) are significantly more expensive, often ranging from **\$80 to over \$600**. These provide higher precision and prevent missed steps.
- **Precision (Step Angle):** Motors with a smaller step angle (e.g., 0.9° instead of the standard 1.8°) offer better positional resolution and are typically more expensive.
- **Gearing:** Motors with an integrated **planetary gearbox** increase torque and precision but also increase the cost, sometimes by two to five times the price of the motor alone.
- **Brand and Quality:** Industrial-grade motors from reputable brands (e.g., Applied Motion, Oriental Motor) designed for continuous, high-reliability operation in harsh environments are far more costly than generic, mass-produced motors often sold on consumer marketplaces.”

[2a] Case Study 2 Prompt: “average servo motor cost”

[2b] Case Study 2 Google Gemini Outcome: “The cost of a servo motor can vary dramatically, ranging from a few dollars for small hobbyist motors to several thousand dollars for high-precision industrial units.

Here is a breakdown of typical price ranges based on the type and application:

Servo Motor Type	Typical Price Range	Key Characteristics
Hobby/Micro Servos	\$5 to \$50	Small, low-power motors often used in RC cars, planes, and basic robotics.
DC Servo Motors	\$100 to \$500	Generally brushed, known for high torque at lower speeds, sometimes requiring separate encoders.
AC Servo Motors	\$200 to \$2,000+	More common in industrial applications, generally more efficient and higher power. Price depends heavily on power and torque ratings.
Brushless DC (BLDC) Servo Motors	\$150 to \$5,000+	Used for high-precision applications like advanced robotics and aerospace. Known for long life and high efficiency.
High-End Industrial Servo Systems	\$1,000 to \$8,000+	High-power motors (e.g., 1 kW to 7.5 kW with high torque, often from major brands like Fanuc, Siemens, or Yaskawa. Prices can go significantly higher for

		specialized direct-drive or extremely high-power units.
--	--	---

Key Factors that Influence Servo Motor Cost:

- **Torque and Power:** Higher torque (measured in Newton-meters, or Nm) and higher power ratings (measured in Watts or kW) directly increase the cost.
- **Precision/Resolution:** Motors with high-quality encoders or resolvers for precise positioning are generally more expensive.
- **Brand and Quality:** Reputable industrial brands often command higher prices due to their established quality, support, and advanced features.
- **Type:** As shown above, the fundamental design (DC, AC, BLDC, Direct Drive) is a primary cost driver.
- **Control System/Drive:** The total system cost includes the motor's dedicated drive unit or controller, which can add another **\$100 to \$5,000+** depending on its complexity (e.g., simple controllers vs. advanced multi-axis CNC controls)."

[3a] Case Study 3 Prompt: "DC Brushless Servo Motor average cost range"

[3b] Case Study 3 Google Gemini Outcome: "The cost of DC Brushless Servo Motors (BLDC servo motors) can vary significantly based on factors like power, torque, integrated features (like a driver/controller and encoder), and intended application (hobby, industrial, or specialized robotics).¹

Based on current market data, here is a general average cost range:

- **Entry-Level / Small Motors (e.g., hobby, low power/torque):**
 - Motors alone can start from as low as **\$15 to \$50** for very small units or basic BLDC motors used in some servo applications.
 - Small motor and driver kits typically range from **\$90 to \$250**.
- **Mid-Range / Industrial Motors (Standard Power, NEMA 23/34 sizes):**
 - Individual industrial-grade motors (e.g., 50W to 1000W) often fall between **\$150 and \$700**.
 - Motor and driver kits for this range are often found between **\$200 and \$1,000**.
- **High-End / High-Power / Specialized Motors (e.g., high torque, integrated harmonic drive, advanced industrial):**
 - High-power units (1kW and up) or motors with specialized gearing/high-resolution absolute encoders can range from **\$1,000 to over \$5,000**, with highly specialized robotic actuators reaching **\$7,000 or more**.

A comprehensive price range for **most BLDC Servo Motors** is approximately **\$150 to \$5,000**.²

Key Factors Influencing Cost:

1. **Power and Torque:** Higher power (Watts or Horsepower) and higher rated torque motors are significantly more expensive.³
2. **Encoder Type:** Motors with high-resolution **absolute encoders** are typically more costly than those with **incremental encoders**.
3. **Integration:** A **motor and driver/controller kit** is often more expensive than the motor alone. Some motors are highly integrated with reduction gearboxes (like harmonic drives) which drives the price up considerably.
4. **Brand and Quality:** Well-known industrial brands (e.g., Yaskawa, Kollmorgen, Parker) often have higher prices than motors from generic or specialized component suppliers.
5. **Application:** Motors designed for high-precision, heavy-duty industrial automation or aerospace are priced much higher than those for general-purpose DIY or light automation.”

[4a] Case Study 4 Prompt: “galvanometer motor average cost range”

[4b] Case Study 4 Google Gemini Outcome: “The average cost of **galvanometer motors** (often sold as part of a **galvanometer scanning head** or **galvo system**) can range broadly, typically falling between a few hundred to tens of thousands of dollars, depending heavily on the component type, performance, and application.¹

Typical Cost Range Breakdown

Component/System	Estimated Cost Range (USD)	Key Factors Affecting Price
Basic Galvo Motor/Single Axis Scanner	\$50 - \$600	Low-speed, smaller aperture (e.g., 5mm), often used for laser light shows or hobby-level marking.
High-Speed 2D Galvo Scanner Head (Pair of Motors + Drivers)	\$300 - \$4,500	Aperture size (e.g., 10mm), speed/precision (kpps rating), brand, and whether it includes a full driver board and optics.
Industrial/High-Performance 2D Galvo Scanner Head	\$3,500 - \$10,000+	High-precision, large aperture (e.g., 15mm+), premium brands, and specialized coatings for high-power lasers (e.g., CO2, Fiber).

3-Axis Dynamic Focusing Galvo System (Full Laser Scan Head)	\$12,000 - \$55,000+	Advanced systems used for large-area marking, 3D printing, or high-power industrial applications, including complex optics and advanced controls.
--	-----------------------------	---

Factors Influencing Galvanometer Motor Cost

The price variation is significant because a "galvanometer motor" can refer to a small, single component or an entire, highly sophisticated scanning system. Key factors include:

- **Axis Configuration:**
 - **Single-axis** systems are cheaper as they only require one motor and mirror.
 - **Dual-axis (2D)** scanner heads use a pair of motors/mirrors (X and Y) and a combined driver system, which is the most common configuration for laser marking and engraving.
 - **3-axis** systems add dynamic focusing (Z-axis control) for marking on curved surfaces or over a large area, making them the most expensive component-wise.
- **Performance (Speed and Precision):**
 - **High-Speed/High-Precision:** Galvanometers with fast step response times and high positioning repeatability (often rated in **kilopoints per second or kpps**) are significantly more expensive, as they require superior motor quality and control electronics.
- **Aperture Size:** This refers to the diameter of the mirror and the beam it can handle (e.g., 5mm, 10mm, 15mm). Larger apertures typically handle higher-power lasers and cost more due to the precision required for larger components.
- **Application/Source:** Systems optimized for different laser wavelengths (e.g., 1065 nm, 355 nm) require specific mirror coatings, impacting the price.
- **Brand and Build Quality:** Premium, industrial-grade manufacturers (e.g., SCANLAB, Raylase, Cambridge Technology) charge higher prices for guaranteed long-term stability, higher resolution, and superior performance compared to mass-market or generic brands.”

[5a] Case Study 5 Prompt: “galvanometer motor, using computer as the controller”

[5b] Case Study 5 Google Gemini Outcome: “A **galvanometer motor** (often called a **galvo scanner** or **galvo motor**) is an oscillating motor, distinct from a typical rotating motor, that is used to rapidly and precisely deflect a laser beam in applications like laser marking, cutting, and welding.

The **computer** acts as the **high-level controller** in a galvanometer motor system.

How the Computer Controls the Galvo Motor

1. **Software Interface:** The process begins with **marking software** or other control applications installed on a host computer. This software allows a user to design the pattern, text, or graphic to be processed by the laser.
2. **Data Processing:** The computer's software processes this design into a large amount of digital **marking data**, including trajectory and laser power information.
3. **Dedicated Controller/Interface Card:** The computer's digital commands are sent to a dedicated **galvo controller card** (sometimes called a laser marking card or digital servo board). This card is crucial for real-time control.
 - The industry-standard **XY2-100 protocol** is often used for communication between the computer's system and the galvo controller.
4. **Signal Conversion and Amplification:** The controller card contains a **Digital-to-Analog Converter (DAC)** to convert the digital position commands into analog voltage signals, which are then amplified by **servo amplifiers**.
5. **Motor Control:** These amplified analog signals are sent to the two galvanometer motors (one for the **X-axis** and one for the **Y-axis**), causing them to rotate their mounted mirrors.
6. **Closed-Loop Feedback:** Modern galvanometer systems are typically **closed-loop**. They use integrated **position sensors** (like optical encoders or capacitive sensors) on the motor axis to continuously measure the mirror's actual angular position. This position data is fed back to the controller, which compares it to the commanded position and makes real-time adjustments to the current, ensuring high precision, accuracy, and quick settling times.

Essentially, the **computer** defines the "what" and "where" of the pattern, and the **galvo controller** handles the "how" by translating those commands into the high-speed, precise electrical signals needed to drive the galvo motors.

The video below explains the inner workings of a closed-loop laser galvanometer. [Inside the Closed Loop Laser Beam Steering Galvanometer](#)"

[6a] Case Study 6 Prompt: “galvanometer motor, using microcontroller as the controller”

[6b] Case Study 6 Google Gemini Outcome: “A **microcontroller (MCU)** can be used as the controller for a galvanometer motor system, particularly in **DIY, research, and lower-speed** applications. However, it requires a specific interface circuit because the MCU's digital output cannot directly drive the analog, high-speed galvo motors.

Microcontroller Galvo Control Architecture

The MCU serves as the **digital brain** that calculates the necessary coordinates and controls the peripheral hardware that interfaces with the galvos.

Component	Function	Detail
Microcontroller (MCU)	Digital Command Generation	Executes the control logic (e.g., drawing a circle or square). It sends position data (digital values) and laser

		on/off commands. Common MCUs include Arduino, Teensy, or STM32 boards.
External DAC Chip	Digital-to-Analog Conversion	Converts the MCU's digital position values into an analog voltage signal . This is critical because galvo drivers require a smooth, continuous analog voltage (± 10 V is common) to command the mirror's angle. Integrated MCU DACs are often too slow or low-resolution.
Driver Circuit/Servo Amplifier	Signal Conditioning & Power	This is the actual motor controller. It takes the low-voltage analog signal from the DAC and: 1. Amplifies it to the required power and voltage levels (e.g., ± 10 V and high current). 2. Drives the motor coils to achieve the commanded angle. 3. Processes the position feedback from the galvo's internal sensor to maintain closed-loop control.
Galvanometer Motors	Mechanical Movement	Two galvo motors (X and Y) with mirrors mounted on them rapidly deflect the laser beam to trace the pattern.

Key Considerations for MCU Control

- **Speed and Resolution:** Commercial laser marking systems require very high speeds (up to 60k points per second or kpps) and high resolution (16-bit DACs), which can strain the data rate of typical hobbyist MCUs. Faster MCUs like the **Teensy** are often preferred for smoother, higher-speed projects.
- **External DAC:** An external **Digital-to-Analog Converter (DAC)** is almost always required. A popular choice is a dual-channel, 12-bit or 16-bit DAC (like the **MCP4822**) to handle the X and Y axes.
- **Analog Signal Requirement:** The galvanometer driver typically expects a **bipolar analog signal** (e.g., -5V to +5V or -10V to +10V). Since most MCUs output a **unipolar digital signal** (e.g., 0V to 3.3V or 0V to 5V), the circuit design must include op-amps and an appropriate power supply to create the required negative voltage and scale the signal range.

For more on DIY galvo control, see how one person achieved it using an Arduino.

[Arduino Laser Show With Real Galvos](#)

This video provides a practical, step-by-step guide for using an Arduino and an external DAC to create a functional galvanometer control system for a laser show.”

[7a] **Case Study 7 Prompt:** “average cost galvo controller card”

[7b] **Case Study 7 Google Gemini Outcome:** “The cost of a galvanometer (galvo) controller card varies widely depending on its **intended application, performance level, and whether it's an integrated industrial solution or a hobbyist component.**”

Here is a general breakdown of the price ranges you can expect:

Price Range	Application & Performance Level	Examples
Budget/Hobbyist	Low-speed laser show or DIY projects. Often simple driver boards for the galvo motor itself, or specialized low-end program boards.	\$40 to \$200 USD
Industrial / Commercial (Mid-Range)	Dedicated laser marking/engraving machine control boards (often referred to as "Galvo Controllers" or "Control Cards" like JCZ/EZCAD). These are high-speed digital controllers that interface between a PC and the galvo driver/laser.	\$300 to \$750 USD
High-Performance / Scientific	High-end industrial, medical, or scientific scanning systems. These are typically part of a larger, complete galvo scan head system and offer extremely high speed, resolution (18-20+ bit), and complex firmware for precision work.	\$1,000 to over \$10,000 USD (often sold as a complete system with the galvos)

Key Takeaways:

- **Industrial Control Card (EZCAD/JCZ Type):** For most commercial laser marking machines, the dedicated control card that handles the job file and interfaces with the galvo drivers (often referred to as an "EZCAD" or similar board) typically costs in the **\$300 - \$750 USD** range.”
- **Hobbyist Components:** If you are building a system using a microcontroller (like an Arduino) and only need the basic **driver board** (servo amplifier) for a pair of galvos, the total cost for the control electronics is often much lower, but this path requires more DIY integration and coding.
- **Complete Scan Heads:** High-performance galvo systems are often sold as a **complete scan head** (galvo motors, mirrors, and drivers) with a dedicated controller, which can cost thousands of dollars.

[8a] Case Study 8 Prompt: “average cost of microcontroller”

[8b] Case Study 8 Google Gemini Outcome: “The average cost of a microcontroller can vary dramatically, ranging from under **\$1 to tens or even hundreds of dollars**, depending heavily on the type, quantity purchased, and features.

Here is a breakdown of typical costs:

- **Low-Cost/Volume Pricing (The Chip Itself):**¹
 - Basic 8-bit microcontrollers (MCUs) can be priced as low as **\$0.03 to under \$0.50 per unit** when purchased in high industrial quantities (e.g., thousands of units).²
 - More capable 32-bit MCUs can be found for around **\$0.50 to \$1.00 per unit** in high volumes.
 - These prices are for the microcontroller chip *itself* and are typical for large-scale manufacturing.
- **Hobbyist/Small Quantity Pricing (The Chip Itself):**
 - When buying single units or small quantities (e.g., from distributors like DigiKey or Mouser), simple MCUs often cost between **\$0.50 and \$5.00** each.
- **Development Boards (For Hobbyists and Engineers):**
 - Many microcontrollers are purchased as part of a **development board** which includes the MCU chip, a USB interface, voltage regulators, and other components to make it easy to program and use. These are significantly more expensive than the chip alone.
 - Popular boards like the **Raspberry Pi Pico** can be around **\$4 to \$6** (or slightly more for the wireless version).³
 - **Arduino Uno** or similar beginner-friendly boards often range from **\$20 to \$35** or more.
 - Higher-performance or specialized development boards (e.g., those with powerful CPUs, built-in large screens, or advanced communication modules) can cost **\$50 to over \$100**.

Key factors that influence the cost include:

1. **Bit Size (Architecture):** 8-bit MCUs (e.g., older AVR, PIC) are generally the cheapest, while 16-bit and 32-bit MCUs (e.g., ARM Cortex-M series) are more powerful and typically cost more.⁴
2. **Quantity:** The price per unit drops dramatically when ordering in large reels or trays for manufacturing compared to buying single chips.
3. **Features:** MCUs with more memory (Flash/RAM), faster clock speeds, advanced peripherals (like built-in Ethernet, Wi-Fi/Bluetooth, higher-precision ADCs), or those designed for specialized markets (like automotive or high-reliability industrial) will cost more.
4. **Supply Chain:** Global semiconductor shortages or demand spikes can temporarily increase prices.⁵

[9a] Case Study 9 Prompt: “average cost of digital to analog converter”

[9b] Case Study 9 Google Gemini Outcome: “The cost of a Digital-to-Analog Converter (DAC) varies widely, depending entirely on whether you're buying the standalone **integrated circuit (IC) chip** for electronics or a **complete audio device**.

1. DAC Integrated Circuit (IC) Chip (For Electronics) 💡

These are the bare components used in circuit board design and are the cheapest option.

- **Average Range (Small Quantity): \$1.00 to \$25.00**
- **Low-End:** Basic 8-bit or 10-bit DAC chips often cost **under \$5.00** per unit.
- **Mid-Range:** Higher-resolution (12-bit to 16-bit) or multichannel industrial DACs typically cost **\$5.00 to \$25.00**.
- **High-End/Specialty:** Extremely high-speed, precision, or RF-sampling DACs (used in telecom or test equipment) can cost **\$50 to over \$1,000** per chip in volume.

2. Consumer Audio DAC Devices (For Hi-Fi/Headphones) 🎧

These are finished products that include the DAC chip, a housing, power supply, input/output ports, and often a headphone amplifier (DAC/Amp).

Category	Typical Price Range	Description
Budget Portable "Dongle" DACs	\$20 to \$150	USB-C dongles (like the AudioQuest DragonFly series or iFi Go Link) that connect to phones/laptops for better audio quality.
Entry-Level Desktop DACs	\$100 to \$350	Standalone units (like the Schiit Modi+ or Topping D10s) that offer excellent measured performance for a home audio system.
Mid-Range/High-Performance DACs	\$400 to \$1,000	Offer high-end features, better power supplies, balanced outputs (XLR), and sophisticated filtering (e.g., Cambridge Audio DacMagic).

<p>Audiophile/Reference DACs</p>	<p>\$1,500 to over \$10,000</p>	<p>Premium devices with extreme attention to internal component quality, chassis design, and proprietary digital processing, targeting the high-fidelity market (e.g., Chord Qutest, RME ADI-2 DAC).</p>
---	--	--

For a consumer looking to significantly upgrade their computer or phone audio, an excellent, high-performing DAC can often be found in the **\$100 to \$200** range.”

[9c] ChatGPT Response: “The cost of a digital-to-analog converter (DAC) can vary widely depending on performance, input/output formats, and use case. Here are some observations and typical price ranges:

 **Price Ranges & Examples**

Here are a few representative products, from simple to very high end:

[Insignia Optical/Coaxial Digital-to-Analog Audio Converter](#)

basic home adapter

\$29.99

[Home Collection 192 kHz Digital to Analog Audio Converter](#)

budget home converter

\$18.49

[FiiO KA11 Portable Digital-to-Analog Converter](#)

portable audio DAC

\$36.99

[Yichuaoxi Digital to Analog Audio Converter 192 kHz](#)

entry home cinema DAC

\$41.86

[Rockville RDAC5B Digital-to-Analog Converter](#)

mid-home audio DAC

\$64.95

[Cambridge Audio DacMagic 200M Digital-to-Analog Converter](#)

high-end audiophile DAC

\$399.00

[NuPrime DAC-10 Digital to Analog Converter](#)

ultra-high-end DAC

\$1,749.00

[HiFi Rose RD160 Stereo Digital-to-Analog Converter](#)

flagship audiophile DAC

\$5,995.00

And here's a quick breakdown:

- [Insignia Optical/Coaxial Digital-to-Analog Audio Converter](#): approx \$30.
- [Home Collection 192 kHz Digital to Analog Audio Converter](#): around \$18–20.
- [FiiO KA11 Portable Digital-to-Analog Converter](#): approx \$37.
- [Yichuaoxi Digital to Analog Audio Converter 192 kHz](#): approx \$41.86.
- [Rockville RDAC5B Digital-to-Analog Converter](#): around \$64.95.
- [Cambridge Audio DacMagic 200M Digital-to-Analog Converter](#): around \$399.
- [NuPrime DAC-10 Digital to Analog Converter](#): about \$1,234 (for a high-end model).
- [HiFi Rose RD160 Stereo Digital-to-Analog Converter](#): up around \$5,995 for ultra-high-end.

Typical “Average Cost”

- For simple home audio/consumer use, many DACs fall in the \$20–\$60 range. (E.g., many optical/coax to analog adapters cost ~\$10–\$30). ([Walmart.com](#))
- For mid-level audiophile use, you'll see prices in the \$300–\$500 range. ([The Master Switch](#))
- For high-performance/flagship models, the price can go well above \$1,000, even into thousands. ([Hi-Fi Heaven](#))

What “Average” Means for You

If you're looking for a typical usable DAC for home/consumer purposes (not ultra-audiophile), you can reasonably budget \$20 to \$100 and find a good one.

If you have more demanding performance requirements (especially for hi-fi, studio, or audiophile uses), plan for \$300+ and upward.

If you like, I can look up average cost specifically for industrial/engineering-grade DACs (for your optics/photonic work) or USB/portable DACs (for computer use) and pull more precise recent market data. Would you like me to do that?”

[10a] Case Study 10 Prompt: “Explain how I can use a variable waveplate to change the polarization of light”

[10b] ChatGPT Response: “A *variable waveplate*—usually a **liquid crystal variable retarder (LCVR)** or **electro-optic modulator**—lets you continuously adjust how much *phase delay* is introduced between two orthogonal polarization components of a beam. By changing that phase delay, you change the polarization state of the light.

Start with the fundamentals

Any linearly polarized light can be thought of as having two components:

- One component along the **fast axis** of the waveplate
- One component along the **slow axis** of the waveplate

The waveplate delays one axis relative to the other.

This **relative delay** is called *retardance* (in units of radians or in fractions of a wavelength like ¼-wave or ½-wave).

So what does adjusting the retardance do?

Retardance	Waveplate type	Effect on polarization (if input is linear at 45° to axes)
0	No waveplate	Output remains linear with same orientation
$\pi/4$ ($\lambda/4$)	Quarter-wave plate	Converts linear → circular (or elliptical depending on input angle)
$\pi/2$ ($\lambda/2$)	Half-wave plate	Rotates the angle of linear polarization
Other values	“Variable retarder”	Produces elliptical polarization

So by tuning the retardance electronically, you can smoothly move between:

Linear → **Elliptical** → **Circular** → **Elliptical** → **Linear (at a new angle)**

How this is done in practice

1. **Send linearly polarized light in.**

Let’s say the polarization is at **45°** to the waveplate axes (this is important—if aligned to an axis, nothing changes).

2. Apply voltage to the variable waveplate.

- Increasing voltage changes the **birefringence** of the material.
- Changing birefringence changes the **retardance**.

3. Observe the polarization change:

- At low voltage → maybe acts like a **half-wave plate** → rotates linear polarization.
- At moderate voltage → becomes **elliptically** polarized.
- At the right voltage → acts like a **quarter-wave plate** → produces **circular polarization**.
- At high voltage → elliptical again, etc.

Example

Suppose your input polarization is linear:

↗ (45° to axes)

- Set retardance = **0** → output is ↗ (same linear)
- Set retardance = $\lambda/4$ → output becomes **circular**
- Set retardance = $\lambda/2$ → output becomes linear rotated to ↘
- Set retardance = **some intermediate amount** → output becomes **elliptical**

So you can *dial* polarization like turning a knob.

Key Practical Points

Factor	Why it matters
Input polarization must not be aligned to waveplate axes	Otherwise no polarization change occurs.
Temperature affects retardance	So many systems include feedback or heating stabilization.
Wavelength dependent	Must match your operating wavelength range.

In short

A variable waveplate works by **changing the phase difference** between two perpendicular components of light.

By adjusting that phase delay (usually via voltage), you can produce **any polarization state** on the Poincaré sphere:

linear ↔ **elliptical** ↔ **circular**, and rotate the polarization angle as well.”

[11a] Case Study 11 Prompt: “I need to collimate light from a LED with a full viewing angle of 80 degrees into a beam with a diameter of no more than 30mm. Can you recommend a lens and give examples?”

[11b] ChatGPT Response: “Nice — you can get that easily with a short-focal-length aspheric/condenser lens. Below I’ll (A) show the arithmetic so you can see the requirement, (B) give two concrete lens examples that meet it, and (C) note practical tips (LED emitter size, mounting, coatings).

Quick design arithmetic (step-by-step)

Your LED full viewing angle = $80^\circ \rightarrow$ half-angle $\theta = 40^\circ$.

For a lens placed near the LED (effectively the lens at the LED’s focal distance), the approximate collimated beam diameter D is

$$D \approx 2f \tan(\theta)$$

where f is the lens focal length.

Compute $\tan(40^\circ)$ precisely:

- $\tan(40^\circ) \approx 0.8390996311772799$.

Now plug in candidate focal lengths:

- If $f = 16.0$ mm: $D \approx 2 \times 16.0 \times 0.8390996311772799 = 26.851$ mm.
- If $f = 17.5$ mm: $D \approx 2 \times 17.5 \times 0.8390996311772799 = 29.368$ mm.
- If $f = 20.0$ mm: $D \approx 33.564$ mm (too large for your 30 mm cap).

So any lens with focal length $\leq \sim 17.9$ mm will produce ≤ 30 mm beam diameter for a point-source LED with 80° full angle. (Calculation above: $30 \text{ mm} / (2 \cdot \tan 40^\circ) \approx 17.87$ mm.)

[Edmund Optics+1](#)

Concrete lens recommendations (examples)

1. **TECHSPEC / Edmund Optics — 30.0 mm dia × 17.5 mm FL molded aspheric condenser**
 - 30 mm diameter, focal length = 17.5 mm \rightarrow calculated beam ≈ 29.37 mm, so it meets your ≤ 30 mm requirement and the aperture is large enough to collect the

full 80° cone. Good choice if you want to *capture the whole LED cone* and have the beam just under 30 mm. [Edmund Optics](#)

2. Edmund Optics — 25.4 mm (1") dia × 16.0 mm FL aspheric condenser

- 25.4 mm diameter, focal length = 16 mm → calculated beam ≈ **26.85 mm**. This produces a slightly smaller beam, but note the lens diameter (25.4 mm) is just a hair *smaller* than the ideal collection aperture for the full 80° cone (so you may clip a little of the outermost rays). If you don't need absolutely every edge ray, this is compact and common. (Part listings: 25.4 mm × 16 mm aspheric condenser.) [Edmund Optics+1](#)

3. Alternatives / secondary optics

- If you prefer very high throughput and compact secondary optics made specifically for LEDs, look at **TIR / molded LED secondary optics** (Carclo, Ledil, Khatod). These are specified by output beam angle rather than focal length; pick a TIR optic that produces $\leq \sim 30$ mm beam at your working distance or that outputs a comparable beam half-angle. TIR optics are very efficient but require matching to the LED package. [Carclo Optics+1](#)

Practical notes & “gotchas”

- **Emitter size matters.** The arithmetic above assumes a pointlike emitter. Many LEDs are extended sources (chip size, phosphor dome). Extended emitters increase divergence and require small adjustments to lens-to-LED spacing; you'll often need to *move the LED a few mm* from the nominal focal plane to minimize wavefront error and get the flattest beam. If you give the LED part number or emitter dimensions I can compute a more accurate expected divergence and optimum spacing.
- **Lens diameter vs collected cone.** To *collect the full 80°* the lens clear aperture D should satisfy $D \geq 2f \tan(40^\circ)$. That's why the 30 mm × 17.5 mm lens is a tidy match (collection aperture ≈ beam diameter). The 25.4 mm × 16 mm lens still gives <30 mm beam but will clip the extreme outer rays of an ideal 80° cone.
- **Coatings / wavelength:** choose an AR coating tuned to your LED wavelength (visible vs NIR) to reduce reflection losses.
- **Mounting:** buy a lens tube or holder sized to the lens diameter (SM1 / 1" accessories are convenient for 25.4 mm optics; for 30 mm look for compatible holders or mount adapters).
- **If you need a perfectly flat top / uniform intensity:** add a condenser + diffuser or a beam homogenizer; that reduces usable throughput but improves uniformity.

Thorlabs/Edmund have diffuser-backed aspheric condensers if you want uniform illumination. [Thorlabs+1](#)

If you want, I can:

- pick exact part numbers with vendor SKUs and (if you want) estimate expected collected optical power given a specific LED part number, or
- show a quick ray sketch and predict how much of the LED's 80° cone will be collected by each lens.

Which would you like next?"

[12a] Case Study 11 Prompt: “can USB-6002 control the SS30Y-AG to have a 0.1 degree movement in 1 ms?”

[12b] Case Study 12 Google Gemini Outcome: “It is **unlikely** that the NI USB-6002 can reliably control the SS30Y-AG galvanometer to achieve a **0.1-degree step movement and settle within 1 ms**, due to limitations in both the DAQ card and the time required for the galvo mirror to physically move and settle.

Here is a breakdown of the limiting factors:

1. DAQ Card Limitation: Analog Output Update Rate

The primary limitation of the NI USB-6002 is its Analog Output (AO) speed.

- **Maximum AO Update Rate:** The NI USB-6002 has a maximum simultaneous AO update rate of 5 kS/s **per channel**.
- **Time per Sample:** This rate corresponds to a minimum time interval of:

$$\Delta t = \frac{1}{5,000 \text{ S/s}} = 0.0002 \text{ s} = 0.2 \text{ ms}$$

- **Implication:** The DAQ card can only issue a new voltage command to the galvo's servo driver every 0.2 ms. To achieve a 1 ms response time, you are trying to complete the entire move and settling within just **five** update steps (1 ms/0.2 ms). This severely limits the control bandwidth and is often too slow for such a tight step response requirement.
-

2. Galvo Limitation: Step Response Time

Galvanometers, even high-performance models, have a physical limit to how fast they can change position and settle (i.e., their step response time).

- The SS30Y-AG is a 30 mm aperture galvo system, designed for high-precision, but high speed is typically achieved with smaller mirrors.

- The required 0.1 degree step is a small mechanical angle, but achieving a 1 ms settling time for a 30 mm mirror is very aggressive.
- Typical **small-angle step response** or **settling times** for high-end galvos in the 30 mm class are often in the range of a few milliseconds (e.g., 1 ms to 5 ms or more, depending on the manufacturer, drive conditions, and the settling tolerance).

Conclusion: Even if the DAQ card could command the change instantly, the physical inertia of the mirror and the bandwidth of the servo system are likely to prevent the galvo from reaching and settling at the new 0.1 degree position within 1 ms.

For high-speed, sub-millisecond step responses, you typically need a DAQ card with an AO rate in the **megasamples per second** (MS/s) range (e.g., NI X-series or specific high-speed cards) to ensure the control waveform is accurately and rapidly generated, paired with a small-aperture, high-speed galvo scanner.”

[13a] Case Study 13 Prompt: “how does a galvanometer motor work and how do you make it a high speed motor”

[13b] Case Study 13 ChatGPT Outcome: “A galvanometer motor (also called a galvo scanner or galvanometer actuator) is a very fast, very precise motor used to rotate a mirror for beam steering in lasers, LIDAR, confocal microscopes, etc. It’s not like a normal DC motor—it's more like a limited-angle, high-precision torque motor with a built-in feedback sensor.

Below is a clean breakdown:

How a Galvanometer Motor Works

1. Basic Structure

A galvo motor usually includes:

- Rotor with permanent magnets
- Stator coil (current creates torque)
- Torsion bar or flexure bearings (super low friction, rotation only \pm a few degrees)
- Position sensor (usually an optical encoder or Hall sensor)
- Servo control amplifier (keeps angle precise)

It’s essentially a rotating voice coil actuator, like a speaker, but built to rotate a small angle with high accuracy.

2. Operating Principle

Torque Generation

It uses the Lorentz force:

$$\tau = K_t I$$

where:

- τ = torque
- K_t = torque constant
- I = current through coil

The rotor only swings a small angle (common ranges ± 10 – 30°).
Because of this small range, you can make the system:

- very low friction
- very light
- very stiff

This allows extremely fast response.

3. Servo Control Loop

A galvo is always run in closed-loop:

1. Controller receives target angle.
2. Reads position sensor.
3. Outputs current to coil.
4. Torque moves rotor until target angle is reached.
5. Loop runs at tens of kHz.

This closed-loop control is why galvos are accurate to microradians and settle very fast.

4. How to Make a Galvanometer “High Speed”

High speed means:

- high bandwidth
- short settling time
- low inertia
- ability to scan at kHz frequencies

To get this, you optimize several factors:

A. Reduce Rotating Inertia (MOST IMPORTANT)

Speed = torque / inertia, so to go fast:

$$\omega \propto \frac{\tau}{J}$$

You reduce J (moments of inertia) by:

- **Using tiny mirrors**
- **Making rotor very small and light**
- **Using hollow or thin ring magnets**
- **Using a lightweight mirror mount**

Galvo manufacturers spend huge effort reducing rotor inertia.

B. Increase Torque Constant (Stronger Magnetic Field)

More torque means faster acceleration.

Ways to increase torque:

- **Increase magnet strength (use NdFeB magnets)**
 - **Use a more efficient magnetic circuit**
 - **Optimize coil geometry to maximize Lorentz force**
 - **Increase allowable coil current (with good cooling)**
-

C. Use Flexure Bearings, Not Ball Bearings

Flexure bearings have:

- **Almost zero friction**
- **No backlash**
- **Very low damping**

Friction kills speed. Flexures enable ultra-fast oscillations.

D. Improve Position Sensor Resolution

Higher resolution allows:

- **tighter control loop**

- **faster settling time**
- **higher closed-loop bandwidth**

Typical sensors: optical analog position detectors (PSD), capacitive sensors, or magnetic encoders.

E. High-Bandwidth Servo Driver

The servo amplifier must be:

- **high slew rate**
- **low noise**
- **able to deliver high current quickly**

This is often the limiting factor. Commercial galvo drivers operate at 20–100 kHz control loop bandwidth.

F. Minimize Mirror Size (Very Important)

Galvo manufacturers offer:

- **1 mm mirrors (very fast)**
- **3–6 mm mirrors (medium)**
- **10–20 mm mirrors (slow)**

Mirror inertia can easily dominate the system.

G. Cooling

Higher speed means:

- **higher RMS current**
- **more power loss**

Cooling allows more current, hence faster acceleration.

5. Actual Achievable Speeds

Depending on design, galvos can achieve:

Mirror Size Scan Speed (typical)

1 mm 3–5 kHz

Mirror Size Scan Speed (typical)

3 mm **1–2 kHz**

6 mm **200–800 Hz**

10–12 mm **50–200 Hz**

This is for closed-loop, accurate scanning.

Open-loop resonant scanners can go much higher (10–50 kHz), but only at fixed frequency.

6. Summary

A galvanometer motor works by:

- Using a torque coil + magnet system for proportional torque.
- Mounting a mirror with extremely low inertia.
- Using a precision position sensor.
- Running a high-speed servo loop to control angle.

To make it high-speed, you focus mainly on:

- Low inertia (small mirror, lightweight rotor)
 - High torque (strong magnets, high current)
 - Flexure bearings
 - High-bandwidth servo electronics
 - High-resolution sensors
-

If you want, I can also explain:

- how a galvo differs from a DC motor,
- how a resonant scanner compares to a galvo,
- or design an example of a high-speed galvo rotor with inertia calculations.”

[14a] Case Study 13 Prompt: “Explain the Poincaré sphere and how to visualize it”

[14b] Case Study 13 ChatGPT Outcome: “The **Poincaré sphere** is one of the most powerful ways to visualize **polarization states of light**. Here’s a clear, intuitive explanation tailored to someone with your optics background:

🌐 What the Poincaré Sphere Represents

The Poincaré sphere is a **unit sphere** where *each point* corresponds to a unique **state of polarization (SOP)**. It maps all possible polarizations—linear, circular, and elliptical—onto a single geometric object.

Think of it as the polarization equivalent of the Bloch sphere in quantum mechanics.

🌀 Axes of the Sphere (Stokes Parameters)

The sphere uses the **normalized Stokes parameters**:

- **S₁**: Horizontal ↔ Vertical polarization
- **S₂**: +45° ↔ -45° linear polarization
- **S₃**: Right-circular ↔ Left-circular polarization

A polarization state is represented by a vector

$$\vec{S} = (S_1, S_2, S_3)$$

with

$$\sqrt{S_1^2 + S_2^2 + S_3^2} = 1$$

📍 Where States Sit on the Sphere

1. Poles (Top and Bottom): Circular Polarization

- **North Pole (S₃ = +1)**: Left-circular
- **South Pole (S₃ = -1)**: Right-circular

2. Equator (S₃ = 0): Linear Polarization

Every point on the equator corresponds to **linear polarization**.

The angle around the equator is **2 × the polarization angle**.

Example:

A linear polarization at 0° (horizontal) → S₁ = +1

A linear polarization at 90° (vertical) → S₁ = -1

A linear polarization at 45° → S₂ = +1

3. Anywhere else: Elliptical Polarization

Between the equator and poles lie **elliptical polarizations**:

- Latitude = **ellipticity**
 - Longitude = **orientation of major axis**
-

What Does a Great Circle Mean?

If you rotate a waveplate or a polarization element, the SOP **moves along a path on the sphere**. A *pure rotation* of the fast axis of a waveplate corresponds to a **great-circle path**.

A **half-wave plate** rotates the polarization state **around the S_2 axis**.

A **quarter-wave plate** rotates it **toward or away from a pole**, creating arcs.

A great circle **must** have radius equal to the sphere (definition of great-circle).

Not all transformations create great circles—only those equivalent to a pure $SU(2)$ rotation about a fixed axis.

How to Visualize the Sphere

✓ 1. Physical Intuition

Imagine a ball where:

- Horizontal band = all linear polarizations
- Vertical axis = circular polarizations
- All else are ellipses

✓ 2. Use an Online Poincaré Sphere Viewer

Search terms:

- "Poincaré sphere interactive"
- "Stokes parameters visualization"

A great one: Thorlabs has a full interactive sphere online that lets you click and see polarization ellipses for any point.

✓ 3. MATLAB Visualization

Since you code in MATLAB, here's a simple way to visualize points or paths:

```
% Plot Poincare sphere
[X,Y,Z] = sphere(100);
surf(X, Y, Z, 'FaceAlpha', 0.3, 'EdgeColor', 'none');
colormap winter; hold on; axis equal;

% Example: linear polarization at 45 degrees
S = [0, 1, 0]; % (S1, S2, S3)
plot3(S(1), S(2), S(3), 'ro', 'MarkerSize', 10, 'MarkerFaceColor', 'r');
xlabel('S1'); ylabel('S2'); zlabel('S3'); grid on;
```

You can also animate a quarter-wave plate transformation by rotating a vector.

Good Videos to Visualize It

Search:

- “Poincaré sphere polarization animation”
- “Great circle polarization waveplate animation”
- “Stokes parameter visualization”

Look for videos showing:

- a sphere with a polarization ellipse drawn at each point
- trajectories caused by waveplate rotation

You’ll especially want videos that show how a quarter-wave plate moves a linear polarization toward the poles (turning it circular).

Key Takeaways

- Every polarization state is a **point** on the sphere.
- Linear = equator
- Circular = poles
- Elliptical = anywhere else

- Waveplates move states along **rotations on the sphere**.
 - The sphere helps visualize complicated polarization evolution simply as curves on a ball.
-

If you want, I can:

- Plot example great-circle trajectories from rotating a waveplate
- Explain how to get the Stokes vector from Jones vectors
- Create MATLAB animations for polarization evolution”

Appendix D: Software Code

```

clc
clear all
close all

tic;

%Variables to be Called
%reference power
ref_power = 1.00*10^-3;
%Rotation Step size
R_step_size = 0.01*pi/180; %0.01 degrees in radians
%Rotation Range
mindegree = 10;
maxdegree = 20;
QWP_rotation_range = pi/90:(pi/90):89*pi/90;
%Operation Time
length_of_time = 1; % ms
%degrees over time
%Velocity is how many ms for 1 degree movement.
Velocity = (1/0.4)*length_of_time;
%Wavelength
lambda1 = 639.5*10^-9;
lambda2 = 521*10^-9;
lambdaarray1 = 457*10^-9;
lambdaarray2 = 483*10^-9;
%wavelength array
bandwidth = 30*10^-9;
lambda_array = lambdaarray1:1*10^-9:lambdaarray2;
%thickness of crystal cm
d = 0.1*10^-2;
%Refractive index of ordinary axis for calcite
n_o1 = sqrt((2.69705+0.0192064./(lambda1.*10^6).^2-0.01820)-0.0151624.*(lambda1.*10^6).^2);
n_o2 = sqrt((2.69705+0.0192064./(lambda2.*10^6).^2-0.01820)-0.0151624.*(lambda2.*10^6).^2);
%Refractive index of extra-ordinary axis for calcite
n_e1 = sqrt((2.18438+0.0087309./(lambda1.*10^6).^2-0.01018)-0.0024411.*(lambda1.*10^6).^2);
n_e2 = sqrt((2.18438+0.0087309./(lambda2.*10^6).^2-0.01018)-0.0024411.*(lambda2.*10^6).^2);

%Rotation angle of crsytal
theta = mindegree*pi/180:R_step_size:maxdegree*pi/180;
%time period
time_period = 0:(maxdegree-mindegree)*Velocity)/length(theta):(Velocity*(maxdegree-mindegree)-(Velocity/length(theta)));
%Beta equals 45 degrees
beta = pi/4;
negbeta = -pi/4;
beta_step = (((0.25*pi/4)-(0.75*pi/4))/(length(theta)));
beta_array = pi/5:beta_step:pi/10-(beta_step);
%Target Extinction ratio
extinction_ratio = 0.001;
%Matrix of a Mirror with Normal Incidence
Retro_Mir = [1 0
             0 -1];
QWP = exp(1i*pi/4)*[1 0
                  0 -1];

%Incident Light matrix
%Vertical linear
E_inc = [1
         0];
%Circular
%E_inc = [(1/sqrt(2))
         (1j/sqrt(2))];
%45 degree polarization
%E_inc = 1/sqrt(2).*[1
                    1];

%FWHM Emission Spectrum Weighting on the LED
emission_table = [456.0 0.44735
457.1 0.49445
458.0 0.53699
459.0 0.59512
460.1 0.64816
461.0 0.68388
462.1 0.74866
463.0 0.78790
464.0 0.83665
465.1 0.85838
466.0 0.88685
467.1 0.91656
468.0 0.94480
469.1 0.96160
469.9 0.98038
471.0 0.99647

```

```

472.1  0.99089
473.0  0.98823
474.1  0.96693
475.0  0.93854
476.0  0.906170
477.1  0.86550
478.0  0.82570
479.1  0.76788
480.0  0.72909
481.1  0.70339
482.0  0.67961
483.0  0.64110
483.9  0.59785];

y = (length(emission_table)/length(lambda_array));

for b = 1:1:length(emission_table)

coeff_emission_table(b,1) = emission_table(b,2);

end

%Sellmeier equations for birefringent crystals

bbo_sell_no = sqrt((2.67579+0.02099./(lambda_array*10^6).^2-0.00470)-0.00528.*(lambda_array*10^6).^2);
bbo_sell_ne = sqrt((2.31197+0.01184./(lambda_array*10^6).^2-0.01607)-0.00400.*(lambda_array*10^6).^2);

cal_sell_no = sqrt((2.69705+0.0192064./(lambda_array.*10^6).^2-0.01820)-0.0151624.*(lambda_array.*10^6).^2);
cal_sell_ne = sqrt((2.18438+0.0087309./(lambda_array.*10^6).^2-0.01018)-0.0024411.*(lambda_array.*10^6).^2);

qrtz_sell_no = sqrt(2.3573-(0.01170.*(lambda_array.*10^6).^2)+(0.01054./((lambda_array*10^6).^2))+(1.3414*10^-4./((lambda_array*10^6).^4))-(4.4537*10^-7./((lambda
qrtz_sell_ne = sqrt(2.3849-(0.01259.*(lambda_array.*10^6).^2)+(0.01079./((lambda_array*10^6).^2))+(1.6518*10^-4./((lambda_array*10^6).^4))-(1.9474*10^-7./((lambda

YV04_sell_no = sqrt(3.77834 + (0.069736./(lambda_array*10^6).^2-0.04724)) - (0.0108133.*(lambda_array*10^6).^2);
YV04_sell_ne = sqrt(4.59905 + (0.110534./(lambda_array*10^6).^2-0.04813)) - (0.0122676.*(lambda_array*10^6).^2);

%MGF2_sell_no = sqrt(1+(0.48755))
%MGF2_sell_ne =
%Calculating of Array for electric field matrix;
%Functions
%Gamma of theta
gamma_theta1 = sqrt(1-(sin(theta).^2/(n_e1^2)))- sqrt(1-(sin(theta).^2/(n_o1^2)));
gamma_theta2 = sqrt(1-(sin(theta).^2/(n_e2^2)))- sqrt(1-(sin(theta).^2/(n_o2^2)));
%Change in Phase
delta_phi1 = ((2*pi*n_o1*d)/lambda1)*gamma_theta1;
delta_phi2 = ((2*pi*n_o2*d)/lambda2)*gamma_theta2;

figure(9);
plot((180.*theta./pi), -1 * delta_phi1/10, LineWidth=2)
title('Delta Phi vs Rotation @ 639.5 nm', FontSize=32)
xlabel('Rotation of Crystal (Degrees)', FontSize=32)
ylabel('Delta Phi (Phase Delay)', FontSize=32)
grid on;
set(gca, "FontSize", 24)

%Matrix Calculations

%Jones Matrix Construction
Qxx = cos(beta)^2 + exp(1i*delta_phi1)*sin(beta)^2;
Qxy = (1-exp(1i*delta_phi1))*sin(beta)*cos(beta);
Qyy = sin(beta)^2 + exp(1i*delta_phi1)*cos(beta)^2;
Qyx = (1-exp(1i*delta_phi1))*sin(beta)*cos(beta);

%retrolight jones matrix -beta
Qxx2 = cos(negbeta)^2 + exp(1i*delta_phi1)*sin(negbeta)^2;
Qxy2 = (1-exp(1i*delta_phi1))*sin(negbeta)*cos(negbeta);
Qyy2 = sin(negbeta)^2 + exp(1i*delta_phi1)*cos(negbeta)^2;
Qyx2 = (1-exp(1i*delta_phi1))*sin(negbeta)*cos(negbeta);

E_darray1 = zeros(2,length(theta));

%Wavelength 2
%Jones Matrix Construction
Qxx3 = cos(beta)^2 + exp(1i*delta_phi2)*sin(beta)^2;
Qxy3 = (1-exp(1i*delta_phi2))*sin(beta)*cos(beta);
Qyy3 = sin(beta)^2 + exp(1i*delta_phi2)*cos(beta)^2;
Qyx3 = (1-exp(1i*delta_phi2))*sin(beta)*cos(beta);

%retrolight jones matrix -beta
Qxx4 = cos(negbeta)^2 + exp(1i*delta_phi2)*sin(negbeta)^2;
Qxy4 = (1-exp(1i*delta_phi2))*sin(negbeta)*cos(negbeta);
Qyy4 = sin(negbeta)^2 + exp(1i*delta_phi2)*cos(negbeta)^2;
Qyx4 = (1-exp(1i*delta_phi2))*sin(negbeta)*cos(negbeta);

```

```

E_darray2 = zeros(2,length(theta));

%For loop solving for the Jones Matrices and then electric field
for n = 1:1:length(theta)

    Q_beta_theta = [Qxx(1,n) , Qxy(1,n)
                   Qyx(1,n) , Qyy(1,n)];

    Q_negbeta_theta = [Qxx2(1,n) , Qxy2(1,n)
                      Qyx2(1,n) , Qyy2(1,n)];

    E_S = Q_beta_theta * E_inc;

    E_d = Q_negbeta_theta * Retro_Mir * E_S;

    %disp(E_d);

    E_darray1(:,n) = E_S;

    %disp(Q_beta_theta);
end
for n = 1:1:length(theta)

    Q_beta_theta = [Qxx3(1,n) , Qxy3(1,n)
                   Qyx3(1,n) , Qyy3(1,n)];

    Q_negbeta_theta = [Qxx4(1,n) , Qxy4(1,n)
                      Qyx4(1,n) , Qyy4(1,n)];

    E_S2 = QWP * Q_beta_theta * E_inc;

    E_d2 = Q_negbeta_theta * Retro_Mir * E_S;

    %disp(E_d);

    E_darray2(:,n) = E_S2;

    %disp(Q_beta_theta);
end

%Electric Field Solution for double pass
%E_1 = 1 - exp(1i*2*delta_phi);
%E_2 = -1*(1+exp(1i*2*delta_phi));
%E = [E_1
      E_2];
%E_D = 0.5.*E;

P_Dmat1 = ((abs(E_darray1)).^2);
P_Dmat2 = ((abs(E_darray2)).^2);

RealE_d1 = real(E_darray1);
RealE_d2 = real(E_darray2);

%calculating PER
%Real Power
Real_power1 = (RealE_d1.^2);
P_E_R1 = 10.*log10(Real_power1(2,:)/Real_power1(1,:));

Real_power2 = (RealE_d2.^2);
P_E_R2 = 10.*log10(Real_power2(2,:)/Real_power2(1,:));

%Solve for Power Shortcut
%P_D = sin(delta_phi).^2;

%Identify local min and max
%P_Dmin = islocalmin(P_D, "MinProminence",extinction_ratio);
%P_Dmax = islocalmax(P_D);

%P_D_max_ind = P_D[:,P_Dmax_v];
%Construct array of indices
%delta_theta_array = find(P_Dmin | P_Dmax);
%[P_Dmax_v, P_Dmaxindex] = max(delta_theta_array);
%[P_Dmin_v, P_Dminindex] = min(delta_theta_array);
%find the differences between consecutive points
%delta_theta = diff(delta_theta_array);
%find the minimum Difference
%delta_theta_min = min(delta_theta);
%Convert to degree change based on stepsize

```

```

%DELTA_THETA = delta_theta_min*(180*R_step_size/pi);

%% find index where the minimum spacing occurs
% [delta_theta_min, idxmin] = min(delta_theta);
% [delta_theta_max, idxmax] = max(delta_theta);
%
%% the two indices in delta_theta_array that define that minimum
% index1min = delta_theta_array(idxmin);
% index2min = delta_theta_array(idxmin+1);
% index1max = delta_theta_array(idxmax);
% index2max = delta_theta_array(idxmax+1);
%
%% convert them to degrees and add initial offset
% theta1min = index1min * (180*R_step_size/pi) + offset;
% theta2min = index2min * (180*R_step_size/pi) + offset;
% theta1max = index1max * (180*R_step_size/pi) + offset;
% theta2max = index2max * (180*R_step_size/pi) + offset;

%Plot of Power change vs rotation (Short Cut)
figure(1);
plot((180.*theta./pi), P_Dmat2(2,:));
title('Power vs Rotation @ 521 nm')
xlabel('Rotation of Crystal (Degrees)')
ylabel('Normalized Power Output (After GTP)')

figure(2);
plot((180.*theta./pi), P_Dmat1(2,:));
title('Power vs Rotation @ 639.5 nm')
xlabel('Rotation of Crystal (Degrees)')
ylabel('Normalized Power Output (After GTP)')

% Plot point on Poincare sphere

figure(4);
plot((180.*theta./pi), P_E_R1,LineWidth=3, Color='r');
hold on;
plot((180.*theta./pi), P_E_R2, LineWidth=3, Color='g');
set(gca, "FontSize", 24)
title('Polarization Extinction Ratio @ 521 & 639.5 nm', FontSize=32)
xlabel('Rotation angle in degrees', FontSize=32)
ylabel('Power in dB', FontSize=32)

legend('639.5 nm', '521 nm', 'Location', 'best');

hold off;

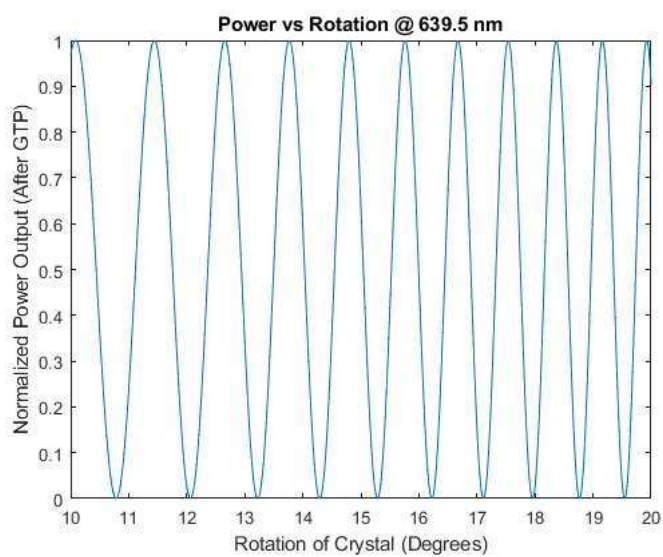
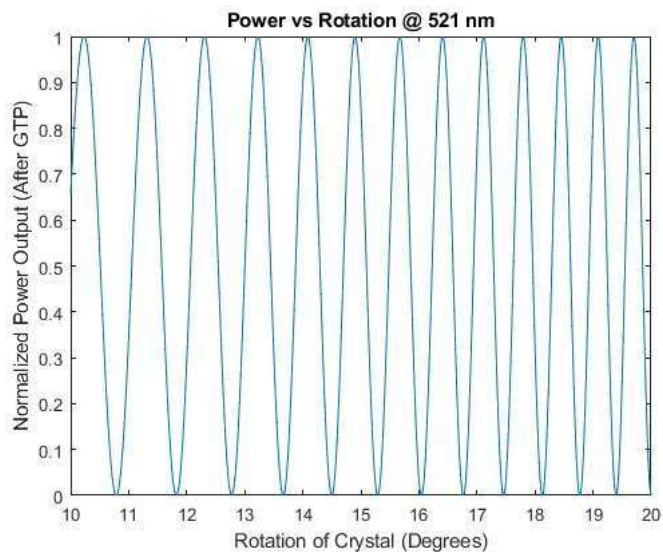
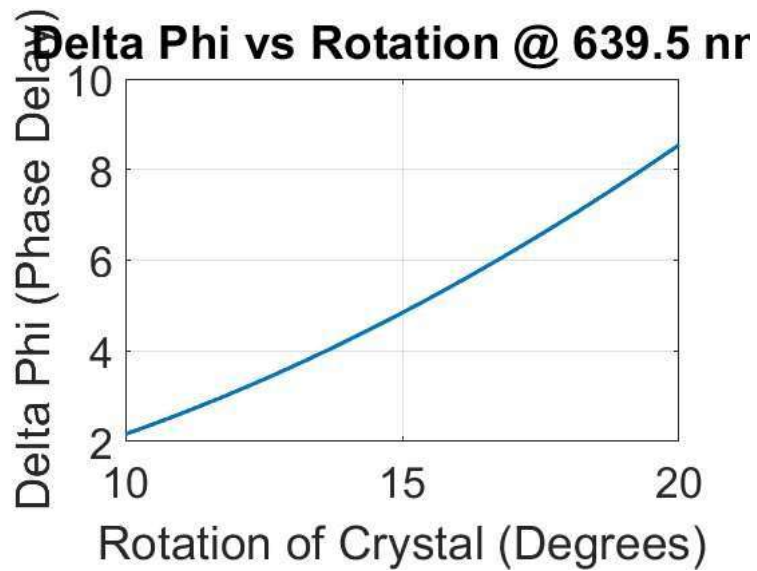
figure(5);
stokes(E_darray1);

figure(3);
stokes(E_darray2);

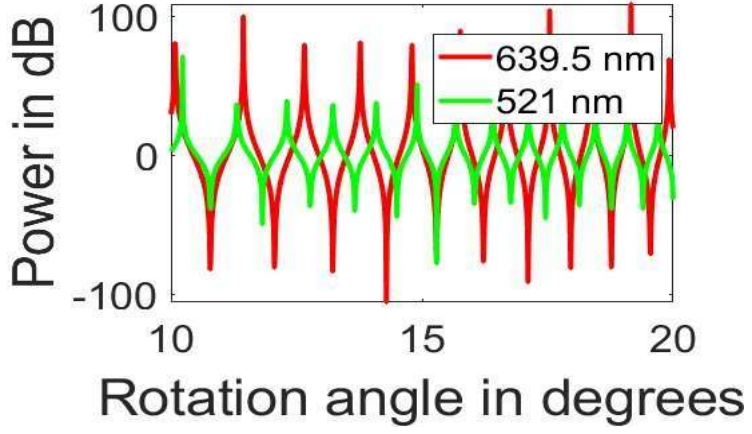
toc;
%Intialization of matrices for broadband claculations
gamma_theta_broad = zeros((length(lambda_array)),(length(theta)));
delta_phi_broad = zeros((length(lambda_array)),(length(theta)));
Qxx_broad = zeros(1,(length(theta)));
Qyy_broad = zeros(1,(length(theta)));
Qyx_broad = zeros(1,(length(theta)));
Qxy_broad = zeros(1,(length(theta)));
Qxx2_broad = zeros(1,(length(theta)));
Qyy2_broad = zeros(1,(length(theta)));
Qyx2_broad = zeros(1,(length(theta)));
Qxy2_broad = zeros(1,(length(theta)));

%E_d_broad_array = zeros((2*length(lambda_array)),(length(theta)));

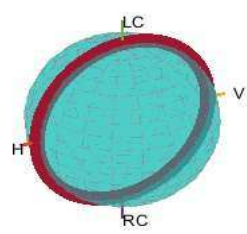
```



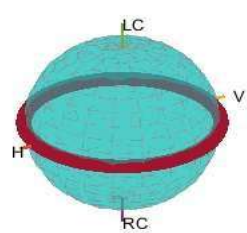
Extinction Ratio @ 521



Poincare Sphere



Poincare Sphere



```
tic;
%broadband source calculation Calcite
```

```
for n = 1:length(lambda_array)
```

```

gamma_theta_broad(n,:) = sqrt(1-(sin(theta).^2/(cal_sell_ne(:,n)^2))) - sqrt(1-(sin(theta).^2/(cal_sell_no(:,n)^2)));

delta_phi_broad(n,:) = ((2*pi*cal_sell_no(:,n)*d)/lambda_array(:,n))*gamma_theta_broad(n,:);

%Matrix Calculations

%Jones Matrix Construction
Qxx_broad(n,:) = cos(beta)^2 + exp(1i*delta_phi_broad(n,:))*sin(beta)^2;
Qxy_broad(n,:) = (1-exp(1i*delta_phi_broad(n,:)))*sin(beta)*cos(beta);
Qyy_broad(n,:) = sin(beta)^2 + exp(1i*delta_phi_broad(n,:))*cos(beta)^2;
Qyx_broad(n,:) = (1-exp(1i*delta_phi_broad(n,:)))*sin(beta)*cos(beta);

%retrolight jones matrix -beta
Qxx2_broad(n,:) = cos(negbeta)^2 + exp(1i.*delta_phi_broad(n,:))*sin(negbeta)^2;
Qxy2_broad(n,:) = (1-exp(1i.*delta_phi_broad(n,:)))*sin(negbeta)*cos(negbeta);
Qyy2_broad(n,:) = sin(negbeta)^2 + exp(1i.*delta_phi_broad(n,:))*cos(negbeta)^2;
Qyx2_broad(n,:) = (1-exp(1i.*delta_phi_broad(n,:)))*sin(negbeta)*cos(negbeta);

%electric field calculation for broadband source

for i = 1:1:length(theta)

    Q_beta_theta_broad = [Qxx_broad(n,i) , Qxy_broad(n,i)
                        Qyx_broad(n,i) , Qyy_broad(n,i)];

    Q_negbeta_theta_broad = [Qxx2_broad(n,i) , Qxy2_broad(n,i)
                            Qyx2_broad(n,i) , Qyy2_broad(n,i)];

    E_S_broad = QWP * Q_beta_theta_broad * (E_inc);

    E_d_broad = Q_negbeta_theta_broad * Retro_Mir * E_S_broad;

    %disp(coeff_emission_table(n));

row_index = (n-1)*2 + (1:2); % two rows per wavelength
E_d_broad_array(row_index,i) = E_S_broad;

    %disp(Q_beta_theta);
end

end

norm_power_broad = abs(E_d_broad_array).^2;

for p = 1:2:2*length(lambda_array)
figure(6)
plot((180.*theta./pi), norm_power_broad(p,:), LineWidth=2)
title('Power vs Rotation @ 456 nm - 484 nm', FontSize=32)
xlabel('Rotation of Crystal (Degrees)', FontSize=32)
ylabel('Normalized Power Output (After GTP)', FontSize=32)
set(gca, "FontSize", 24)
hold on;

%pause(.1);

end

hold off;

Real_E_d_broad = real(E_d_broad_array);

Real_power_broad = Real_E_d_broad.^2;

for b = 1:2:2*length(lambda_array)

PER_broad = 10.*log10(Real_power_broad(b,:)./Real_power_broad(b+1,:));

PER_broad_array(b,:) = PER_broad;

end

figure(7);

for c = 1:2:2*length(lambda_array)

plot((180.*theta./pi), PER_broad_array(c,:), LineWidth=2)
title('Polarization Extinction Ratio @ 456 nm - 484 nm', FontSize=32)

```

```

xlabel('Rotation angle in degrees', FontSize=32)
ylabel('Power in dB', FontSize=32)
set(gca, "FontSize", 24)

hold on;

end

hold off;

%for m = 1:10:length(theta)
figure(8)
for d = 1:2:2*length(lambda_array)

    stokes(E_d_broad_array([d,d+1,:]);
    hold on;

end
%end

hold off;

toc;
time_response_narrow = zeros(length(P_Dmat1),length(time_period));

for b = 1:1:length(P_Dmat1)

    time_response_narrow(b,:)= P_Dmat1(1,b);

end

Rotation_v_time = zeros(1,length(P_Dmat1));

for b = 1:1:length(P_Dmat1)

    Rotation_v_time(b) = time_response_narrow(b,b);

end

figure(11);
plot(time_period, Rotation_v_time(1,:), LineWidth=2);
title('Power vs Time @ 639.5 nm', FontSize=32)
xlabel('Time Period (ms)', FontSize=32)
ylabel('Normalized Power Output (After GTP)', FontSize=32)
set(gca, "FontSize", 24)

%pause(.1);

%%Initialization of Matrices
Qxx_tot = zeros(length(theta),length(theta));
Qxy_tot = zeros(length(theta),length(theta));
Qyx_tot = zeros(length(theta),length(theta));
Qyy_tot = zeros(length(theta),length(theta));

%Beta dependent test
for m = 1:1:length(theta)
for k = 1:1:length(beta_array)

%Jones Matrix Construction beta array
Qxx_b_array = cos(beta_array(k)).^2 + exp(1i*delta_phi1(m)).*sin(beta_array(k)).^2;
Qxy_b_array = (1-exp((1i*delta_phi1(m)))).*sin(beta_array(k)).*cos(beta_array(k));
Qyy_b_array = sin(beta_array(k)).^2 + exp(1i*delta_phi1(m)).*cos(beta_array(k)).^2;
Qyx_b_array = (1-exp((1i*delta_phi1(m)))).*sin(beta_array(k)).*cos(beta_array(k));

%retrolight jones matrix -beta
Qxx2_b_array = cos((-1)*beta_array(k)).^2 + exp(1i*delta_phi1(m)).*sin((-1)*beta_array(k)).^2;
Qxy2_b_array = (1-exp((1i*delta_phi1(m)))).*sin((-1)*beta_array(k)).*cos((-1)*beta_array(k));
Qyy2_b_array = sin((-1)*beta_array(k)).^2 + exp(1i*delta_phi1(m)).*cos((-1)*beta_array(k)).^2;
Qyx2_b_array = (1-exp((1i*delta_phi1(m)))).*sin((-1)*beta_array(k)).*cos((-1)*beta_array(k));

Qxx_tot(m,k) = Qxx_b_array;
Qxy_tot(m,k) = Qxy_b_array;
Qyx_tot(m,k) = Qyx_b_array;
Qyy_tot(m,k) = Qyy_b_array;

end
end

%
%Matrix construction
for n = 1:1:length(beta_array)
for o = 1:1:length(theta)

```

```

Q_beta_theta_tot = [Qxx_tot(o,n) , Qxy_tot(o,n)
                    Qyx_tot(o,n) , Qyy_tot(o,n)];

E_S_tot = Q_beta_theta_tot * E_inc;

column_index = (n-1)*2 + (1:2); % two columns per beta
E_S_tot_array(o,column_index) = E_S_tot;

end
end

norm_E_S_tot_array = abs(E_S_tot_array).^2;

figure(10);

for c = 1:2:length(norm_E_S_tot_array)

plot((180.*theta./pi), norm_E_S_tot_array(:,c+1), LineWidth=2)
title('Beta and Rotation Dependent Response', FontSize=32)
xlabel('Rotation angle in degrees', FontSize=32)
ylabel('Normalized Power', FontSize=32)
set(gca, "FontSize",20)

hold on;

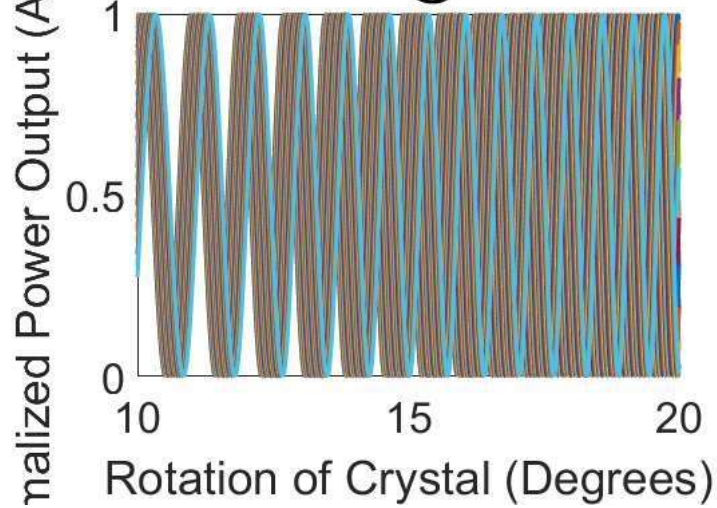
end

hold off;

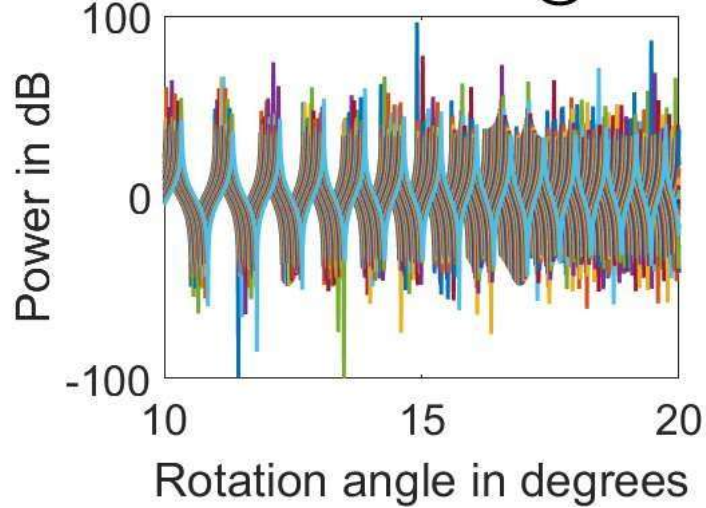
```

Elapsed time is 2.260447 seconds.

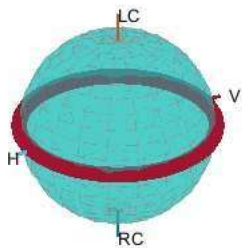
Power vs Rotation @ 456 nm - 484

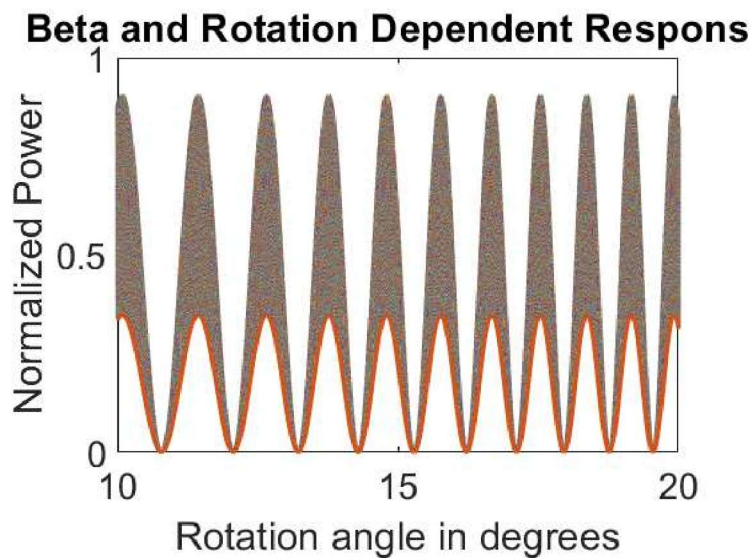
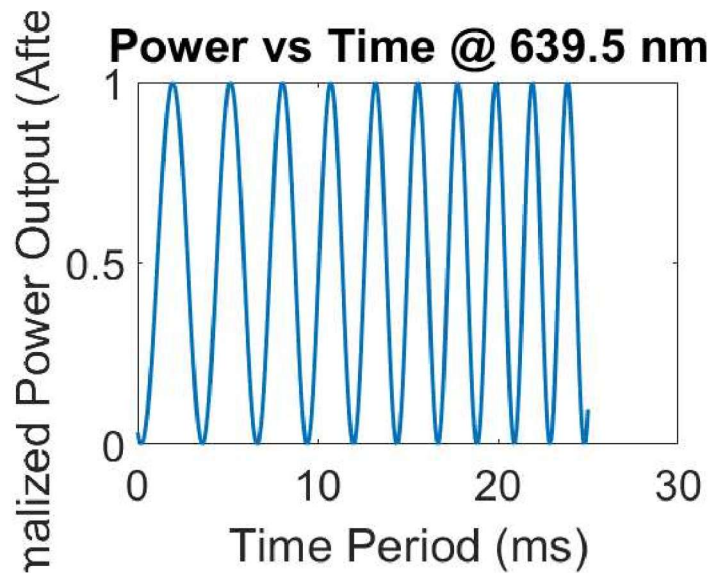


Polarization Extinction Ratio @ 456 nm



Poincare Sphere





```

%for s = 1:1:length(QWP_rotation_range)

%adjust_QWP = (exp(-1i*pi/4)).*[(cos(QWP_rotation_range(s))^2)+1i*(sin(QWP_rotation_range(s))^2) (1-1i)*sin(QWP_rotation_range(s))*cos(QWP_rotation_range(s))
% (1-1i)*sin(QWP_rotation_range(s))*cos(QWP_rotation_range(s)) (sin(QWP_rotation_range(s))^2)+1i*(cos(QWP_rotation_range(s))^2)];

% for t = 1:10:length(E_darray1)

%adjust_E_darray1 = adjust_QWP * E_darray1(:,t);

%figure(16)
%stokes(adjust_E_darray1);

%hold on

% end

%end
%hold off

```

```

1  #include <Arduino.h>
2  #include <SPI.h>
3  #include <esp32-hal-adc.h>
4  #include <esp_adc/adc_continuous.h>
5  #include <freertos/FreeRTOS.h>
6  #include <freertos/task.h>
7  #include <freertos/queue.h>
8
9  const int SPI_MOSI = 35; //MOSI = GPIO 35
10 const int SPI_CLK = 36; //SCLK = GPIO 36
11 const int SPI_CS = 39; //SS = GPIO 39
12
13 const int LED_EN_PIN = 48; //Input from DAQ Card for LED, GPIO 48
14 const int LED_on_PIN = 2; //To LED Enable Pin, GPIO 2
15 const int LED_test = 12; //To Status LED, GPIO 12
16 //GPIO 6 for ADC Reading
17
18 TaskHandle_t ADCTaskHandle = NULL;
19 TaskHandle_t SPITaskHandle = NULL;
20
21 QueueHandle_t ADCQueue = NULL;
22
23 adc_continuous_handle_t adc_handle = NULL;
24
25 void ADCTask(void *parameter){
26
27     int LED_State = LOW; //Check to see if LED is on or off
28     int LED_Status = LOW; //Status LED starts turned off

```

```

29
30 unsigned long previousMillis = 0; //Store last time LED was updated
31 unsigned long currentMillis;
32 const long interval = 1000; //LED will blink every 1000 ms (1 s)
33
34 uint32_t ADC_con_Value = 0; //To store the ADC continuous Reading value
35 uint8_t buffer[256];
36 uint32_t bytes_read = 0;
37
38 for(;;){
39
40     LED_State = digitalRead(LED_EN_PIN); //Read Input from DAQ Card for LED
41
42     if(LED_State == HIGH){
43         digitalWrite(LED_on_PIN, HIGH); //turn on LED
44     }
45     else {
46         digitalWrite(LED_on_PIN, LOW); //turn off LED
47     }
48
49     if(LED_State == HIGH){
50
51         LED_Status = HIGH;
52         digitalWrite(LED_test, LED_Status); //Turn on Status LED
53
54         adc_continuous_start(adc_handle); //Start ADC continuous reading

```

```

55
56     while(LED_State == HIGH){
57         if(adc_continuous_read(adc_handle, buffer, 256, &bytes_read, 0) == ESP_OK){
58             //Process each ADC continuous reading sample (4 bytes per sample)
59             for(int i = 0; i < bytes_read; i += 4){
60                 adc_digi_output_data_t *data = (adc_digi_output_data_t*)&buffer[i];
61                 ADC_con_Value = data->type2.data;
62
63                 xQueueSend(ADCQueue, &ADC_con_Value, 0); //Send ADC Continuous Reading to SPI Task
64             }
65         }
66
67         LED_State = digitalRead(LED_EN_PIN); //Read Input from DAQ Card for LED
68
69     }
70
71     adc_continuous_stop(adc_handle); //Stop ADC continuous reading
72
73 }
74
75 currentMillis = millis();
76
77 if(currentMillis - previousMillis >= interval){
78     previousMillis = currentMillis; //Save the last time the LED was blinked
79

```

```

80     if(LED_Status == LOW){
81         LED_Status = HIGH; //Blink Status LED
82     }
83     else {
84         LED_Status = LOW; //Blink Status LED
85     }
86 }
87 digitalWrite(LED_test, LED_Status); //Turn on/off Status LED
88
89 }
90 }
91
92 void SPITask(void *parameter){
93
94     uint32_t ADC_con_Value;
95     uint32_t sum = 0;
96     int counter = 0;
97     uint16_t average = 0;
98
99     for(;;){
100         if(xQueueReceive(ADCQueue, &ADC_con_Value, portMAX_DELAY)){
101
102             counter++;
103             sum = sum + ADC_con_Value;
104
105             if(counter == 16){
106                 average = sum >> 4; //Divide by 16
107                 sum = 0;

```

```

108     counter = 0;
109
110     //Bit Shift ADC Reading to be sent to the DAC
111     uint16_t SPI_Value = (average >> 2) & 0x3FF; //12-bit ADC Reading to 10-bit DAC Output
112     uint16_t DAC_Value = SPI_Value << 4; //0-3 Bits - I do not care bits
113
114     digitalWrite(SPI_CS, LOW); //Start SPI Communication
115     SPI.transfer16(DAC_Value); //Output ADC Value
116     digitalWrite(SPI_CS, HIGH); //End SPI Communication
117 }
118
119 //Code for testing purposes of the ADC Reading
120
121 //uint16_t SPI_Value = ADC_con_Value;
122
123 //if(counter%10==0){
124 | //Serial.printf("%d \n", SPI_Value);
125 | //}
126 | //counter = counter + 1;
127 | }
128 | }
129 | }
130
131 void setup() {
132     // put your setup code here, to run once:
133     Serial.begin(115200);

```

```

134
135     pinMode(LED_EN_PIN, INPUT);
136
137     pinMode(LED_on_PIN, OUTPUT);
138     pinMode(LED_test, OUTPUT);
139
140     SPI.begin(SPI_CLK, -1, SPI_MOSI, SPI_CS);
141     SPI.setFrequency(1000000); //1 MHz , keep up with ADC Reading
142     SPI.setDataMode(SPI_MODE1); //CLK idles low, data is read on falling edge of CLK
143     SPI.setBitOrder(MSBFIRST); //MSB First
144
145     pinMode(SPI_CS, OUTPUT);
146     digitalWrite(SPI_CS, HIGH); //SPIT Communication is off at start of code
147
148     //Initialize the ADC Continuous Mode Driver
149     adc_continuous_handle_cfg_t adc_config = {
150     | .max_store_buf_size = 1024, //DMA Buffer Size
151     | .conv_frame_size = 256, //Read Size
152     };
153     ESP_ERROR_CHECK(adc_continuous_new_handle(&adc_config, &adc_handle));
154
155     //Configure ADC pin and how to sample
156     adc_continuous_config_t dig_cfg = {
157     | .sample_freq_hz = 50000, //50 kHz
158     | .conv_mode = ADC_CONV_SINGLE_UNIT_1,
159     | .format = ADC_DIGI_OUTPUT_FORMAT_TYPE2,

```

```

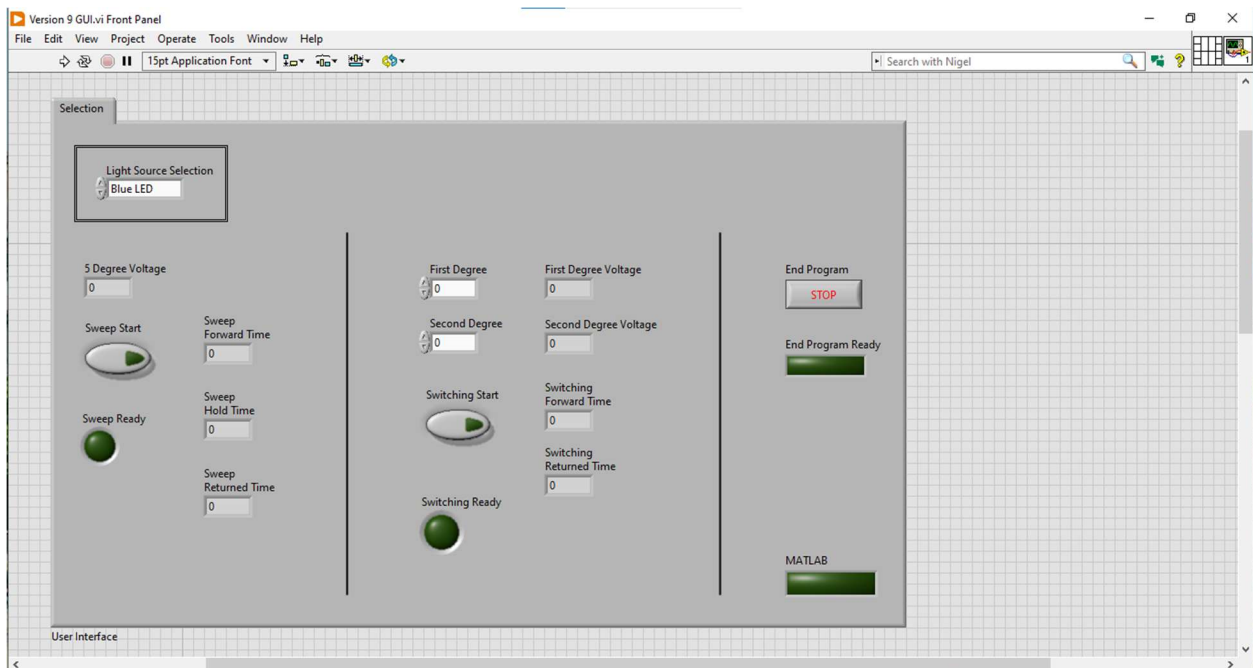
160 };
161
162 adc_digi_pattern_config_t adc_pattern = {
163     .atten = ADC_ATTEN_DB_12, //0 - 3.3 V Reading
164     .channel = ADC_CHANNEL_5, //GPIO 6 for ADC Reading
165     .unit = ADC_UNIT_1,
166     .bit_width = ADC_BITWIDTH_12, //12-bit
167 };
168
169 dig_cfg.pattern_num = 1;
170 dig_cfg.adc_pattern = &adc_pattern;
171
172 ESP_ERROR_CHECK(adc_continuous_config(adc_handle, &dig_cfg));
173
174 ADCQueue = xQueueCreate(
175     4096, //Queue Size
176     sizeof(uint32_t) //Data Size
177 );
178 if(ADCQueue == NULL){
179     Serial.println("Failed to create LED Queue!\n");
180     while(1);
181 }
182
183 xTaskCreatePinnedToCore(
184     ADCTask, //Task Function
185     "ADCTask", //Task Name
186     4096, //Stack Size (bytes)

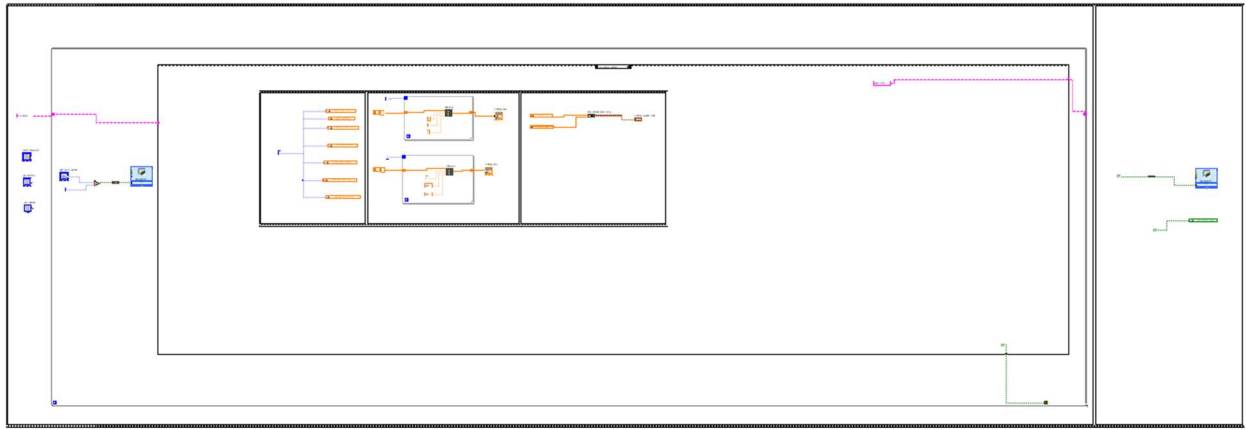
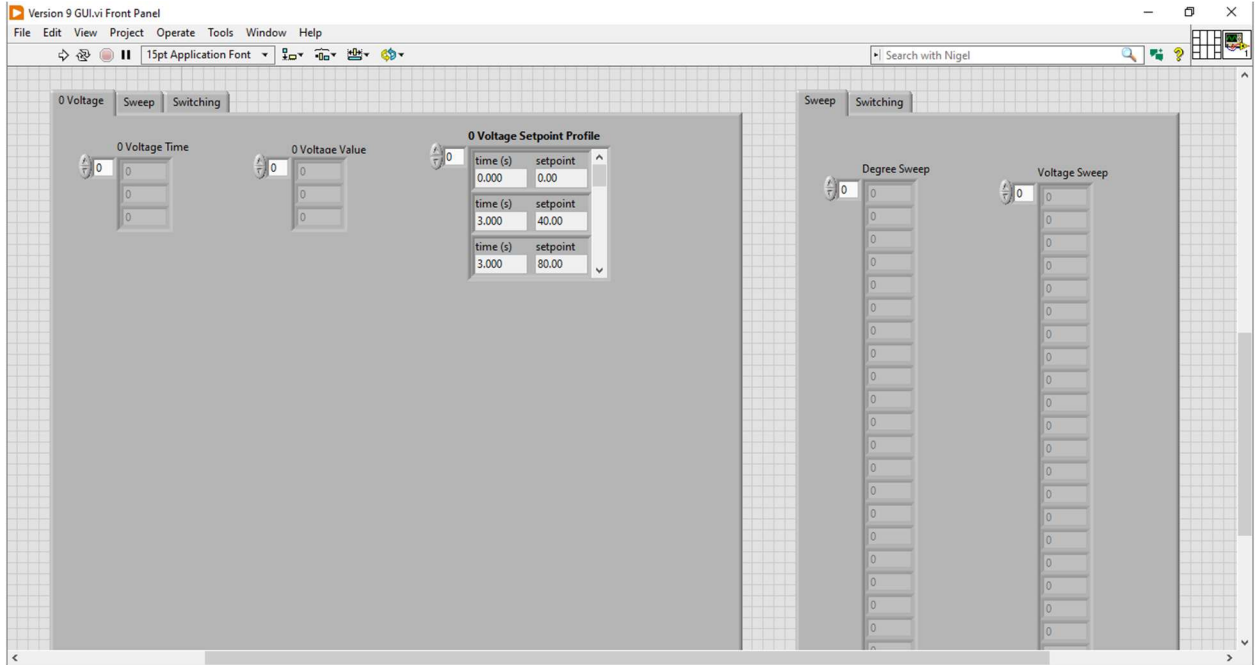
```

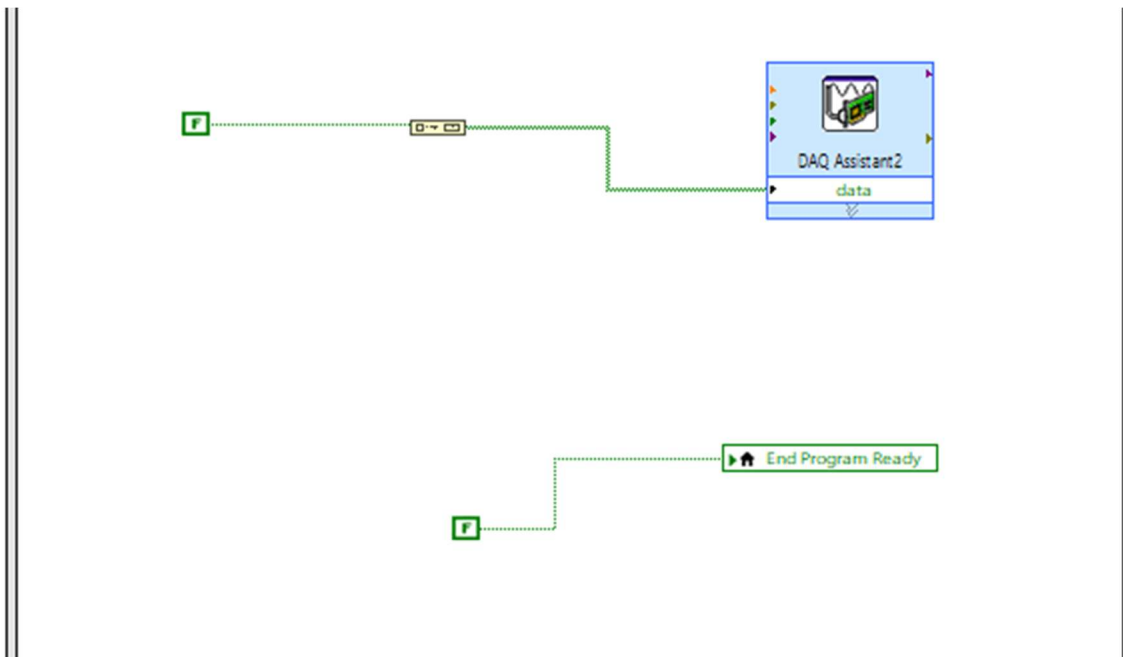
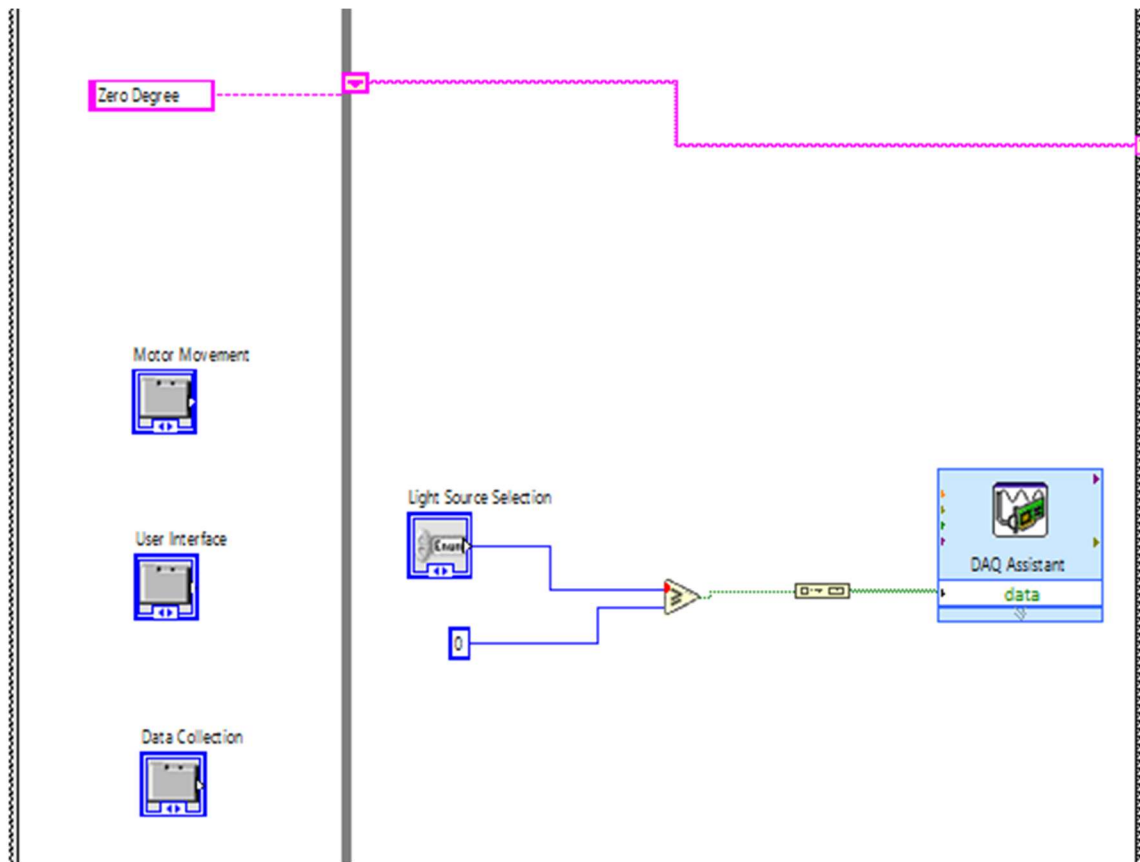
```

187     NULL, //Parameters
188     1, //Priority
189     &ADCTaskHandle, //Task Handle
190     1 //Core 1
191 );
192
193 xTaskCreatePinnedToCore(
194     SPITask, //Task Function
195     "SPITask", //Task Name
196     4096, //Stack Size (bytes)
197     NULL, //Parameters
198     1, //Priority
199     &SPITaskHandle, //Task Handle
200     0 //Core 0
201 );
202
203 }
204
205 void loop() {
206     // put your main code here, to run repeatedly:
207 }

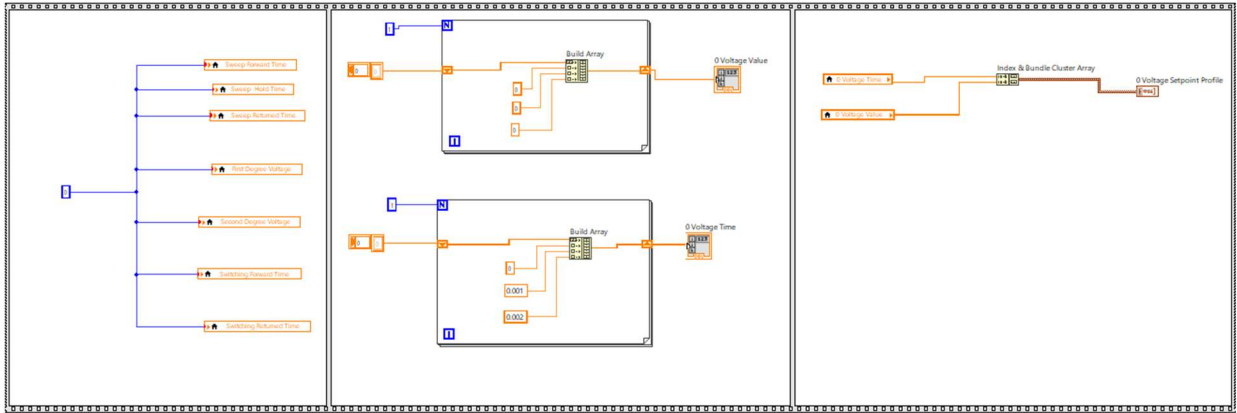
```



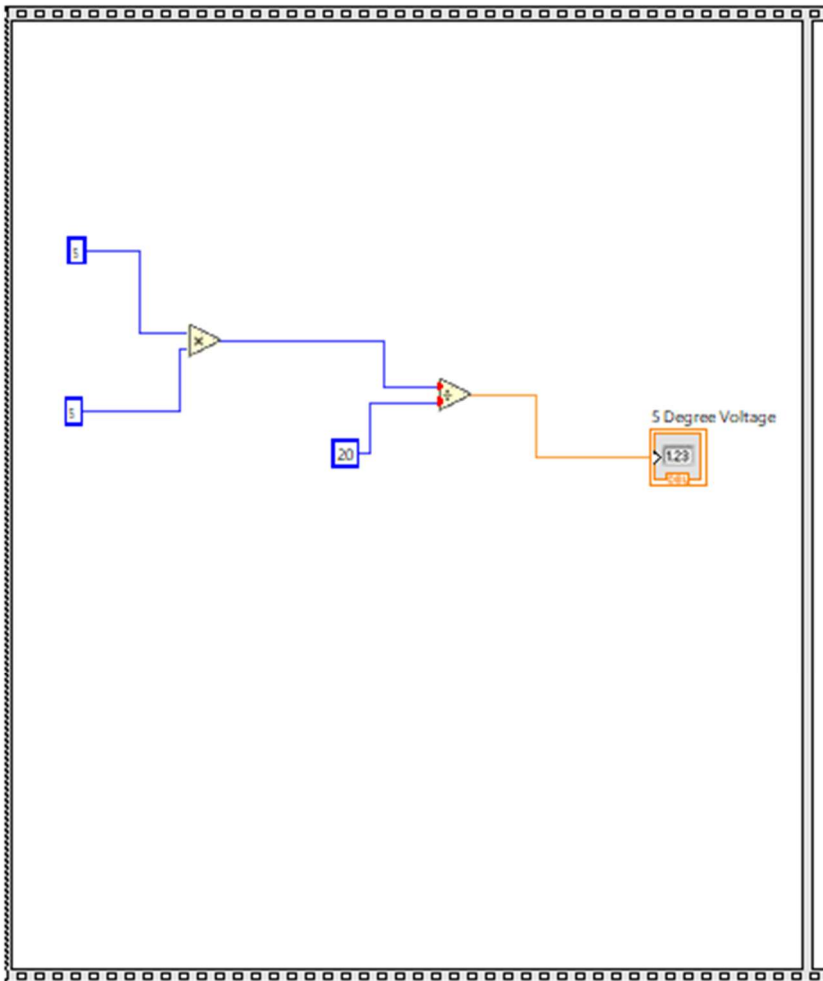


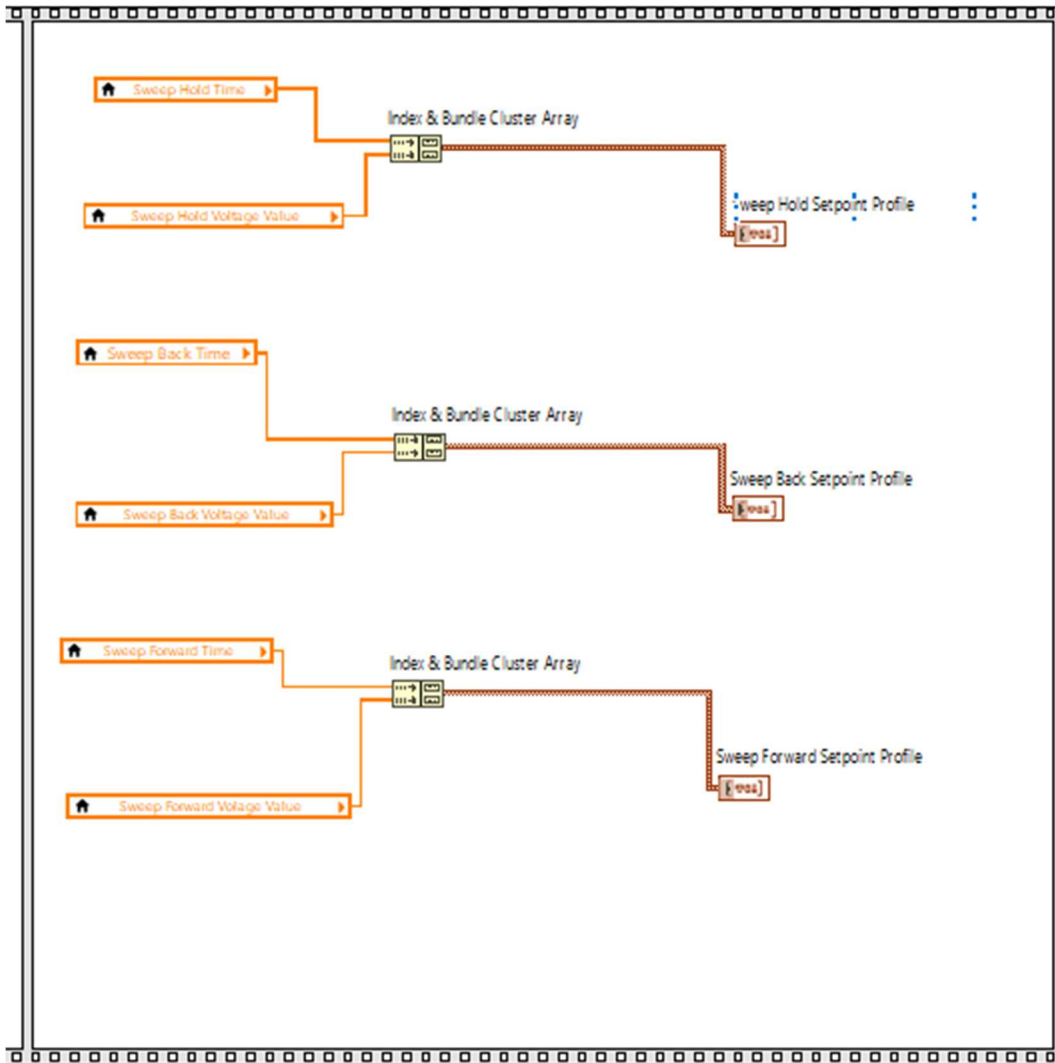
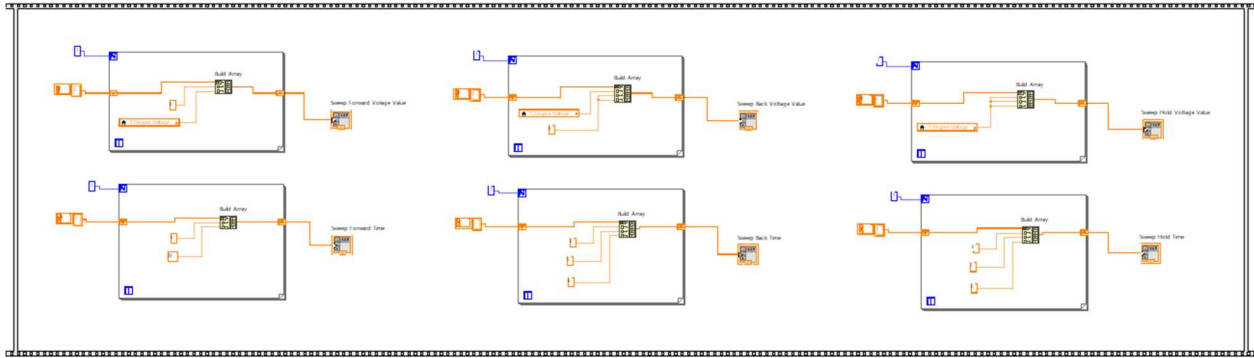


Case Structure: Zero Degree

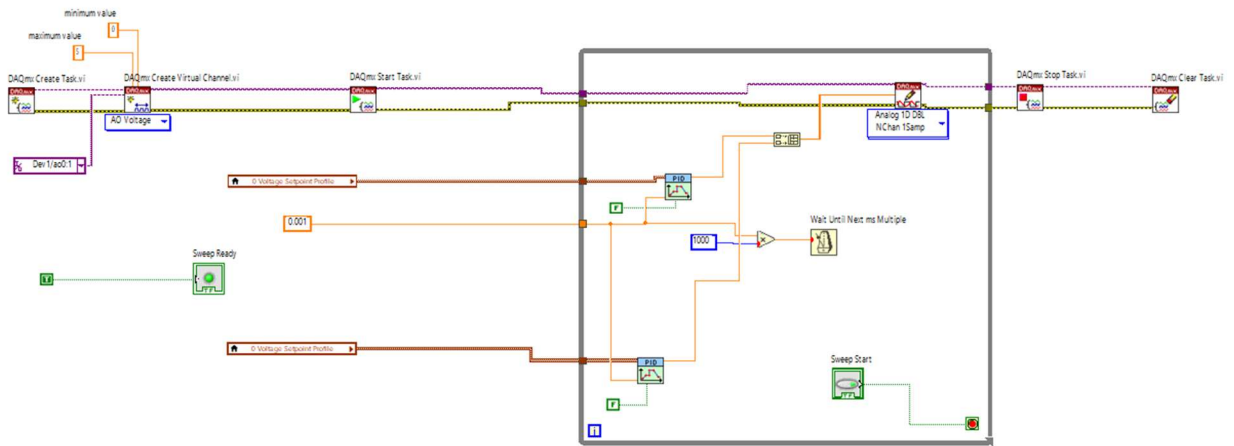


Case Structure: Sweep Setup

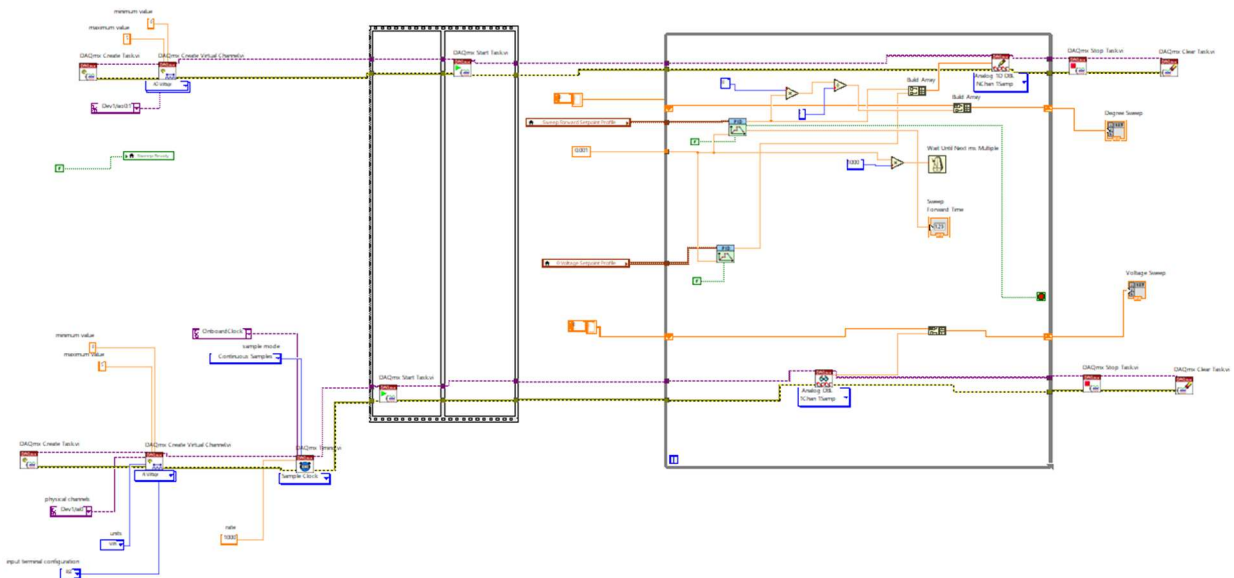




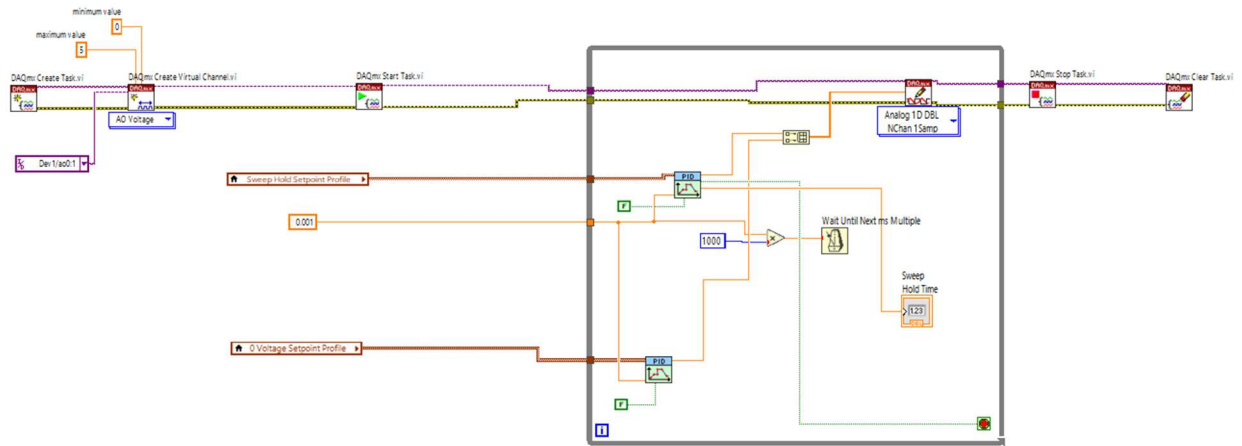
Case Structure: Sweep Start



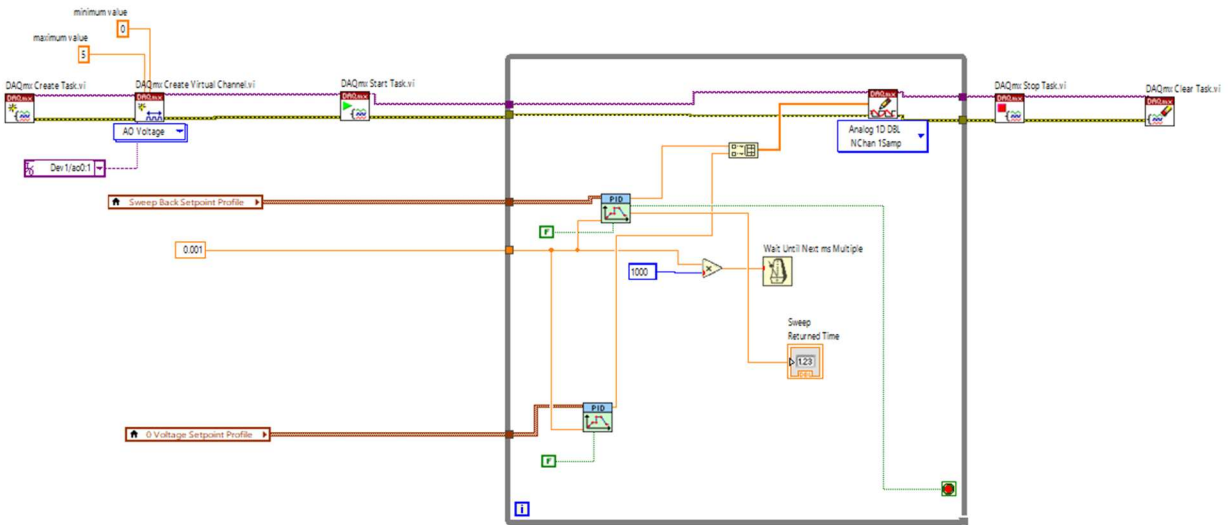
Case Structure: Sweep Forward



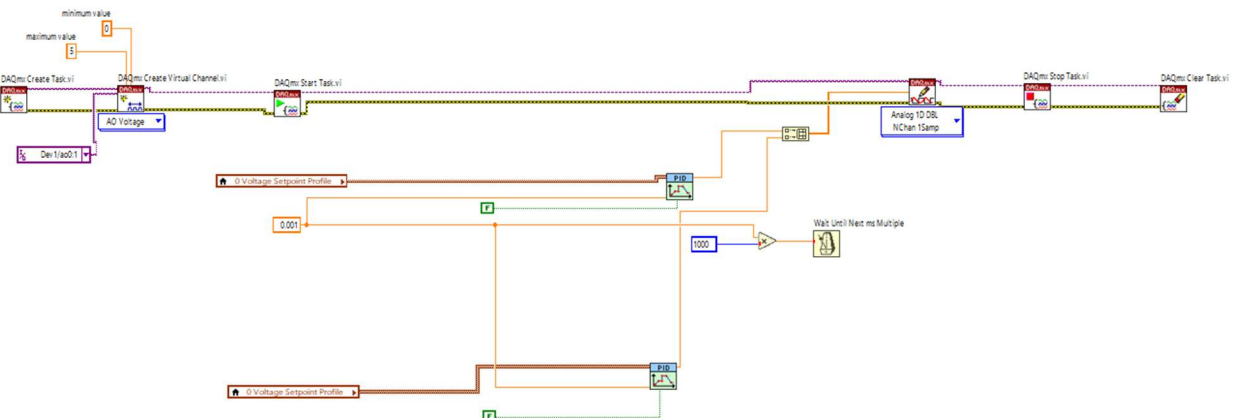
Case Structure: Sweep

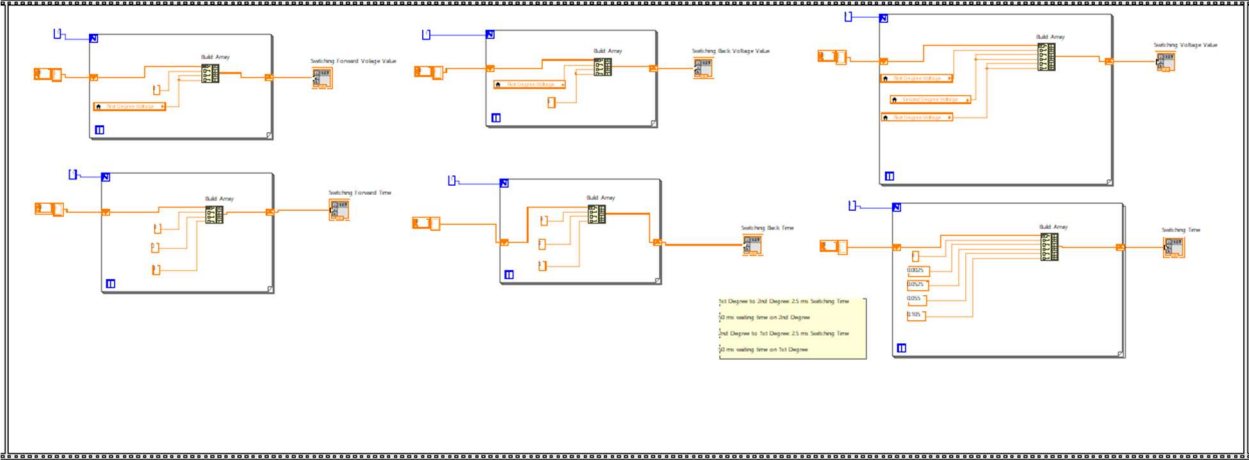
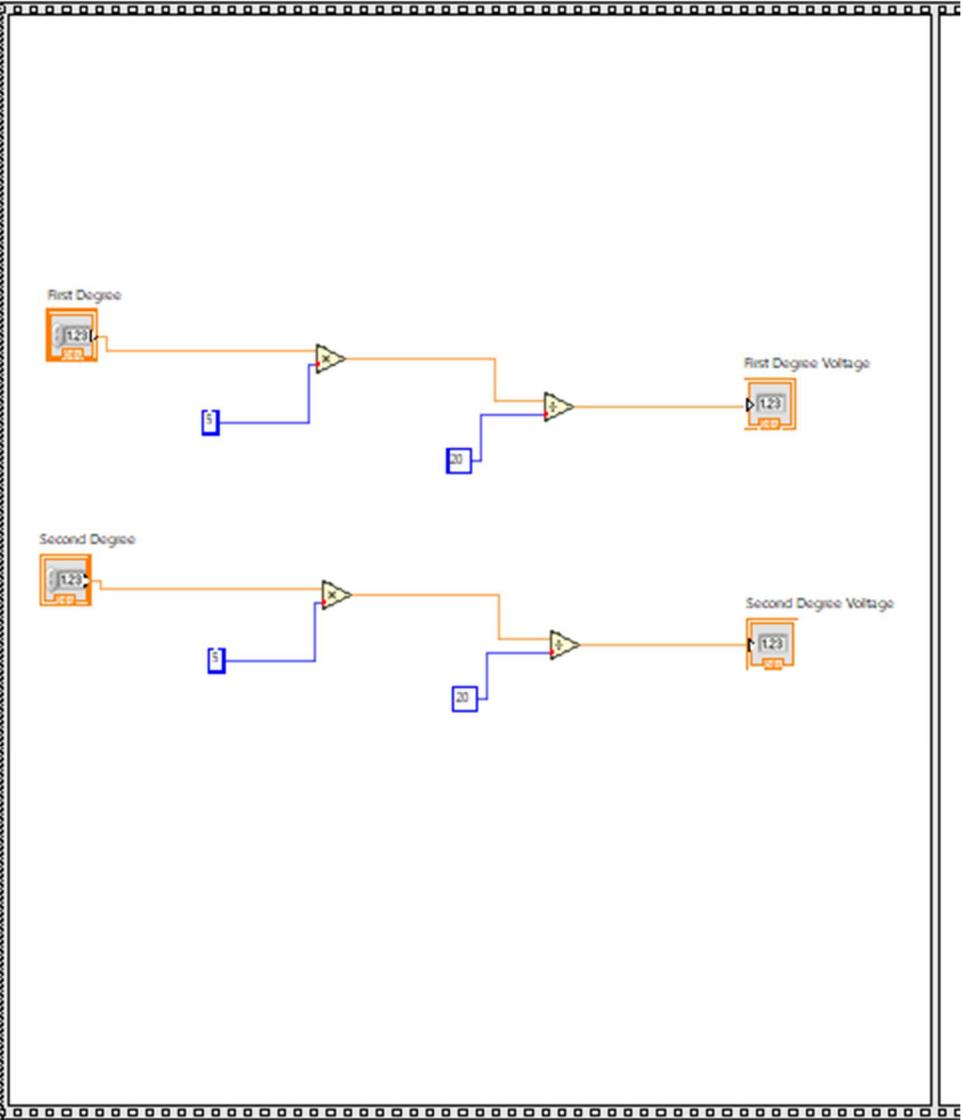


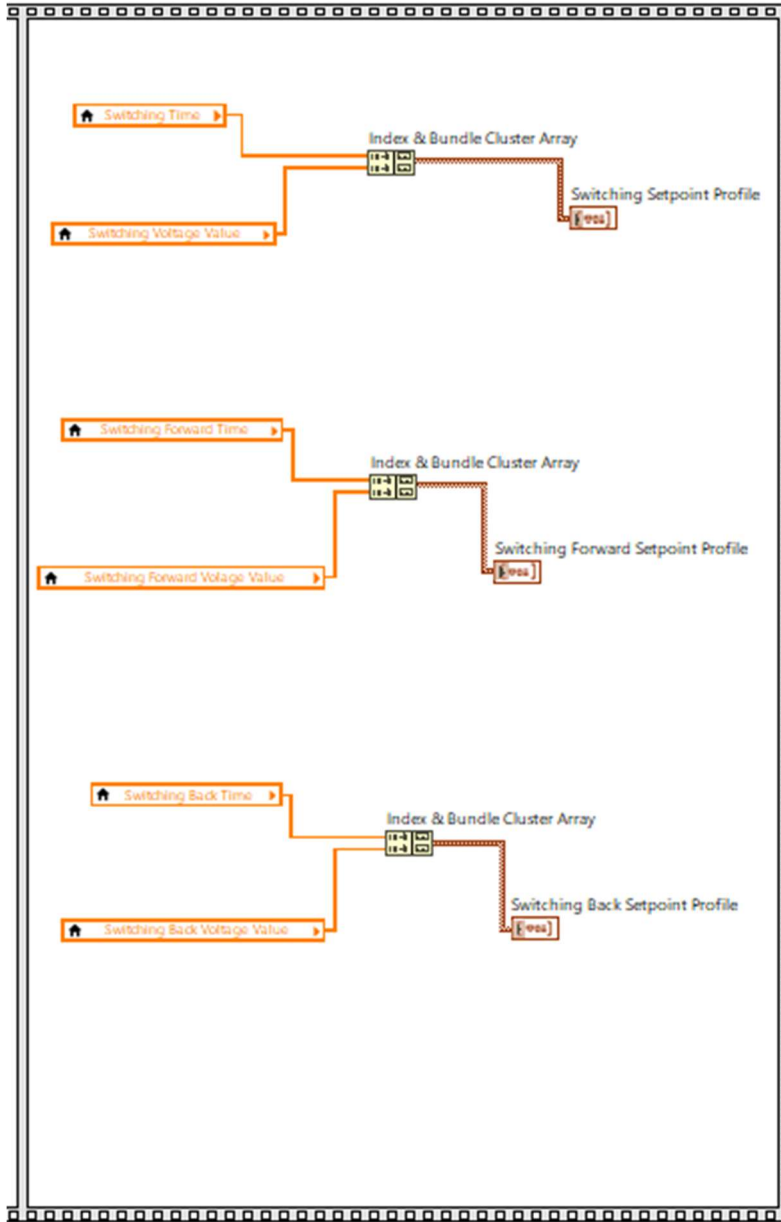
Case Structure: Sweep Back



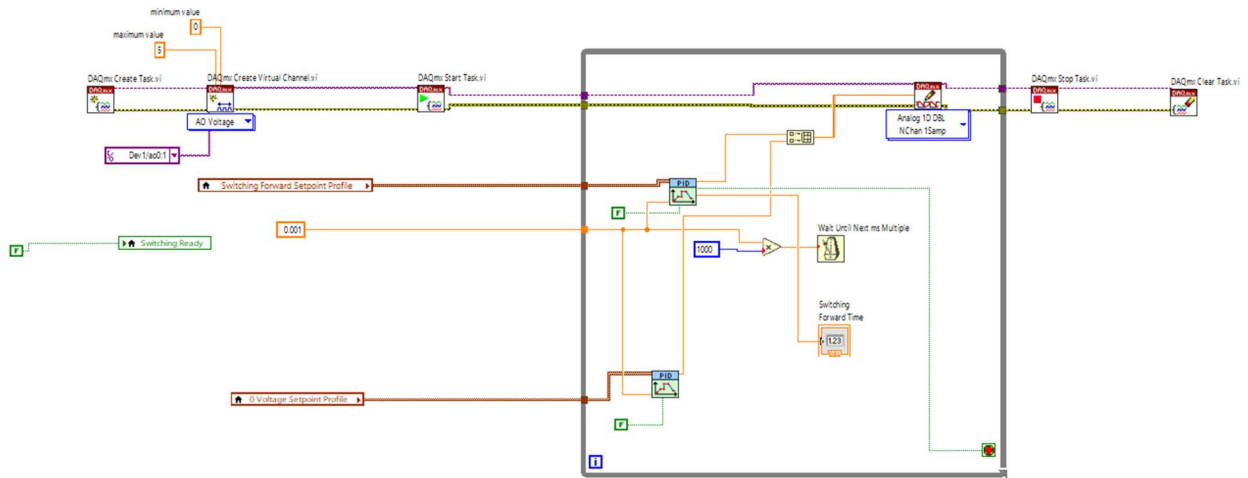
Case Structure: Sweep Stop



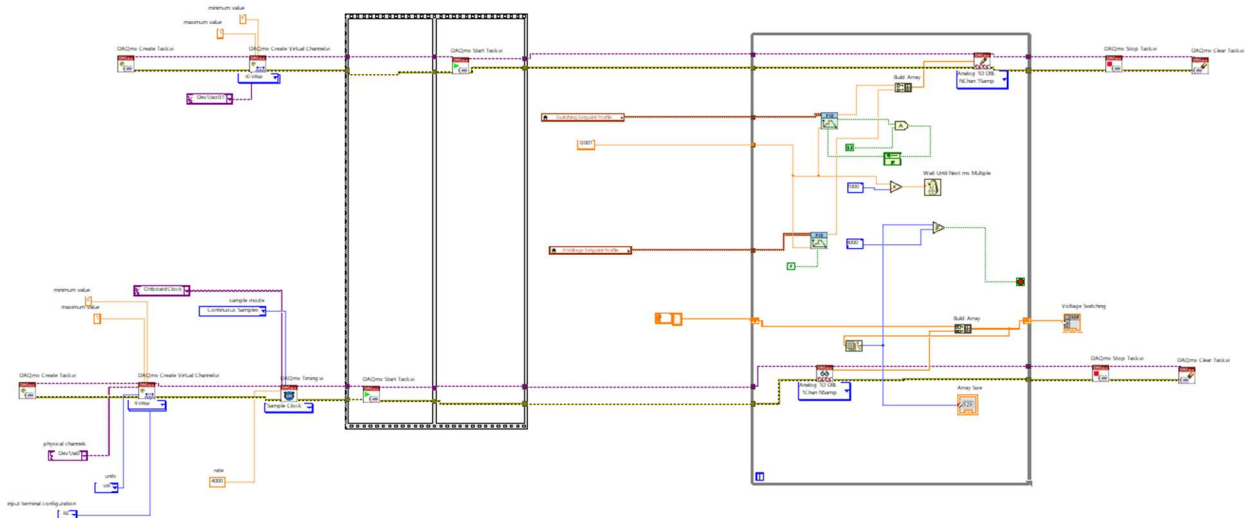




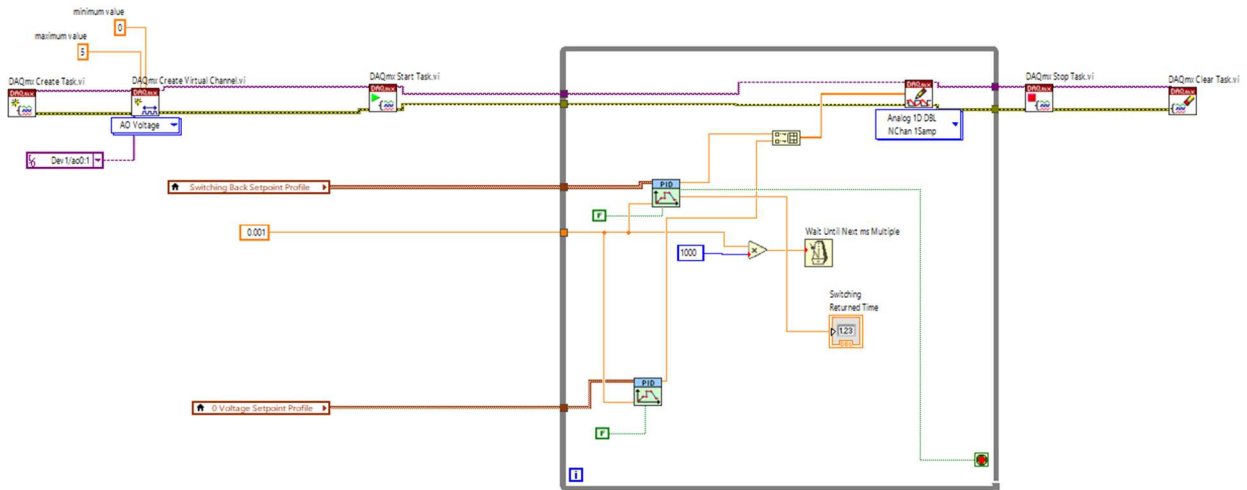
Case Structure: Switching Forward



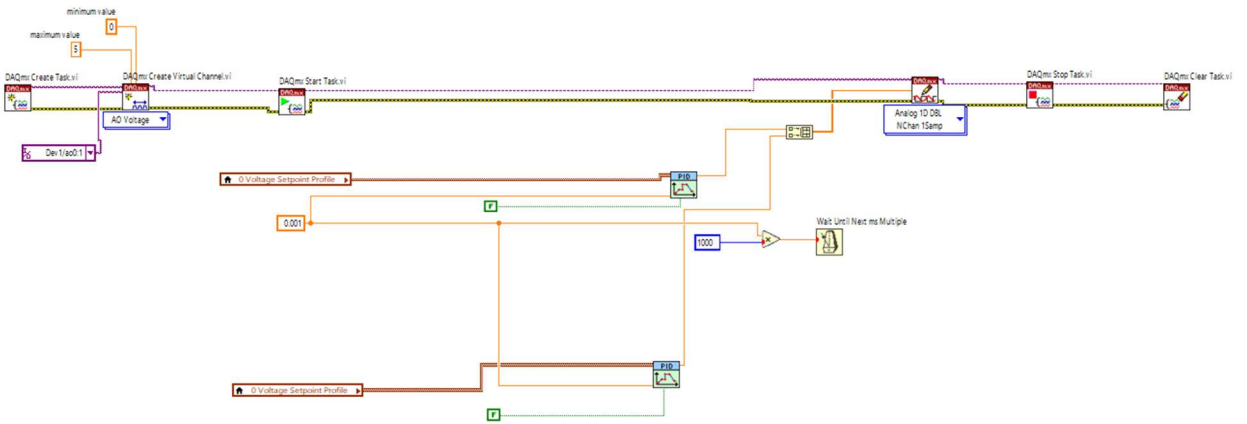
Case Structure: Switching



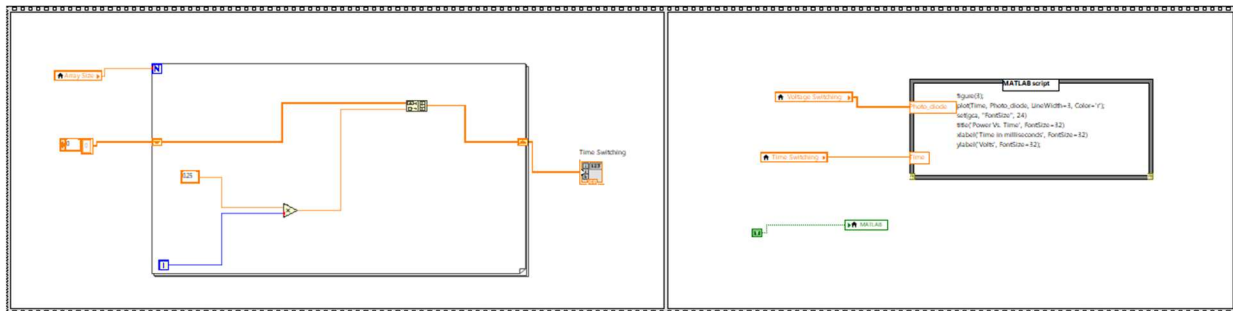
Case Structure: Switching Back



Case Structure: Switching Stop



Case Structure: Switching Data



Case Structure: Button Stop

